VOLUME 11 NUMBER 1 2018 ISSN 2218-7979

International Journal of Biology and Chemistry

Al-Farabi Kazakh National University

International Journal of Biology and Chemistry is published twice a year by al-Farabi Kazakh National University, al-Farabi ave., 71, 050040, Almaty, the Republic of Kazakhstan
website: http://ijbch.kaznu.kz/

Any inquiry for subscriptions should be sent to:
Prof. Mukhambetkali Burkitbayev, al-Farabi Kazakh National University
al-Farabi ave., 71, 050040, Almaty, Republic of Kazakhstan
e-mail: Mukhambetkali Burkitbayev@kaznu.kz

 Printed in Kazakhstan

EDITORIAL

The most significant achievements in the field of natural sciences are reached in joint collaboration, where important roles are taken by biology and chemistry. Therefore publication of a Journal, displaying results of current studies in the field of biology and chemistry, facilitates highlighting of theoretical and practical issues and distribution of scientific discoveries.

One of the basic goals of the Journal is to promote the extensive exchange of information between the scientists from all over the world. We welcome publishing original papers and materials of biological and chemical conferences, held in different countries (after the process of their subsequent selection).

Creation of special International Journal of Biology and Chemistry is of great importance, because a great amount of scientists might publish their articles and it will help to widen the geography of future collaboration. We will be glad to publish also the papers of the scientists from the other continents.

The Journal aims to publish the results of the experimental and theoretical studies in the field of biology, biotechnology, chemistry and chemical technology. Among the emphasized subjects are: modern issues of technologies for organic synthesis; scientific basis of the production of physiologically active preparations; modern issues of technologies for processing of raw materials, production of new materials and technologies; study on chemical and physical properties and structure of oil and coal; theoretical and practical issues in processing of hydrocarbons; modern achievements in the field of nanotechnology; results of studies in the fields of biology, biotechnology, genetics, nanotechnology, etc.

We hope to receive papers from a number of scientific centers, which are involved in the application of the scientific principles of biology, biotechnology, chemistry and chemical technology on practice and carrying out research on the subject, whether it relates to the production of new materials, technology and ecological issues.

IRSTI 31.19.29

[1*]D. Orazbayeva, [1]B. Kenessov, [2]J.A. Koziel

[1]Al-Farabi Kazakh National University, Faculty of Chemistry and Chemical Technology,
Center of Physicochemical Methods of Research and Analysis, Almaty, Kazakhstan
[2]Iowa State University, Department of Agricultural and Biosystems Engineering, Ames, IA 50011, USA
[*]e-mail: orazbayeva@cfhma.kz

Quantification of naphthalene in soil using solid-phase microextraction, gas-chromatography with mass-spectrometric detection and standard addition method

Abstract: Development of simple, fast and accurate methods for quantification of volatile organic compounds (VOCs) in soil samples is important for providing greater efficiency of analytical laboratories in Kazakhstan and other developing countries. Naphthalene is a model polycyclic aromatic hydrocarbon (PAH), belonging to a group of compounds of significant concern due to environmental impact. Solid-phase microextraction (SPME) is an optimal method for solvent-free automated sample preparation for determination of VOCs in environmental samples. In this work, the method for quantification of naphthalene in soil based on headspace SPME, gas chromatography with mass spectrometric detection, and standard addition calibration was developed. The parameters of SPME and sample equilibration after spiking with standards were optimized for better control of the soil matrix effect. The SPME temperature 80 °C provided the greatest accuracy of naphthalene responses for soils with different matrix and humidity. Equilibration of soil samples after spiking with standards for 6 h at 80 °C provided stabilization of responses in soils with different matrix and water content. The greatest accuracy and precision were achieved after equilibration of the samples for 8 h. The method provides recoveries of 105-119% in the concentration range 0.01-0.1 ng g^{-1} with detection limit 0.001 ng g^{-1}. The developed method was applied for quantification of naphthalene in real soil samples collected in Almaty, Kazakhstan. The measured concentration of naphthalene in real soil samples varied in the range of 1.4 to 47 ng g^{-1}. In five out of ten collected soil samples concentration exceeded a maximum permissible concentration of 15 ng g^{-1}.
Key words: naphthalene, soil analysis, solid-phase microextraction, standard addition, gas chromatography.

Introduction

Naphthalene is a ubiquitous pollutant found in many environmental samples of air, water, soil. It is a confirmed carcinogen and mutagen linked to hemolytic anemia and cataracts in humans [1,2]. Along with other polycyclic aromatic hydrocarbons (PAHs), naphthalene can be released into the environment during transportation, storage, and use of crude oil and oil products [2]. The soil is often the main sink of PAHs spills.

Standard methods for quantification of naphthalene in soil require waste-generating, costly and time-consuming sample preparation using toxic organic solvents (e.g., acetonitrile, acetone, chloroform, diethyl ether, methanol). The extraction of an analyte from soil is followed by purification of the extracts by passing through adsorbent (e.g., aluminum oxide, silica gel) and an evaporative concentration [3–5], which can result in the emission of toxic compounds to an environment.

The most promising "green" method of sample preparation for the determination of volatile and semi-volatile organic compounds (VOCs and SVOCs) in soils is solid-phase microextraction (SPME) [6]. SPME combines sampling, extraction, concentration, and purification steps into one easily automated operation. During SPME, VOCs are transferred onto the polymer coating from a headspace (HS) above a soil sample. Extracted analytes are then desorbed in an inlet of a gas chromatograph for analysis (Figure 1). This method does not require organic solvents and provides an ideal combination of simplicity and sensitivity.

Available SPME-based methods for quantification of naphthalene and other PAHs in soil include preliminary extraction with a surfactant solution [7]

 Printed in Kazakhstan

or an organic solvent [8], while SPME is conducted in direct-immersion (DI) mode. For headspace SPME, extraction is conducted with simultaneous heating of the sample and cooling of a fiber coating (cold-fiber SPME) [9–11], or at low-pressure conditions (vacuum-assisted HS-SPME) [12]. The main limitations of CF-SPME and vacuum-assisted HS-SPME are the complexity of method instrumentation and its automation, along with no commercial availability.

The accuracy of SPME-based quantification of VOCs and SVOCs in soil is affected by a matrix effect, which results in variable extraction efficiencies of analytes from samples having different physicochemical properties. To overcome the matrix effect, two main approaches are used: control of the matrix effect by obtaining a calibration plot for each type of soil; and a decrease of the matrix effect by increasing the extraction temperature, addition of water, or using cold-fiber SPME [13]. The main difficulty in using the first approach is a long and often inefficient equilibration of samples after their spiking with standards [14; 15].

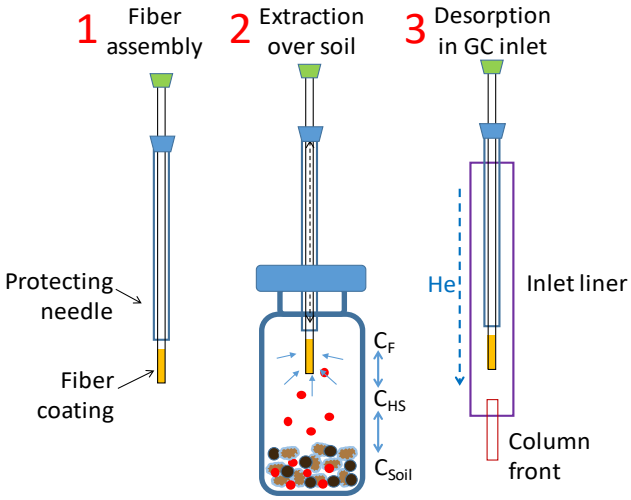

Figure 1 – Solid-phase microextraction of organic compounds from soil
Note: Stages of SPME: 1 – Fiber holder (before extraction); 2 – extraction; 3 – desorption; C_F – analyte concentration in fiber; C_{HS} – analyte concentration in headspace; C_{Soil} – analyte concentration in soil

In this work, a fast, green, and accurate method for quantification of naphthalene in soil samples using headspace (HS) SPME, GC with MS detection, and the standard addition calibration was developed. Parameters of HS-SPME were optimized to provide the best accuracy of naphthalene responses for soils with different matrix and humidity. Soil equilibration temperature and time after spiking with naphthalene standard were optimized. The developed method was successfully applied for the analysis of real soil samples.

Materials and methods

Reagents, materials, and samples

Naphthalene (99%) was purchased from Meryer (China). Methanol (HPLC grade) purchased from AppliChem (Germany) was used for the preparation of standard solutions. SPME fiber – 100 µm polydimethylsiloxane (PDMS) was purchased from Supelco (USA). Soil sampling and calibration were performed in 20-mL crimp-top headspace vials (HTA, Italy) with PTFE/silicone septa (Zhejiang Aijiren Technology Co., China). All vials and septa were washed with distilled water and pre-conditioned at 140 °C for 2 h before analysis.

Two different soil types were used: clay and chernozem having humus content 0.90 and 45%, respectively. These soils will be referred hereinafter as soils with 'low' and 'high' humus content (LHC and HHC), respectively. Both soils were collected near Almaty, Kazakhstan. Soils were cleaned from possible naphthalene residues and water by heating in a drying furnace at 150 °C for 6 h.

Parameters of gas chromatography-mass spectrometry (GC-MS) analysis

GC-MS analyses were performed on the 6890N/5973N system (Agilent, USA) equipped with a Combi-PAL autosampler (CTC Analytics, Switzerland). Separation was conducted using a polar 60 m x 0.25 mm DB-WAXetr (Agilent, USA) column with a 0.50 µm film thickness at constant helium (>99.995%, Orenburg-Tehgas, Russia) flow 1.0 mL min^{-1}. The oven temperature was programmed from 80 °C to 160 °C with the heating rate 20 °C min^{-1}, and further heating to 240 °C (held for 3 min) with the heating rate 10 °C min^{-1}. GC run time was 15 min (sample chromatogram is shown in Figure 2). Temperatures of the ion source, quadrupole and MS interface were 230, 150 and 240 °C, respectively. Detection was conducted using electron impact ionization at 70 eV in selected ion monitoring (SIM) mode at m z^{-1} of 128.

Headspace solid-phase microextraction (HS-SPME) procedure

Soil samples weighing 1.00 g were placed into 20-mL crimp-top headspace vials and spiked with 10 μL of standard solution of naphthalene (C = 10 ng μL^{-1}). Vials were placed into the agitator of the autosampler and incubated at a preset temperature for 10 min. The headspace extraction was conducted for 5 min at a preset temperature of the agitator of the autosampler using 100 μm PDMS fiber. After extraction, the analyte was completely desorbed from the SPME fiber in the GC inlet at 240 °C for 60 s.

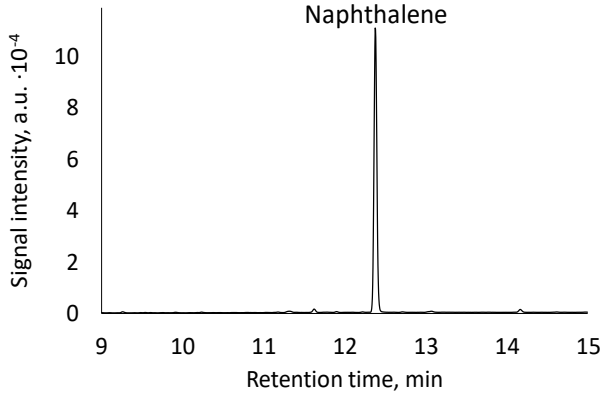

Figure 2 – Selected ion monitoring (m z^{-1} 128) chromatogram obtained after SPME-GC-MS analysis of soil spiked with naphthalene standard solution

Study of the effect of soil water content and extraction temperature on intensity and precision of naphthalene responses

Soils with water content of 0%, 25%, and 50% were prepared by addition of 0, 250 or 500 μL of water to 1.00 g soil samples pre-spiked with 10 μL of a standard solution of naphthalene (C = 10 ng μL^{-1}). Studied extraction temperatures were 60, 70 and 80 °C. Responses were measured in three replicates.

Study of the effect of temperature and time on equilibration of naphthalene in soils with different humus and water content

Vials with HHC and LHC soils of the different water content (0, 25, and 50%) were placed into the agitator of the autosampler and equilibrated at 60, 70, and 80 °C. The HS-SPME was conducted immediately after spiking and every 2 h until stabilization of the naphthalene responses. All experiments were conducted in three replicates.

Method validation

Model samples of HHC and LHC soils with concentrations of naphthalene 10 and 100 ng g^{-1} were prepared by spiking 1.00 g of soil with 10 μL of standard solutions with concentrations of naphthalene 1 and 10 ng μL^{-1}, respectively. After spiking, the model samples were held for 48 h at 60 °C. Calibration standards for standard addition calibration were obtained by spiking 1.00 g of model samples with 10 μL of standard solutions with concentrations of naphthalene 0, 0.5, 2.0, 5.0, and 10 ng μL^{-1}. After spiking with standards, the soils samples were equilibrated for 8 h at 60 °C. Slope factors of calibration plots, measured concentrations, and their standard deviations were calculated using least squares method and standard addition approach.

Results and discussion

Optimization of HS-SPME of naphthalene from soil samples

The precision of the analytical responses has a significant effect on the accuracy of quantification of analytes using the standard addition method. To achieve the acceptable accuracy at high standard deviation, an increase in the number of calibration standards is required, which results in the increase of the cost of the analysis. The aim of this experiment was to study the effect of extraction temperature from soil samples with different matrices on the intensity and precision of naphthalene responses.

Naphthalene extraction effectiveness from soils with low humus content (LHC) decreased with increasing extraction temperature from 60 to 80 °C (Figure 3A). The increase of the extraction temperature from 60 to 70 °C resulted in the decrease of the response by 50%. In soils with high humus content (HHC), such increase in the extraction temperature resulted in the increase of the response by 10 to 14%. At 80 °C, responses of naphthalene for soils with low and high humus content became practically similar meaning that this temperature allows such analysis at minimum matrix effects. However, the increase of the extraction temperature to 80 °C resulted in the increase of the relative standard deviations (RSDs) of naphthalene responses in soils with different matrix (Figure 2B). The optimal temperature of naphthalene extraction from soil samples for minimization of the matrix effect is 80 °C. However, optimization of sample equilibration after spiking with standards is required in order to provide proper precision and accuracy of responses.

The increase of water content of soil did not affect naphthalene extraction effectiveness from soils with high humus content (Figure 4). RSDs of responses increased with the increase of soil humidity. At 0% humidity, the RSDs of naphthalene in high humus content soil (HHC) was 2.9%, at water content 25% and 50%, RSDs were 3.2 and 7.1%, respectively.

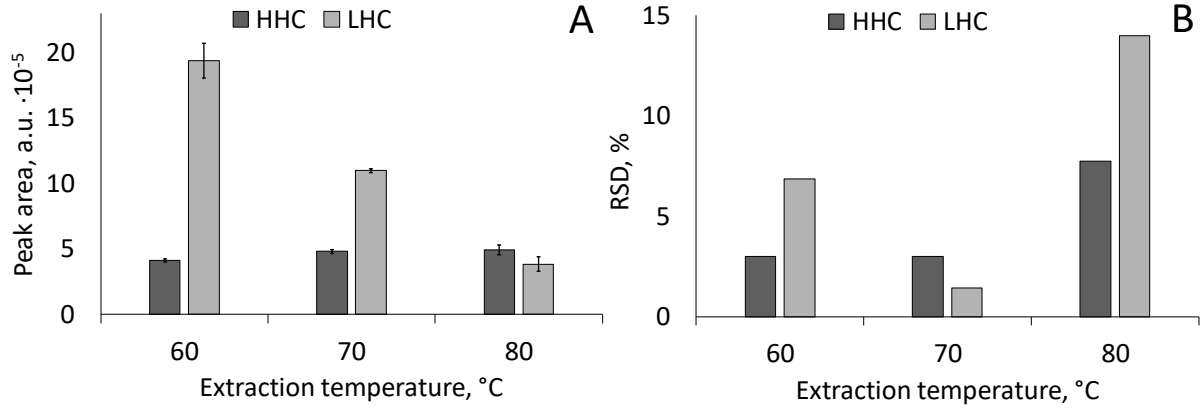

Figure 3 – Effect of SPME temperature on intensity (A) and precision (B) of the naphthalene responses from soils with high and low humus content. *Note:* water content: 0%, extraction time 5 min, C = 100 ng g^{-1}

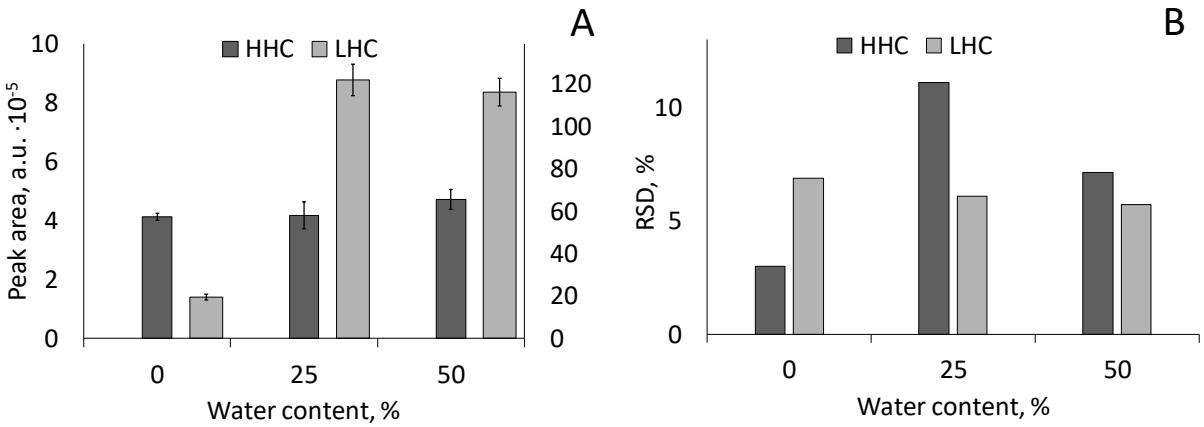

Figure 4 – Effect of water content on intensity (A) and precision (B) of the naphthalene responses for soils with HHC (on the primary axis) and LHC (on the secondary axis).
Note: extraction temperature 60 °C, extraction time 5 min, C = 100 ng g^{-1}

In soils with low humus content, the increase in soil humidity up to 25 and 50% resulted in the increase of responses by the factor of ~7. The addition of water to the soil, therefore, increases the difference in the effectiveness of naphthalene extraction from soils with different matrix. The increase of soil water content leads to a more efficient desorption of naphthalene from soils with low humus content and can lead to analyte losses during the sample preparation for calibration using the standard addition method. Thus, for SPME-GC-MS determination of naphthalene by the standard addition method, it is undesirable to introduce water additives into the samples before extraction.

Equilibration of naphthalene in soils of different type and water content

Equilibration of soils after spiking by standards is required in order to achieve high accuracy using the standard addition method [14,15]. Equilibration of spiked soil samples ensures the same extraction efficiency of analytes already present in the sample and spiked standards.

Stabilization of naphthalene responses for soils with high humus content proceeded with the decrease of their intensity (Figure 5). At all studied equilibration temperatures, the stabilization of the naphthalene responses for the HHC soil was achieved within 2 h. When equilibrated for 8 h, the naphthalene responses in all parallel experiments and at different equilibration and extraction temperatures were equalized.

For LHC soil equilibrated at 60 °C, the signal was fluctuating in the range of standard deviation

during 6 h without a decrease of the responses, decrease of the responses was observed only after 6 h of equilibration. When equilibrating LHC soil at 70 and 80 °C, the responses after 8 h of equilibration decreased by 20 and 70%, respectively, showing that increase of temperature enhances equilibration of LHC soils. The rate of equilibration of LHC soils after spiking with naphthalene is lower than for HHC soils, and equilibration was observed only after 6 to 8 h at 80 °C.

RSDs of responses of naphthalene decreased as the equilibration time increased at all studied temperatures (Figure 6). The lowest RSDs were obtained at equilibration temperature 70 °C.

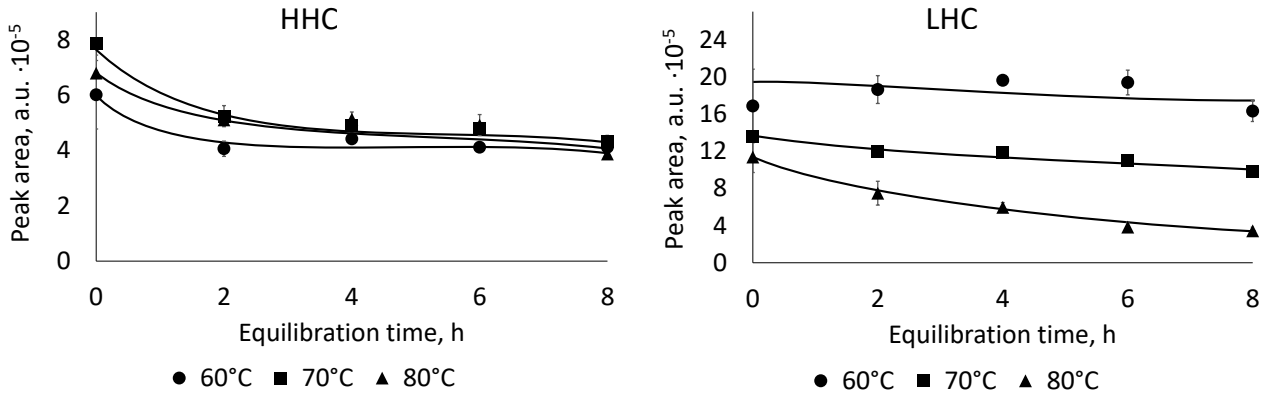

Figure 5 – Effect of temperature and time of equilibration on responses of naphthalene from soils with HHC and LHC.
Note: water content 0%, extraction time 5 min, C = 100 ng g^{-1}

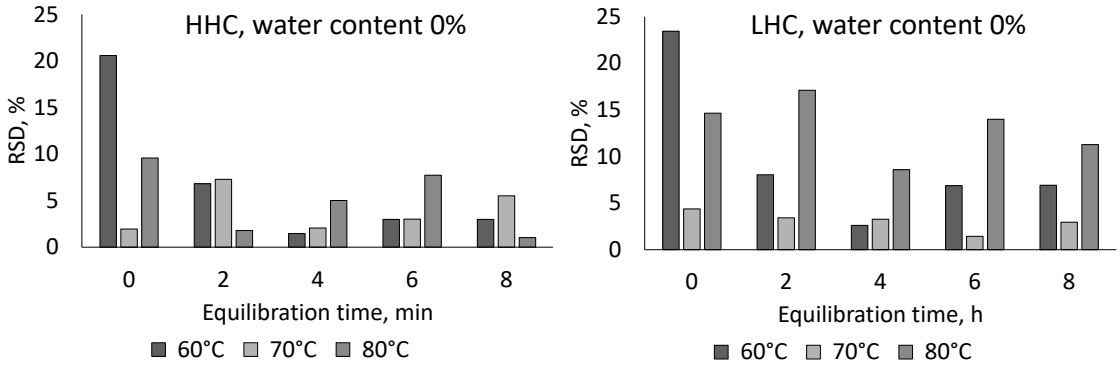

Figure 6 – Effect of equilibration time on precision of naphthalene responses from soil samples

Soil humidity affects equilibration of soil samples after spiking with naphthalene (Figure 7). In HHC soils the stabilization of the naphthalene responses was observed in 6 h for all studied water contents. With the increase of water content in HHC soil, the increase of naphthalene responses during equilibration was observed. When the HHC soil was equilibrated in a wide range of water contents (0 to 50%) for 6 h or more, the responses of naphthalene were equalized, and the precision of the results increased. In LHC soils with 0% water content, the equilibration was not observed at all studied equilibration times. For LHC soils with water contents 25 and 50%, equilibration was achieved in 4 h (Figure 7).Thus, the optimum temperature of soil equilibration after spiking with naphthalene standards is 80 °C. Stabilization of responses in all types of soil and water contents was achieved after 6 h of equilibration. The optimal equilibration time providing best combination of accuracy and precision of the results was 8 h.

Validation of the method

The developed method was applied for quantification of naphthalene in model soil samples with

concentrations 10 and 100 ng g^{-1}. The method provided good linearity of the calibration plots obtained using standard addition approach and least squares method with coefficients of determination ranging from 0.968 to 0.998 for concentrations 1 to 250 ng g^{-1} (Table 1). Higher coefficients of determination of the calibration plots were obtained for LHC soils. Method detection limit is 1 ng g^{-1}.

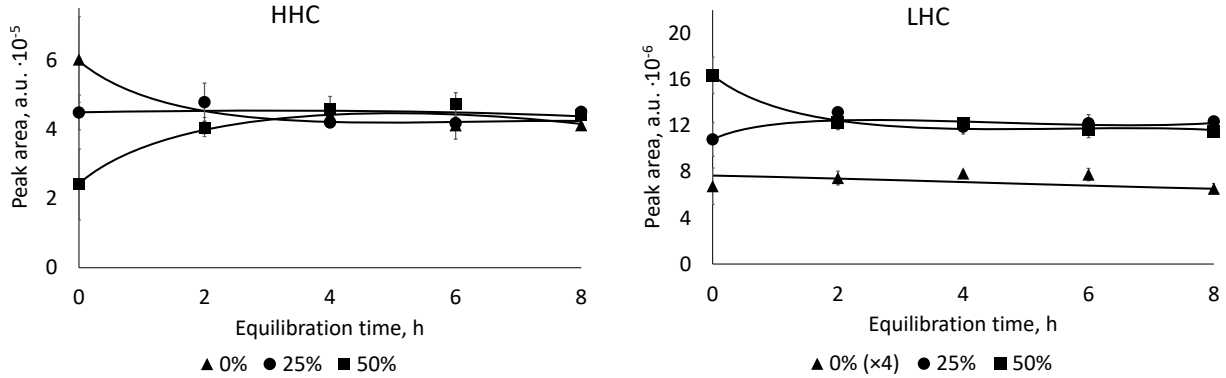

Figure 7 – Effect of soil water content on the equilibration of soils with different matrix after spiking with naphthalene at 60 °C

The accuracy of quantification of naphthalene in soils with a high concentration (100 ng g^{-1}) is higher than in soils with a low concentration (Table 1). Deviations from the spiked concentrations were 10 to 18%. In soils with a low concentration of naphthalene, deviations from the spiked concentrations were 5 to 29%. The greatest deviations between measured and spiked concentrations were obtained in LHC soils with low analyte concentration. This can be explained by the low affinity of naphthalene to the soil, which leads to its less homogeneous distribution in the soil.

Table 1 – Results of quantification of naphthalene in model samples using the developed method

Soil type	Spiked concentration (ng g^{-1})	Measured concentration (ng g^{-1})	Recovery (%)	R^2
HHC	10	10.5+0.9	105+9	0.968
LHC	10	12.9+1.7	129+13	0.993-0.998
HHC	100	110+11	110+10	0.969-0.982
LHC	100	118+11	118+9	0.989-0.993

Application of the developed method on real soil samples

The developed method was applied for the analysis of ten soil samples collected in different locations in Almaty, Kazakhstan (map of sampling locations is shown in [16]) in September 2017. Sampling and sample preparation were optimized to minimize the loss of analytes (Figure 8). Samples for response measurement were collected separately into preweighed vials and analyzed from sealed vials without any sample preparation. Samples for preparation of calibration samples were collected at the same location and prepared as described in the optimized method.

Naphthalene was detected in all collected samples (Table 2). In five samples, concentrations of naphthalene were close to or higher than the maximum permissible concentration (MPC, 15 ng g^{-1}). Concentrations of naphthalene in samples 4 and 5 collected in park area and gas station territory, respectively, were three and two times higher than MPC.

The slope factors of obtained calibration plots varied in the range 1991-12842. This significant difference in slope factors could be caused by different humidity of the samples, as it was shown previously that increase of water content results in significant response differences of naphthalene from soils. These results imply the importance of matrix control by standard addition calibration, since external standard calibration will not provide acceptable accuracy of quantification.

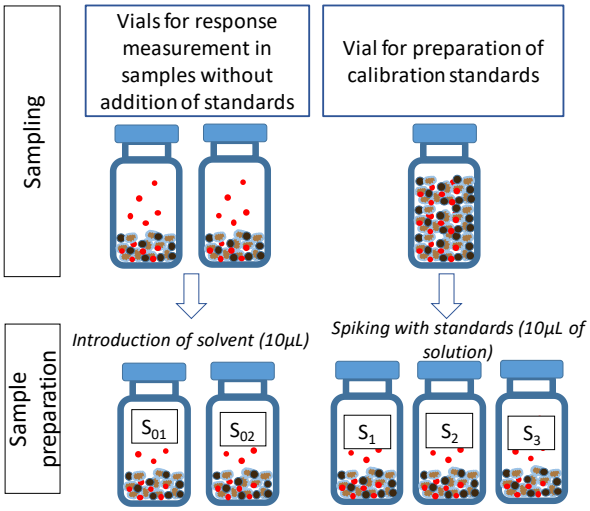

Figure 8 – Scheme of soil sampling and analysis using the developed method

Table 2 – Naphthalene concentrations determined in real soil samples using of the developed method

#	Measured concentration (ng g^{-1})	RSD (%)	Slope factors of calibration plots	R^2	Location description
1	18 ± 3	17	2785	0.972	Private residential sector
2	13 ± 2	17	1991	0.977	Near the roadway
3	47 ± 5	11	3823	0.991	Park area
4	31 ± 3	9	6674	0.998	Gas station area (Gas Energy)
5	15 ± 2	13	8615	0.984	Residential area
6	10.2 ± 1.2	12	12842	0.986	Student residential area (KazNU)
7	1.4 ± 0.2	15	11745	0.995	Near the major roadway (Timiryazev st.)
8	16 ± 3	22	9785	0.963	Park area next to roadway
9	2.1 ± 0.4	17	11916	0.982	Gas station area (KazMunaiGaz)
10	8.9 ± 1.4	16	9552	0.993	Near the major roadway (Gagarin st.)

Conclusion

Fast, green, and automated method for quantification of naphthalene in soil samples based on solid-phase microextraction and gas-chromatography with mass-spectrometric detection was developed and tested. Optimal temperature of SPME providing best matrix effect minimization is 80 °C. The optimal temperature for soil equilibration after spiking with naphthalene standards is 70 °C. Stabilization of responses in all types of soil and water contents at 80 °C is achieved in 6 h. The greatest accuracy and precision are achieved after equilibration of the samples for 8 h. The uncertainty in the determination of naphthalene in soils with concentration higher than 100 ng g^{-1} does not exceed 18%; for soils with a

concentration higher than 0.01 ng g^{-1}, uncertainty is less than 29%.

The developed method provides simple and fast quantification of naphthalene with sufficient accuracy without using toxic organic solvents. The method can be applied in environmental analytical laboratories for quantification of naphthalene in different soils.

Acknowledgments

This work was conducted under the project 3661/GF4 "Development and implementation of "green" methods for determination of organic pollutants in soils" and Ph.D. project of Dina Orazbayeva both funded by the Ministry of Education and Science of Kazakhstan.

References

1. Agency for Toxic Substances and Disease Registry (ATSDR) (2005). Toxicology profile for naphthalene, 1-methylnaphalene, and 2-methylnaphthalene. – Atlanta, GA: U.S. Department of Health and Human Services, Public Health Service, 347 p.

2. Abdel-Shafy H.I., Mansour M.S.M. (2016) A review on polycyclic aromatic hydrocarbons: Source, environmental impact, effect on human health and remediation. Egyptian Journal of Petroleum, Vol. 25, Is. 1, P. 107–123.

3. MUK 4.1.1062-01 (2001) Khromato-mass-spektrometricheskoye opredeleniye trudnoletuchikh organicheskikh veshchestv v pochve i otkhodakh proizvodstva i potrebleniya (Chromato-mass spectrometric determination of non-volatile organic substances in soil and production and consumption wastes). – M.: Minzdrav Rossii, 27 p. [In Russian]

4. ISO 13859. (2014) Determination of polycyclic aromatic hydrocarbons (PAH) by gas chromatography (GC) and high-performance liquid chromatography (HPLC) – ISO, 37 p.

5. EPA Method 8310 (1986). Polynuclear Aromatic Hydrocarbons – EPA, 13 p.

6. Reyes-Garcés N., Gionfriddo E., Gómez-Ríos G.A., Alam M.N., Boyacı E., Bojko B., Singh V., Grandy J., Pawliszyn J. (2018) Advances in Solid Phase Microextraction and Perspective on Future Directions // Analytical Chemistry, Vol. 90, Is. 1, P. 302–360.

7. Pino V., Ayala J.H., Afonso A.M., González V. Micellar microwave-assisted extraction combined with solid-phase microextraction for the determination of polycyclic aromatic hydrocarbons in a certified marine sediment // Analytica Chimica Acta. – 2003. – Vol. 477, Is. 1. – P. 81–91.

8. Wang Y., Zhang J., Ding Y., Zhou J., Ni L., Sun C. Quantitative determination of 16 polycyclic aromatic hydrocarbons in soil samples using solid-phase microextraction // Journal of Separation Science. – 2009. – Vol. 32, Is. 22. – P. 3951–3957.

9. Ghiasvand A.R., Hosseinzadeh S., Pawliszyn J. New cold-fiber headspace solid-phase microextraction device for quantitative extraction of polycyclic aromatic hydrocarbons in sediment // Journal of Chromatography A. – 2006. – Vol. 1124, Is. 1–2. – P. 35–42.

10. Martendal E., Carasek E. A new approach based on a combination of direct and headspace cold-fiber solid-phase microextraction modes in the same procedure for the determination of polycyclic aromatic hydrocarbons and phthalate esters in soil samples // Journal of Chromatography A. – 2011. – Vol. 1218, Is. 13. – P. 1707–1714.

11. Guo J., Jiang R., Pawliszyn J. Determination of polycyclic aromatic hydrocarbons in solid matrices using automated cold fiber headspace solid phase microextraction technique // Journal of Chromatography A. – 2013. – Vol. 1307. – P. 66–72.

12. Yiantzi E., Kalogerakis N., Psillakis E. Vacuum-assisted headspace solid phase microextraction of polycyclic aromatic hydrocarbons in solid samples // Analytica Chimica Acta. – 2015. – Vol. 890. – P. 108–116.

13. Kenessov B., Koziel J.A., Bakaikina N.V., Orazbayeva D. Perspectives and challenges of on-site quantification of organic pollutants in soils using solid-phase microextraction // Trends in Analytical Chemistry. – 2016. – Vol. 85. – P. 111–122.

14. Orazbayeva D., Kenessov B., Koziel J.A., Nassyrova D., Lyabukhova N.V. Quantification of BTEX in soil by headspace SPME–GC–MS Using combined standard addition and internal standard calibration // Chromatographia. – 2017. – Vol. 80, Is. 8. – P. 1249–1256.

15. Yegemova S., Bakaikina N.V, Kenessov B., Koziel J.A., Nauryzbayev M. Determination of 1-methyl-1H-1,2,4-triazole in soils contaminated by rocket fuel using solid-phase microextraction, isotope dilution and gas chromatography – mass spectrometry // Talanta. – 2015. – Vol. 143. – P. 226–233.

16. Orazbayeva D. Map of soil sampling for quantification of naphthalene [Electronic resource] available: https://goo.gl/vFLaH7 (Accessed: 06.01.2018).

IRSTI 31.25.15

*A.N. Imangaliyeva, G.A. Seilkhanova, A.Zh. Ondasheva, M.S. Telkhozhayeva

Al-Farabi Kazakh National University, Faculty of Chemistry and Chemical Technology,
Al-Farabi av. 71, 050040, Almaty, Kazakhstan
*e-mail: imangaly.ainur@gmail.com

Adsorption studies of Cu (II), Pb (II) and Cr (VI) by chitosan/unitiol composite

Abstract: Chitosan-unithiol composite for the first time was synthesized by simple and short period procedure. The sorption process was carried out under static conditions at temperature 298 K and at pH=4.5. The concentration of ions of toxic metals before and after sorption was determined by the atomic absorption method. The removal characteristics such as the removal degree and equilibrium time of Cu^{2+}, Pb^{2+} and Cr^{6+} were illustrated. The adsorption equilibrium for Cu^{2+} ions was best described by Langmuir model and for Pb^{2+} and Cr^{6+} ions by Freundlich model. It was found that adsorption of Cu^{2+} and Cr^{6+} by chitosan-unithiol followed first-order kinetics. Adsorption of Pb^{2+} was followed second-order kinetics. The sorption process was also investigated under co-presence of heavy metal ions. The obtained results indicate that the synthesized chitosan-unithiol composite is the effective sorbent for removing toxic metal ions.
Key words: sorption, composite, chitosan, unithiol, degree of removal.

Introduction

One is the main purpose of the adsorption of heavy metals is to find an effective modification method of material. The synthesized material has to be approach to several requirements such as low toxicity, high biocompatibility, adsorption capacity, selective sorption and the absence of side effects during the sorption [1]. In recent years the application of biomaterials such as algae, bacteria, fungi, high plants, and products derived from these organisms have represented big interest [2].

Chitosan is a natural polysaccharide widely used in fundamental studies as well as practical applications, including in treatment of wastewater, heterogeneous catalysts, delivery vaccines materials, agricultural stimulators, antibacterial agent and medical entersorbents [3; 4]. It consists of β-(1→4)-linked D-glucosamine and *N*-acetyl-D-glucosamine units. Chitosan is a well-known adsorbent for toxic and heavy metal ions. Due to the lone pair of electrons on nitrogen in acetoamido group and hydroxyl group can posse high chelating ability. Furthermore, the ability of chitosan depending on the acidity of the medium to form flaky precipitation can be used in sorption. For instant, in the recent years biosorbents based on chitosan has been synthesized and their sorption characteristics were studied for use in separation of heavy metal ions. Intoxication by heavy metal ions can lead to serious diseases of organism. These metal ions non-degradable and are persistent in the medium. Therefore chitosan has been applied in the synthesis various functional composites, by using clays, inorganic substances, natural and synthetic polymers [5].

In this way, a system which consists of chitosan and polyvinyl alcohol was studied. It was found that the adsorption efficiency of this sorbent has the maximum recovery of cadmium ions at pH = 6 and t = 40 C [6].

Also, in the work [7] the adsorption of composite material composed from chitosan and polyvinyl chloride was demonstrated. One of the advantages of this polymer is physical and chemical stability in organic solutions as well as in concentrated acidic and alkaline media. The study showed that the adsorption capacity of the chitosan and polyvinyl chloride system were 90% for Cu (II) and Ni (II) [7]. In the study [8] effect of modification by different compounds were illustrated. For instant, sorption activities of chitosan compounds were increased according to the following sequence: chitosan-cotton [9], [10], chitosan-magnetite [11], chitosan-cellulose [12], chitosan-perlite [13], chitosan-alginate [14; 15] and chitosan- clinoptilolite [16].

It is known that unithiol (2,3-dimercapto-1-propanesulfonic acid) is widely used in medicine as an

 Printed in Kazakhstan

antidote drug against heavy metal and radionuclide ions. Unithiol was found to have good solubility in water and strong chelation by virtue of sulfhydryl group [17]. Despite these additional features, unithiol has a disadvantage due to its high price.

Thus, using the positive features of both chitosan and unithiol materials, the novel chitosan-unithiol composite was synthesized. The sorption of heavy metal ions by chitosan-unithiol composite was investigated. This work was done with the purpose to establish the effect of concentration of metal ions and kinetics of sorption process. In our work was also shown the capability of chitosan-unithiol to sorb copper, lead and chromium ions during their simultaneous presence.

Materials and methods

Chitosan flakes with the deacetylation degree of about 85% and molecular weight of 300,000 produced from crab shells (Tokyo Chemical Industry UK Ltd) were used for experiments. Uniothiol in ampoules with a concentration of 50 mg/ml ("Belmed drugs", Belarus) were used as a modifier.

Preparation of chitosan-unithiol composite was carried out as follows:

An aqueous solution of chitosan was prepared by dissolving chitosan (0.25 g) in 5 ml of acetic acid (75 wt. %) for 30 min. And then 5 ml of H_20 and 5 ml of acetic acid (75 wt. %) were added in course of stirring. Chirosan after keeping 1 day at room temperature was put on 100 cm^3 solution of unithiol with concentration of 1 mg/ml.

All the experiments were carried out under bath conditions with solutions containing $CuCl_2$, $Pb(NO_3)_2$, $K_2Cr_2O_7$. Sorption was performed in 100 ml vessels by pouring metal ions containing solutions onto 1 g of chitosan-unithiol composite and occasional stirring.

The concentration of Cu (II) and Pb (II) before and after sorption was determined by the AAS method using an atomic absorption spectrophotometer "Shimadzu 6200". Cr (VI) concentrations were determined photometrically on the Specord 200 (Analytic Jena) at λ=530 nm using 1,5 -diphenylcarbazide as an indicator.

Results and discussion

The removal degree is an important characteristic because it shows efficiency of the sorbent. Sorption of Cu^{2+}, Pb^{2+} and Cr^{6+} ions by initial chitosan and unithiol-chitosan was investigated at 25 °C in the time interval from 0 to 180 min and results are provided in Figure 1. The addition of a modifier to the sorbent composition significantly increased the recovery of metal ions, practically reaching 100 %, while the initial chitosan recovered only about 80 % of the ions. On the course the time the initial concentration of metals was reduced. After 3 hours removal degree of ions were achieved the maximum extent. Hence 3 hours was found to be equilibrium sorption time.

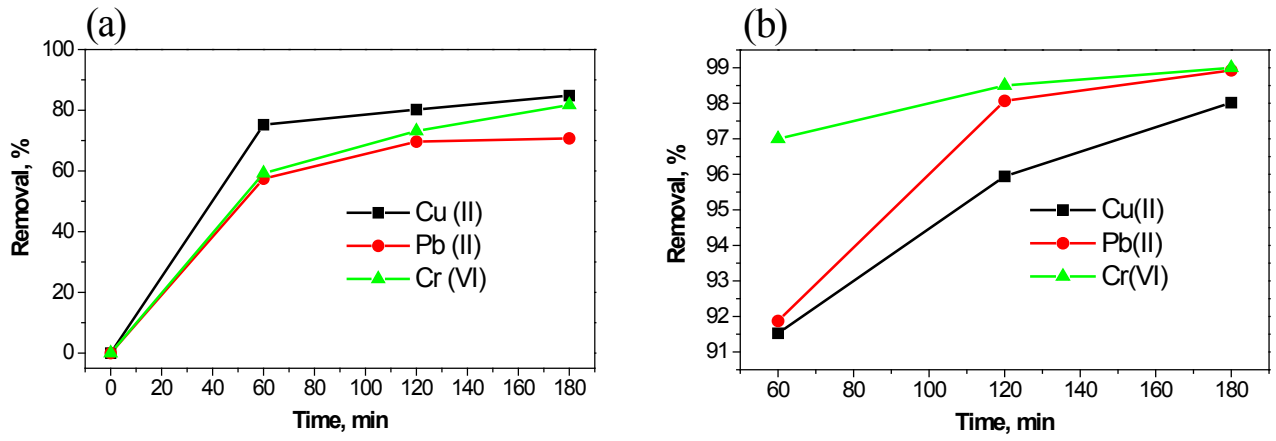

Figure 1 – Adsorption characteristics of (a) chitosan and (b) chitosan-unithiol composite for Cu (II), Pb (II) and Cr (VI) ions

Sorption isotherms can be used to determine the nature of the distribution of metal ions between the adsorbent and the liquid phase in a state of equilibrium, depending on their concentration. In this study, in order to describe adsorption of heavy metal ions by chitosan-unithiol were applied the Langmuir and Freundlich isotherms.

The linearised form of Langmuir model is:

$$\frac{C_e}{A} = \frac{1}{A_\infty K_L} + \frac{1}{A_\infty} C_e \quad (1)$$

where K_L – equilibrium adsorption constant ($l \cdot mg^{-1}$), A_∞ – limiting adsorption capacity ($mg \cdot g^{-1}$), A – adsorption ($mg \cdot g^{-1}$) and C_e – metal ion concentration in the solution at equilibrium ($mg \cdot l^{-1}$).

Freundlich's isotherm is an empirical equation that describes heterogeneous systems. The Freundlich model can be expressed by:

$$ln A = ln K_F + \frac{1}{n} ln C_e \quad (2)$$

where K_F ($(mg \cdot g^{-1})(l \cdot g^{-1})^n$) is indicative of the relative sorption capacity and $1/n$ – is measure of the nature of the sorption, A- adsorption ($mg\ g^{-1}$) and C_e – metal ion concentration in the solution at equilibrium ($mg \cdot l^{-1}$).

On the Table 1 was illustrated the constant values for the corresponding sorption isotherms (Figure 2), calculated according to the Langmuir and Freundlich theories. According to the results, reported in Table 1, Langmuir equation best described the sorption of Cu (II) ions (correlation coefficients R^2=0.934). Therefore, according to the literature [19], all the sorbed particles interact only with the sorption centers and do not contact each other. For Pb (II) and Cr (VI) ions according to the regression coefficients proved that correlation of Freundlich model was strong with respect to the Langmuir model.

In the present work, pseudo-first-order and pseudo-second-order kinetic models were used to check the experimental data. The pseudo-first-order and pseudo-second-order models were described by the following equations:

$$lnC_t = lnC_0 - k_1 t \quad (3)$$

$$\frac{1}{C_t} = \frac{1}{C_t} + k_2 t \quad (4)$$

where C_0 – initial concentration of metal ions, C_t – concentration of metal ions at time t. k_1 (min^{-1}) and k_2 ($ml\ mg^{-1}\ min^{-1}$) are rate constants.

Table 1 – Parameters of adsorption isotherms

Metal ions	pH	Langmuir isotherm			Freundlich isotherm		
		K_L ($l\ mg^{-1}$)	A∞ ($mg\ g^{-1}$)	R^2	K_F $(mg\ g^{-1})(l\ g^{-1})^n$	1/n	R^2
Cu (II)	4.5	53.94	1.03	0.934	1.74	0.31	0.765
Pb (II)	4.5	13.00	1.71	0.641	3.70	0.62	0.779
Cr (VI)	4.5	2.54	1.44	0.866	1.16	0.54	0.874

The constants were calculated from the slope and the intercept of the plots are given in Table 2 and Figure 3. The results are given in Table 2 illustrate that for both Cu (II) and Cr (VI) ions, the R^2 values (R^2 = 0.999 and 0.983) for pseudo-first-order model higher than results obtained using pseudo-second-order model (R^2=0.950 and 0.892). Thus, the pseudo-first-order model explains the kinetics better. But kinetics of sorption Pb (II) ions is better described by pseudo-second-order model (R^2 = 0.941). Heavy metals such as lead, copper, chromium are poisons for the body. They enter the human body not only in an individual form, but also in the joint presence of metals. Getting into the human body, they cause symptoms of poisoning: headache, vomiting, convulsions. Therefore, in this paper, the sorption process was studied in the joint presence of the Cu (II), Pb (II) and Cr (VI) ions, the result of which is given below.

Thus, the results of sorption show that the degree of chromium removal was reached 90%. Hence, this composite proved to be effective in the removal of chromium ions.

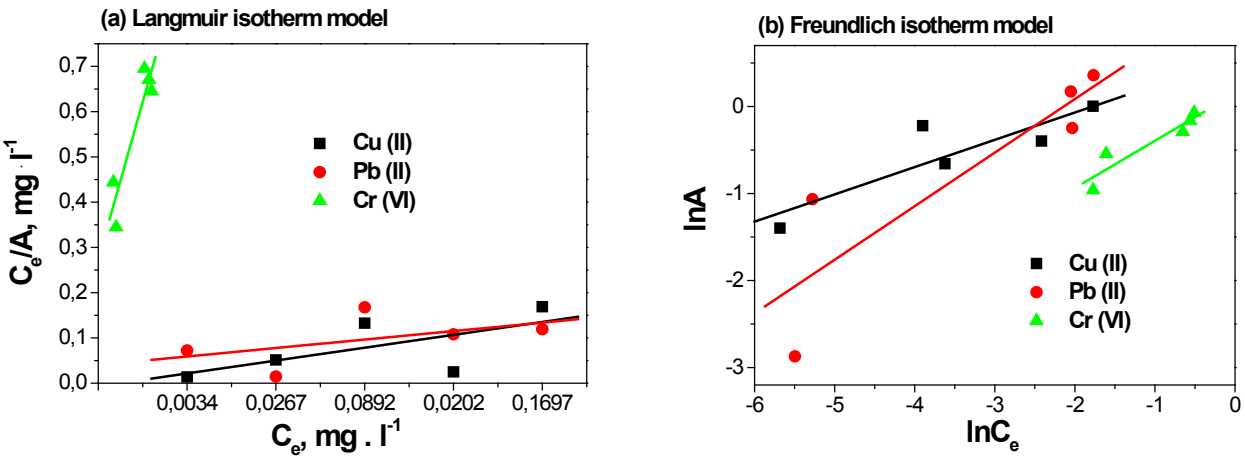

Figure 2 – (a) Langmuir and (b) Freundlich isotherm adsorption model of the Cu (II), Pb (II) and Cr (VI)

Table 2 – Kinetic characteristics of adsorption of metal ions

Metal ion	Pseudo-first-order kinetic model			Experimental value	Pseudo-second-order kinetic model		
	C_0 (mg/l)	k_1 (min^{-1})	R^2	C_0 (mg/l)	C_0 (mg/l)	k_2 (l mg^{-1} min^{-1})	R^2
Cu (II)	6.13	0.014	0.999	5.21	0.04	0.618	0.950
Pb (II)	4.44	0.003	0.918	7.94	0.25	0.025	0.941
Cr (VI)	6.24	0.015	0.983	2.00	0.03	0.694	0.892

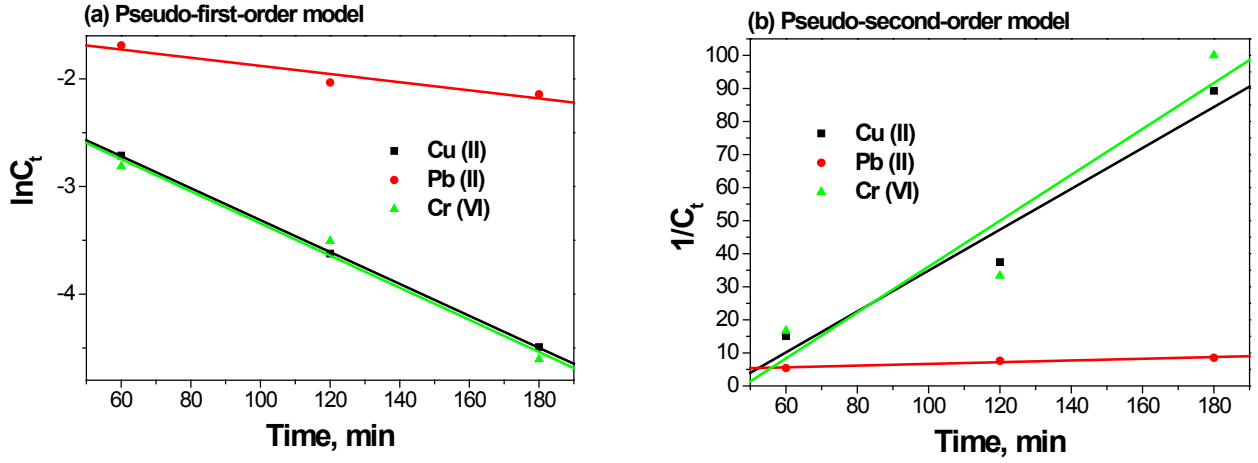

Figure 3 – Plots of (a) pseudo-first-order and (b) pseudo-second-order kinetics of sorption by chitosan-unithiol composite

Table 3 – The results of sorption at a joint presence of metal ions

Metal ions	Removal, %	Adsorption capacity, mg/g
Cu (II)	25	$2.5\ 10^{-4}$
Pb (II)	30	$11.4\ 10^{-4}$
Cr (VI)	90	$40.5\ 10^{-4}$

Conclusion

In the present work, synthesis of a sorbent based on chitosan and unithiol for the first time was reported. Analysis of the sorption characteristics of the obtained composite showed a significant increasing of adsorption. The removal degrees of Cu (II), Pb (II), and Cr (VI) ions were equal to 98%, 99% and 99%, respectively. It was found that the Langmuir isotherm better describes the sorption of Cu (II) ions than the Freundlich isotherm, which indicates the formation of a monomolecular sorption layer. Freundlich isotherm displayed a better fitting model than Langmuir isotherm for adsorption of Pb (II) and Cr (VI). The kinetic process can be predicted by pseudo-first-order model and rate constants for Cu^{2+} and Cr^{6+} sorption were found to be 0.014 and 0.015 min^{-1}, respectively at 25°C. Adsorption of Pb^{2+} was followed second-order kinetics and rate constant were equal to 0.025 l mg^{-1} min^{-1}. The effect of sorbent on the joint presence of heavy metal ions showed high sorption properties respect to Cr (VI) ions. The removal degrees are Cr^{6+} – 90%, Pb^{2+}- 30%, Cu^{2+}-25%. The obtained results show that this material is a highly effective composite for the removal of toxic metal ions.

Acknowledgments

This work was supported by the grant of Ministry of Education and Science of Republic of Kazakhstan 3444/GF4 “Scientific bases development of phosphorus-containing compounds obtained on the basis of technogenic mineral raw materials”.

References

1. Saravanan D., Hemalatha R., Sudha P. N., Synthesis and characterization of cross linked chitin / bentonite polymer blend and adsorption studies of Cu (II) and Cr (VI) on chitin // Der Pharma Chem. – 2011. – 3(6). – P. 406–423.

2. Domszy J.G., Roberts G.A.F. Evaluation of infrared spectroscopic techniques for analysing chitosan // Makromolecular Chemie. – 1985. – 186(8). – P. 1671–1677.

3. Raghavendra G. M., Jung J., Kim D., J. Seo Chitosan-mediated synthesis of flowery-CuO , and its antibacterial and catalytic properties // Carbohydr. Polym. – 2017. – 172. – P.78–84.

4. Gyliene O., Binkiene R., Baranauskas M., Mordas G., Plauškaite K., and Ulevičius V. Influence of dissolved oxygen on Fe(II) and Fe(III) sorption onto chitosan // Colloids Surfaces A Physicochem. Eng. Asp. – 2014. – 461(1). – P. 151–157.

5. Wang Jianlong, Chen Can Chitosan-based biosorbents: Modification and application for biosorption of heavy metals and radionuclides // Bioresour. Technol. – 2014. – 160. – P. 136–140.

6. Bingjie Liu, Dongfeng Wang, Guangli Yu, Xianghong Meng Adsorption of heavy metal ions, dyes and proteins by chitosan composites and derivatives – a review // J. Ocean Univ. China. – 2013. – 12. – P. 500–508.

7. Popuri S. R., Vijaya Y., Boddu V. M., Abburi K. Adsorptive removal of copper and nickel ions from water using chitosan coated PVC beads // Bioresour. Technol. – 2009. – 100. – P. 194–199.

8. Rinaudo M. Chitin and chitosan: properties and applications // Prog. Polym. Sci. – 2006. – 31. – P. 603–632.

9. Solovtsova O.V., Grankina T.Y., Krasilnikova O.K., Serebriakova N.V., Shinkarev S. M. Absorption methods of copper cations using lyophilized chitosan // Prot. Met. Phys. Chem. Surfaces. – 2009. – 45(1). – P. 36–41.

10. Wan Ngah W., Teong L., Hanafiah M. Adsorption of dyes and heavy metal ions by chitosan composites: a review // Carbohydr. Polym. – 2011. – 83(4). P. 1446–1456.

11. Tran H.V., Tran L.D., Nguyen T.N. Preparation of chitosan/magnetite composite beadsand their application for removal of Pb(II) and Ni(II) from aqueous solution // Material Sci. and Eng. – 2010. – 30. – P. 304–310.

12. Sun X., Peng B., Ji Y., Chen J., Li D. Chitosan(chitin)/cellulose composite biosorbents prepared using ionic liquid for heavymetal ions adsorption // Separations. – 2008. – 55. – P. 2062–2069.

13. Kalyania S., Ajitha Priyaa J., Srinivasa Raoa P., Krishnaiah A. Removal of copper and nickel from aqueous solutions using chitosan coated on perlite as biosorbent // Separation Sci. and Technol. – 2000. – 40. – P. 1483–1495.

14. Vijayaa Y., Popurib S.R., Bodduc V.M., Krishnaiaha A. Modified chitosan and calcium alginate biopolymer sorbents for removal of nickel (II) through adsorption // Carbohydr. Polym. – 2008. – 72. – P. 261–271.

15. Wan Ngah W.S., Fatinathan S. Adsorption of Cu (II) ions in aqueous solution using chitosan beads, chitosan–GLA bead sand chitosan–alginate beads // Chem. Eng. Journal. – 2008. – 143. – P. 62–72.

16. Dragan E.S., Dinu M.V., Timpu D. Preparation and characterization of novel composites based on chitosan and clinoptilolite with enhanced adsorption properties for Cu^{2+} // Bioresour. Technol. – 2010. – 101. – P. 812–817.

17. Yablokov V. E., Ishchenko N. V., Alekseev S. A. Sorption preconcentration of cadmium and lead ions as complexes with unithiol on a silica surface modified by quaternary ammonium salt groups // J. Anal. Chem. – 2013. – 68 (3). – P. 206–211.

18. Green-Ruiz C., Rodriguez-Tirado V., Gomez-Gil B., Cadmium and zinc removal from aqueous solutions by Bacillus jeotgali: pH, salinity and temperature effects // Bioresour. Technol. – 2008. – 99. – P. 3864–3870.

19. Dang V.B.H., Doan H.D., Dang-Vu T., Lohi A.Equilibrium and kinetics of biosorption of cadmium (II) and copper (II) ions by wheat straw // Bioresour. Technol. – 2009. – 100. – P. 211–219.

IRSTI 31.27.31; 34.15.23; 34.15.25; 76.03.31; 76.29.49

[1*]D.E. Aisina, [1]A.T. Ivashchenko, [1]R.E. Niyazova, [1]S.A. Atambayeva, [2]E.N. Imyanitov

[1]Laboratory of Biotechnology, Almaty, Kazakhstan
[2]N.N. Petrov National Medical Research Center of Oncology, St. Petersburg, Russia
[*]e-mail: dana.aisina03@gmail.com

Characteristics of interaction of miRNA with mRNA of breast cancer candidate genes

Abstract: To establish associations of miRNAs with their target genes, the binding characteristics of miRNAs with mRNAs of candidate genes of various subtypes of breast cancer have been determined. The binding characteristics of miRNAs with mRNAs in 5'UTR, CDS and 3'UTR were found using the MirTarget program. Of the 600 genes involved in the development of breast cancer, 33 genes specific for the triple negative subtype, 16 genes specific for the luminal A, B subtype and 28 genes specific for the her2 subtype. For the triple negative subtype of breast cancer, *CBL, DRAM1, FGFR2, LAMC1, MMP2, NTRK2, PFN1, PTGS2, PRRT2, RAB5A* genes can be characterized as candidate target genes for miRNAs which binding sites are located in the 5'UTR. Candidate genes for binding miRNAs in the CDS are *JHDM1D, RUNX1* and in the 3'UTR – *RUNX1*. In the luminal A,B subtype of breast cancer, candidate genes for binding miRNAs in the 5'UTR are *FOXA1, GTF2IRD1, HMGA2, ITGA6, MAPT, SMAD3, TGFB1*. Candidate genes for binding miRNAs in the CDS are *FOXA1, ITGB1, SOX4* and in the 3'UTR – *SMAD3, TGFB1*. For the her2 subtype of breast cancer, candidate genes for binding miRNAs in the 5'UTR are *A4GALT, EPOR, MAZ, NISCH* and *RAD21*. Candidate genes for miRNA binding in the CDS are *EPOR, MAPK3, MAZ, NHS, RYR1* and in the 3'UTR – *H2AFX*. Based on the obtained characteristics of miRNA interaction with mRNA of candidate genes, associations of miRNA with mRNA have been proposed for use in the diagnosis of breast cancer subtypes.
Key words: miRNA, mRNA, genes, subtypes, breast cancer.

Introduction

Breast cancer (BC) is the leading cause of death in women and is the most common type of cancer. Although advances in the diagnosis and treatment of breast cancer have greatly reduced its incidence and mortality, there are still 500,000 breast cancer deaths per year worldwide [1; 2]. Annually more than 500 thousand cases of disease are registered in the world, as a rule, at the stage of expressed morphological signs. The disease proceeds in different forms, which differ in the degree of aggression, the rate of cell proliferation, invasiveness, the ability to metastasis, etc. The characteristics of each form of disease are the basis for the application of different treatment methods. The success of treatment depends on the correct diagnosis of subtype of the disease. The disturbance of the gene expression which determines the subtype of the disease lies on the basis of all subtypes of the disease. Therefore, in recent years, it is actively searched for genes involved in oncogenesis, taking into account the characteristics of subtypes. This task is extremely difficult, since even one or more genes causing disease interact with many other genes and molecular factors, from which it is difficult to identify the contribution of each participant of oncogenesis. Therefore, the primary interest in oncogenesis lies in the establishment of molecular bases for the initial stages of oncogenesis, when the participants in this process are still few. Currently, more than 600 genes involved in the development of breast cancer are known, of which we have chosen genes based on literature sources, which, according to the authors of the publications, are involved in the development of specific subtypes of breast cancer.

Among the low-molecular factors involved in the regulation of gene expression, miRNAs are actively studied. These molecules directly or indirectly regulate the expression of almost genes of the human genome. The miRNAs predominantly control the expression of transcription factor genes and protein genes involved in signaling systems. Many publications focus on the role of miRNAs in the development of breast cancer. However, the interaction of

 Printed in Kazakhstan

miRNAs with mRNA genes determining subtypes of breast cancer has been little studied. In this regard, the aim of our study was to establish associations of miRNAs and their target genes that can be used as molecular markers for the definition of subtypes of BC.

Materials and methods

The nucleotide sequences of candidate genes of the BC subtypes were downloaded from GenBank (http://www.ncbi.nlm.nih.gov). The miRNA nucleotide sequences were downloaded from miRBase database (http://www.mirbase.org). The MirTarget program [3] was used to search for binding sites, free energy of binding (ΔG), and interaction schemes. The value of ΔG/ΔGm was used as a comparative quantitative criterion of the interaction strength of miRNA with mRNA, where ΔGm is equal to the free energy of miRNA binding with a completely complementary nucleotide sequence. The MirTarget program calculates the ratio ΔG/ΔGm, determines the location of microRNA site in the 5'-untranslated region (5'UTR), in the protein-coding region (CDS) or in the 3'-untranslated region (3'UTR). Table 1 shows list of miRNAs interacting with candidate genes of breast cancer subtypes. Table 2 shows sources of information on candidate genes of breast cancer subtypes which were targeted for miRNAs from miRBase.

Results and discussion

Characteristics of miRNAs interaction with mRNAs of candidate genes of the triple negative subtype

The ANXA3 protein is a member of calcium-dependent phospholipid-binding proteins and is involved in proliferation, apoptosis, development, migration of metastasis, and invasion of breast cancer cells [4]. The mRNA gene of *ANXA3* gene has binding sites for two miRNAs in the 5'UTR (Table 3), which helps stop protein synthesis before the start of the translation. The mRNA of ASAH1 gene contains two miRNA binding sites in the 5'UTR. ATM and AXL genes are targets for one miRNA and their binding sites are located in the 5'UTR, respectively. The mRNA of BIRC5 gene contains binding sites for two miRNAs located in the 5'UTR starting at one position (Table 3). Therefore, identical nucleotide sequences of binding site could interact with different miRNAs.

Table 1 – List of miRNAs interacting with candidate genes of breast cancer subtypes

Triple-negative (basal-like) subtype: miR-1-1093-3p; miR-1-1101-3p; miR-1-155-3p; miR-1-163-3p; miR-1-1819-3p; miR-1-1922-3p; miR-1-2121-3p; miR-1-2180-3p; miR-1-2228-3p; miR-1-2558-3p; miR-1-3554-3p; miR-1-4241-5p; miR-1-875-3p; miR-2-3313-3p; miR-2-3962-5p; miR-2-4005-5p; miR-2-4119-3p; miR-2-4804-5p; miR-2-5355-3p; miR-2-5674-3p; miR-2-6166-5p; miR-2-6328-5p; miR-2-6862-5p; miR-2-7434-3p; miR-2-7838-5p; miR-3-10329-5p; miR-3-10870-3p; miR-3-7886-3p; miR-3-8100-5p; miR-3-8242-5p; miR-3-9317-3p; miR-4-11437-3p; miR-4-11565-3p; miR-4-11828-5p; miR-4-12861-5p; miR-5-14114-5p; miR-5-14202-5p; miR-5-14959-3p; miR-5-15432-3p; miR-5-15564-3p; miR-5-15733-3p; miR-5-15926-3p; miR-5-16438-3p; miR-5-17240-3p; miR-6-12155-5p; miR-6-16980-5p; miR-6-17815-3p; miR-6-17875-3p; miR-6-18496-3p; miR-7-18337-3p; miR-7-19239-3p; miR-7-20203-3p; miR-7-20411-3p; miR-7-20752-3p; miR-7-21068-3p; miR-7-21133-5p; miR-7-21139-3p; miR-7-22377-3p; miR-8-21445-5p; miR-8-21978-5p; miR-8-23953-5p; miR-9-20317-3p; miR-9-23270-3p; miR-9-23803-5p; miR-9-23969-3p; miR-9-24743-3p; miR-9-25082-3p; miR-9-25335-5p; miR-9-25681-5p; miR-9-25955-3p; miR-9-27797-5p; miR-9-28523-5p; miR-10-11641-3p; miR-10-12491-5p; miR-10-13655-3p; miR-10-16862-5p; miR-10-26483-5p; miR-11-29461-3p; miR-11-29831-3p; miR-11-29998-3p; miR-12-17092-3p; miR-13-32613-3p; miR-13-34600-3p; miR-13-35476-3p; miR-14-35161-5p; miR-14-35446-5p; miR-15-16874-3p; miR-16-35004-5p; miR-16-36024-3p; miR-16-36548-3p; miR-16-36971-3p; miR-16-37915-3p; miR-16-38416-3p; miR-16-38458-3p; miR-16-38712-3p; miR-16-40163-5p; miR-17-10097-3p; miR-17-12514-5p; miR-17-39143-3p; miR-17-39416-3p; miR-17-39440-3p; miR-17-39753-3p; miR-17-39859-5p; miR-17-40012-5p; miR-17-41183-5p; miR-18-39953-5p; miR-18-40163-3p; miR-18-41189-3p; miR-19-30988-5p; miR-19-33623-3p; miR-19-34067-3p; miR-19-41131-3p; miR-19-41746-3p; miR-19-41910-5p; miR-19-42189-5p; miR-19-42710-3p; miR-19-42772-5p; miR-19-43342-3p; miR-19-43662-5p; miR-19-43860-3p; miR-19-43963-5p; miR-19-44540-3p; miR-20-41939-3p; miR-20-43555-5p; miR-20-44079-5p; miR-20-44999-3p; miR-20-45152-5p; miR-20-45753-5p; miR-21-45132-5p; miR-21-45324-5p; miR-22-23987-3p; miR-22-46461-3p; miR-22-46522-5p; miR-X-13195-3p; miR-X-20136-3p; miR-X-25977-5p; miR-X-45905-3p; miR-X-46422-5p; miR-X-46723-3p; miR-X-47540-3p; miR-X-48174-3p

Luminal A,B subtypes: miR-1-1510-5p; miR-1-155-3p; miR-1-1714-3p; miR-1-1819-3p; miR-1-1904-5p; miR-1-1922-3p; miR-1-2121-3p; miR-1-265-3p; miR-1-275-3p; miR-1-3037-5p; miR-1-3554-3p; miR-1-356-5p; miR-2-2621-5p; miR-2-3313-3p; miR-2-4697-3p; miR-2-4782-5p; miR-2-4826-5p; miR-2-5674-3p; miR-2-7331-5p; miR-2-8239-5p; miR-2-8257-5p; miR-3-6515-3p; miR-3-7886-3p; miR-3-8100-5p; miR-3-9441-3p; miR-3-9461-3p; miR-4-11009-3p; miR-4-11421-3p; miR-4-11437-3p; miR-4-12154-5p; miR-4-13460-3p; miR-4-6496-3p; miR-5-14114-5p; miR-5-14202-5p; miR-5-14873-3p; miR-5-15432-3p; miR-5-15733-3p; miR-5-3563-5p; miR-5-6716-5p; miR-5-8853-5p; miR-6-12155-5p; miR-6-16980-5p; miR-7-15849-3p; miR-7-20142-5p; miR-7-20203-3p; miR-7-20411-3p; miR-7-21249-3p; miR-8-19447-3p; miR-8-21162-5p; miR-8-21445-5p; miR-8-23353-3p; miR-8-23953-5p; miR-8-24549-5p; miR-9-13610-3p; miR-9-20317-3p; miR-9-25846-3p; miR-9-26042-5p; miR-9-26255-5p; miR-9-27181-5p; miR-9-27797-5p; miR-9-5204-5p; miR-10-13655-3p; miR-10-26214-5p; miR-10-26423-3p; miR-10-26528-5p; miR-10-26815-5p; miR-10-28986-3p; miR-11-28041-3p; miR-11-29077-3p; miR-11-29827-3p; miR-11-31496-5p; miR-12-17704-3p; miR-12-26632-3p; miR-12-29625-3p; miR-12-30075-3p; miR-12-30416-5p; miR-12-31544-5p; miR-12-32764-3p; miR-12-32997-5p; miR-12-33279-5p; miR-12-33610-3p; miR-14-35670-5p; miR-15-11315-5p; miR-15-31763-5p; miR-15-32047-5p; miR-15-33256-3p; miR-15-36925-3p; miR-15-38620-5p; miR-16-13062-5p; miR-16-20199-5p; miR-16-36024-3p; miR-16-36745-3p; miR-16-40261-3p; miR-17-38733-3p; miR-17-39011-3p; miR-17-39023-3p; miR-17-39273-3p; miR-17-40081-5p; miR-17-40348-5p; miR-17-40711-5p; miR-17-40968-3p; miR-17-41168-3p; miR-18-39953-5p; miR-18-41332-3p; miR-18-41949-5p; miR-19-21199-3p; miR-19-30988-5p; miR-19-33623-3p; miR-19-41131-3p; miR-19-42772-5p; miR-19-42853-3p; miR-19-43315-5p; miR-19-43351-3p; miR-19-43373-3p; miR-19-43614-3p; miR-19-43966-3p; miR-19-44127-3p; miR-19-44540-3p; miR-19-9434-3p; miR-20-22562-3p; miR-20-43381-5p; miR-20-43873-3p; miR-20-45152-5p; miR-20-45753-5p; miR-22-16963-5p; miR-22-23987-3p; miR-22-46979-5p miR-X-13195-3p; miR-X-25977-5p; miR-X-48174-3p
Her2 subtype: miR-1-155-3p; miR-1-1630-3p; miR-1-163-3p; miR-1-1852-5p; miR-1-2121-3p; miR-1-2372-3p; miR-1-2597-5p; miR-1-2802-3p; miR-1-3554-3p; miR-1-356-5p; miR-1-3919-5p; miR-2-3313-3p; miR-2-4733-3p; miR-2-6809-5p; miR-2-7331-5p; miR-2-8257-5p; miR-3-4734-5p; miR-3-7886-3p; miR-3-8100-5p; miR-4-11421-3p; miR-4-11828-5p; miR-4-11923-3p; miR-4-12861-5p; miR-4-6496-3p; miR-5-12460-5p; miR-5-13733-5p; miR-5-14114-5p; miR-5-15026-5p; miR-5-15432-3p; miR-5-15733-3p; miR-5-16562-3p; miR-5-17008-3p; miR-5-17494-5p; miR-5-3563-5p; miR-5-6716-5p; miR-6-12155-5p; miR-6-17519-3p; miR-6-17811-3p; miR-7-12728-5p; miR-7-16350-5p; miR-7-21068-3p; miR-7-21142-5p; miR-7-21249-3p; miR-8-21445-5p; miR-8-21978-5p; miR-8-23986-3p; miR-9-20317-3p; miR-9-22187-3p; miR-9-23270-3p; miR-9-23969-3p; miR-9-25917-3p; miR-9-26042-5p; miR-9-26506-3p; miR-9-27797-5p; miR-10-13655-3p, miR-10-27682-5p; miR-10-28986-3p; miR-10-8412-5p miR-11-27076-3p; miR-11-28204-5p; miR-11-28656-5p; miR-11-29077-3p; miR-11-29324-3p; miR-11-29461-3p; miR-11-29998-3p; miR-12-17092-3p; miR-12-30578-5p; miR-12-31544-5p; miR-12-31979-3p; miR-12-32764-3p; miR-12-33610-3p; miR-13-32368-5p; miR-13-32613-3p; miR-13-33774-5p; miR-13-35476-3p; miR-14-15069-5p; miR-14-31624-3p; miR-14-35161-5p; miR-14-36092-3p; miR-15-32047-5p; miR-15-33256-3p; miR-15-36862-3p; miR-15-38560-5p; miR-16-20406-3p; miR-16-33136-3p; miR-16-36024-3p; miR-17-25894-5p; miR-17-39313-3p; miR-17-39440-3p; miR-17-39593-3p; miR-17-40081-5p; miR-17-40348-5p; miR-18-39953-5p; miR-18-41189-3p; miR-19-21199-3p; miR-19-25044-3p; miR-19-28028-5p; miR-19-30988-5p; miR-19-33623-3p; miR-19-36095-3p; miR-19-41131-3p; miR-19-42218-3p; miR-19-42224-5p; miR-19-43329-3p; miR-19-43644-3p; miR-19-43966-3p; miR-19-44540-3p; miR-20-22562-3p; miR-20-42898-3p; miR-20-43381-5p; miR-20-43646-5p; miR-20-43873-3p; miR-20-44980-3p; miR-20-45152-5p; miR-20-45753-5p; miR-22-16963-5p; miR-22-45335-5p; miR-22-45834-5p; miR-22-46522-5p; miR-22-46603-5p; miR-22-46979-5p; miR-X-13195-3p; miR-X-48174-3p; miR-X-48265-3p

Table 2 – List of candidate genes of subtypes of breast cancer

Triple-negative (basal-like) subtype: *ANXA3* (doi: 10.1016/j. clbc.2017.11.009)*;* *ASAH1 (doi:10.1158/1078-0432.CCR-06-1109); ATM* (doi: 10.1007/s40262-017-0587-4); *AXL* (doi: 10.1155/2017/1686525); *BIRC5* (doi: 10.1186/1756-9966-31-58); *CBL* (doi: 10.1073/pnas.1300873110); *CD44* (doi: 10.1093/protein/gzx063); *CEACAM5 (CEA)* (doi: 10.1016/j.cca.2017.04.023); *DRAM1 (doi: 10.1016/j.febslet.2012.12.027);* *ERBB3* (doi: 10.18632/oncotarget.13284); *FGFR2* (doi: 10.1007/s00428-016-1950-9); *FH* (doi: 10.2147/OTT.S101677)*; FIS1 (LINC01554)* (doi: 10.1186/bcr3588); *IL11* (doi: 10.1371/journal.pone.0037361); *JHDM1D(KDM7A)* (doi: 10.1002/ijc.27629); *LAMC1* (doi: 10.1016/j.molonc.2012.03.003); *LASP1* (doi: 10.1186/1756-9966-31-58); *MAGEA10* (doi: 10.1016/j.acthis.2014.01.003); *MDK (doi: 10.1007/s13277-015-3710-x)*; *MMP2* (doi: 10.1038/srep28623); *MTCH2* (doi: 10.1016/j.ajpath.2013.02.046); *MTSS1 (doi: 10.1371/journal.pone.0074525)*; *MYL9 (doi: 10.1002/ijc.27629)*; *NTRK2* (doi: 10.1186/bcr2867); *PARP1* (doi: 10.1016/j.yexcr.2017.12.032); *PFN1* (doi: 10.1080/15384101.2017.1346759); *PTGS2* (doi: 10.1073/pnas.1709119114); *PRRT2 (PKC)* (doi: 10.1002/cmdc.201700640); *RAB5A (doi: 10.3390/ijms17040443)*; *RUNX1* (doi: 10.1016/j.ebiom.2016.04.032); *SERPINE1 (PAI1)* (doi: 10.1186/1471-2407-13-268); *SFN* (doi: 10.1073/pnas.1315022110); *STMN1* (doi: 10.3892/ijo.2017.4085).

Luminal A,B subtype: *ANGPTL4* (doi: 10.1038/ncb2672)*; EZH1* (doi: 10.1371/journal.pgen.1002751); *FOXA1* (doi: 10.1038/modpathol.2017.107); *GTF2IRD1* (doi: 10.2353/ajpath.2010.090837); *HMGA2* (doi: 10.1371/journal.pgen.1002751); *ITGA6* (doi: 10.1038/ncb2672); *ITGB1* (doi: 10.1080/15548627.2016.1213928); *JAK1* (doi: 10.1371/journal.pgen.1002751); *LOX* (doi: 10.3390/ijms18122775); *MAP3K14 (doi: 10.1186/bcr3683); MAPT* (doi: 10.1007/s00428-012-1357-1); *MCM7* (doi: 10.1371/journal.pgen.1002751); *SMAD3* (doi: 10.1074/jbc.M113.506535); *SOX4* (doi: 10.1371/journal.pgen.1002751); *TGFB1 (TGFB)* (doi: 10.1038/ncb2672); *TNC (doi: 10.2147/IJN.S56070)*.
Her2 subtype: *A4GALT (PMID: 24324107); ACSS2 (doi: 10.1186/ar4486.); ADAM10* (doi: 10.1038/s41598-016-0013-4)*; ADAM17* (doi: 10.1016/j.acthis.2011.03.009); *AURKA* (doi: 10.1038/s41523-017-0049-z); *BRCA2* (doi: 10.1155/2016/5718104); *BRIP1* (doi: 10.18632/oncotarget.7027); *CDK2* (doi: 10.1093/annonc/mdr340); *CDK6* (doi: 10.2147/BCTT.S150540); *EPOR* (doi: 10.1007/s10549-012-2316-x); *EPO* (doi: 10.5114/aoms.2016.62723)*; ERBB3 (HER3)* (doi: 10.18632/oncotarget.22027); *FKBPL* (doi: 10.1038/s41523-017-0049-z)*; GTF2E1 (doi: 10.1186/1471-2407-11-140); H2AFX (H2AX)* (doi: 10.18632/oncotarget.2259); *KDM5D (doi: 10.1021/mp5007618); MAPK3 (ERK1)* (doi: 10.1016/j.bbrc.2017.06.001); *MAZ* (doi: 10.1371/journal.pone.0026122); *NHS (doi: 10.1002/jlcr.3287); NISCH* (doi: 10.1016/j.artmed.2016.10.003); *PARP1* (doi: 10.1053/j.seminoncol.2017.06.006)*; RAD21* (doi: 10.1186/bcr3176)*; RASSF1* (doi: 10.18632/oncotarget.4062)*; RPLP2 (doi: 10.1038/onc.2011.584.); RYR1 (HUON.2006.50.4.0349); STAR (doi: 10.1016/j.ajpath.2014.12.018); TIMP3* (doi: 10.1016/j.humpath.2011.12.022), *TNF* (doi: 10.17219/acem/62120).
Notes: In parentheses, sources of information of candidate genes of breast cancer subtypes

Table 3 – Characteristics of miRNAs binding with mRNAs of candidate genes of the triple negative subtype

ANXA3: miR-20-43555-5p, 56, -119, 88, 22; miR-16-38458-3p, 94, -121, 86, 24
ASAH1: miR-20-44079-5p, 17, -119, 89, 22; miR-19-42772-5p, 232, -121, 85, 23
ATM: miR-7-21133-5p, 9777**, -121, 89, 24
AXL: miR-17-39143-3p, 2690*, -119, 86, 24
BIRC5: miR-16-35004-5p, 110, -125, 89, 23; miR-16-36548-3p, 110, -125, 89, 23
CBL: miR-9-20317-3p (6), 12 ÷ 28, -127 ÷ -140, 86 ÷ 94, 24; miR-18-39953-5p (4), 15 ÷ 24, -123, 85, 23; miR-16-33136-3p (4), 16 ÷ 25, -117, 86, 22; miR-5-15733-3p (5), 16 ÷ 34, -127 ÷ -138, 86 ÷ 93, 24; miR-17-39416-3p (4), 17 ÷ 26, -121, 92, 22; miR-5-15564-3p, 27, -123, 89, 22; miR-X-48174-3p (2), 28 ÷ 31, -121, 85, 24; miR-1-1819-3p, 32, -125, 91, 23; miR-16-38712-3p, 174*, -123, 85, 24; miR-11-29461-3p, 176*, -125, 89, 23; miR-2-4804-5p, 7728**, -117, 93, 24
CD44: miR-16-40163-5p, 129, -121, 90, 23; miR-5-14959-3p, 352, -121, 85, 24; miR-1-2180-3p, 359, -121, 89, 22; miR-X-25977-5p, 362, -119, 87, 22
CEACAM5: miR-7-21133-5p, 3220**, -119, 87, 24; miR-17-39753-3p (2), 3223÷ 3267**, -115 ÷ -117, 87 ÷ 89, 21
DRAM1: miR-20-45753-5p, 57, -121, 89, 22; miR-19-30988-5p, 62, -123, 85, 23; miR-X-13195-3p, 73, -123, 87, 23; miR-14-35446-5p, 302, -121, 85, 24; miR-9-25335-5p, 410, -119, 89, 22
ERBB3: miR-3-8100-5p, 148, -125, 86, 24
FGFR2: miR-17-41183-5p, 37, -119, 86, 23; miR-4-11437-3p, 38, -121, 86, 23; miR-18-39953-5p, 42, -123, 85, 23; miR-19-41131-3p, 43, -123, 85, 23; miR-7-21139-3p, 48, -132, 89, 24; miR-11-29831-3p, 55, -129, 86, 24; miR-19-34067-3p, 60, -123, 92, 23; miR-1-2228-3p, 152, -125, 89, 24
FH: miR-14-35446-5p, 96*, -121, 85, 24
FIS1: miR-X-46422-5p, 529, -119, 86, 24; miR-X-47540-3p, 529, -119, 86, 24; miR-21-45132-5p, 535, -119, 89, 22
IL11: miR-7-21068-3p, 54, -125, 86, 24; miR-16-36971-3p, 630*, -123, 85, 24
JHDM1D: miR-9-20317-3p, 7*, -127, 86, 24; miR-5-15564-3p, 12*, -119, 86, 22; miR-7-19239-3p, 88*, -123, 88, 23; miR-1-155-3p, 92*, -119, 86, 22
LAMC1: miR-11-29998-3p, 28, -121, 86, 23; miR-20-44754-3p, 42, -119, 86, 23; miR-19-43342-3p, 51, -119, 90, 22; miR-19-44540-3p, 107, -121, 85, 23; miR-10-13655-3p (2), 111 ÷ 115, -117 ÷ -123, 86 ÷ 91, 22; miR-2-3313-3p, 112, -136, 85, 25; miR-19-42772-5p, 114, -121, 85, 23; miR-1-155-3p, 115, -119, 86, 22; miR-4-11437-3p, 244, -121, 86, 23; miR-3-7886-3p, 277*, -123, 85, 24; miR-6-18496-3p, 388*, -119, 90, 22
LASP1: miR-20-42659-3p, 47, -119, 89, 22; miR-16-36476-5p, 68, -119, 90, 22; miR-5-16438-3p, 206, -119, 90, 22; miR-1-2121-3p, 207, -134, 85, 25; miR-19-33623-3p, 207, -127, 86, 24
MAGEA10: miR-5-14114-5p, 599*, -119, 86, 23

MDK: miR-8-23986-3p, 16, -129, 90, 24; miR-5-14114-5p, 421*, -121, 88, 23; miR-7-20815-5p, 483*, -119, 86, 23
MMP2: miR-1-1819-3p, 110, -123, 89, 23; miR-9-25082-3p, 110, -121, 85, 24; miR-9-20317-3p, 112, -129, 87, 24; miR-X-48174-3p, 112, -121, 85, 24; miR-17-39416-3, 113, -121, 92, 22; miR-5-15733-3p, 115, -127, 86, 24; miR-7-20203-3p, 115, -121, 90, 22; miR-9-27797-5p (2), 118 ÷ 124, -121 ÷ -127, 85 ÷ 90, 24; miR-12-17092-3p, 124, -123, 89, 22; miR-2-6166-5p, 279, -119, 86, 23; miR-21-45324-5p, 379*, -125, 91, 23; miR-X-20136-3p, 380*, -121, 86, 24
MTCH2: miR-22-46522-5p, 26, -123, 89, 22; miR-5-15926-3p, 74, -123, 94, 22
MTSS1: miR-11-28201-3p, 26, -123, 85, 24; miR-20-42676-3p, 26, -121, 86, 23; miR-12-30578-5p, 1653*, -123, 85, 24
MYL9: miR-19-43662-5p, 639**, -121, 93, 23; miR-16-37915-3p, 873**, -119, 86, 24
NTRK2: miR-2-5674-3p, 57, -121, 88, 23; miR-17-39416-3p, 61, -125, 95, 22; miR-9-20317-3p, 63, -129, 87, 24; miR-5-15564-3p, 65, -127, 92, 22; miR-10-13940-3p, 171, -110, 96, 18; miR-9-23270-3p, 266, -129, 86, 24; miR-20-43555-5p, 285, -121, 89, 22
PARP1: miR-19-36095-3p, 1275*, -119, 90, 23
PFN1: miR-3-8242-5p, 78, -119, 89, 23; miR-9-23803-5p (3), 78 ÷ 90, -121 ÷ -129, 86 ÷ 92, 24; miR-19-44540-3p, 101, -121, 85, 23; miR-X-13268-5p, 103, -119, 90, 21; miR-19-42772-5p, 105, -125, 88, 23; miR-20-45753-5p, 108, -119, 88, 22; miR-17-41183-5p, 504, -119, 86, 23; miR-8-21978-5p, 508, -121, 85, 24; miR-19-41131-3p, 509, -123, 85, 23; miR-7-18337-3p, 512, -119, 87, 23; miR-11-30258-3p, 522, -119, 86, 24; miR-6-12155-5p, 606, -119, 86, 22; miR-20-41939-3p, 782*, -119, 87, 22; miR-3-10329-5p, 1130**, -119, 87, 24; miR-16-37915-3p, 1240**, -123, 89, 24
PTGS2: miR-5-15432-3p, 107, -121, 85, 23; miR-9-23969-3p, 108, -123, 92, 21; miR-X-13195-3p, 112, -121, 85, 23; miR-6-12155-5p, 113, -119, 86, 22
PRRT2: miR-11-28560-5p, 39, -119, 87, 23; miR-2-5674-3p, 44, -119, 86, 23; miR-9-20317-3p, 44, -127, 86, 24; miR-7-17529-3p, 48, -125, 86, 25; miR-X-48174-3p, 51, -125, 88, 24
RAB5A: miR-19-41910-5p, 37, -125, 86, 24; miR-X-48174-3p (4), 143 ÷ 192, -121 ÷ -127, 85 ÷ 90, 24; miR-18-40163-3p (2), 179 ÷ 185, -121, 86, 23; miR-18-39953-5p, 182, -125, 87, 23; miR-6-17815-3p, 184, -132, 89, 24; miR-8-23953-5p, 184, -125, 86, 24; miR-5-15733-3p (2), 186 ÷ 189, -127, 86, 24; miR-2-6862-5p (3), 187 ÷ 191, -117 ÷ -121, 86 ÷ 89, 23; miR-9-27797-5p, 189, -121, 85, 24; miR-1-1819-3p, 190, -121, 88, 23; miR-13-32613-3p, 190, -121, 85, 24; miR-13-32613-3p, 193, -121, 85, 24; miR-9-25082-3p, 193, -123, 87, 24; miR-19-42772-5p (2), 324 ÷ 327, -121, 85, 23; miR-2-3313-3p (2), 325 ÷ 329, -136 ÷ -140, 85 ÷ 88, 25; miR-10-13655-3p, 328, -119, 87, 22; miR-1-155-3p (3), 328 ÷ 334, -119 ÷ -127, 86 ÷ 92, 22; miR-9-28523-5p, 328, -121, 97, 20
RUNX1: miR-9-25955-3p, 12, -121, 90, 21; miR-5-14114-5p, 1417, -123, 89, 23; miR-5-14114-5p, 1434, -119, 86, 23; miR-10-13655-3p, 1605*, -121, 89, 22; miR-20-44999-3p, 1668*, -123, 88, 23; miR-10-16862-5p, 1684*, -119, 89, 21; miR-16-36024-3p, 2215*, -121, 85, 23; miR-8-21445-5p, 2807*, -119, 86, 22; miR-4-11828-5p, 2957**, -117, 87, 22; miR-16-38712-3p, 3038**, -123, 85, 24; miR-18-41189-3p, 3061**, -127, 87, 23; miR-2-4005-5p, 3119**, -129, 87, 24; miR-20-45152-5p, 3124**, -127, 86, 24
SERPINE1: miR-16-38458-3p, 30, -123, 88, 24; miR-2-3962-5p, 542*, -125, 88, 24
SFN: miR-6-16980-5p, 824**, -123, 88, 23; miR-6-16980-5p, 829**, -121, 86, 23; miR-19-30988-5p, 835**, -129, 90, 23
STMN1: miR-5-17240-3p, 1096**, -119, 89, 23; miR-2-5355-3p, 1987**, -119, 93, 22
Notes: miRNA; in brackets, the number of binding sites; the beginning of the binding site; without * – 5'UTR; * – CDS; ** – 3'UTR; binding energy, kJ / mole; the value ΔG / ΔGm,%; length, nt

The proto-oncogene *CBL* encodes ubiquitin ligase [5]. The *CBL* gene is highly expressed in the testes, and weakly in other organs and tissues. The *CBL* gene is the target for 11 miRNAs, several of which have multiple binding sites (Table 3). miR-9-20317-3p has six sites, miR-5-15733-3p – five sites, miR-17-39416-3p and miR-18-39953-5p – four sites, miR-X-48174-3p – two sites. The beginning of all these binding sites are located in the 5'UTR region from 12 nt to 34 nt, i.e., the nucleotide sequences of binding sites of these miRNAs are partially common. For miR-16-38712-3p and miR-11-29461-3p, the binding sites are also common and located in the CDS. One miRNA is bound in the 3'UTR. The *CBL* gene encodes oligopeptides GGGSGSGGSGSGG, HHHHHHH, DDDDDE and PPPPPP in the protein structure, the function of which is unknown.

CD44 protein is a glycoprotein involved in intercellular interactions, adhesion, cell migration, hematopoiesis, apoptosis and metastasis at the triple-negative subtype of the breast cancer [6]. The *CD44* gene is the target for three miRNAs which bind in the 5'UTR of mRNA with a free energy of -119 kJ/mole and -121 kJ/mole, which provides sufficient interaction of miRNA and mRNA. These miRNAs bind to mRNA in the 5'UTR region with the beginning at 352 nt, 359 nt and 362 nt, that is,

the binding sites overlap. This position of RISK interaction with mRNA prevents the initiation of translation.

The mRNA of *CEACAM5* gene links two miRNAs in the 3'UTR starting at positions of 3220 nt, 3223 nt and 3267 nt, that is, with a partial overlap of the nucleotide sequences of the binding sites.

The *DRAM1* gene is the target for five miRNAs, three of which bind with mRNA in the 5'UTR in one region from 57 nt to 73 nt.

The *ERBB3* gene encodes a member of the epidermal growth factor receptor family (EGFR) tyrosine kinase. Overexpression of this protein is detected in various organs, including the prostate, bladder, mammary gland [7]. The *ERBB3* gene is a target of a single miRNA that binds in the 5'UTR (Table 3). In mRNAs longer than 4000 nucleotides, there are no miRNA binding sites.

The protein encoded by *FGFR2* gene is a member of the epidermal growth factor receptor family (EGFR). It is highly conservative in the process of evolution [8]. In mRNA of *FGFR2* gene, there are eight miRNA binding sites in the 5'UTR (Table 3). Binding sites of seven miRNAs are located with a partial coincidence of nucleotide sequences in the region from 37 nt to 60 nt. Free binding energy changed from -119 kJ/mole to -132 kJ/mole. miR-7-21139-3p has the advantage in the binding with mRNA of *FGFR2* gene.

The *FIS1* gene is a target for three miRNAs that may bind in the 5'UTR in the region of 529 nt to 535 nt. The *FH* and *IL11* genes are targets for one and two miRNAs, respectively.

The mRNA of *JHDM1D* gene binds four miRNAs in the CDS. The starts of binding sites for two miRNAs are located at positions 7 nt and 12 nt, and for other two miRNAs at positions 88 nt and 92 nt. That is, CDS is characterized by the cluster location of miRNA binding sites. Typically, sites of miRNA binding in the protein coding region evolved long ago and they are conservative.

There are two sites for miRNA binding in the 5'UTR mRNA of *LAMC1* gene. In the first region from the position of 28 nt to 51 nt, binding sites for three miRNAs are located. In the second region from the position of 107 nt, the binding sites of five miRNAs are located.

In the 5'UTR mRNA of *LASP1* gene the binding site of the first miRNA immediately starts after the binding site of the second miRNA. Next three miRNAs have the beginning of binding sites at 206 nt and 207 nt. The genes *MAGEA10* and *MDK* are targets for miRNAs which bind in the CDS.

In mRNA of *MMP2* gene, the starts of binding sites of nine miRNAs are located from 110 nt to 124 nt in the 5'UTR. In the protein coding region of mRNA, the beginning of binding sites of two miRNAs is coincided. Therefore, the location of miRNA binding sites in mRNA of *MMP2* gene also has a clear tendency to form clusters of miRNA binding sites. This number of binding sites suggests a strong dependence of *MMP2* gene expression on miRNAs, which compete with each other for mRNA binding.

There are few sites for miRNAs binding in mRNA of *MTCH2, MYL9* and *MTSS1* genes, and only two miRNA binding sites in the 5'UTR mRNA of *MTSS1* gene are coincided.

The *NTRK2* gene is a target for seven miRNAs whose binding sites are located in the 5'UTR. The first four miRNAs have very close positions at the beginning of binding sites.

The mRNA of *PFN1* gene has binding sites for 15 miRNAs. The first six miRNAs has the beginning of binding sites from 78 nt to 108 nt. The next five miRNAs have the beginning of binding sites from 508 nt to 522 nt in the 5'UTR. Therefore, the expression of *PFN1* gene is strongly controlled by miRNA.

All binding sites of the four miRNAs in mRNA of *PTGS2* gene are located in the 5'UTR and constituted one cluster. Similarly, all binding sites of the five miRNAs in mRNA of *PRRT2* gene are located in the 5'UTR and constitute one cluster.

The beginning of binding sites for 14 miRNAs are located in the 5'UTR mRNA of *RAB5A* gene in a region from 143 to 193 nt. Moreover, miR-X-48174-3p has four and miR-2-6862-5p three binding sites. miR-13-32613-3p, miR-18-40163-3p, miR-5-15733-3p have two binding sites. From 324 nt to 334 nt, there are binding sites for five miRNAs, three of which have two binding sites. The *RAB5A* gene is unique among 17,000 genes we studied for the ability to bind miRNA in the 5'UTR of mRNA. The free binding energy of these miRNAs varies from -115 kJ/mole to – 140 kJ/mole, which indicates a strong interaction of miRNA with mRNA of *RAB5A* gene. The need to suppress gene expression with miRNA has been experimentally confirmed. It was found that increasing the expression of *RAB5A* gene increases the mobility of tumor cells and increases the lymph node metastases [9]. Suppressing the expression of *RAB5A* gene leads to a decrease in the mobility of cancer cells and a decrease in invasiveness [10].

The *RUNX1* gene is the target for nine miRNAs that have been bind in the 5'UTR, CDS and 3'UTR (Table 3). In each of these mRNA regions, two miRNAs form clusters of common binding sites.

The mRNA of *SERPINE1* and *STMN1* genes has two miRNA binding sites. The mRNA of *SFN* gene has binding sites for three miRNAs in the 3'UTR with beginning at positions 824 nt, 829 nt and 835 nt.

Characteristics of the interaction of miRNAs with mRNAs of candidate genes of the luminal subtype

The *ANGPTL4* gene in breast cancer is expressed higher than in the control [11] and the gene is associated with the regulation of invasion in breast cancer [12]. The mRNA of *ANGPTL4* gene has binding sites for two miRNAs, one of which is fully complementarily bound in the CDS (Table 4). The mRNA of *EZH1* gene has binding sites for one miRNA in the 3'UTR.

Table 4 – Characteristics of miRNAs binding with mRNA of candidate genes of the luminal subtype

ANGPTL4: miR-19-44540-3p, 227*, -125, 88, 23; miR-19-43315-5p, 259*, -134, 100, 23
EZH1: miR-17-39273-3p, 3085**, -115, 89, 23; miR-19-43614-3p, 3832**, -125, 91, 23
FOXA1: miR-8-19447-3p, 55, -125, 87, 24; miR-11-31496-5p, 56, -125, 88, 23; miR-11-28041-3p, 62, -119, 86, 23; miR-1-1904-5p, 99, -123, 89, 24; miR-22-16963-5p, 100, -123, 88, 22; miR-17-40081-5p, 101, -129, 88, 23; miR-20-22562-3p, 101, -129, 86, 24; miR-20-22562-3p, 102, -129, 86, 24; miR-1-155-3p (3), 109 ÷ 130, -119 ÷ -129, 86; ÷ 94, 22miR-20-43873-3p, 110, -123, 89, 23; miR-1-1510-5p, 111, -140, 94, 24; miR-1-2121-3p (5), 112 ÷ 118, -134 ÷ -140, 85 ÷ 89, 25; miR-5-3563-5p, 112, -127, 92, 22; miR-X-13195-3p, 112, -121, 85, 23; miR-10-26423-3p, 113, -129, 87, 24; miR-19-30988-5p, 113, -127, 88, 23; miR-20-45152-5p, 115, -129, 87, 24; miR-19-33623-3p (3), 115 ÷ 122, -129 ÷ -134, 87 ÷ 90, 24; miR-19-44127-3p, 117 ÷ 126, -127 ÷ -129, 86 ÷ 87, 24; miR-3-8100-5p (2), 117 ÷ 121, -127, 87, 24; miR-1-1714-3p, 118, -121, 97, 20; miR-1-1922-3p, 118, -119, 89, 22; miR-15-32047-5p, 118, -125, 86, 24; miR-X-13195-3p, 118, -123, 87, 23; miR-19-21199-3p (3), 118 ÷ 121, -134 ÷ -136, 85 ÷ 86, 25; miR-19-44540-3p, 118 ÷ 137, -121 ÷ -123, 85 ÷ 87, 23; miR-17-40348-5p, 120, -123, 91, 23; miR-19-21199-3p, 120, -140, 89, 25; miR-4-11421-3p, 120, -121, 86, 23; miR-5-6716-5p, 121, -125, 88, 23; miR-2-3313-3p, 122, -136, 85, 25; miR-19-42772-5p, 123, -121, 85, 23; miR-20-22562-3p, 123, -129, 86, 24; miR-10-13655-3p, 124, -123, 91, 22; miR-19-43966-3p, 125, -121, 86, 23; miR-4-6496-3p (2), 127 ÷ 130, -119 ÷ -121, 92 ÷ 93, 21; miR-8-21445-5p, 133, -121, 88, 22; miR-2-8257-5p, 135, -123, 87, 23; miR-6-12155-5p, 231, -119, 86, 22; miR-2-2621-5p, 238, -121, 86, 22; miR-19-9434-3p, 756*, -119, 87, 23; miR-8-19447-3p, 766*, -125, 87, 24; miR-5-15733-3p, 768*, -132, 89, 24; miR-12-33610-3p, 1128*, -127, 86, 24; miR-19-43351-3p, 1128*, -119, 87, 23; miR-4-12154-5p, 1129*, -125, 87, 24; miR-8-23953-5p, 1130*, 125, 86, 24; miR-9-27797-5p, 1135*, -121, 85, 24; miR-9-20317-3p, 1150*, -134, 90, 24; miR-7-20203-3p, 1159*, -119, 89, 22; miR-X-25977-5p, 1279*, -119, 87, 22; miR-15-33256-3p, 1280*, -127, 86, 24; miR-17-40081-5p, 1287*, -129, 88, 23; miR-1-1819-3p, 1325*, -119, 86, 23; miR-5-14202-5p, 1325*, -119, 88, 22; miR-12-31544-5p, 1396*, -119, 87, 23
GTF2IRD1: miR-2-8257-5p, 124, -121, 85, 23; miR-10-26423-3p, 127, -129, 87, 24; miR-4-11421-3p, 133, -121, 86, 23; miR-1-2121-3p, 135, -136, 86, 25; miR-1-3037-5p, 160, -119, 86, 23; miR-12-32997-5p, 208, -125, 89, 23; miR-16-36024-3p, 210, -121, 85, 23; miR-6-12155-5p, 234, -123, 89, 22; miR-8-23353-3p, 340, -123, 92, 22; miR-8-21162-5p, 959*, -121, 92, 23
HMGA2: miR-2-3313-3p, 99, -138, 87, 25; miR-1-155-3p (4), 515 ÷556, -119 ÷-132, 86 ÷95, 22; miR-19-43373-3p, 539, -119, 93, 21; miR-X-13195-3p, 541, -123, 87, 23; miR-15-32047-5p (3), 541÷ 545, -125 ÷-134, 86 ÷91, 24; miR-1-265-3p, 542, -125, 91, 22; miR-17-41168-3p, 542, -117, 95, 20; miR-17-40348-5p (2), 543÷ 547, -119, 87, 23; miR-19-21199-3p (3), 543 ÷549, -134 ÷-136, 85 ÷86, 25; mir-1-2121-3p (4), 544÷ 548, -134 ÷-146, 85 ÷93, 25; miR-19-33623-3p, 544÷ 548, -129 ÷-142, 87 ÷96, 24; miR-1-275-3p, 547, -121, 85, 23; miR-1-1922-3p, 550, -119, 89, 22; miR-22-23987-3p, 553, -119, 90, 21; miR-10-26815-5p, 575, -121, 88, 24; miR-1-1819-3p, 788, -123, 89, 23; miR-18-41949-5p, 822*, -119, 89, 22; miR-2-7331-5p, 1270**, -119, 86, 23
ITGA6: miR-4-11009-3p, 71, -125, 88, 23; miR-9-26042-5p, 73, -119, 87, 22; miR-1-3554-3p, 180, -117, 86, 23; miR-9-25846-3p, 200, -117, 86, 23; miR-5-15432-3p, 248*, -121, 85, 23
ITGB1: miR-10-26815-5p, 61*, -127, 92, 24; miR-22-46979-5p, 91*, -127, 92, 23; miR-9-5204-5p, 91*, -119, 89, 22; miR-10-13655-3p, 95*, -123, 91, 22; miR-5-8853-5p, 98*, -117, 93, 20; miR-16-40261-3p, 101*, -117, 93, 20; miR-3-9441-3p, 101*, -121, 86, 23
JAK1: miR-11-29827-3p, 66, -129, 90, 24; miR-7-21249-3p, 66, -123, 87, 23; miR-17-40968-3p, 75, -123, 85, 24
LOX: miR-12-32764-3p, 711*, -123, 87, 23; miR-17-40081-5p, 723*, -125, 86, 23
MAP3K14: miR-15-31763-5p, 30, -123, 85, 24; miR-19-42853-3p, 854*, -119, 86, 23; miR-12-33279-5p, 2342*, -127, 91, 24; miR-2-8239-5p, 3041**, -121, 89, 22; miR-2-4697-3p, 3333**, -132, 87, 24
MAPT: miR-19-44540-3p, 108, -121, 85, 23; miR-12-26632-3p, 147, -123, 88, 23; miR-3-6515-3p, 174, -119, 86, 24; miR-17-40348-5p, 224, -119, 87, 23; miR-19-33623-3p, 225, -129, 87, 24; miR-9-26042-5p, 3168**, -119, 87, 22; miR-7-20411-3p, 3743**, -119, 87, 23
MCM7: miR-17-39023-3p, 23, -123, 87, 24; miR-7-20142-5p, 26, -119, 89, 23; miR-8-23353-3p, 111, -121, 90, 22

SMAD3: miR-16-13062-5p, 3, -129, 87, 24; miR-7-15849-3p, 4, -115, 100, 18; miR-20-45753-5p, 54, -119, 88, 22; miR-10-26214-5p, 89, -123, 88, 23; miR-9-26255-5p, 139, -123, 87, 24; miR-15-11315-5p, 194, -117, 100, 19; miR-16-20199-5p, 201, -121, 88, 22; miR-12-29625-3p, 243, -125, 92, 23; miR-6-16980-5p, 2070*, -127, 91, 23; miR-12-17704-3p, 2071**, -123, 88, 23; miR-15-38620-5p, 2072*, -119, 90, 22; miR-14-35670-5p, 4330*, -119, 89, 23
SOX4: miR-16-36745-3p, 739, -123, 87, 24; miR-10-28986-3p, 766, -121, 86, 23; miR-4-13460-3p, 1291*, -123, 91, 22; miR-5-14873-3p, 1293*, -121, 90, 22; miR-18-39953-5p, 1295*, -125, 87, 23; miR-4-11437-3p, 1402*, -125, 89, 23; miR-X-48174-3p, 1454*, -125, 88, 24; miR-3-8100-5p, 1482*, -125, 86, 24; miR-2-3313-3p, 1483*, -136, 85, 25; miR-1-155-3p, 1486*, -121, 88, 22; miR-3-7886-3p, 1624*, -123, 85, 24; miR-12-30075-3p, 1721*, -127, 88, 24; miR-9-27181-5p, 1723*, -127, 92, 22; miR-X-13195-3p, 1799*, -123, 87, 23; miR-1-356-5p, 1837*, -127, 87, 23; miR-15-36925-p, 1838*, -127, 87, 24; miR-11-31496-5p , 1884*, -123, 87, 23; miR-9-13610-3p, 1900*, -121, 92, 21; miR-16-36024-3p, 2405**, -121, 85, 23; miR-11-29077-3p, 2428**, -123, 88, 24; miR-2-5674-3p, 2994**, -123, 89, 23; miR-17-39011-3p, 3000**, -125, 95, 23; miR-X-48174-3p, 3000**, -127, 90, 24
TGFB1: miR-19-43966-3p, 1, -121, 86, 23; miR-20-43381-5p, 1, -121, 92, 21; miR-1-155-3p, 3, -121, 88, 22; miR-9-13610-3p, 6, -121, 92, 21; miR-2-4782-5p, 78, -119, 86, 22; miR-12-30416-5p, 186, -117, 92, 22; miR-10-13655-3p, 209, -129, 95, 22; miR-1-155-3p, 212, -119, 86, 22; miR-20-43381-5p, 213, -119, 90, 21; miR-19-41131-3p, 235, -123, 85, 23; miR-17-38733-3p, 241, -119, 89, 24; miR-3-8100-5p (2), 900 ÷ 903*, -127, 87, 24; miR-3-9461-3p, 910*, -119, 87, 23; miR-17-40711-5p, 1053*, -121, 88, 23; miR-6-16980-5p (3), 2057 ÷ 2087**, -121 ÷ -123, 86 ÷ 88, 23; miR-19-30988-5p (2), 2058 ÷ 2073**, -123, 85, 23; miR-1-356-5p, 2059**, -127, 87, 23; miR-9-13610-3p, 2060**, -123, 94, 21; miR-8-24549-5p, 2066**, -125, 88, 24; miR-12-17704-3p, 2088**, -123, 88, 23; miR-15-38620-5p, 2089**, -119, 90, 22; miR-5-14114-5p, 2091**, -119, 86, 23; miR-1-2121-3p, 2093**, -140, 89, 25; miR-19-33623-3p, 2093**, -129, 87, 24; miR-18-41332-3p, 2095**, -121, 88, 23
TNC: miR-10-26528-5p, 1165*, -119, 86, 24; miR-2-4826-5p, 8073**, -115, 92, 23
Notes: miRNA; in brackets, the number of binding sites; the beginning of the binding site; without * – 5'UTR; * – CDS; ** – 3'UTR; binding energy, kJ / mole; the value ΔG / ΔGm,%; length, nt

FOXA1 transcription factor involves in the regulation of differentiation of breast cancer cells and other processes of oncogenesis [13-17]. Suppressing the expression of *FOXA1* gene significantly reduces the mobility of BC cells [18]. The mRNA of *FOXA1* gene has 50 binding sites in the 5'UTR including three miRNAs in the region from 55 nt to 62 nt. 33 miRNAs have binding sites in the region from 99 nt to 137 nt.

miR-1-2121-3p has five binding sites and miR-19-21199-3p has three binding sites with a free binding energy equal to -134 kJ/mole ÷ -140 kJ/mole for both miRNAs. miR-19-33623-3p has three binding sites with a free binding energy equal to -129 kJ/mole ÷ -134 kJ/mole. miR-1-155-3p also has three binding sites in this region. miR-2-3313-3p has binding site with a free binding energy equal to -136 kJ/mole. The mRNA of *FOXA1* gene has nine binding sites in the CDS of which seven are located from 1128 to 1150 nt. Three miRNAs are bound in the CDS at positions 1279 nt, 1280 nt, and 1287 nt. Two miRNAs have binding sites in the CDS starting at 1325 nt and three miRNAs have the beginning of binding sites at 756 nt, 766 nt, and 768 nt. Therefore, clusters of miRNA binding sites are detected in both 5'UTR and CDS. The established characteristics of miRNA binding with mRNA of *FOXA1* gene indicate that this gene is under the strong control of more than 50 miRNAs. In addition, five miRNAs have free binding energy more than -130 kJ/mole. According to these data, *FOXA1* gene expression will not occur if all these miRNAs are present in the medium at concentrations comparable to the mRNA concentration. Therefore, it is necessary to consider which miRNA and in what concentration are present during the expression of *FOXA1* gene. According to the gene bank, the *FOXA1* gene is expressed only in the prostate.

Expression of the transcription factor GTF2IRD1 varies with BC [19]. The mRNA of *GTF2IRD1* gene binds with four miRNAs which binding sites are located in the 5'UTR in the region from 124 nt to 135 nt. Out of ten miRNAs, only miR-8-21162-5p is bound in the CDS. GTF2IRD1 is expressed in half of the tissues.

HMGA2 factor modulates transcription, is involved in the regulation of growth and invasion of breast cancer [20-22]. 14 miRNAs bind with mRNA of *HMGA2* gene in the 5'UTR in a region from 515 nt to 575 nt. Of these, miR-1-2121-3p has four binding sites with a binding energy equal to -134 kJ/mole ÷ -146 kJ/mole. miR-19-21199-3p has three binding sites with a free binding energy equal to -134 kJ/mole ÷ -136 kJ/mole. miR-1-155-3p has four binding sites with a free binding energy equal to -119 kJ/mole ÷ -132 kJ/mole. miR-19-33623-3p has three binding sites with a free binding energy equal to -129 kJ/mole ÷ -142 kJ/mole. miR-15-32047-5p has two binding sites with a free binding energy equal to -125 kJ/mole ÷ -129 kJ/mole. miR-2-3313-3p has a binding site with a free binding energy equal to -138 kJ/

mole. All binding sites for all miRNAs are located in the 5'UTR. The genes are similar in the number of miRNAs that bind with mRNA of *HMGA2* and *FOXA1* genes. The gene encoding the HMGA protein is actively expressed at the embryonic stage of development, while in adult cells its expression is at the background level [23]. However, with the development of malignant tumors of epithelial origin, the expression level of this gene significantly increases again. The increase in the level of expression of HMGA2 was noted in colon cancer [24], bladder [25], thyroid gland [26], skin [27], ovaries [28], etc.

The mRNA of *ITGA6* gene has five miRNA binding sites, of which only one is located in the CDS, and others in the 5'UTR.

Integrin ITGB1 is a member of the family of membrane receptors including cell adhesion, embryogenesis, immune and metastasis [29; 30]. The mRNA of *ITGB1* gene is associated with seven miRNAs in the CDS with the beginning of binding sites of six of them in a region from 91 nt to 101 nt, which is a rare case of a cluster of miRNA binding sites in the CDS.

The three sites for binding miRNAs with mRNA of *JAK1* gene are a cluster located in the 5'UTR. The mRNA of *LOX* gene has binding sites for two miRNAs located in the CDS with partial common nucleotide sequences. The *MAP3K14* gene is a target for five miRNAs. The binding sites of two of them are located in the CDS, two in the 3'UTR and one in the 5'UTR. In mRNA of *MAPT* gene, there are five miRNA binding sites in the 5'UTR and two in the 3'UTR. In mRNA of *MCM7* gene, three miRNA binding sites in the 5'UTR were identified. The *SMAD3* gene is a target for 12 miRNAs, the binding sites of eight miRNAs are located in the 5'UTR and four miRNAs in the 3'UTR. miR-15-11315-5p is fully complementary to its binding site.

In mRNA of *SOX4* gene, 23 miRNA binding sites were identified. Only two miRNAs are bind in the 5'UTR and five miRNAs in the 3'UTR. Three miRNAs are included in the cluster in the CDS with the beginning of miRNA binding sites at position 1291 nt. Three miRNAs are in clusters with a start at position 1482 nt and at position 1837 nt. Two miRNAs are bind at positions 1721 nt and 1723 nt.

In mRNA of *TGFB1* gene, 25 miRNA binding sites were identified. The first cluster constitutes the binding sites of four miRNAs beginning with 1 nt of 5'UTR. The next cluster consists of binding sites for five miRNAs in the 5'UTR starting at 209 nt. In 3'UTR, a cluster for 11 miRNAs with binding sites starting at position 2057 nt was identified. One miRNA has three binding sites and two miRNAs have two binding sites in this cluster. Two miRNAs are bound in the CDS with a nearest location of beginning of binding sites. The TGFB1 polymorphism has been associated with breast cancer risk inducing an increase in TGF-β1 cellular expression and elevating plasma TGF-β1 levels, which might suppress the immune regulatory activities of macrophages and increase the risk of breast cancer [31], although other authors suggest that lower levels of circulating TGF-β1 are associated with a higher metastatic risk and poor disease prognosis [32]. The *TNC* gene is a target for two miRNAs binding in CDS and 3'UTR.

Characteristics of the interaction of miRNAs with mRNAs of candidate genes of her2 subtype

The mRNA of *A4GALT* gene binds 15 miRNAs, two out of which have binding sites in the CDS and others in the 5'UTR (Table 5).

The free binding energy value varies from -119 kJ/mole to -129 kJ/mole. The starts of the binding sites of 13 miRNAs in the 5'UTR are located at a region from 9 nt to 41 nt, that is, the nucleotide sequences for miRNA binding are partially common. The presence of a such strong dependence of gene expression on miRNA both on the free interaction energy value and on the number of miRNA is difficult to explain. It seems that the mRNA of gene is unlikely to be translated with such control by miRNA. However, one must take into account that not all miRNAs can be synthesized simultaneously and their total concentration in the cell may be less than the concentration of mRNA. As a result, the protein can be synthesized depending on the ratio of concentrations of miRNA and mRNA. Another factor limiting the effect of miRNA is the presence in the cell of miRNA-free RISC complexes. It should be noted that about half of miRNAs are synthesized when the host gene is expressed from introns during the splicing process and this gene may not be expressed permanently or temporarily in the tissue cell.

mRNA of *ACSS2, ADAM17* and *AURKA* genes have binding sites for only one miRNA. However, if the concentrations of the respective miRNAs are comparable or exceed the concentration of mRNA, the effect of inhibition of mRNA translation will be significant.

Table 5 – Characteristics of miRNAs binding with mRNAs of candidate genes of the her2 subtype

A4GALT: miR-8-21445-5p, 9, -123, 89, 22; miR-1-356-5p, 12, -127, 87, 23; miR-9-23969-3p, 13, -127, 95, 21; miR-12-32764-3p, 19, -121, 85, 23; miR-19-30988-5p, 19, -123, 85, 23; miR-11-29077-3p, 28, -123, 88, 24; miR-4-11828-5p, 30, -119, 89, 22; miR-11-28656-5p, 32, -121, 86, 23; miR-1-356-5p, 33, -125, 86, 23; miR-2-8257-5p, 37, -125, 88, 23; miR-10-28986-3p, 39, -121, 86, 23; miR-20-22562-3p, 39, -129, 86, 24; miR-5-3563-5p, 39, -119, 86, 22; miR-17-40348-5p, 41, -121, 89, 23; miR-5-12460-5p, 457*, -123, 85, 24; miR-11-29324-3p, 995*, -121, 86, 23
ACSS2: miR-2-8257-5p, 231*, -123, 87, 23
ADAM10: miR-9-26506-3p, 165, -117, 95, 22; miR-5-15733-3p, 416, -132, 89, 24; miR-9-20317-3p, 416, -129, 87, 24
ADAM17: miR-20-43873-3p, 2378*, -121, 88, 23
AURKA: miR-9-22187-3p, 197, -115, 86, 23
BRCA2: miR-19-42224-5p, 25, -115, 93, 21; miR-22-45335-5p, 10821**, -113, 90, 23
BRIP1: miR-18-39953-5p, 7, -129, 90, 23; miR-16-20406-3p, 14, -125, 86, 23; miR-17-39440-3p, 4342**, -117, 86, 24; miR-20-43646-5p, 6567**, -119, 87, 24; miR-14-35161-5p, 6607**, -115, 87, 24
CDK2: miR-12-31544-5p, 116, -117, 86, 23
CDK6: miR-5-15733-3p, 258, -129, 87, 24; miR-12-30578-5p, 466, -123, 85, 24; miR-6-17811-3p, 483, -127, 86, 24; miR-15-36862-3p (2); 1900 ÷ 1906**, -115, 95, 23; miR-8-23986-3p, 7773**, -127, 88, 24
EPOR: miR-19-42218-3p, 79, -119, 89, 23; miR-16-20406-3p, 80, -125, 86, 23; miR-19-41131-3p, 80, -129, 90, 23; miR-22-46522-5p, 83, -121, 88, 22; miR-5-16562-3p, 173*, -119, 88, 24; miR-17-39313-3p, 340*, -125, 86, 24; miR-2-6809-5p, 922*, -123, 85, 25
EPO: miR-12-31979-3p, 12, -121, 89, 23; miR-2-8257-5p, 18, -123, 87, 23
ERBB3: miR-1-3554-3p, 105, -117, 86, 23; miR-1-163-3p, 114, -113, 93, 21; miR-3-8100-5p, 148, -125, 86, 24
FKBPL: miR-13-33774-5p, 35, -121, 86, 24; miR-20-45753-5p, 42, -119, 87, 22; miR-2-8257-5p, 49, -121, 85, 23; miR-3-4734-5p, 769*, -115, 89, 23
GTF2E1: miR-19-25044-3p, 1750**, -117, 87, 24
H2AFX: miR-20-45152-5p, 506**, -136, 91, 24; miR-5-3563-5p, 509**, -123, 89, 22; miR-1-1630-3p, 511**, -119, 89, 22; miR-10-27682-5p, 604**, -123, 85, 24; miR-1-3919-5p, 632**, -123, 89, 24; miR-6-12155-5p, 641**, -121, 88, 22; miR-1-2121-3p, 643**, -134, 85, 25; miR-17-40081-5p (2), 647÷ 724**, -125, 86, 23; miR-22-16963-5p, 683**, -121, 86, 22; miR-2-8257-5p, 688**, -123, 87, 23; miR-5-15432-3p, 688**, -121, 85, 23; miR-16-33136-3p, 827**, -123, 91, 22
KDM5D: miR-22-46603-5p, 2489*, -119, 87, 24; miR-9-22187-3p, 3065*, -119, 89, 23
MAPK3: miR-11-29461-3p, 103*, -123, 88, 23; miR-13-32613-3p, 110*, -121, 85, 24; miR-7-21142-5p, 113*, -121, 86, 23; miR-1-2802-3p, 1144*, -117, 93, 22; miR-2-8257-5p, 1381**, -123, 87, 23; miR-5-14114-5p, 1527**, -119, 86, 23
MAZ: miR-12-17092-3p, 16, -123, 89, 22; miR-18-41189-3p, 16, -134, 91, 23; miR-9-25917-3p, 26, -125, 88, 23; miR-11-29998-3p, 27, -127, 91, 23; miR-12-33610-3p, 27, -129, 87, 24; miR-13-32368-5p, 29, -121, 85, 23; miR-1-2372-3p, 43, -121, 85, 24; miR-14-36092-3p, 79, -121, 85, 23; miR-11-28204-5p, 107, -121, 90, 21; miR-14-31624-3p, 112, -127, 88, 24; miR-7-12728-5p, 114, -121, 92, 22; miR-16-36024-3p, 118, -125, 88, 23; miR-5-17008-3p, 363*, -125, 89, 23; miR-4-12861-5p, 372*, -119, 92, 22; miR-22-16963-5p, 373*, -121, 86, 22; miR-7-21249-3p, 377*, -121, 85, 23; miR-7-21068-3p, 433*, -125, 86, 24; miR-2-4733-3p, 439*, -121, 88, 22; miR-3-8100-5p (5), 457 ÷ 472*, -125 ÷ -138, 86 ÷ 94, 24; miR-7-16350-5p, 459*, -119, 93, 21; miR-2-6809-5p, 461*, -125, 87, 25; miR-19-44540-3p, 462*, -121, 85, 23; miR-2-3313-3p (3), 464 ÷ 467*, -136 ÷ -140, 85 ÷ 88, 25; miR-11-28656-5p, 470*, -121, 86, 23; miR-1-155-3p, 470*, -123, 89, 22; miR-3-7886-3p, 671*, -129, 90, 24; miR-19-21199-3p, 473*, -134, 85, 25; miR-20-43381-5p, 489*, -121, 92, 21; miR-4-11923-3p, 489*, -125, 94, 22; miR-14-31624-3p, 495*, -123, 85, 24; miR-15-33256-3p, 499*, -129, 87, 24; mir-1-2121-3p (4), 500 ÷ 615*, -134 ÷ -138, 85 ÷ 88, 25; miR-16-36024-3p, 500*, -125, 88, 23; miR-19-33623-3p (3), 500 ÷ 608*, -127 ÷ -134, 86 ÷ 90, 24; miR-X-13195-3p, 503*, -125, 88, 23; miR-9-27797-5p, 898*, -123, 87, 24; miR-2-7331-5p, 900*, -123, 89, 23; miR-13-35476-3p, 901*, -125, 97, 22; miR-8-23986-3p, 905*, -123, 85, 24; miR-X-48174-3p, 2072**, -127, 90, 24; miR-8-23986-3p, 2340**, -123, 85, 24
NHS: miR-19-44540-3p, 426*, -121, 85, 23; miR-1-2597-5p, 431*, -129, 87, 24; miR-2-3313-3p, 532*, -146, 92, 25; miR-10-13655-3p (2), 534 ÷ 537, -121 ÷ -123, 89 ÷ 91, 22; miR-15-32047-5p, 534*, -132, 90, 24; miR-22-46979-5p, 535*, -123, 89, 23; miR-3-8100-5p, 536*, -125, 86, 24; miR-19-21199-3p (3), 539 ÷ 543*, -134 ÷ -138, 85 ÷ 88, 25; miR-1-155-3p (2), 540 ÷ 546*, -127 ÷ -134, 92 ÷ 97, 22; miR-4-11421-3p, 541*, -121, 86, 23; miR-22-16963-5p, 543*, -121, 86, 22; miR-4-6496-3p, 543*, -121, 93, 21; miR-19-43966-3p, 544*, -123, 88, 23; miR-19-43329-3p, 608*, -123, 91, 24; miR-9-23270-3p, 630*, -129, 86, 24; miR-5-15733-3p, 674*, -127, 86, 24; miR-22-45834-5p, 676*, -121, 86, 23

NISCH: miR-9-20317-3p, 31, -127, 86, 24; miR-X-48174-3p, 31, -125, 88, 24; miR-7-21142-5p, 35, -121, 86, 23; miR-1-1852-5p, 38, -121, 86, 23; miR-19-43644-3p, 38, -123, 89, 23; miR-8-21978-5p, 41, -125, 88, 24; miR-16-20406-3p, 42, -127, 87, 23; miR-18-39953-5p, 43, -123, 85, 23; miR-22-46522-5p, 47, -123, 89, 22; miR-17-39313-3p, 2198*, -125, 86, 24; miR-1-2121-3p, 3421*, -134, 85, 25; miR-10-8412-5p, 3432*, -123, 85, 23
PARP1: miR-19-36095-3p, 1275*, -119, 90, 23
RAD21: miR-9-26042-5p, 57, -121, 89, 22; miR-18-39953-5p, 120, -125, 87, 23; miR-1-3919-5p, 180,-121, 88, 24; miR-12-31979-3p, 214, -119, 87, 23
RASSF1: miR-5-15432-3p, 63, -121, 85, 23; miR-14-36092-3p, 83, -121, 85, 23
RPLP2: miR-15-32047-5p, 68, -125, 86, 24; miR-19-43966-3p, 81, -121, 86, 23; miR-17-25894-5p, 328*, -125, 87, 24
RYR1: miR-19-28028-5p, 51, -136, 91, 24; miR-5-12460-5p, 56, -123, 85, 24; miR-5-6716-5p, 5291*, -121, 85, 23; miR-19-41131-3p (2), 12919 ÷ 12934*, -125 ÷ -127, 87 ÷ 88, 23; miR-13-32613-3p, 12929*, -123, 87, 24; miR-9-20317-3p, 12931 ÷ 12994*, -127 ÷ -132, 86 ÷ 89, 24; miR-12-33610-3p, 12934*, -127, 86, 24; miR-17-39593-3p, 12958*, -136, 89, 24; miR-20-44980-3p, 13015*, -121, 86, 23; miR-15-38560-5p, 13053*, -123, 85, 24; miR-12-33610-3p, 13174*, -132, 89, 24; miR-5-15733-3p, 13174*, -127, 86, 24; miR-22-45834-5p, 13176*, -123, 88, 23; miR-X-48265-3p, 13415*, -129, 87, 24
STAR: miR-5-13733-5p, 1001*, -115, 89, 23
TIMP3: miR-14-15069-5p, 659, -119, 87, 22; miR-6-17519-3p, 1102, -121, 90, 22; miR-11-27076-3p, 3153**, -119, 86, 24; miR-5-15026-5p, 3176**, -119, 86, 23
TNF: miR-20-42898-3p, 230*, -121, 92, 23
Notes: miRNA; in brackets, the number of binding sites; the beginning of the binding site; without * – 5'UTR; * – CDS; ** – 3'UTR; binding energy, kJ / mole; the value ΔG / ΔGm,%; length, nt

In mRNA of *ADAM10* metallopeptidase gene, the binding sites of three miRNAs are located in the 5'UTR. The starts of binding sites of two miRNAs are coinciding. miR-5-15733-3p binds with the highest free binding energy equal to -132 kJ/mole. These data indicate the dependence of the expression of *ADAM10* gene on miRNAs. Note that when mutations occur in the binding site of two miRNAs, the gene leaves their control and can become an oncogene. It was found that the expression of *ADAM10* gene is higher in the tumor than in normal tissue and suppression of gene expression significantly reduces the *in vitro* migration of cells [33]. Therefore, the gene can serve as a marker for the HER2 subtype and the therapeutic target [34].

The mRNA of *BRCA2* gene has one binding site in the 5'UTR and one site in the 3'UTR. The free energy of miRNA binding with mRNA varies from -113 kJ/mole to -115 kJ/mole, which indicates their weak interaction. Interestingly, the CDS mRNA of *BRCA2* gene has more than 10,000 nucleotides and does not contain any miRNA binding site, which also reflects a weak dependence of the expression of *BRCA2* gene on miRNA. Since the *BRCA2* gene is considered as a tumor suppressor [35; 36], its weak dependence on the direct effect of miRNA reflects the preservation of its function and only mutations in the gene can affect on its function as a tumor suppressor.

The *BRIP1* gene is a target for five miRNAs, of which three binding sites are located in the 3'UTR and two sites in the 5'UTR (Table 5). miR-18-39953-5 and miR-16-20406-3p bind with mRNA of *BRIP1* gene with a free energy value varies from -129 kJ/mole to -125 kJ/mole, respectively. The free energy value of the interaction of miRNA in the 3'UTR is significantly lower: from -115 kJ/mole to -119 kJ/mole. *BRIP1* is a candidate gene for the development of BC [37].

The mRNA of *CDK2* gene has only one miRNA binding site in the 5'UTR. The *CDK6* gene is a target for five miRNAs. Three miRNA binding sites are located in two regions in the 5'UTRs: 258 nt (one miRNA) and 466 nt and 483 nt (two miRNAs). MiRNAs which bind in the 3'UTR are also bind in two regions: from 1900 nt to 1,906 nt (two sites for miR-15-36862-3p) and at 7773 nt. The *CDK6* gene encodes a cyclin dependent kinase. CDK4/6 can be used as a target for inhibition of oncogenesis.

The *EPOR* gene can affect on the growth of the tumor. The *EPOR* gene serves as a target for four miRNAs that bind in the 5'UTR mRNA in one site from 79 nt to 83 nt. Four miRNAs interact with mRNA in the CDS. The free energy of miRNA binding with mRNA varies from -117 kJ/mole to -129 kJ/mole. EPOR expression has been detected in several cancer forms [38].

The *EPO* gene is involved in the proliferation of BC cells. The mRNA of *EPO* gene has two binding sites in one 5'UTR region. The mRNA of *ERBB3* gene has three binding sites in the 5'UTR. The mRNA of

FKBPL gene has binding sites for three miRNAs in one 5'UTR region and one site in the CDS (Table 5).

The mRNA of *H2AFX* gene binds 12 miRNAs that are located in the 3'UTR. In the region from 632 to 688 nt, the binding sites of seven miRNAs are located arranged with nucleotide sequences. The *H2AFX* gene was considered as a prognostic marker of breast cancer.

The *MAPK3* gene participates in proliferation, differentiation, cell cycle. At the beginning of MAPK3 protein, there is the oligopeptide AAAAAQGGGGGE, which is encoded by the miR-11-29461-3p, miR-13-32613-3p and miR-7-21142-5p binding sites. The sites of these miRNAs binding with mRNA of *MAPK3* gene are located in one cluster in the CDS and two miRNAs are bound in the 3'UTR.

Transcription factor MAZ is associated with participation in the development of BC. The protein contains oligopeptides: AAAAAAAAAAAA, PPPPPP, GAGGGGG. 11 miRNA bind in the 5'UTR with nucleotide sequence overlap in two sites from 16 nt to 47 nt and from 107 to 118 nt. The binding sites of six miRNAs form a cluster from 495 nt in the CDS. Another cluster of binding sites for nine miRNAs starts at 457 nt. miR-18-41189-3p, miR-3-8100-5p, miR-2-3313-3p, miR-19-21199-3p, miR-1-2121-3p, miR-19-33623-3p bind with mRNA of *MAZ* gene with free energy from -132 kJ/mole to -140 kJ/mole.

The mRNA of *NHS* gene binds with 18 miRNAs only in the CDS, the binding sites are located in three regions: from 426 nt to 431 nt (2 miRNA), from 532 nt to 544 nt (12 miRNA) and from 608 to 674 nt (4 miRNA). The free energy of interaction is large in all binding sites varies from -121 kJ/mole to -146 kJ/mole. miR-19-21199-3p binds in three sites with a free energy value equal to -134 kJ/mole ÷ -138 kJ/mole. Naturally, the question arises again how this gene can be expressed with such a number of miRNAs that potentially can interact with mRNA of *NHS* gene. This gene has complex pattern of temporally and spatially regulated expression, which, together with the pleiotropic features of NHS, suggests that this gene has key functions in the regulation of eye, tooth, brain, and craniofacial development [39].

The synthesis of NISCH protein is lower in BC than in normal tissue, while the overexpression induces apoptosis, inhibits cell migration and invasion, decreases tumor growth and metastases. A gene can be a potential target for breast cancer therapy. In the NISCH protein, there are two domains consisting of polyglutamic acid, which are encoded by miRNA binding sites. Nine sites of miRNA binding with mRNA of *NISCH* gene are located in the same 5'UTR cluster with beginning from 31 nt to 47 nt. The free energy of the interaction of miRNA with mRNA varies from -121 kJ/mole to -127 kJ/mole, which indicates a strong binding of these molecules. Two binding sites for two miRNAs are available in the CDS. miR-1-2121-3p binds with mRNA of *NISCH* gene with free interaction energy equal to -134 kJ/mole. In general, all miRNAs can significantly reduce the expression of the *NISCH* gene even in the absence of several miRNAs. Expression of NISCH significantly negatively correlated with estrogen receptor status [40].

The mRNAs of *RAD21* and *RASSF1* genes have miRNA binding sites only in the 5'UTR. The mRNA of *RYR1* gene has binding site for 13 miRNAs, of which 11 are bound in the CDS and two in the 5'UTR [41]. In all sites the free energy of binding fluctuates from -121 kJ/mole to -136 kJ/mole. There are several domains of polyglutamic acid in the protein RYR1. It is described the relationship of *RYR1* gene with the calcification at BC is and the gene is proposed as a target for BC therapy.

The *TIMP3* gene is a target for four miRNAs, two of which bind in the 5'UTR and two in the 3'UTR with a free energy value from -119 kJ/mole to -121 kJ/mole [42]. The *TIMP3* gene regulates apoptosis. The *TNF* gene tumor necrosis factor regulates apoptosis.

Based on the results of establishing the characteristics of the interaction of miRNAs with mRNAs of studied candidate genes of different subtypes of the breast cancer, several features of these interactions can be identified.

The studied genes have a different number of miRNAs that bind with mRNAs. The largest number of miRNAs bind with mRNA of *FOXA1* (56 miRNA), *MAZ* (41 miRNA), *TGFB1* (25), *SOX4* (23 miRNA) genes. Sites for miRNA binding with mRNA are predominantly clustered. That is, in a small region of mRNA, several different miRNAs can bind with overlapping nucleotide sequences of binding sites. These sites more often are located in the 5'UTR at the triple negative subtype, in the CDS at the luminal A, B subtype and in the 3'UTR at the her2 subtype. This indicates a non-random distribution of miRNA binding sites throughout the mRNA sequence. For example, in mRNA of *GTF21RD1* and *HMGA2* genes, miRNA binding sites are located only in the 5'UTR, in mRNA of *NHS* gene only in the CDS and in mRNA of *H2AFX* gene only in the 3'UTR (Tables 4, 5).

A role of a large number of miRNA binding sites in mRNA of one gene is still not clarified. It is likely that such a gene is necessary for life, but it should be poorly expressed, at least in most organs. An increase in its expression leads to various pathologies. Above mentioned *FOXA1, MAZ* and *SOX4* genes, having in their mRNAs a large number of binding sites for miRNAs, are transcription factors and poorly expressed in the norm. The *TGFB1* gene is functionally associated with the SMAD transcription factor family.

The miRNA binding sites are more often located in the 5'UTR, then in the CDS and less in the 3'UTR. This preference can be explained by the biological role of miRNA – stopping the translation process. It is energetically more advantageous to stop protein synthesis at the beginning of the process, than to interrupt it later, resulting in abortive proteins, the synthesis of which was spent energy.

Subtypes of breast cancer differ in the candidate genes, whose mRNAs in the triple negative subtype bind miRNAs preferably in the 5'UTR. At the luminal A,B subtype, miRNAs is preferably bind in the CDS and, in the her2 subtype, miRNAs is preferably bind to 3'UTR (Tables 4, 5). Based on this, one of the functions of 5'UTR and 3'UTR is the need to include miRNA binding sites. For example, genes with an extended nucleotide sequence contain more miRNA binding sites.

Selection of associations of miRNA with their target genes for the diagnosis of subtypes of breast cancer is a complex task, since there are from one to several dozens of miRNA which influence on each gene. Of these, the most specific should be selected to reduce the likelihood of including miRNAs, which may have other target genes. To do this, it is necessary to determine the expected impact of each candidate miRNA on all genes of the human genome.

Conclusion

In the present study, we performed a bioinformatics analysis of interaction of miRNA with mRNA of breast cancer candidate genes. We selected 33 genes specific for the triple negative subtype, 16 genes specific for the luminal A, B subtype and 28 genes specific for the her2 subtype. It was identified the features of interactions of these genes with miRNAs. The miRNA binding sites are more often located in the 5'UTR, then in the CDS and less in the 3'UTR. Genes *CBL, DRAM1, FGFR2, LAMC1, MMP2, NTRK2, PFN1, PTGS2, PRRT2, RAB5A* responsible for the triple negative subtype of breast cancer can be characterized as candidate target genes for miRNAs which binding sites are located in the 5'UTR of mRNA. For candidate genes *JHDM1D, RUNX1* miRNAs binding sites are located in the CDS and for *RUNX1* – in the 3'UTR of mRNA. Genes *FOXA1, GTF2IRD1, HMGA2, ITGA6, MAPT, SMAD3, TGFB1* responsible for the luminal A,B subtype of breast cancer can be characterized as candidate target genes for miRNAs which binding sites are located in the 5'UTR of mRNA. For candidate genes *FOXA1, ITGB1, SOX4* miRNAs binding sites are located in the CDS and for *SMAD3, TGFB1* – in the 3'UTR of mRNA. For the her2 subtype of breast cancer, candidate genes for binding miRNAs in the 5'UTR are *A4GALT, EPOR, MAZ, NISCH, RAD21*. Candidate genes for miRNA binding in the CDS are *EPOR, MAPK3, MAZ, NHS, RYR1* and in the 3'UTR – *H2AFX*.

In summary, our study provides associations of the above miRNAs and their target genes that can be used to develop a method for diagnosis subtypes of breast cancer.

Acknowledgments

The work was carried out within the framework of the grant AP05132460 "Development of test systems for early diagnosis of cardiovascular, oncological and neurodegenerative diseases based on miRNA associations and their target genes" with the financial support of the Ministry of Education and Science of the Republic of Kazakhstan.

References

1. Torre L.A., Bray F., Siegel R.L., Ferlay J., Lortet-Tieulent J., Jemal A. (2015) Global cancer statistics. *CA-Cancer J Clin.,* vol. 65, no. 2, pp. 87-108.

2. DeSantis C., Siegel R., Bandi P., Jemal A. (2011) Breast cancer statistics. *CA-Cancer J Clin,* vol. 61, no. 6, pp. 409-418.

3. Ivashchenko A., Berillo O., Pyrkova A., Niyazova R. (2014) MiR-3960 binding sites with mRNA of human genes. *Bioinformation*, vol. 7, pp. 423-427.

4. Zhou T., Li Y., Yang L., Liu L., Ju Y., Li C. (2017) Silencing of ANXA3 expression by RNA interference inhibits the proliferation and invasion of breast cancer cells. *Oncol Rep.*, vol. 37, no. 1, pp. 388-398.

5. Wang Y., Chen L., Wu Z., Wang M., Jin F., et al. (2016) miR-124-3p functions as a tumor suppres-

sor in breast cancer by targeting CBL. *BMC Cancer*, vol. 16, no. 1, p. 826.

6. Matsumoto Y., Itou J., Sato F., Toi M. (2018) SALL4 – KHDRBS3 network enhances stem ness by modulating CD44 splicing in basal-like breast cancer. *Cancer Med.*, p. 22.

7. Morrison M.M., Hutchinson K., Williams M.M., Stanford J.C., Balko J.M., et al. (2013) ErbB3 down regulation enhances luminal breast tumor response to antiestrogens. *J Clin Invest*., vol. 123, no. 10, pp. 4329-4343.

8. Wang S., Ding Z. (2017) Fibroblast growth factor receptors in breast cancer. *Tumour Biol*., vol. 39, no. 5, pp. 1010428317698370.

9. Yang P.S., Yin P.H., Tseng L.M., Yang C.H., Hsu C.Y., Lee M.Y., Horng C.F., Chi C.W. (2011) Rab5A is associated with axillary lymph node metastasis in breast cancer patients. *Cancer Sci*., vol. 102, no. 12, pp. 2172-2178.

10. Liu S.S., Chen X.M., Zheng H.X., Shi S.L., Li Y. (2011) Knockdown of Rab5a expression decreases cancer cell motility and invasion through integrin-mediated signaling pathway. *J Biomed Sci*., vol. 17, pp. 18-58.

11. Shafik N.M., Mohamed D.A., Bedder A.E., El-Gendy A.M. (2015) Significance of Tissue Expression and Serum Levels of Angiopoietin-like Protein 4 in Breast Cancer Progression: Link to NF-κB/P65 Activity and Pro-Inflammatory Cytokines. *Asian Pac J Cancer Prev*., vol. 16, no. 18, pp. 8579-8587.

12. Adhikary T., Brandt D.T., Kaddatz K., Stockert J., Naruhn S., Meissner W., et al. (2013) Inverse PPARβ/δ agonists suppress oncogenic signaling to the ANGPTL4 gene and inhibit cancer cell invasion. *Oncogene*, vol. 31, pp. 5241-5252.

13. Anzai E., Hirata K., Shibazaki M., Yamada C., Morii M., Honda T., Yamaguchi N., Yamaguchi N. (2017) FOXA1 Induces E-Cadherin Expression at the Protein Level via Suppression of Slug in Epithelial Breast. *Cancer Cells. Biol Pharm Bull*., vol. 40, no. 9, pp. 1483-1489.

14. Ademuyiwa F.O., Thorat M.A., Jain R.K., Nakshatri H., Badve S. (2010) *Expression of Forkhead-box protein A1, a marker of luminal A type breast cancer, parallels low oncotype DX 21-gene recurrence scores. Mod Pathol*., vol. 23, pp. 270–275.

15. Gawrzak S., Rinaldi L., Gregorio S., Arenas E.J., Salvador F., Urosevic J., Figueras-Puig C. (2018) MSK1 regulates luminal cell differentiation and metastatic dormancy in ER+ breast cancer. *Nat Cell Biol*., vol. 20, no. 2, pp. 211-221.

16. Fu X., Jeselsohn R., Pereira R., Hollingsworth E.F., Creighton C.J., Li F., et al. (2016) *FOXA1 overexpression mediates endocrine resistance by altering the ER transcriptome and IL-8 expression in ER-positive breast cancer. Proc Natl Acad Sci USA*, vol. 113, pp. E6600–E09.

17. Bernardo G.M., Bebek G., Ginther C.L., Sizemore S.T., Lozada K.L., Miedler J.D., et al. (2013) *FOXA1 represses the molecular phenotype of basal breast cancer cells. Oncogene,* vol. 32, pp. 554-563.

18. Park S., Koh E., Koo J.S., Kim S.I., Park B.W., Kim K.S. (2017) Lack of both androgen receptor and forkhead box A1 (FOXA1) expression is a poor prognostic factor in estrogen receptor-positive breast cancers. *Oncotarget*, vol. 8, no. 47, pp. 82940-82955.

19. Huo Y., Su T., Cai Q., Macara I.G. (2016) An in vivo gain-of-function screen identifies the Williams-Beuren Syndrome gene GTF2IRD1 as a mammary tumor promoter. *Cell Rep*., vol. 15, no. 10, pp. 2089-2096.

20. Li X., Wang S., Li Z., Long X., Guo Z., Zhang G., Zu J., Chen Y., Wen L. (2017) The lncRNA NEAT1 facilitates cell growth and invasion via the miR-211/HMGA2 axis in breast cancer. *Int J Biol Macromol*., vol. 105, pp. 346-353.

21. Zou Q., Wu H., Fu F., Yi W., Pei L., Zhou M. (2016) RKIP suppresses the proliferation and metastasis of breast cancer cell lines through up-regulation of miR-185 targeting HMGA2. *Arch Biochem Biophys*., vol. 610, pp. 25-32.

22. Wu J., Zhang S., Shan J., Hu Z., Liu X., Chen L., Ren X., Yao L., Sheng H., et al. (2016) Elevated HMGA2 expression is associated with cancer aggressiveness and predicts poor outcome in breast cancer. *Cancer Lett*., vol. 376, no. 2, pp. 284-292.

23. Cleynen I., Van de Ven W.J. (2008) The HMGA proteins: a myriad of functions. *Int J Oncol*., vol. 32, no. 2, pp. 289-305.

24. Wang X., Liu X., Li A.Y. et al. (2011) Overexpression of HMGA2 promotes metastasis and impacts survival of colorectal cancers. *Clin Cancer Res*., vol. 17, no. 8, pp. 2570-2580.

25. Ding X., Wang Y., Ma X. et al. (2014) Expression of HMGA2 in bladder cancer and its association with epithelial-tomesenchymal transition. *Cell Prolif*., vol. 47, no. 2, pp. 146-151.

26. Chiappetta G., Tallini G., De Biasio M.C. et al. (1998) Detection of high mobility group I HMGI(Y) protein in the diagnosis of thyroid tumors: HMGI(Y) expression represents a potential diagnostic indicator of carcinoma. *Cancer Res*., vol. 58, no. 18, pp. 4193-4198.

27. Raskin L., Fullen D.R., Giordano T.J. et al. (2013) Transcriptome profiling identifies HMGA2 as

a biomarker of melanoma progression and prognosis. *J Invest Dermatol*., vol. 133, no. 11, pp. 2585-2592.

28. Malek A., Bakhidze E., Noske A. et al. (2008) HMGA2 gene is a promising target for ovarian cancer silencing therapy. *Int J Cancer*., vol. 123, no. 2, pp. 348-356.

29. Li W.X., Sha R.L., Bao J.Q., Luan W., Su R.L., Sun S.R. (2017) Expression of long non-coding RNA linc-ITGB1 in breast cancer and its influence on prognosis and survival. *Eur Rev Med Pharmacol Sci*., vol. 21, no. 15, pp. 3397-3401.

30. Yang J., Hou Y., Zhou M., Wen S., Zhou J., Xu L., Tang X., Du Y.E., Hu P., Liu M. (2016) Twist induces epithelial-mesenchymal transition and cell motility in breast cancer via ITGB1-FAK/ILK signaling axis and its associated downstream network. *Int J Biochem Cell Biol*., vol. 71, pp. 62-71.

31. Dunning AM, Ellis PD, McBride S, et al. (2003) A transforming growth factorbeta1 signal peptide variant increases secretion in vitro and is associated with increased incidence of invasive breast cancer. *Cancer Res*., vol. 63, no. 10, pp. 2610-2615.

32. Panis C, Herrera AC, Victorino VJ, Aranome AM, Cecchini R. (2013) Screening of circulating TGF-beta levels and its clinicopathological significance in human breast cancer. *Anticancer Res*., vol. 33, no. 2, pp. 737-742.

33. Ergün S., Ulasli M., Igci Y.Z., Igci M., Kırkbes S., Borazan E., et al. (2015) The association of the expression of miR-122-5p and its target ADAM10 with human breast cancer. *Mol Biol Rep*., vol. 42, no. 2, pp. 497-505.

34. Feldinger K., Generali D., Kramer-Marek G., Gijsen M., Ng T.B., et al. (2014) ADAM10 mediates trastuzumab resistance and is correlated with survival in HER2 positive breast cancer. *Oncotarget*, vol. 5, no. 16, pp. 6633-6646.

35. Soenderstrup I.M.H., Laenkholm A.V., Jensen M.B., Eriksen J.O. (2018) Clinical and molecular characterization of BRCA-associated breast cancer: results from the DBCG. *Acta Oncol*., vol. 57, no. 1, pp. 95-101.

36. Parvin S., Islam M.S., Al-Mamun M.M., Islam M.S., Ahmed M.U., Kabir E.R., Hasnat A. (2017) Association of BRCA1, BRCA2, RAD51, and HER2 gene polymorphisms with the breast cancer risk in the Bangladeshi population. *Breast Cancer*, vol. 24, no. 2, pp. 229-237.

37. Ouhtit A., Gupta I., Shaikh Z. (2016) BRIP1, a potential candidate gene in development of non-BRCA1/2 breast cancer. *Front. Biosci*., vol. 8, pp. 289-298.

38. Reinbothe S., Larsson A., Vaapil M., et al. (2014) EPO-independent functional EPO receptor in breast cancer enhances estrogen receptor activity and promotes cell proliferation. *Biochem Biophys Res Commun*., vol. 445, no. 1, pp. 163-169.

39. Burdon K., McKay J., Sale M., et al. (2003) Mutations in a novel gene, NHS, cause the pleiotropic effects of Nance-Horan syndrome, including severe congenital cataract, dental anomalies, and mental retardation. *Am J Hum Genet*., vol. 73, no. 5, pp. 1120-1130.

40. Chang C., Wei W., Han D., et al. (2017) Expression of Nischarin negatively correlates with estrogen receptor and alters apoptosis, migration and invasion in human breast cancer. *Biochem Biophys Res Commun*., vol. 484, no. 3, pp. 536-542.

41. Atambayeva S., Niyazova R., Ivashchenko A., Pyrkova A., Pinsky I., Akimniyazova A., Labeit S. (2017) The Binding Sites of miR-619-5p in the mRNAs of Human and Orthologous Genes. *BMC Genomics*, vol. 18, no. 1, p. 428.

42. Ivashchenko A., Berillo O., Pyrkova A., Niyazova R., Atambayeva Sh. (2014) The properties of binding sites of miR-619-5p, miR-5095, miR-5096 and miR-5585-3p in the mRNAs of human genes. *Biomed Res Int*, vol. 2014, p.e8.

IRSTI 34.25.39

[1*]A.M. Alexandrova, [1]O.V. Karpova, [1]R.M. Nargilova, [1]R.V. Kryldakov, [1]A.S. Nizkorodova, [1]A.V. Zhigaylov, [2]E.M. Yekaterinskaya, [3]S.V. Kushnarenko, [4]R.Zh. Akbergenov, [1]B.K. Iskakov

[1]M. Ajtkhozhin Institute of Molecular Biology and Biochemistry, Almaty, Kazakhstan
[2]A. Baitursynov Kostanay State University, Kostanay, Kazakhstan
[3]Institute of Plant Biology and Biotechnology, Almaty, Kazakhstan
[4]Institute of Medical Microbiology, University of Zurich, Switzerland
[*]e-mail: alena_pisarenko@inbox.ru

Distribution of potato (*Solanum tuberosum*) viruses in Kazakhstan

Abstract: Potato is one of the most popular crops, cultivated around the world. The decrease in potato yield is caused by the degeneration of the seed material associated with the defeat of various diseases. Viruses pose a great threat to potato farming all over the world. Viral infections are dangerous not only by a significant decrease in the potato yield, but also by the absence of a phenotypic manifestation of diseases. The use of modern mpRT-PCR and ELISA methods for the diagnostics allows detecting viral infection quickly and reliably. The purpose of our research was to compare the efficiency of the molecular diagnostic methods of ELISA and mpRT-PCR and on their basis to study the degree of potato damage by the PLRV, PVM, PVS, PVX and PVY viruses in the southeast and north of Kazakhstan. There were analyzed 119 samples from Almaty and 138 samples from Kostanay regions. Most of tested potato samples were infected by PVM and PVS. PLRV was absent in the southeast and north of Kazakhstan. Complex viral infections were dominance over the monoviral infection. The reliability of ELISA and mpRT-PCR methods for the diagnostics of PVX, PVY, PVM, PVS and PLRV was assessed. Viruses PVS, PVX and PVY were more effectively detected by the mpRT-PCR than ELISA. ELISA was more effective for PVM. The reliability and efficiency of analytical methods highly depended on the variability of the nucleotide and amino acid sequences of virus isolates. We found two isolates of the PVS and three PVM isolates in the course of optimization of the mpRT-PCR method.
Key words: potato viruses, PVX, PVY, PVM, PVS, PLRV, mpRT-PCR, ELISA.

Introduction

Originally grown in the Andes, introduced to Europe in the 16th century, potato is one of the main agricultural crops cultivated all over the world, which production is growing every year [1]. It is the second most popular crop stable food after wheat, which is cultivated in all areas of Kazakhstan except Mangystau region. The potato crop area was 183.4 thousand hectares in 2017 and the largest areas were in Almaty and Kostanay (39 and 27.8 thousand hectares, respectively) [2]. In our country, this culture of foreign and domestic selection are grown [3]. However, potato production in the southeast part of Kazakhstan does not provide the needs of the local population due to its low yields. The productively of potato was 1852 kg per hectare in Almaty and 1957 kg per hectare in Kostanay in 2017. The decrease in potato yield is caused by the degeneration of the seed material associated with the nature defeat of various diseases (viral, bacterial, and fungal).

One of the most important problems of potato growing is viral infections, leading to annual significant crop losses [3]. To date, about 40 potato viruses have been identified [4]. The most common and harmful potato viruses are Potato leaf roll virus (PLRV), Potato virus M (PVM), Potato virus S (PVS), Potato virus X (PVX) and Potato virus Y (PVY). Propagation of viruses occurs in nature by insect vectors (various types of aphids, leafhoppers, whitefly), nematodes, and also by mechanical contact between infected and healthy plants. There are cases of transfer of viruses through pollen and seeds [5].

There are primary and secondary infections of plants. In the case of a primary infection, the infection of the plant occurs during the growing season and is characterized by the spread phase of the viral infection from the diseased stalk to the healthy, and

 Printed in Kazakhstan

then the infection accumulates in the tubers, while a part of the tubers may remain uninfected. In secondary infection, the virus spreads systematically from the mother tuber throughout the plant and is transmitted to all daughter tubers [6].

The symptoms of viral infection are different types of mosaic: wrinkled, banded, ordinary as well as necrosis, leaf curling, broom tops, etc. [3]. However, often the phenotypic manifestation of viral infections is absent or weakly expressed. It is not possible to determine the presence of a particular virus by external manifestations reliably in this case.

At present, the methods of enzyme-linked immunosorbent assay (ELISA) and reverse transcription polymerase chain reaction (RT-PCR) are widely used to diagnose viral infections of potato plants [7-9]. These methods are fairly simple to use and have a high degree of reliability of the results of the analysis.

Diagnosis of potato for the presence of viral infections is a necessary stage of the evaluation of seed material, potato recovery technologies, as well as a general assessment of the viral background in a separate area.

This paper describes the compare of efficiency of molecular diagnostic methods, including double antibody sandwich enzyme-linked immunosorbent assay (DAS-ELISA) and multiplex RT-PCR (mpRT-PCR) and gives the characteristics of the prevalence level of potato viruses on the territory of Almaty and Kostanay regions in 2013-2017.

Materials and methods

In vitro potato plant samples obtained by the method described earlier [10] from tubers growing in Almaty region and potatoes leaves and tubers from fields of Kostanay region were used for the analysis. The potato tubers were germinated before testing in individual pots in laboratory conditions.

There were analyzed 119 plant samples from Almaty (from field collection of Kazakh Research Institute of Potato and Vegetables Growing) and 138 samples from Kostanay (from field collection North-Kazakhstan Research Institute of Agriculture and Kostanay Research Institute of Agriculture) regions in total. Leaves and tubers were collected in 2013-2017.

Potato leaves were tested for PVX, PVY, PVM, PVS and PLRV infection by DAS-ELISA using the kits "BIOREBA" (Switzerland). The 405 nm values were recorded using a plate reader (model Stat Fax-2100, "Awareness Technology", USA). Samples were considered positive if the absorbance values were high than the value of corresponding negative control and higher than 0.1 after incubation for 45 min at room temperature. Assay for each sample was carried out at least three times.

Total RNAs were extracted from fresh or freeze leaves (0.5-1.0 g) using TRIzol reagent (Sigma-Aldrich, USA) according to the manufacture instruction. The pellets were dissolved in 50 µl RNase-free water.

To synthesized first-strand complementary DNA (cDNA) we used 2 µg of total RNA, an oligo$(dT)_{18}$ as reverse primer at 10 pmol final concentration and Maxima (Moloney murine leukemia virus) Reverse Transcriptase (Thermo Fisher Scientific, Lithuania).

Reaction was carried out in 30 µl according the manufacture's instruction. Synthesized cDNA was amplified using *Taq* DNA polymerase (Thermo Fisher Scientific, Lithuania).

The primers were designed to conservative regions of coat protein-coding sequences of PVX, PVS, PVY and PVM or a large capsid protein P3 of PLRV (Table 1). PCR was carried out in volume of 25 µl using 2.5 µl cDNA and five primer pairs at final concentration of 2 pmol.

The PCR program consisted of 5 min at 94°C, 30 cycles of 30 s at 94°C, 30 s at 57°C and 45 s at 72°C followed by the final extension for 5 min at 72°C. PCR was conducted on Gene Amp PCR System 9700 (Applied Biosystems, USA). PCR products were analyzed in 2% agarose (TopVision Agarose, Thermo Fisher Scientific, Lithuania) gel.

Results and discussion

Potato viruses in Kazakhstan. We have studied the potato samples from Almaty and Kostanay regions. Some viruses were detected PVM, PVS, PVY, while PVX and PLRV could not be diagnosed in tested plant samples, although it was believed that these viruses were spread throughout the potato growing regions of Kazakhstan [2; 3]. This indicates that there is currently no PLRV in the southeast and north of Kazakhstan. Perhaps this is due to the peculiarities of interaction between the virus and the insect vector, however this issue is still insufficiently studied.

PVM was the most common potato virus in Kazakhstan (Figure 1, A). As can be seen from the Figure 1 (A), the total number of samples infected with the virus, was as follows: for the Almaty region – 84.03%, for the Kostanay region – 80.84%. PVS was more common in the north of the Republic (46.11% vs. 36.97% in southeast), and PVY, on the contrary, was more typical for southeast Kazakhstan (24.37% vs. 5.99% in north). The incidence of PVX was almost equal for Almaty and Kostanay areas and was 2.52% and 2.99%, respectively.

Table 1 – Nucleotide sequences of primers used for mpRT-PCR

Primer names	Genome position*	Full nucleotide sequences	Fragment size (bp)	References
#PVX-Forward	5664-5683	5' – tagcacaacacaggccacag – 3'	562	8
#PVX-Reverse	6205-6225	5' – ggcagcattcatttcagcttc – 3'		8
#PVY-Forward	8723-8742	5' – acgtccaaaatgagaatgcc – 3'	480	8; 17
#PVY-Reverse	9183-9202	5' – tggtgttcgtgatgtgacct – 3'		8; 17
#PVM-Forward	7242-7264	5' – gaaagctgaaactgccaaagatg – 3'	521	19
#PVM-Reverse	7737-7762	5' – catctgcagttatagcacctcttgg – 3'		19
#PLRV-Forward	3653-3672	5' – cgcgctaacagagttcagcc – 3'	336	8; 18
#PLRV-Reverse	3969-3988	5' – gcaatgggggtccaactcat – 3'		8; 18
#PVS – Forward	7543-7561	5' – tggcgaacaccgagcaaatg – 3'	187	16
#PVS – Reverse	7707-7728	5' – atgatcgagtccaagggcactg – 3'		16
#PVS-new-Forward	7457-7477	5' – atgaaatgcggaggaatccgg – 3'	280	This paper
#PVS-new-Reverse	7690-7715	5' – actgctccagttgggaactcaacagt – 3'		This paper

*Primer positions of gRNA were chosen according following NCBI GenBank acc. numbers: EU571480.1 (PVX), NC001616.1 (PVY), NC001361.2 (PVM), AF453394.1 (PLRV), KC430335.1 (PVS)

Variants of viruses and maximal values for each infection are indicated on the abscissa. The percent of infected plant samples on ordinate. A – The general level of distribution of viruses in Almaty and Kostanay regions; B – Levels of individual and complex viral infections in Almaty and Kostanay regions

According to literature data, in 1994-1996 the degree of virus infections was as follows in the territory of the Republic of Kazakhstan: PLRV – up to 85.7%, PVM – up to 85.7%, PVS – up to 100%, PVX – up to 96%, PVY – up to 85.7% [6; 11-12]. Consequently, PVS and PVX were the most common, although the level of infection with other viruses was also very high.

In the Southern region of Kazakhstan in 2014, rate of potato infestation was: PLRV – 5%, PVM – 8.5%, PVS – 31.7%, PVX – 41.9%, PVY – 14.5% [13].This fact also indicates the prevalence of PVX and PVS, although the overall level of virus infection of potato plants was lower by 2-3 times compared to the mid-1990s.

The study of the prevalence of viral infections in East Kazakhstan indicated the prevalence of PVM (10 varieties of 15 were infected), the incidence of PVS and PVY was the same (4 out of 15) [14]. The lowest level of spread was observed for PVX – 3 of 15 varieties were infected. Unfortunately, there was no information about the level of PLRV infection.

Based on the results obtained, at present the level of potato infection in Kazakhstan for PVX and PVY had decreased, but for PVM and PVS had increased. These results not only testify to the significant spread of viruses in the territory of Kazakhstan, but also that the degree of prevalence of a particular virus is not constant and changes over time.

Individual and complex viral infection. When we were studying the potato virus diseases, we compared the prevalence of individual and complex infections in Almaty to Kostanay regions (Figure 1, B). The individual (monovirus) infections were caused by PVM, PVS or PVY as it can be seen at Figure1, B. By the literature information in the complex infection (when plants infected two or more types of viruses) were found up to five different types of viruses simultaneously [4].

Potato samples were found infected with three types of viruses at the same time. PVX was found only as part of a complex infection with PVM or in a mixture of PVM + PVS. The incidence of potato by monoviral infection was as follows: PVM – 36.13%, PVS – 0.84%, PVY – 5.88% for the southeast of Kazakhstan. In the northern region, PVM was the single example of monoinfection (28.74%). PVS and PVY were detected only as part of complex infection. The overall level of a single infection was 42.85% for the Almaty region and 28.74% for the Kostanay region.

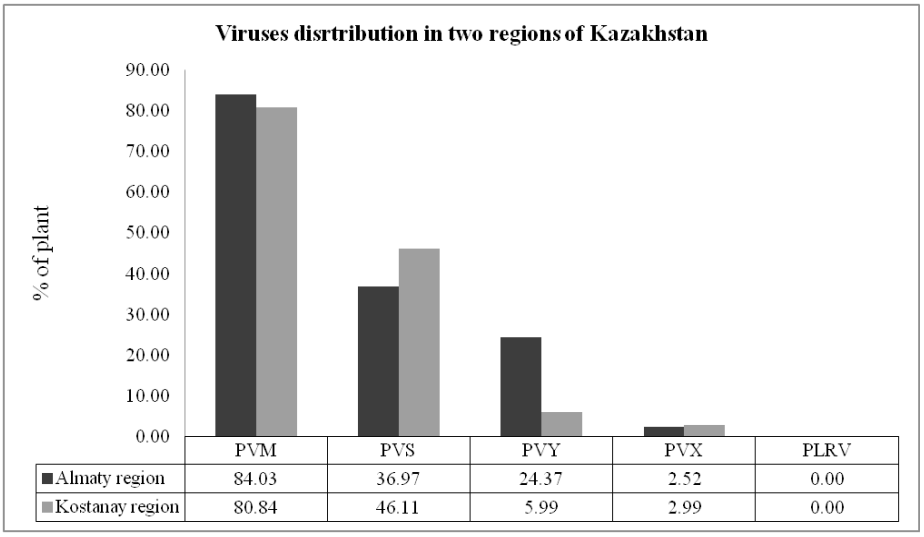

	PVM	PVS	PVY	PVX	PLRV
Almaty region	84.03	36.97	24.37	2.52	0.00
Kostanay region	80.84	46.11	5.99	2.99	0.00

a

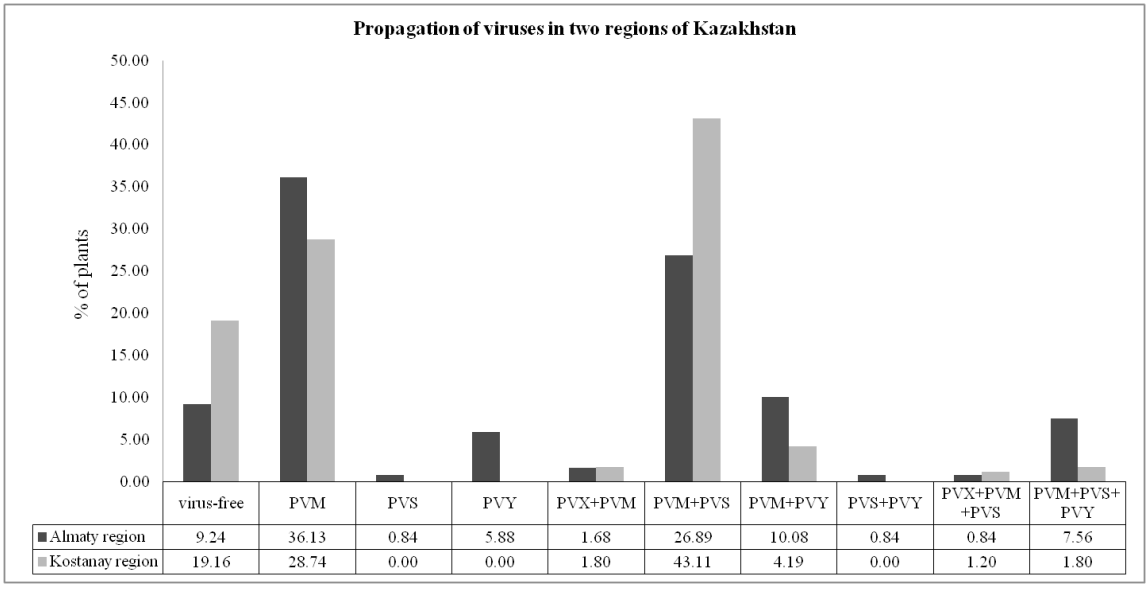

	virus-free	PVM	PVS	PVY	PVX+PVM	PVM+PVS	PVM+PVY	PVS+PVY	PVX+PVM +PVS	PVM+PVS+ PVY
Almaty region	9.24	36.13	0.84	5.88	1.68	26.89	10.08	0.84	0.84	7.56
Kostanay region	19.16	28.74	0.00	0.00	1.80	43.11	4.19	0.00	1.20	1.80

b

Figure 1 – Distribution of virus infections in Kazakhstan

The prevalence of complex infection varied between the two regions. It was 47.91% in Almaty area, while it was 52.1% in Kostanay area. Among the most common the complex infection was a combination of PVM + PVS: 26.89% in Almaty and 43.11% in Kostanay region. The ratio of mixed infection PVM + PVY was assessed as 10.08% in Almaty and 4.19% in Kostanay. Whereas the level of virus combination PVM + PVX was approximately the same for both regions 1.68% and 1.8%, respectively. The presence of PVS + PVY in samples was found only in the Almaty region (0.84%), and completely was absent in the Kostanay region. The main viruses (PVM and PVS) of the three-part infection belonged to carlaviruses, the third virus was either PVX or PVY. Complex infection of PVM + PVS + PVX was observed in samples from Almaty region (0.84%) and Kostanay region (1.2%) and was approximately at the same level. However, complex infection PVM + PVS + PVY was more distributed in Almaty region (7.56%) than in Kostanay (1.8%).

The total number of potato plant samples free from viral damage was 9.24% in Almaty region, and 19.16% in Kostanay region. Because in the south there are several periods of mass flying of aphids, which are the main vectors of viruses, the probability

of potato infection is increased in the these regions than in the north.

Thus, it was confirmed that potatoes grown in a cool climate are less susceptible to viral infection. The incidence of potato by PVX does not depend on the climatic conditions of the regions. The combination of PVM + PVS is currently the main type of viral infections of potatoes in the Republic of Kazakhstan.

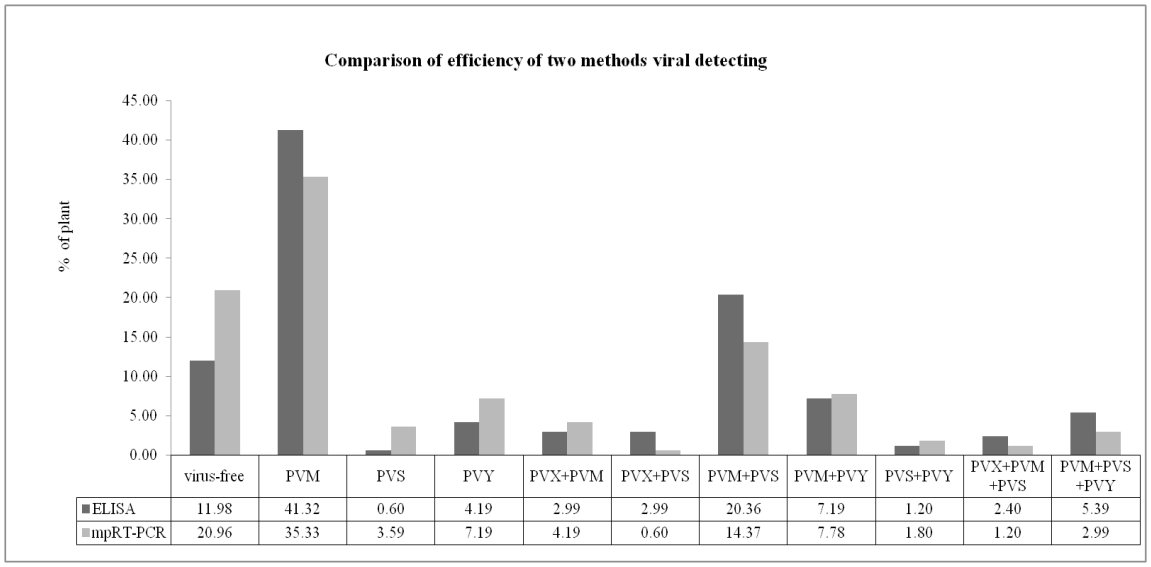

	virus-free	PVM	PVS	PVY	PVX+PVM	PVX+PVS	PVM+PVS	PVM+PVY	PVS+PVY	PVX+PVM +PVS	PVM+PVS +PVY
ELISA	11.98	41.32	0.60	4.19	2.99	2.99	20.36	7.19	1.20	2.40	5.39
mpRT-PCR	20.96	35.33	3.59	7.19	4.19	0.60	14.37	7.78	1.80	1.20	2.99

Figure 2 – Comparison of efficiency of ELISA and mpRT-PCR

Variants of viruses and maximal values for each infection are indicated on abscissa.
Percentage of infected plant samples on ordinate

Comparison of the efficiency of ELISA and RT-PCR methods. Since the sensitivity of the analytic methods is a fundamental factor in the diagnostics of viral infections, we compared the efficiency of ELISA and mpRT-PCR methods to detect viruses in plant samples from Almaty and Kostanay areas (Figure 2).

There was shown from Figure 2, individual PVS or PVY virus was more effectively detected by mpRT-PCR (3.59% and 7.19%), in contrast to ELISA (0.6% and 4.19%, respectively). The ELISA method proved to be the more effective for PVM than mpRT-PCR (41.32% versus 35.33% respectively). PVM was not detected by mpRT-PCR if its ELISA reading was less than 0.4 units from negative control. Although according to the manufacturer recommendations of the ELISA kit, this value considered positive. Apparently, this was due to the peculiarities of the nucleotide sequence of genomic RNA (gRNA) and the amino acid sequence of the PVM isolate coat proteins, distributed in the territory of Kazakhstan. There is evidence that the efficiency of the ELISA kits is directly correlated with the amino acid sequence features of different PVM isolates, had various territorial distribution [5]. The primers for mpRT-PCR we used are complementary to the conservative regions of the gRNA encoding the PVM coat protein. Thus, PVM could more reliably detect by the ELISA both in single and complex infection.

The complex infections PVX + PVM, PVM + PVY and PVS + PVY were more accurately detected by mpRT-PCR method (4.19%, 7.78% and 1.8%, versus ELISA 2.99%, 7.19% and 1.2%, respectively). Diagnostics by ELISA was more effective for combinations of viruses PVX + PVS (2.99% vs. mpRT-PCR 0.6%), PVM + PVS (20.36% vs. 14.37%), PVX + PVM + PVS (2.4% vs. 1.2%) and PVM + PVS + PVY (5.39% vs. 2.99%).

It should be noted that the PVM was the dominant virus in complex infection. The low efficiency of the mpRT-PCR could be associated with the dominance of PVM gRNA compared to other virus RNAs in reaction mix. Other kinds of RT-PCR products could be found in minor amount. ELISA method permits to detect only one type of virus, so there is no competition for the reaction components. Also, this method allows using of frozen material for analysis, whereas it is preferable to investigate fresh one by mpRT-PCR.

The discrepancy between the results of ELISA and mpRT-PCR often occurred in the diagnostics of PVS, while the presence of the virus was confirmed

only by the ELISA. In our opinion, this is due to the variety of PVS isolates common in Kazakhstan. Different isolates are characterized by the presence of features of the nucleotide composition of the gRNA, while the amino acid composition of proteins remains almost identical. Currently, there is no information on the diversity of PVS and PVM viruses isolates in the Republic of Kazakhstan. Therefore, to confirm viral diseases in the field, ELISA method is suitable because it is simple and not uses expensive equipment. The ELISA method does not allow the identification of different virus isolates, in which case the use of mpRT-PCR is more preferable. However, there were cases in our practice when the presence of a viral infection was confirmed only by the mpRT-PCR. Thus, it is sufficient to use ELISA for the analysis of potato plants for the presence of viral infections in the field. However, if it is necessary to confirm the purity of the plant material under study, we consider it expedient to use two diagnostic methods.

Variety of PVM and PVS isolates in the Republic of Kazakhstan. PVM and PVS are related viruses and belong to the Carlavirus group. According to NCBI GeneBank, there are many local populations of these viruses, distributed in various regions of the world and having the features of the nucleotide composition of the gRNA. PVS is subdivided into three subgroups: Andean (PVS^A), Ordinary (PVS^O) and Antioquia (PVS^P) [15]. Two subgroups of PVS^A and PVS^O are distributed around the world and are represented by a variety of different isolates. It is believed that the PVS^A subgroup is more aggressive with respect to the host plant. While PVS^O does not cause significant damage to potato plantings and is a moderate virus.

The hypothesis about the presence of different isolates of the Carlavirus group in our Republic was confirmed during the computer analysis of the gRNA sequences encoding the coat proteins of various PVS isolates. So, it turned out that the primers #PVS – Forward and #PVS – Reverse were used to identify the European PVS isolate (the size of the PCR-amplificated fragment was 187 bp [15], Table 1) had incomplete complementarity to the isolates first discovered in China and South America. When primers #PVS-new-Forward and #PVS-new-Reverse were used matched to the most conservative region of PVS gRNA (after sequencing), the efficiency of PVS detection significantly increased.

The results of analysis of some potato samples from the Almaty region were shown in the Figure 3 (A). Samples 1 and 2 contained DNA fragments of PVM (520 bp) and PVS (280 bp). In addition, there were no fragments of DNA 187 bp in size, which would indicate the presence of a European PVS isolate. Samples 7, 8 and 9 had both DNA fragments 187 bp specific for the European PVS isolate as well as 280 bp fragments, were universal for different isolates and identified in all samples.

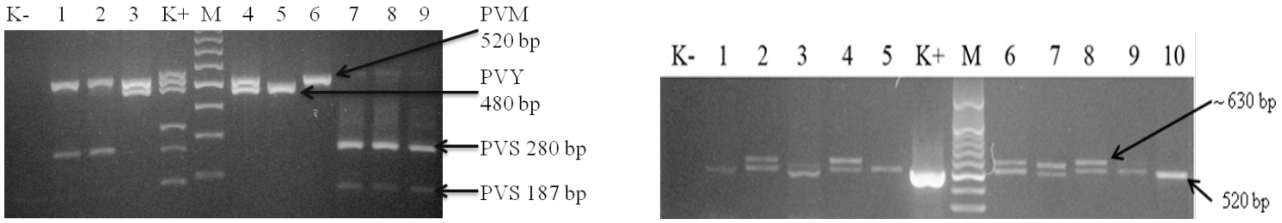

a b

Figure 3 – Results of agarose gel electrophoresis of RT-PCR products. K – negative control, K+ positive control, M – marker DNA (GeneRuler™ 100 bp)

A – Results of electrophoresis in a 2% agarose gel after mpRT-PCR diagnostics of potato samples from the Almaty region. 1-9 – sample numbers, arrows indicate amplified DNA fragments for PVM (fragment size 520 bp), PVY (fragment size 480 bp), and PVS (fragment size 280 bp and 187 bp);

B – Results of electrophoresis in a 1.5% agarose gel of uniplex RT-PCR products in the diagnosis of PVM in samples from the Kostanay region. 1-10 – numbers of samples, arrows indicate the corresponding DNA fragments

Thus, we can detect the European isolate of PVS and distinguish it from other isolates.

When we analyzed some potato samples obtained from the Kostanay region, it was found differences during diagnostics of PVM by two methods. As a result it was decided to use the uniplex RT-PCR to PVM diagnostics. Two DNA fragments were identified in samples 2, 4, 6, 7, 8 and 9, expected fragment

of 520 bp in size, and a heavier one of 630 bp in size (Figure 3 (B)). Samples 1, 5 and 10 contained one DNA fragment corresponding to the expected size of 520 bp. It was found a shorter DNA fragment measuring ~ 500 bp in sample 3. Accordingly, there are three different PVM populations in the territory of the Kostanay area.

As a result, we detected two various PVS isolates and three PVM isolates on the territory of Kazakhstan.

Conclusion

There are PVX and PVY among the most dangerous viruses on the territory of Kazakhstan, which lead to death, as well as PVM and PVS, which provoke a secondary infection. Potato is less prone to viral infections in the northern regions. After comparing the degree of potato infection with viral diseases in two regions of Kazakhstan, the most common virus is PVM, the infection level of which reaches 84.03% in Almaty and 80.84% in Kostanay regions.

The ELISA method is advisable for diagnostics of potato viruses in the field conditions, when there is a need for an overall assessment of the level of contamination of potatoes. However, if necessary to analyze individual samples accurately, two supplementary methods ELISA and mpRT-PCR should be used. The efficiency of detecting viral infections by mpRT-PCR depends on the nucleotide sequence of genomic RNAs of the viruses being analyzed. The mpRT-PCR allows not only to detect a viral infection, but also to determine isolates of viruses.

References

1. Birch R.J.P., Bryan G., Fenton B., Gilroy E. G., Hein I., Jones J. T., Prashar A., Taylor M.A., Torrance L., Toth I.K. (2012) Crops that feed the world 8 – Potato: are the trends of increased global production sustainable? *Food Security*, vol. 4, pp. 477-508.

2. The Committee on Statistics Ministry of National Economics of the Republic of Kazakhstan (www.stat.gov.kz).

3. Krasavin V.F. (2009) Selekcija kartofelja na jugo-vostoke Kazahstana [Potato selection in the southeast of Kazakhstan], 1st ed., *Almaty: Oner*, p. 224.

4. Antonova O.Ju., Apalikova O.V., Uhatova Ju.V., Krylova E.A., Shuvalov O.Ju., Shuvalova A.R., Gavrilenko T.A. (2017) Ozdorovlenie mikrorastenij treh kul'turnyh vidov kartofelja (*Solanum tuberosum* L., *S. phureja* Juz. & Buk. i *S. stenotomum* Juz. & Buk.) ot virusov metodom kombinirovannoj termo-himioterapii [Eradication of viruses in microplants of three cultivated potato species (*Solanum tuberosum* L., *S. phureja* Juz. & Buk., *S. stenotomum* Juz. & Buk.) using combined thermo-chemotherapy method]. *Sel'skohozjajstvennaja biologija*, vol. 52, no. 1, pp. 95-104.

5. Gavrilenko T.A., Rogozina E.V., Antonova O. Ju. (2005) Sozdanie ustojchivyh k virusam rastenij kartofelja na osnove tradicionnyh podhodov i metodov biotehnologii [The creation of plant-resistant potatoes based on traditional approaches and biotechnology methods]. Identificirovannyj genofond rastenij i selekcija. *St.-Piterburg: Gosudarstvennyj nauchnyj centr Rossijskoj Federacii Vserossijskij nauchno-issledovatel'skij institut rastenievodstva im. N.I. Vavilova*, p. 896.

6. Askarova M.A., Manadilova A., Sadvakasova G.G., Kunaeva R.M., Lobenshtajn G. (1997) Issledovanie kartofel'nyh polej Kazahstana na virusnoe zarazhenie [Research of potato by viral infection in Kazakhstan's fields]. *Biotehnologija. Teorija i praktika*, vol. 2, pp. 26-32.

7. Huttinga, H. (1996) General Aspects on diagnostic Methods: Viruses Microorganisms. Proceedings of the 4th International Symposium of the European Foundation for Plant Pathology (September 9–12), *Germany: Bonn*, p. 556.

8. Nie X., Singh R.P. (2001) A novel usage of random primers for multiplex RT-PCR detection of virus and viroid in aphids, leaves, and tubers. *J of Virology Meth.*, vol. 91, pp. 37-49.

9. Crosslin J.M., Hamlin L.L. (2011) Standardized RT-PCR conditions for detection and identification of eleven viruses of potato and *Potato spindle tuber viroid*. *Am. J of Potato Research,* vol. 88, pp. 333-338.

10. Kushnarenko S.V., Romadanova N.V., Aralbaeva M.M., Matakova G.N., Bekebaeva M.O., Babisekova D.I. (2013) Sozdanie kollekcii *in vitro* sortov i gibridov kartofelja kak ishodnogo materiala dlja kriokonservacii [Creation of *in vitro* collection of cultivars and hybrids of potatoes as a raw material for cryopreservation]. *Biotehnologija. Teorija i praktika*, no. 1, pp. 28-33.

11. Manadilova A.M., Sadvakasova G.G., Bekel'man E., Lobenshtajn G. (1998) Diagnostika Y-virusa kartofelja metodom immunoferentnogo analiza [Diagnostics of Potato virus Y by ELISA]. *Biotehnologija. Teorija i praktika*, no. 3, pp. 50-54.

12. Sadvakasova G.G., Bekel'man E., Lobenshtajn G. (1997) Ochistka virusa S kartofelja iz *Chenopodium amaranticolor* i ego detekcija immunofermentnym metodom [Purification of the Potato virus S from the

Chenopodium amaranticolor and its detection by ELISA]. *Biotehnologija. Teorija i praktika*, no. 2, pp. 33-38.

13. Ospanova G.S., Bozshataeva G.T., Turabaeva G.K., Alihanova A. (2014) Virusnye bolezni paslenovyh v Kazahstane [Virus diseases of *Solanaceae* in Kazakhstan]. *Mezhdunarodnyj zhurnal prikladnyh i fundamental'nyh issledovanij. Sel'skohozjajstvennye nauki*, no. 3, pp. 62-64.

14. Kuz'mina G.N., Akzambek A.M., Kabataeva Zh. K. (2017) Zarazhennost' kartofelja virusnymi infekcijami v Vostochnom Kazahstane [Contamination of potato by viral infections in East Kazakhstan]. *Materialy XLI Mezhdunarodnoj nauchno-prakticheskoj konferencii KazATK im. M. Tynyshpaeva na temu: «Innovacionnye tehnologii na transporte: obrazovanie, nauka, praktika»*, vol. 1, pp. 520-522.

15. Vallejo C. Daniela, Gutiérrez S., Pablo Andrés, Marín M. Mauricio (2016) Genome characterization of a Potato virus S (PVS) variant from tuber sprouts of *Solanum phureja* Juz. *et* Buk. *Agronomía Colombiana*, vol. 34, no. 1, pp. 51-60.

16. Matoušek J., Schubert J., Didic P. (2000) A broad variability of potato S carlavirus (PVS) revealed by analysis of RT-PCR-amplified virus sequences. *Can J of Plant Path*., vol. 22, pp. 29-37.

17. Singh R.P., Kurz J., Boiteau G. (1996) Detection of stylet-borne and circulative potato viruses in aphids by duplex reverse transcription polymerase chain reaction. *J of Vir Meth.,* vol. 59, pp. 189-196.

18. Singh R.P., Kurz J., Boiteau G., Bernard G. (1995) Detection of potato leaf roll virus in single aphids by reverse transcription polymerase chain reaction and its potential epidemiological application. *J of Vir Meth*., vol. 55, pp. 133-143.

19. Kushnarenko S., Romadanova N., Aralbayeva M., Zholamanova S., Alexandrova A., Karpova O. (2017) Combined ribavirin treatment and cryotherapy for efficient Potato virus M and Potato virus S eradication in potato (*Solanum tuberosum* L.) *in vitro* shoots. *In Vitro Cellular & Developmental Biology Plant,* vol. 53, pp. 425-432.

IRSTI 34.31.37

[1]G.A. Shalakhmetova, [2]S. Nayekova, [3]M. Sagi, [2*]Z. Alikulov

[1]Al-Farabi Kazakh National University, Almaty, Kazakhstan
[2]L.N.Gumilov Eurasian National University, Astana, Kazakhstan
[3]Ben Gurion University, Beer Sheva, Israel
[*]e-mail: zer-kaz@mail.ru

The effect of presowing saturation with molybdatenum and presence of nitrate on the allantoin content in sprouted wheat grain

Abstract: It is generally known that when the grain is primed, saturated with a solution of biologically important elements and subsequently dried, the aleurone layer selectively permits ions of various metals. It is also known that in the case of a deficiency of molybdenum in the soil, a non-molybdenum inactive population of molecules of xanthine dehydrogenase and nitrate reductase is synthesized in plant cells. Presowing priming of wheat grain in molybdate solution of optimal concentration allows grain to germinate more actively. Upon germination of the wheat grain, in the process of embryo cells division, exogenous molybdenum is incorporated into the molecule of the non-molybdenum forms of the newly synthesized molybdoenzymes – nitrate reductase and xanthine dehydrogenase. This leads to the complete activation of the non-molybdenum forms of nitrate reductase and xanthine dehydrogenase in sprouted wheat grain. Since nitrate assimilation induces nitrate reductase synthesis, which uses reduced nicotinamide adenine dinucleotide as donor of electrons, nicotinamide adenine dinucleotide oxidized pool is formed in the cells, what is specifically required for the oxidation of xanthine to allantoin (via uric acid) by xanthine dehydrogenase. Our results show that prior to sowing priming of wheat grain of the "Baiterek" cultivar in molybdate solution and further growth in a nitrate containing medium abruptly increases the content of the antioxidant allantoin in germinated grain.

Key words: allantoin, xanthine dehydrogenase, nitrate reductase, priming, wheat, molybdenum.

Introduction

Allantoin is an important reserve and transport form of nitrogen in plants, that is to say allantoin is the source of the amino group for the biosynthesis of amino acids and is easily transported by plant conducting pathways [1; 2]. Numerous studies show that purine catabolism plays a role not only in the metabolism of nitrogen, but also affects plant resistance to adverse abiotic factors (soil salinity and drought) [3; 4]. Exogenous allantoin increased the viability and the growth rate of *Arabidopsis thaliana* sprouts grown in a medium containing sodium chloride (NaCl) [3]. A direct correlation was observed between the level of allantoin in seeds and the resistance of seedlings to low temperature and drought [4].

Molybdenum (Mo) is an essential element for higher plants and plays a vital role in many physiological and biochemical processes. Four of molybdoenzymes have been found in plants, namely nitrate reductase (NR),aldehyde oxidase (AO), xanthine dehydrogenase (XDH) and sulfite oxidase (SO) [5]. These molybdoenzymes participate in diverse metabolic processes, such as nitrate assimilation, phytohormone synthesis, purine catabolism and sulfite detoxification in plants [6]. Among them, AO has been shown to catalyse the final steps in the conversion of indole-3-acetaldehyde to indole-3-abscisic acid (IAA), and the oxidation of abscisic aldehyde to ABA [7]. Mutations in either AO apoprotein or enzymes involved in Mo-cofactor (Moco) biosynthesis and Moco activation (sulfuration) disrupt ABA synthesis [5; 8]. A low ABA level results in a wilty appearance of plants as a result of excessive transpiration, loss of stomatal control, altered seed dormancy and impaired defense responses to environmental stress [6; 7]

Stress activates AO as well as Moco-hydroxylase-sulfurylase (MHS) enzyme, which in turn activates AO and XDH, changing one of Mo's atoms of oxygen for sulfide [9; 10].

The two inorganic N-forms readily available for uptake by plants, NO_3^- and NH_4^+, switch on N-assimilation specifity pathways to synthesize fundamental

 Printed in Kazakhstan

cell components such as amino acids, nucleic acids, proteins and photosynthetic pigments [11].

The key and rate-limiting enzyme for NO_3^-assimilation is nitrate reductase (NR, EC 1.6.6.1). This enzyme catalyzes the first step in the NO_3^- reduction pathway to yield NO_2^-, which is then further reduced to NH_4^+. The latter ion is incorporated into organic N-compounds by the activity of the enzymes glutamine synthetase and glutamate synthase (the GS/GOGAT pathway). The resulting amino acids, glutamine and glutamate then serve as substrates to produce additional amino acids [12]. While NO_3^- transport and assimilation occur practically throughout the entire plant, NH_4^+ is taken up directly into the roots and the resulting assimilation products are transported to the growing plant parts [13; 14].

Generally, plants may transport N in the form of amides (glutamine and asparagine) and/or ureides (allantoin and allantoate). Ureides are more rich in N (4N:4C) in comparison to amides and amino acids and, therefore, their involvement in the transport of assimilated ammonia from the root to the shoot minimizes loss of carbon originating from photosynthesis [15].

Xanthine dehydrogenase (XDH, EC 1.2.1.37) is an important enzyme in purine catabolism where it catalyzes the oxidative hydroxylation of hypoxanthine to xanthine and xanthine to uric acid that ultimately yields the purine degradation products, ureides (allantoin and allantoate) [16; 17]. Recently, AtXDH1 transcript was shown to be induced by drought, salinity and abscisic acid treatments [18-20], indicating a role for XDH in purine catabolism in plants subjected to environmental stresses.

A common consequence of the influence of abiotic factors on plants is an increase in the intracellular concentration of reactive oxygen species (ROS) [21]. One of the least active forms of oxygen, superoxide, spontaneously or in the presence of transition metals is converted into more aggressive forms, for instance, hydroxyl radical, which can cause damage to many cellular biomolecules – lipids, proteins and DNA. Oxidation of lipids causes lipid peroxidation, i.e. destruction of plasma membranes, oxidation of proteins leads to loss of their function, formation of reactive oxygen species, DNA oxidation might directly induce mutations [21].

Therefore, one of the possible measures, reducing the negative effect of these stresses on plants, can be realized through a system of natural antioxidants. Antioxidants are substances that have the ability to suppress free radical oxidation, are capable of reacting with ROS to form either molecular products or radicals with lower reactivity [21]. One of these potential antioxidants is allantoin. Stability of *Arabidopsis thaliana* to NaCl stress caused by exogenous allantoin was accompanied by a decrease in the formation of ROS in seedlings. Exogenous allantoin stimulated growth and decreased the content of malondialdehyde (the product of membrane peroxidation) in rice seedlings [22], increased the expression of two antioxidant genes in *Arabidopsis thaliana* seedlings under saline conditions [3]. It was shown that allantoin induces ABA adaptive phytohormone synthesis under high salt concentrations [23; 24]. Thus, allantoin is an effective environmental protector against the effects of environmental stressors mediated by oxidative stress.

Allantoin is also used for medicinal purposes. It has been proved that allantoin possesses a keratolytic effect, which promotes cellular regeneration of the skin, rapid healing of abrasions and cracks, and the removal of irritations. Therefore, allantoin is a part of more than 1300 different cosmetic products. When administered orally, it increases the leukocyte count and improves lymph flow, protects the tissues of the stomach and intestines, and facilitates the repair of the gastrointestinal tract [25]. Allantoin is non-toxic and does not cause inflammatory reactions, is effective even in small concentrations.

Allantoin of plant origin is derived from the roots of the comfrey (*Symphytum officinale*), sprouted wheat, soybean and rice hulls [25]. It is well known that wheat germination is a functionally rich stage of wheat growth and germinated grain extract contains a large number of biologically active compounds and antioxidants, including allantoin [26; 27].

One promising approach to improve salt tolerance during germination is seed priming, which implies controlled seed inhibition followed by drying and facilitates the improvement of later development of seedlings [28]. The process of seed priming involves prior exposure to an abiotic stress, making a seed more resistant to future exposure. Seed priming stimulates the pre-germination metabolic processes and makes the seed ready for radicle protrusion. Priming of tomato seeds with 1M NaCl is recommended prior to sowing directly in saline soils [29]. Priming of seeds results in increased activities of the antioxidant enzymes superoxide dismutase, catalase and glutathione reductase. After priming, plant seeds reach higher level of proteins and nucleic acidssynthesis.Priming increases the antioxidant system activity and the process of membranesrepair, promotes seed vigor during germination, and further growth under salinity stress [28].

Based on the above-mentioned information it is of great importance and actuality to study the application of seed priming with relatively high concentrations of essential mineral elements as a fertilization technology to minimize soil and foliar fertilization, thus reducing environmental contamination. Thus, the improvement seed germination and seedling stand under high salinity may enhance not only forestation processes in the Aral Sea region but also reclamation of salt-affected land for crop production in the region.

This paper presents the results of the influence of presowing processing of wheat grain in molybdate solution by priming and germination in the presence of nitrate on the activity of XDH and on the content of allantoin in the germinated grains of this plant.

Materials and methods

Grain and 5-day old seedlings of "Baiterek" soft spring wheat cultivar were used as objects of the study.

The effects of so-called presowing seed priming are now widely studied. Priming means complete saturation of seeds with water and subsequent drying under controlled conditions [28]. The results of numerous studies have shown that simple saturation of plant seeds with water (or solutions of various salts) and subsequent drying leads to an increase in the percentage of their germination, growth and development of seedlings [29]. In our studies, used wheat grain was sterilized for 5 min in 1% potassium permanganate and then thoroughly washed with distilled water.

Priming of wheat seeds was carried out according to the method of Koehler K.H et al. [28]. The activity of NR and XDH was determined without priming on the whole grain and grain parts, endosperm and embryo, and in seeds after priming in water and with various concentrations of sodium molybdate. Dry wheat grain was completely saturated with water for 15 h at the room temperature and dried for 20 h [29]. Untreated and primed seeds were divided into endosperm part and embryo. These parts of the grain were mixed with 10 mM sodium phosphate buffer (pH 6.5 containing 10 μM EDTA) in a ratio of 1:10 (g/ml) and homogenized in a porcelain mortar. The homogenate was centrifuged at room temperature for 15 min at 15,000 g.

In the following experiments, we conducted presowing priming of the seeds in water, in a solution of molybdate and in a solution of tungstate. These seeds were then germinated in a medium containing potassium nitrate. As a control, wheat 5-day old seedlings with emerged radicals were homogenized in sodium phosphate buffer, and the activity of NR and XDH molybdoenzymes was determined without treatment and after heating at 80 °C for 5 min in the presence of 10 mM glutathione (GSH) and 10 mM sodium molybdate. After heat treatment, NR activity was determined by the reduced diaphorasive active benzylviologen by appeared NADH. It is very sensitive to high temperature (the diaphorase domain of NR attaches NADH and transfers electrons to the Moco, and the reduced benzylviologen directly transfers electrons to it).

The activity of NR was determined by a well-known method, where the enzyme was isolated from the wheat grain by chilled buffer containing 25 mM Tris-HCl, pH 8.4, 1 mM DTT, 5 mM cysteine, 3 mM EDTA, 10 μM FAD, 5 μM Na_2MoO_4, and 0.1 mM phenylmethyl sulfofluoride in a ratio of 1:3 [8]. The homogenated plant material was centrifuged at 15,000 g in Sorvall RC-5 centrifuge with cooling at 3-5 °C for 10 min. The nitrate reductase activity was determined in a reaction mixture containing 30 mM K-phosphate buffer (pH 7.5) of 25 mM KNO_3 and 0.25 mM NADN. The enzymatic reaction was carried out at 28°C for 15 min. The reaction was stopped by adding 50 μl of the mixture in a 1:1 ratio (v/v) of 0.3 mM phenazine methosulfate and 1 M Zn acetate followed by precipitation to remove residual NADH. Nitrite was determined in 1 ml of the mixture in a ratio of 1:1 (v/v) 1% sulfanilamide in 3.0 M HCl and 0.02% N-naphthyl (1)-dihydrochloride. Absorption was measured at 540 nm after 20 min. The NR activity was expressed as μmol NO_2^- g^{-1} wet weight per h^{-1}

A well-known method for enzyme extract ion using a buffer containing 10 mM Tris-HCl or 10 mM phosphate buffer (pH 6.5) was used for determination of XDH activity: 0.1 mM EDTA, 1 mM DTT, 10 mM GSH, 5 μM FAD. 1 g of plant material was extracted in the buffer in a ratio of 1:10 [20]. Plant material was centrifuged in a Sorvall RC-centrifuge at 15,000 g and 4°C for 15 min. Obtained supernatant was studied by spectrophotometric measurement of NADH at 340 nm. The reaction mixture contained 1 mM hypoxanthine, 2.5 mM NAD, 1 mM DTT, and 100-200 ml desalted extract 300-500 μg/mg^{-1} protein in 1.5 ml 50 mM phosphate buffer (pH 7.8) at 25 °C.

Extraction of enzyme with buffer containing 10 mM Tris-HCl or 10 mM phosphate buffer (pH 6.5): 0.1 mM EDTA, 1 mM DTT, 10 mM GSH, 5 μM FAD was used to determine the XDH activity [20].1 g of plant material was extracted in the buffer in a ratio of 1:10. The homogenized plant material was

centrifuged in a Sorvall RC-centrifuge at 15,000 g and 4 °C for 15 min, the supernatant obtained was used followed by spectrophotometric measurement of NADH at 340 nm. The reaction mixture contained 1mM hypoxanthine, 2.5 mM NAD, 1 mM DTT, and 100-200 ml desalted extract 300-500 μg/mg^{-1} protein in 1.5 ml 50 mM phosphate buffer (pH 7.8) at 25 °C.

The total amount of allantoin in the germinated grains was determined by the method of Vogels et al. [31]. Ureides were extracted with 80% ethanol in a ratio of 1:4 (v/v). Following extraction, allantoin and allantoic acid were determined using the appropriate standards as described by Vogels and van der Drift [31]. The resulting color formation was estimated spectrophotometrically at 535 nm.

Results and discussion

The precursor of allantoin is uric acid, which is formed during the oxidation of the purine base of xanthine, catalyzed by XDH Mo-containing enzyme [32].

Therefore, we conducted estimation of XDH and allantoin activity in "Baiterek" soft spring wheat cultivar, which were at rest in wheat, and after treatment in distilled water by priming, the activity of XDH and the content of allantoin were determined in the supernatants obtained. The results are shown in Table 1.

Table 1 – XDH activity and allantoin content (mg/g) obtained from wheat grains treated with priming

Variants	XDH activity, nmol UA/mg/min	Allantoin content, mg/g of grain dry weight
Control (whole grain)	>0.3	~0.2
Control (endosperm)	5.4 ± 0.7	>0.1
Control (embryo)	>0.3	1.3 ± 0.2
Priming H_2O (whole grain)	~0.5	~0.2
Priming H_2O (endosperm)	>0.3	>0.1
Priming H_2O (embryo)	7.2 ± 1.3	1.4 ± 0.1

As can be seen from the Table 1, the main content of allantoin is found in the embryo of both forms of wheat grain. Processing of grain using the priming method hardly increased the content of allantoin in the embryo and the endosperm part of the grain. Earlier, we found that the aleurone layer in the endosperm, the germ-free part, in the wheat grain contains XDH [29].

It is well known that the deficiency of molybdenum in the soil leads to a low activity of molybdoenzymes in plants [32].

According to the data of the Institute of Soil Science of the Academy of Sciences, KazSSR, Kazakhstani soils, although alkaline, contain molybdenum 3-5 times less than the critical concentration (0.1 mg Mo/kg for temperate soils) necessary for normal plant growth and development [33]. Earlier, we showed that a non-molybdenum population of XDH is synthesized in the germ of wheat grains, which is activated in vivo by heating (80°C) in the presence of GSH and sodium molybdate [35].

Apparently, the existence of the non-molybdenum forms of XDH is associated with a lack of molybdenum in the soils.

It is supposed that the formation of uric acid and allantoin depends on the level of assimilation of nitrate by plants. Assimilation of nitrates is a fundamental process in the plant kingdom, and therefore the NR enzyme restoring nitrate is regarded as a limiting factor in the growth, development, protein formation and final crop yield. NR is an inducible enzyme, i.e. it is synthesized only in the presence of a medium containing nitrate. In the catabolism of purines, XDH oxidizes xanthine to uric acid. Complete degradation of purines includes the stages of transformation: purine nucleotides → hypoxanthine → xanthine → uric acid (UA) → allantoin [34]. For the oxidation of xanthine, XDH uses oxidized NAD^+ as an electron acceptor. As mentioned above, the product of enzymatic oxidation of xanthine is UA, which is further oxidized with the participation of uricase, or non-enzymatically in the presence of ROS, forming allantoin. Thus, the formation of UA and allantoin directly depends on the concentration of oxidized NAD^+ in the plant cell.

When assimilating nitrate, NR restores it to nitrite (NO_2^-). In the reduction of nitrate, NR as an electron donor uses NADN, thus forming NAD^+. The more nitrate is reduced in the plant cell, the more NAD^+ is formed, required for XDH catalytic reaction. In the oxidation of xanthine, its electrons restore the NAD^+ again, turning it into NADH. The more active is XDH, the more allantoin is formed via UA.

Allantoin, as a potential antioxidant, neutralizing ROS, increases the resistance of plants to oxidative stress caused by unfavorable environmental conditions. It has been established that nitrate nutrition increases plant tolerance to salinity, which might be explained as follows. Since the reduced pyridine

nucleotide NADH is the only physiological electron donor for the catalytic reaction of NR, a high level of nitrate reduction under stress conditions maintains a high level of NAD^+. For the enzymatic reduction of one nitrate molecule, 4 molecules of NADH (8 electrons) of 6 protons are required, thuswise, the assimilation of nitrate is when set beside with of other molecules, the most effective NAD^+–generating reaction [36; 37].

Thus, an important antioxidant role of NR is the constant maintenance of the high level of NAD^+, required for the synthesis of allantoin. Therefore, in our next experiments, we studied the effect of presowing priming of wheat grains in a solution of sodium molybdate on the activity of NR, XDH, and the content of allantoin in sprouted wheat grains. Wheat grains after Mo-priming were grown on a medium containing potassium nitrate.

Our preliminary results showed that the priming of wheat grains in solutions of molybdate sodium to 75 mM concentration does not affect the process of their germination [34]. It was also established that 0.45 mM potassium nitrate concentration is sufficient to induce NR, and therefore, the germination medium contained this concentration of KNO_3 [37]. On the 5th day after the appearance of the radicals in germinated grain, the activity of XDH, NR and allantoin was determined.

Table 2 shows the results of wheat grain priming with molybdenum and tungsten, it can compete with molybdenum for incorporation into the enzyme complex and results in enzyme inactivation [38], their subsequent germination in a medium with nitrate on the activity of NR, XDH, and the content of allantoin in 5-day wheat seedlings.

Table 2 – Influence of presowing priming of wheat grain on the activity of NR, XDH and on the content of allantoin in 5-day seedlings of wheat grain

Variants	NR activity, nmol NO_2^-/ mg protein/min	XDH activity, nmol UA/мmg/min	Allantoin, mg/g grain dry weight
Control	0.0	6.5 ± 0.7	13.2 ± 1.4
Priming in H_2O	0.0	7.2 ± 1.2	13.8 ± 1.6
Priming in 75 мМ MoO_4^- solution	0.0	8.3 ± 1.3	19.4 ± 2.5
Priming in 0.45 мМ NO_3^- solution	15.7 ± 2.3	7.5 ± 0.9	14.0 ± 2.1
Priming in 75 мМ MoO_4^-+0.45 мМ NO_3^-	20.3 ± 2.7	11.3 ± 1.9	21.2 ± 1.7
Priming in 75 мМ WO_4^- + 0.45 мМ NO_3^-	0.0	~1.3	~1.2

The results presented in Table 2 show that the presupposition of accumulation of exogenous molybdenum in the grain increases the content of allantoin in the germinated grains. And with germination of wheat grain, saturated with molybdenum, in a medium with nitrate sharply increases the level of allantoin in sprouted grains. These results confirm the relationship between the assimilation of nitrate and the formation of allantoin. A presowing saturation of grain with tungsten, a chemical analogue of molybdenum, somewhat reduced the content of allantoin in such grains. As is known, in the absence of molybdenum in a growth medium, its chemically analogous tungsten is easily included in the active center (instead of molybdenum) of molybdoenzymes. Since unlike molybdenum, tungsten atoms do not possess the ability to transfer electrons in the active center of NR and XDH, they become inactive, no regeneration of NAD^+ and new syntheses of urate, the precursor of allantoin is seen.

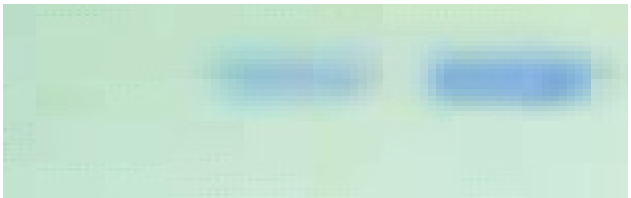

Figure 1 – Zymogramma of sprouted seeds after priming in a solution of tungsten (1), in water (2) and in molybdate solution (3)

As mentioned above, we previously found that in the embryo of dormant wheat seeds there is a non-molybdenum population of XDH, which is activated

by exogenous molybdate after heating at 80 °C in the presence of GSH. This indicated the existence of a non-molybdenum population of this enzyme intact wheat seeds. Therefore, in order to clarify the effect of presowing priming in molybdate solution in the following experiments, we conducted priming of the seeds in water, in molybdate solution and in a solution of tungstate. These seeds were then germinated in a medium containing potassium nitrate. The results are shown in Table 3.

Table 3 – Effect of heat treatment on nitrate reductase and xanthine dehydrogenase activity of wheat seedlings after priming under various conditions

Variants	Seeds treatments	NR activity	XDH activity
Control (without priming)	Without treatment	0.0	6.7 ± 1.2
	heat treatment + MoO_4^- + GSH	0.0	9.2 ± 1.4
Priming in H_2O	Without treatment	15.4 ± 25	7.5 ± 0.9
	heat treatment + MoO_4^- + GSH	22.1 ± 3.8	11.3 ± 1.9
Priming in MoO_4^- solution	Without treatment	20.3 ± 3.7	9.8 ± 1.4
	heat treatment + MoO_4^- + GSH	22.4 ± 2.8	12.7 ± 1.9
Priming in WO_4^- solution	Without treatment	0.0	1.2 ± 0.2
	heat treatment + MoO_4^- + GSH	19.5 ± 3.2	10.9 ± 1.5

As can be seen from the Table 3, in order to restore the lack of molybdenum in the non-molybdenum XDH and NR forms in germinating seeds, it is sufficient to presow them in the molybdate solution. Molybdoenzymes in such sprouted seeds are activated only by slightly exogenous molybdenum, i.e. molybdenum accumulated during priming of seeds germinated is a part of the newly synthesized NR and XDH molecules. Inactive molecules after priming in tungstate solution are fully activated after heat treatment in the presence of exogenous molybdenum and GSH. Such in vitro activation of non-molybdenum forms of molybdoenzymes is explained as follows.

As is known, in the active center of molybdoenzymes, the molybdenum atom is directly bound to the Moco, in the non-molybdenum forms of enzymes this cofactor is contained. During heat treatment, the molecules of molybdoenzymes are partially denatured and the access of molybdenum and GSH to the active center of enzymes is opened. Since the sulfhydryl cofactor groups binding the molybdenum atom in the presence of oxygen rapidly oxidize, the presence of GSH protects their oxidation. In such a situation, exogenous molybdenum is easily bound by these co-factor thiols. Moreover, with denaturation, the active molybdenum-containing molecules of NR and XDH are formed.

Conclusion

It is generally known that in the cells of various organisms (plants and animals), the non-molybdenum forms of molybdoenzymes are synthesized. One of the ways to activate them in plants is presowing seed priming. It is also known that molybdenum accumulated in plant seeds by presowing priming during their germination is transported to roots and ground parts. At the same time, all molecules of molybdoenzymes are provided with this metal, i.e. they all become active. Presowing priming of wheat seeds in solution increases the activity of nitrate reductase and xanthine dehydrogenase, and accordingly the formation of allantoin. It is known that different types of wheat differ in the level of activity of molybdoenzymes. It is known that different types of wheat differ in the level of activity of molybdoenzymes. Therefore, the identification of wheat with high nitrate reductase and xanthine dehydrogenase activity in the seed embryo will allow them to be used as a source of allantoin after presowing priming in a molybdate solution.

Thus, the obtained results convincingly show the important role of the interrelation of molybdoenzymes of xanthine dehydrogenase and nitrate reductase in the formation of allantoin in the germ of

wheat grain during its germination. In addition, the existence of the molybdenum-free forms of not only xanthine dehydrogenase in the embryo of wheat grain, but also of another nitrate reductase molybdoenzyme is shown again. Based on the analysis of the results of studies, it can be concluded that the biosynthesis of the natural antioxidant – allantoin increases in the embryo of wheat grain when it is saturated with the molybdate solution by presowing priming and when germinating in the presence of nitrate. Thus, our data suggest that wheat seeds of varieties with a high content of molybdoenzymes xanthine dehydrogenase and nitrate reductase can be one of the sources of an important biologically active substance – allantoin.

References

1. Werner A.K., Witte C.P. (2011) The biochemistry of nitrogen mobilization: purine ring catabolism. *Trends Plant Sci*., vol. 16, pp. 381-387.

2. Werner A.K., Medina-Escobar N., Zulawski M., Sparkes I.A., Cao F.Q., Witte C.P. (2013) The enzymes of in vivo ureide catabolism. *Plant Physiol.*, vol. 211, pp. 1-30.

3. Irani S., Todd C.D. (2018) Exogenous allantoin increases Arabidopsis seedlings tolerance to NaCl stress and regulates expression of oxidative stress response genes. *J Plant Physiol*., vol. 221, pp. 43-50.

4. Alamillo J.M., Diaz-Leal J.L., Sanchez-Moran M.V., Pineda M. (2010) Molecular analysis of ureide accumulation under drought stress in Phaseolus vulgaris L. *Plant Cell Environ*., vol. 33, pp. 1828-1837.

5. Schwarz G., Mendel R.R. (2006) Molybdenum cofactor biosynthesis and molybdenum enzymes. *Annu. Rev. Plant Biol*., vol**.** 57, pp. 623-647.

6. Mendel R.R., Hansch R. (2002) Molybdoenzymes and molybdenum cofactor in plants. *J Exp Bot*., vol.53, pp.1689-1698

7. Kaiser B.N., Gridley K.L., Brady, J.N., Phillips, T., Tyerman, S.D. (2005) The role of molybdenum in agricultural plant production. *Ann. Bot.*, vol. 96, pp. 745-754.

8. Sagi M., Savidov N.A., L'vov N.P., Lips S.H. (1997) Nitrate reductase and molybdenum cofactor in annual ryegrass as affected by salinity and nitrogen source. *Physiol. Plantarum.*, vol. 99, pp. 546-553.

9. Omarov R.T., Sagi M., Lips S.H. (1999) Regulation of aldehyde oxidase and nitrate reductase in roots of barley (Hordeum vulgare L.) by nitrogen source and salinity. *J. Exp. Bot.*, vol. 49, pp. 897-902.

10. Sagi M., Fluhr R., Lips S.H. (1999) Aldehyde oxidase and xanthine dehydrogenase in a flacca tomato mutant with deficient abscisic acid and wilty phenotype. *Plant Physiol*., vol. 120, pp. 571-577.

11. Pilbeam D.J, and Kirkby E.A. Some aspects of the utilization of nitrate and ammonium by plants. In: Mengel, K., Pilbeam, D.J. (Eds.) (1992) Nitrogen metabolism of plants*. Oxford: Clarendon Press*, pp. 55-70.

12. Tischner R. (2000) Nitrate uptake and reduction in higher and lower plants. *Plant Cell Environ.*, vol.23, pp. 1005-1024.

13. Lips S.H., Leidi E.O., Silberbush M. (1990) Nitrogen assimilation of plants under stress and high CO_2 concentrations. In: Inorganic nitrogen metabolism. *Berlin: SpringerVerlag*, pp. 341-348.

14. Tischner R. (2000) Nitrate uptake and reduction in higher and lower plants. *Plant Cell Environ*., vol. 23, pp. 1005-1024.

15. Zrenner R., Stitt M., Sonnewald U., Boldt R. (2006). Pyrimidine and purine biosynthesis and degradation in plants. *Ann. Rev. Plant Biol*. vol. 57, pp. 805-836.

16. Brychkova G., Alikulov Z., Fluhr R., Sagi M. (2008). A critical role for ureides in dark and senescence-induced purine remobilization is unmasked in the Atxdh1 Arabidopsis mutant. *Plant J.*, vol.54, pp. 496-509.

17. Brychkova G., Fluhr R., Sagi M. (2008). Formation of xanthine and the use of purinemetabolites as a nitrogen source in Arabidopsis plants. *Plant Signal Behav*., vol. 3, p. 12

18. Hesberg C., Hansch R., Mendel R.R., Bittner F. (2000). Tandem orientation of duplicated xanthine dehydrogenase genes from Arabidopsis thaliana. *J. Biol. Chem.*, vol.42, no. 79, pp. 13547-13554.

19. Yesbergenova, Z., Yang, G., Oron, E., Soffer, D., Fluhr, R., Sagi, M. (2005). The plant Mo-hydroxylases aldehyde oxidase and xanthine dehydrogenase have distinct reactive oxygen species signatures and are induced by drought and abscisic acid. *Plant J*., vol. 42, pp. 862-876.

20. Ventura Y., Wuddineh W.A., Ephrath Y., Shpigel M., Sagi M. (2010). Molybdenum as an essential element for improving total yield in seawater-grown Salicornia europaea L. *Scientia Horticulturae*, vol. 126, pp. 395-401.

21. Shao H.B., Chu L.Y., Zhao H.L., Kang C. (2008) Primary antioxidant free radical scavenging and redox signalling pathways in higher plant cells. *J Biol Sci*., vol. 4, pp. 8-14.

22. Peng Wang, Chui-Hua Kong, Bei Sun, Xiao-Hua Xu (2012) Distribution and function of allantoin (5-ureidohydantoin) in rice grains. *J Agric Food Chem.,* vol. 60, no. 11, pp. 2793-2798.

23. Watanabe S., Matsumoto M., Hakomori Y., Takagi H., Shimada H., Sakamoto A. (2014) The purine metabolite allantoin enhances abiotic stress tolerance through synergistic activation of abscisic acid metabolism. *Plant Cell Environ*., vol. 37, no. 4, pp. 1022-1036.

24. Takagi H., Ishiga Y., Watanabe Sh., Konishi T., Egusa M., Akiyoshi N., Matsuura T., Mori I.C., Hirayama T., Kaminaka H., Shimada H., Sakamoto A. (2016) Allantoin, a stress-related purine metabolite, can activate jasmonate signaling in a MYC2-regulated and abscisic acid-dependent manner. *J Exp Bot.*, vol. 67, no. 8, pp. 2519-2532.

25. Guskov E.P., Prokofev V.N.,Kleztkiy M.E., Kornienko E.V., Gapurenko O/A., Olekhnovich L.P., Chistyakov V.A., Shestopalov A.V., Sazyekina M.A., Markeyev A.V., Shkurat T.P., Malhosyan S.R., Zhdanov U.A. (2004) Allantoin as vitamin [Allantoin kak vitamin]. *DAN*, vol. 398, no. 6, pp. 1-6.

26. Kapoor M., Waygood E.R. (1962) Initial steps of allantoin biosynthesis in wheat germ. *Bioch Bioph Res Comm.*, vol. 9, pp. 7-10.

27. Perni S., Calzuola I., Caprara A.G., Gianfranceschi L.G., Marsili V. (2014) Natural antioxidants in wheat sprout extracts. *Curr Org Chem*., vol. 18, pp. 2950-2960.

28. Koehler K.H, Voigt B., Spittler H., Schelenz M. Biochemical events after priming and osmoconditioning of seeds. In: Ellis R.H., Black M., Murdoch A.J. (Eds.) (1997) Basic and applied aspects of seed biology. *Dotrecht: Kluwer Acad. Publ.*, pp. 531-536.

29. Alikulov Z., Altaeva A.S., Agibetova I., Altayuly C.A. (2009) Pre-sown hydration of wheat seeds in the presence of molybdenum may prevent the pre-harvest sprouting in cereal seeds. Biotechnology, biodegradation, water and foodstaffs. *NY: Nova Science Publishers*, pp. 59-65.

30. Alikulov Z., Lips H.S. (2002) Molybdenum containing enzymes in developing wheat seed. *Proc VIth annual meeting of American Society of Plant Biologists, USA*. pp. 135-138.

31. Vogels and Van der Drift (1970). Improved methods of ureide determination. *Anal. Biochem.*, vol. 33, pp. 143-157.

32. Hille R. (2005) Molybdenum-containing hydroxylases, *Biochem Biophys.*, vol. 433, no. 1, pp. 107-116.

33. Modi A.T., Cairn A.L. (1994) Molybdenum deficiency in wheat results in lower dormancy levels via reduced ABA. *Seed Sci Res*., vol. 4, pp. 329-333.

34. Eleshev R.E., Smagulov T.S. (1997) Agrochemistry [Agrochimiya]. *Almaty*, vol. 3, p.276.

35. Alikulov Z.O. (2009) Existance of molybdenum-free forms of molybdoenzymes [Sushestvovaniye bezmolibdenovykh form molibdo-fermentov]. *Vestnik ENU*, vol. 9, no. 76, pp. 41-49.

36. Guerrero M.G., Vega J.M., Losada M. (1981). The assimilatory nitrate-reducing system and its regulation. *Ann Rev Plant Physiol*., vol. 32, pp. 169-204.

37. Kamin H., Privalle L.S. Nitrate reductase. In: Ullrich W.R., Aparicio P.J. Syrret P.J. Castillo F. (Eds) (1987) Inorganic nitrogen metabolism. *Berlin: Schpringer Verlag*, pp. 112-117.

38. Babenko O., Alikulov Z. (2013) Effect of pre-sowing seed priming with molybdate tungstate on the seed germination and growth of crops plant. *Proc of Modern Science: Problems and Perspectives international conference, USA*, vol. 4, pp. 48-51.

IRSTI 34.39.55

[1*]M.A. Altay, [1]M.S. Kulbaeva, [1]S.T. Tuleukhanov,
[2]Yu.A. Kim, [1]L.K. Baktybaeva, [1]T.T. Kulbaev, [1]B.K. Kairat,
[1]A.I. Zhumadilla

[1]Laboratory of Chronobiology and Ecological Physiology, Almaty, Kazakhstan
[2]Institute of Cell Biophysics Russian Academy of Sciences, Pushchino, Moskovskaya obl., Russia
[*]e-mail: altay.moldir@mail.ru

Study of the influence of tonsillitis on other organs based on biophysical properties of skin biologically active points

Abstract: One of the most frequently encountered, especially at the adolescents and students, respiratory disease is chronic tonsillitis. It emerges under the influence of infectious agents, such as bacteria, viruses and fungi. The main causes leading to the spread of this disease are changing climate conditions (more often in fall and winter) with increased humidity and cold, when the resistance of body to infection decreases. However, tonsillitis may occur during the summer. In summer, the main causes for the spread of tonsillitis are air recirculating conditioning systems, ice cream, cold drinks, humid and dirty air. 14 students aged 19-23 years old were enrolled into the experiment, divided into two groups by seven students each (with tonsillitis as test and healthy as control). Biologically active points (BAP) symmetrically located to the right and left sides of the human body served as object of the study and were studied by their temperature indicators. Temperature measurements were recorded with "Biotemp-2". The results were statistically calculated. There were no significant differences in the temperature data of points located on the right and left sides of the body in control group; seven points from five meridians were statistically reliant when considering the temperature indices ($p<0.05$). According to the seven BAP, for which statistical validity was calculated, physiological changes from chronic tonsillitis of these biologically points indicate that they might be used as diagnostic markers.

Key words: biologically active points, biophysical properties, meridian, tonsillitis, temperature.

Introduction

Hundreds of millions of people suffer from chronic respiratory diseases; four million people die prematurely from chronic respiratory diseases each year. Acute respiratory infections are the leading cause of death in children in developing countries. Although the Global Burden of Disease Study 2020 revealed fewer deaths related to lower respiratory tract infections than 2 decades ago, too many people are still dying.

The "Kazakhstan-2030" Strategy outlined a long-term way of development of the Republic of Kazakhstan, in which one of the main priorities is "Health, Education and Wellness of Kazakhstani Citizens", which states that our citizens need to be healthy until the end of their lives and lead a healthy lifestyle.

Overall world statistics shows that more than half of the global population suffers from tonsillitis, which constitutes about 50 to 70% of the individual population in developed countries. 63% of patients consulted with otolaryngologists in the Outpatient Center in 2017 were diagnosed with tonsillitis. Of them: 40% were women and 23% were men [1; 2].

When comparing the spread of the disease in our country to the world statistics, 29-30 thousand in 100 thousand people, namely 29-30%complained about the disease [3-5].

Chronic tonsillitis is one of the most common illnesses in the pathology. It emerges under the influence of infectious agents such as bacteria, viruses, fungi. For example, it can cause sore throat illness when catching cold [6; 7]. The main causes of the prevalence of these diseases are climate change, adverse environmental effects, increased urban and motor traffic, increased smoking and industrial wastes, prevalence of various viral diseases [8; 9].

The main reasons for tonsillitis are common or local cold, cold drinks. Tonsillitis spreads in cold weather (autumn, winter), when the air humidity elevates and the body's resistance to infection decreases. The main causes of tonsillitis in summer are

 Printed in Kazakhstan

air recirculating conditioning systems, ice cream and cold drinks, humid and dirty air [10].

Air recirculating conditioning systems are placed everywhere, even in private homes. When entering the environment with temperatures below the ambient air temperature, there is a rather high chance for tonsillitis or lung inflammation. Decrease in temperature by 10 degrees is a major stress for the body. The immune system weakens and the body cannot resist the causative agents of infection [11].

During the summer, large number of people eat cold desserts, drink cold drinks in their attempt to quench thirst. However, there is a clear controversy, as firstly, "ice-cold" drinks do not quench thirst, and secondly, consumers of such might catch a cold, creating perfect conditions for the causative agent of tonsillitis – *Streptococcus pyogenes* [12; 13].

The humidity of air also has a significant effect on the heat exchange of the organism with the external environment. During the low temperature and high humidity time, the heat transfer process increases and the human body cools down [14]. Winter and summer time in Almaty are characterized as highly humid. Frequent precipitation and snow melting increase the air humidity. Lack of ventilation in the buildings sums up the development of this process in the city. Prevailing number of youngsters studying at the higher education institutions often suffer from respiratory diseases due to such environmental factors [15].

Tonsils is an organ that is a part of the lymphatic system, which together with the other organs of the immune system forms immunity. Has many functions: first is protective – tonsils produce a large number of macrophages, which have the ability to "absorb" viruses and bacteria. Secondly, they participate in the process of blood formation, forming the lymphocytes – blood cells responsible for the immune response. The infected tonsils plays a major role in childhood as the protective processes in it lead to the formation of acquired immunity in the future.

During the development of tonsillitis, patient has difficulty in drinking and swallowing, elevated body temperature and general weakness. Upon inspection, it is possible to observe the reddening of the mucous membranes of the mouth and throat, inflammation of the mucous membranes, and 1-3 times escalation in the size of the tonsils. According to the literature sources, tonsillitis may lead to brain damage, rheumatism and kidney disease [16; 17].

BAP are specifically activated points in the body. They are not characterized by certain anatomical structure. However, they have spectral potential of areas of their localization, own metabolism, high heat, low electrical resistance and they are extremely sensitive to varying temperatures [18; 19].

700-1000 BAP are located in the human body [20]. Irritation of each one may cure the illness due to a special feeling and can be used as a preventive measure for diagnostic purposes. In order to affect BAP silver, vanadium, and bone needles, ultrasounds, electromagnetic fields and laser beam are used [21; 22]. On areas around them, the temperatures are higher in comparison to the surrounding skin and in the pathological state this difference increases. In some of the pathological conditions, BAP temperature may be less than that of the surrounding skin [23; 24].

Due to the increased incidence of tonsillitis in recent years, it is interesting to study BAP effects on the body. Study of the temperature data of skin BAP in students suffering from tonsillitis has been made for the first time and reflects the relevance of the work.

Materials and methods

The study of the BAP temperature indicators (Figure 1) in the skin was performed at the Laboratory of Chronobiology and Ecological Physiology, Department of Biophysics and Biomedicine, Faculty of Biology and Biotechnology, Al-Farabi Kazakh National University. 14 students aged 19-23 years old were enrolled into the experiment, divided into two groups by seven students each (with tonsillitis as test and healthy as control).

During the experiment 24 BAP were taken from the standard meridians, on the right and left sides of the body [25, 26], associated with tonsillitis: *P9 Tai-Yuan, P11 Shao-Shan* from the lung meridian; *GI4 He-Gu, GI5 Yan-Si* from the large intestine meridian; *E41 Tsze-Si, E45 Li-Duy* from the stomach meridian; *RP2 Da-Du, RP5 Shan-Tsyu* from the spleen-pancreas meridian; *C7 Shen-Men, C9 Shao-Chun* from the heart meridian; *IG1 Shao-Tse, IG19 Tin-Gun* from the small intestine meridian; *V1 Tsin-Min, V2 Tsuan-Chzhu* from the bladder meridian; *R1 Yun-Tsyuan, R6 Chzhao-Hai* from the kidney meridian; *MC7 Da-Lin, MC8 Lao-Gun* from the pericardium meridian; TR21 *Er-Men, TR23 Sy-Chzhu-Kun* from triple heater meridian; *VB14 Yan-Bai, VB44 Tszu-Tsao-Yin* from the gallbladder meridian; *F1 Da-Dun, F2 Sin-Tsyan* from the liver meridian.

The results of many researches show that there is no real BAP anatomical structure, only the places

where the points have good nerve endings, blood vessels and loose tissues are known [27; 28].

"Biotemp-2" (modeled on the basis of BA Biotemp, Research Institute of Medical Cybernetics and Biophysics, Novosibirsk, 2006) apparatus for recording BAP temperature indices of two groups of students was produced by the special order at the experimental production center of our University. Apparatus consists of plastic cover, front panel indicator, light-emitting diode (LED) and a sensor. It includes two sources of power supply, a digital unit, an indication block, a voltage amplifier, two currents generator and a temperature sensor, active and passive electrodes. The results obtained were statistically calculated; Student's t-test was used to examine the validity of the data.

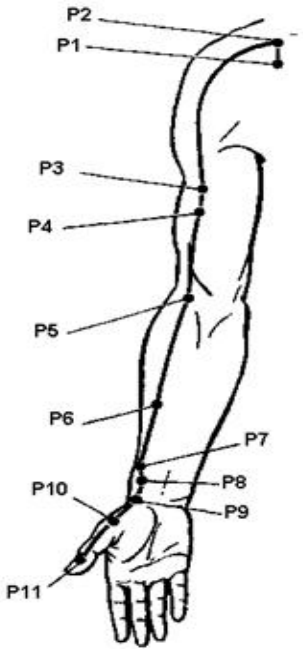

Lung meridian

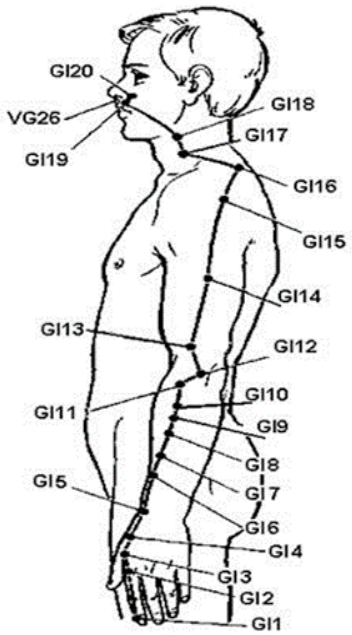

Large intestine meridian

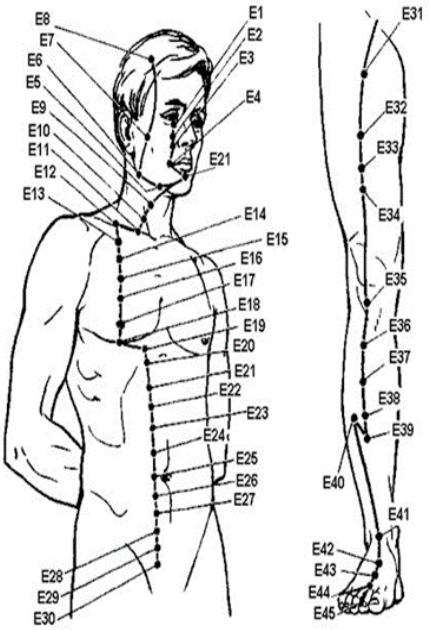

Stomach meridian

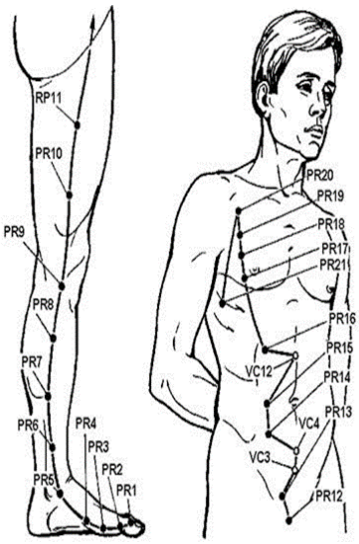

Spleen-pancreas meridian

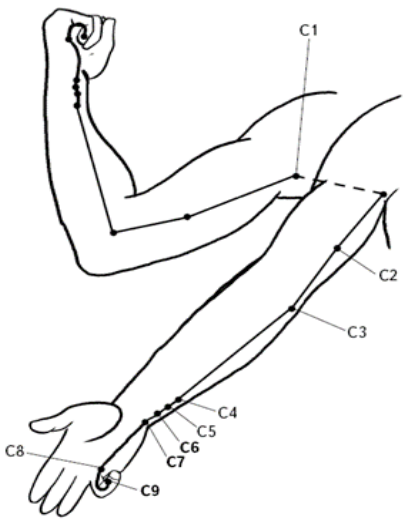

Heart meridian

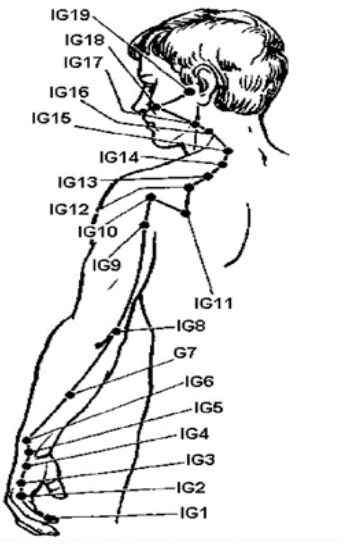

Small intestine meridian

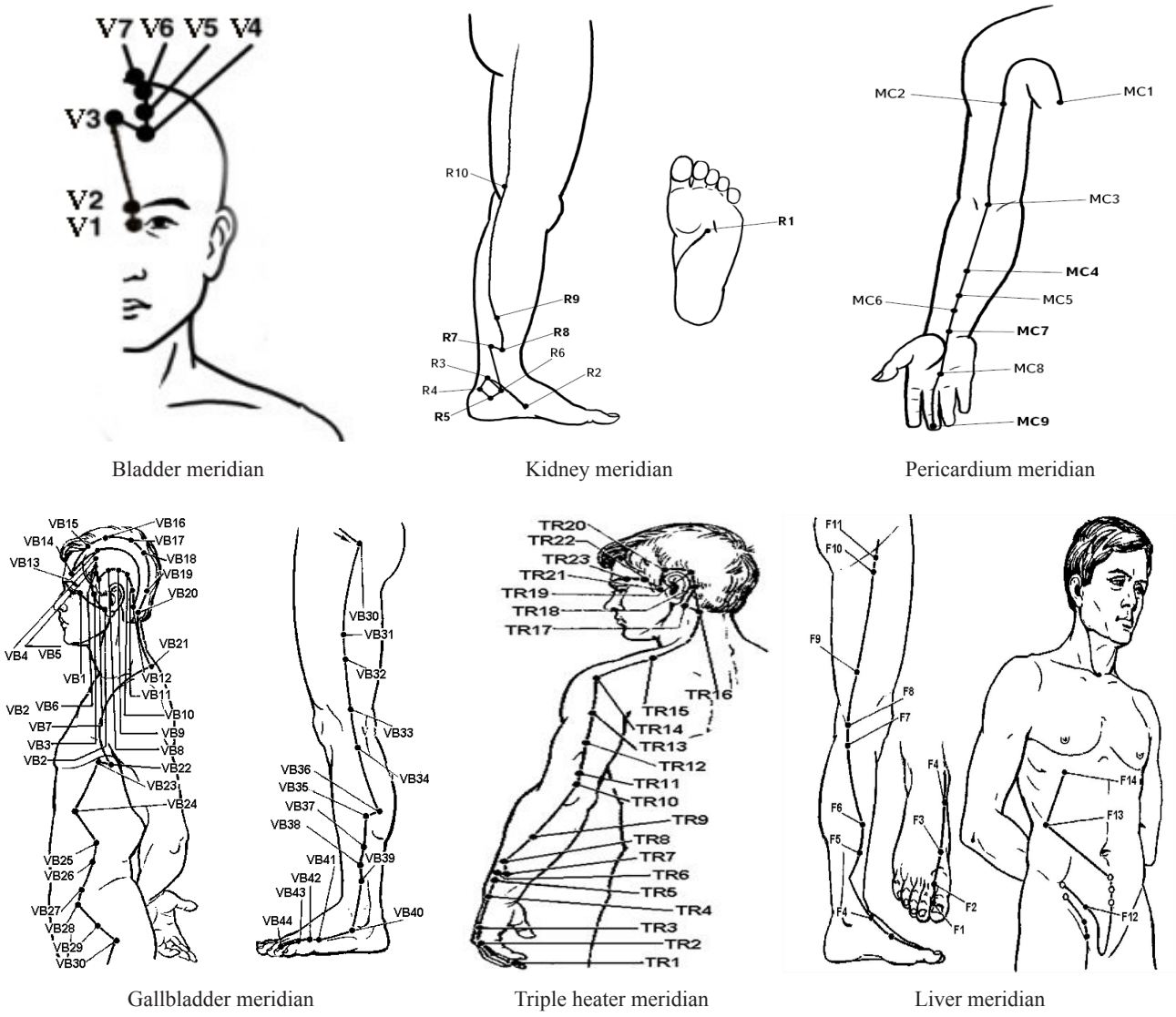

Figure1 – Localization of the biologically active points of the skin on the body

Results and discussion

In the normal condition and in students with chronic tonsillitis, in the right side of the body the temperature indicators from the biologically points is equal to 24.9÷5.4°C and 30.8÷35.1°C.

In the normal condition and in students with chronic tonsillitis, in the right side of the body the temperature indicators from the biologically points *P9 Tai-Yuan, P11 Shao-Shan* from the lung meridian; *GI4 He-Gu, GI5 Yan-Si* from the spleen-pancreas meridian; *E41 Tsze-Si* from the stomach meridian, *C7 Shen-Men, C9 Shao-Chun* from the heart meridian; *IG1 Shao-Tse, IG19 Tin-Gun* from the small intestine meridian are in between 30.0-35.0°C (Figure 2).

As can be seen from the Figure 2 in normal condition the temperature of *E45 Li-Duy* biologically point from the stomach meridian is 25.2±1.0°C, during tonsillitis it is increased by 33.0±0.5°C ($p<0.05$), in normal condition the temperature of *RP2 Da-Du* from the spleen-pancreas meridian is 26.8±0.6°C, during tonsillitis increases up to 32.1±1.0°C ($p<0.05$), in normal condition the temperature of *RP5 Shan-Tsyu* from the spleen-pancreas meridian is 28.7±0.9°C, during tonsillitis it is changed to 32.6±1.1°C ($p<0.05$).

As can be seen from the Figure3 *V1 Tsin-Min, V2 Tsuan-Chzhu* from the bladder meridian; *R6 Chzhao-Hai* from the kidney meridian; *MC7 Da-Lin, MC8 Lao-Gun* from the pericardium meridian; *TR21 Er-Men, TR23 Sy-Chzhu-Kun* from the triple

heater meridian; biologically point *VB14 Yan-Bai* the gallbladder meridian are in between 30.0-35.0°C. But in normal condition the temperature of biologically point *R1 Yun-Tsyuan* from the kidney meridian is 28.4±0.9°C, during tonsillitis it is increased by 33.1±0.7°C ($p<0.05$), in normal condition the temperature of biologically point *VB44 Tszu-Tsao-Yin* from the gallbladder meridian is 25.6±0.5°C, during tonsillitis showed a high indicator of 31.8±1.1°C ($p<0.05$), in normal condition the temperature of biologically point *F1 Da-Dun* from the liver meridian is 24.9±0.6°C, under pathology it is increased by 31.1±1.0°C ($p<0.05$), in normal condition the temperature of biologically point *F2 Sin-Tsyan* is 27.5±0.6°C, but during tonsillitis it increases up to 33.4±0.3°C ($p<0.05$).

In the normal condition, the temperature of the BAP in the selected skin from the left side of the body of students is 24.7÷35.4°C, in chronic tonsillitis – 31.4÷34.7°C (Figure 4).

As can be seen from the Figure 4 in the normal condition and in students with chronic tonsillitis, in the left side of the body the temperature indicators from the biologically points *P9 Tai-Yuan, P11 Shao-Shan* from the lung meridian; *GI4 He-Gu, GI5 Yan-Si* from the spleen-pancreas meridian; *E41 Tsze-Si*from the stomach meridian; *C7 Shen-Men, C9 Shao-Chun* from the heart meridian; *IG1 Shao-Tse, IG19 Tin-Gun* from the small intestine meridian are in between 30.0-35.0°C. But in normal condition the temperature of *E45 Li-Duy* biologically active point from the stomach meridian is 24.7±0.7°C, during tonsillitis increases up to 32.5±1.0°C, in normal condition the temperature of *RP2 Da-Du* point from the spleen-pancreas meridian is 26.6±0.7°C, during tonsillitis it increases up to 32.6±0.7°C, in normal condition the temperature of *RP5 Shan-Tsyu* from the spleen-pancreas meridian is 29.0±0.7°C, under pathology it increase up to 32.8±0.9°C. Statistically significant increase in these three biologically active points in tonsillitis compared to control ($p<0.05$) is noted.

Biologically active points *V1 Tsin-Min, V2 Tsu-an-Chzhu* from the bladder meridian; *R6 Chzhao-Hai* from the kidney meridian; *MC7 Da-Lin, MC8 Lao-Gun* from the pericardium meridian; *TR21 Er-Men, TR23 Sy-Chzhu-Kun* from the triple heater meridian; *VB14 Yan-Bai* from the gallbladder meridian the temperature is in between 30.0-35.0°C (Figure 5).

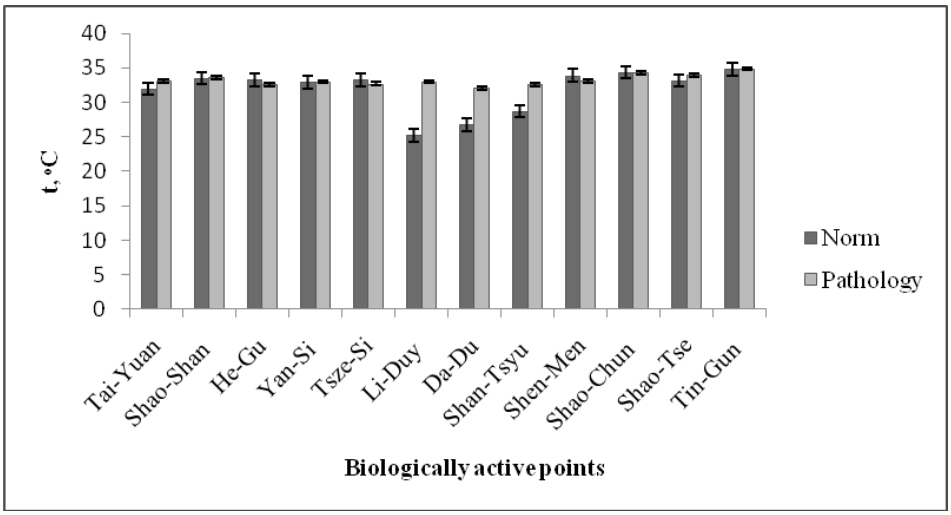

Figure 2 – Temperature in normal and pathological conditions of the BAP located on the right side of the organism (t, °C)

According to the literature sources, pain in the stomach leads to illness throat. The acid in the gastric juice causes irritation of the mucous membranes and thereby the disease of the throat. Sometimes this feeling of pain also causes ear disease. At tonsillitis, there is an increase in the spleen pancreas and liver. Tonsillitis is often accompanied by kidney insufficiency. The gallbladder system at the tonsillitis deteriorates and from the gall bladder of a sick person the allocating agents of tonsillitis – *Streptococcus pyogenes*. It means in case of sore throat microbes get into the system of the gallbladder. The results obtained in the experience have proven the conclusions in literary data [29; 30].

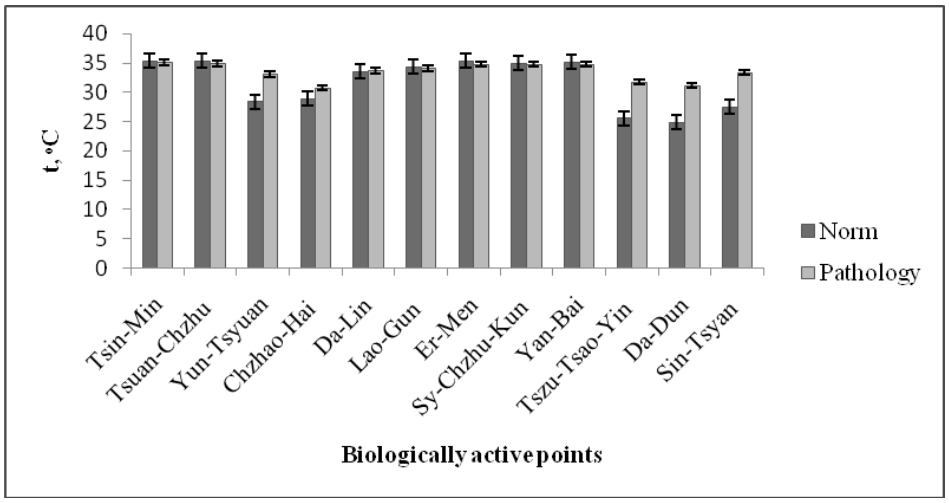

Figure 3 – Temperature in normal and pathological conditions of the BAP located on the right side of the organism (t, °C)

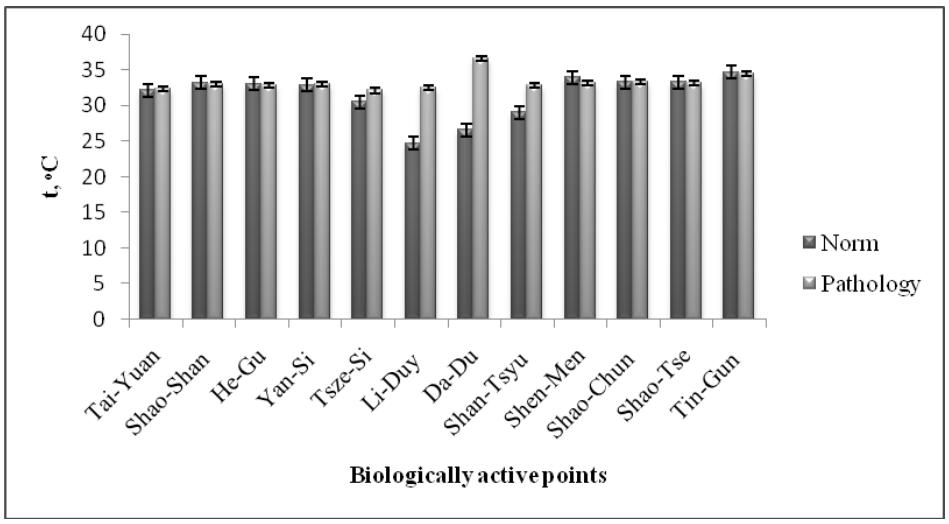

Figure 4 – Temperature in normal and pathological conditions of the BAP located on the left side of the organism (t, °C)

As can be seen from the Figure 5 the temperature of biologically point *R1 Yun-Tsyuan* from the kidney meridian in normal condition is 28.2±0.4°C, during tonsillitis it increases up to 33.8±0.5°C, in normal condition the temperature of *VB44 Tszu-Tsao-Yin* from the gallbladder meridian is 25.8±0.3°C, during tonsillitis it increases up to 31.9±0.5°C, in normal condition the temperature of biologically point *F1Da-Dun* from the liver meridian is 24.9±0.3°C, under pathology it increases up to 33.2±0.7°C, in normal condition the temperature of biologically point *F2 Sin-Tsyan* is 28.2±0.2°C, but during tonsillitis 32.4±1.0°C it is equal to the high temperature indicator. Statistically significant increase in these four biologically active points in tonsillitis compared to control ($p<0.05$) is noted.

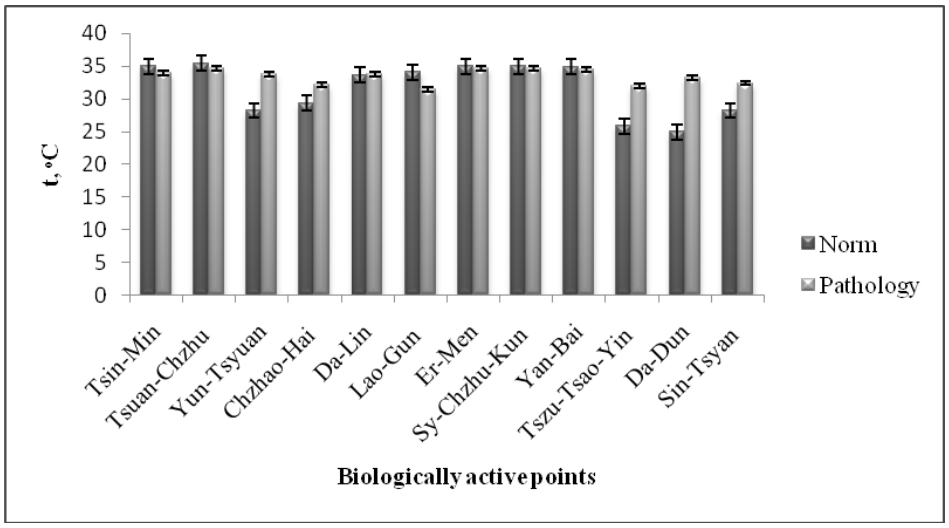

Figure 5 – Temperature in normal and pathological conditions of the BAP located on the left side of the organism (t, °C)

Conclusion

According to our studies the temperature indices on the right and left sides of the body with statistical validity of $p<0.05$ was obtained for seven points from five meridians. They are: *E45 Li-Duy* from the stomach meridian, *RP2 Da-Du, RP5 Shan-Tsyu* from the spleen-pancreas meridian, *R1 Yun-Tsyuan* from the kidney meridian, *VB44 Tszu-Tsao-Yin* from the gallbladder meridian, *F1 Da-Dun, F2 Sin-Tsyan* from the liver meridian. Temperature indicators were high. According to seven BAP, which statistical validity was calculated, physiological changes from chronic tonsillitis in these meridian organs of these biologically points indicate that these points might further be studied and potentially used as diagnostic markers.

References

1. Portenko G.M. (2012) Chronic tonsillitis from the standpoint of modern information technologies. *Center of Tver State Medical Academy*, p. 79.

2. Hickner J.M., Bartlet J.G., Besser R.E., Gonzales R., Hoffman J.R. (2012) Principles of appropriate antibiotic use for acute rhinosinusitis in adults: background. *Ann Intern Med.*, vol. 134, no. 6, pp. 498-505.

3. Maulenova S.Zh. (2001) Conditions and factors of economic development of Kazakhstan [Usloviya i factory ekonomicheskogo razvitiya Kazakhstana]. *Kazakhstan na puti k novoi modeli razvitiya, ch.1, Almaty: Kazakh university*, p. 180.

4. Andre M., Odenholt I., Schwan A. (2012) Upper respiratory tract infections in general practice: diagnosis, antibiotic prescribing, duration of symptoms and use of diagnostic tests. *Scand J Infect Dis*., no. 34, pp. 880-886.

5. Kunelskaya N.L., Turovsky A.B., Kudryavtseva Yu.S. (2010) Angina: diagnosis and treatment. *Rus Med J*., vol. 18, no. 7, pp. 438-440.

6. *Klug T.E., Rusan M., Fuursted K., Ovesen T. (2016) Peritonsillar abscess: complication of acute tonsillitis or weber's glands infection? Off J Am Ac Tool-Head and Neck Surg, vol. 155, no. 2, pp. 199-207.*

7. Pluzhnikov M.S. (2010) Chronic tonsillitis: clinical picture and immunological aspects, *St. Petersburg: Dialogue*. pp. 105-106.

8. Koblizek V. (2011) Impairment of nasal mucociliary clearance in former smokers with stable chronic obstructive pulmonary disease relates to the presence of a chronic bronchitis phenotype. *Am J Rhinol*, vol. 49, no.4, pp. 397-406.

9. Ron Dagan, Keith P. Klugman, William Craig, Fernando Baquero. (2013) Evidence to support the rational that bacterial eradication in respiratory tract infection is an important aim of antimicrobial therapy. *J Antimicrob Chemother.*, no. 47, pp. 129-140.

10. Maltseva G.S., Grinchuk O.N. (2011) Conservative treatment of chronic tonsillitis of streptococcal etiology. *Otorhinolaryngology, M.: Non-commercial partnership to promote the development of the healthcare and medicine system "Rusmedical Group"*, no. 6, pp. 20-23.

11. Medzhitov R., Janeway C.A. (2012) Decoding the pattern ofself and nonself by the innate immune system. *Science*, vol. 296, pp. 298-300.

12. Kreth J., Meritt J., Qi F. (2009) Bacterial and host interactions of oral Streptococci. *DNA Cell Biol.*, vol. 28, no. 8, pp. 397-403.

13. Orrling A., Karlsson E., Melhus A. (2011) Penicillin treatment failure in-group A streptococcal tonsillopharyngitis: no genetic difference found between strains isolated from failures and nonfailures. *Ann Otol Rhinol Laryngol.*, vol. 110, no. 7, pp. 690-695.

14. Cvejic L. (2011) Laryngeal penetration and aspiration in individuals with stable COPD. *Am J Respir.*, vol. 16, no. 2, pp. 269-275.

15. Kennedy, D.W. (2012) International Forum of Allergy & Rhinology to become a monthly publication in 2013. *Int Forum Allergy Rhinol.*, vol. 2, no. 4, pp. 269-270.

16. Fokkens W.J., Lund W.J., Mullol J. (2012) European position paper on nasal polyps. *Am J Rhinol*., vol. 50, no. 23, pp. 1-298.

17. Hurst J. R. (2014) Upper airway symptoms and quality of life in chronic obstructive pulmonary disease (COPD). *Am J Respir. Med.*, vol. 98, no. 8, pp. 767-770.

18. Vasileva L.K., Gorskii A.N. (2000) Electro technical aspects of the impact of low-frequency electromagnetic fields on human [Elektrotexnicheskie aspekty vliania nizkochastotnyx elektromagnitnyx poley na cheloveka]. *MANEB.*, vol. 4, no. 28, pp. 31-35.

19. Eleceeva U.Y. (2006) Acupuncture. Complete Guide [Igloreflekcoterapia. Polnyispravochnik], *M.: Ekcmo*, p. 608.

20. Toleusarinova A.M., Duisegalieva G.I., Kunanbai K., Toleukhanov S.T., Toleucarinova C.T. (2007) Shygys medicinacy: okukuraly, Almaty: Kazakh university, p. 148.

21. Gromova L.B. (2005) Acupuncture: technique, practice, application tips [Igloterapiametodika, praktika, sovety po premeneniuy], *M.: IKC "MarT"*, p. 128.

22. Moloctov V.D. (2008) Acupuncture and chiropractic: a practical guide for the treatment of diseases. [Igloterapia i manual naia terapia prakticheskoe rukovodstvo po lecheniu zabolevanii], *M.: Eksmo*, p. 784.

23. Altay M.A., Kulbaeva M.S., Ablayhanova N.T., Baktybaeva L.K., Tauasarova M.K., Kulbaev T.T., Zhumadilla A.I. (2018) Studying of physiological state of students with tonsillitis by temperature indicators BAP of the skin. *Proceedings of the International Scientific-Practical Conference "Modern issues of ecological genetics and current biology", Almaty: Qazaq university,* pp. 58-59.

24. ZhorzhCule de Moron. (2005) Chinese acupuncture. Classified and refined Chinese tradition [Kitaickaia akapunktura. Klassificirovannaia i utochnennaia kitaiskai atradiciia], *M.: Izdatelskii Dom "Profitctail"*, no. 4, p. 384.

25. Chan W.W., Weissensteiner H., Rausch W.D., Chen K.Y., We L.S., Lin J.H. (2008) Comparison of substance P concentration in acupuncture pointsin different tissues in dogs. *Am J Chin Med.*, vol. 26, no. 1, pp. 13-18.

26. Kulbayeva M.S. (2017) Daily dynamics of electrophysiological properties of acicular bioactive dots in the skin of rabbits in the conditions of noise and vibration, *Almaty: Qazaq University*, p. 152.

27. Hobbs B. (2004) The application of electricity to acupuncture needles: A review of the current literature and research with a brief outline of the principles involved. *Compl Ther Med*, vol. 2, no.1, pp. 36-40.

28. Boytsov I., Adaskevitch V. (2008) Planning of acupuncture effects basing on results of electroacupunctural diagnostic after Riodoraku. *Abstracts of the XVIII: Congressus Acupuncturae Bohemiae et Slovacae cum participatione internationali*, p. 20.

29. Mayanskiy N., Alyabieva N., Ponomarenko O., Lazareva A., Katosova L., Ivanenko A., KulichenkoT., Namazova-Baranova L., Baranov A. (2014) Serotypes and antibiotic resistance of non-invasive *Streptococcus pneumaniae* circulating in pediatric hospitals in Moscow, Russia: *Int J Infect Dis*, no. 20, pp. 58-62.

30. *Windfuhr J.P., Toepfner N., Steffen G., Waldfahrer F., Berner R. (2016) Clinical practice guideline: tonsillitis I. Diagnostics and nonsurgical management. Eur Arch Oto Rhino Laryngol., vol. 273, no. 4, pp. 73-87.*

IRSTI 34.45.21; 34.43.35

[1*]L.K. Baktybayeva, [1]M.K. Tauassarova, [2]B.K. Darrell, [3]V.K. Yu, [3]A.G. Zazybin

[1]al-Farabi Kazakh National University, Almaty, Kazakhstan
[2]Oklahoma State University, Center for Health Sciences, Stillwater, Oklahoma City, USA
[3]A.B. Bekturov Institute of Chemical Sciences, Almaty, Kazakhstan;
Kazakh-British Technical University, School of Chemical Engineering, Almaty, Kazakhstan
[*]e-mail: Layilia.Baktybaeva@kaznu.kz

Immunostimulating properties of the azaheterocyclic compounds BIV-3, BIV-4, BIV-7

Abstract: In animals and humans, immune system performs an important function to maintain the constancy of the body internal environment, carried out by recognizing and eliminating alien substances of antigenic nature from the body. This immune system function is carried out with the congenital and acquired immunity factors. Different types of radiation, heavy metal salts, vitamin and micronutrient deficiency, stressful situations, age-related changes in the lympho-myeloid complex, therapy with anti-tuberculosis, antibacterial, hormonal, cytostatic drugs and a number of other factors lead to the development of immune diseases. These diseases can be treated with a set of immunotherapy methods; use of immunostimulants is one of them. Today, immunostimulants are distinguished as of microbial, thymic, bone marrow, cytokine, nucleic, plant and synthetic origin. Azaheterocyclic compounds comprise a class of compounds that have demonstrated significant biological activities against various human diseases. We suggest that azaheterocyclic compounds with a piperidine nucleus are perspective for the search for new effective immunostimulating drugs. To study their immunostimulating activity, the following compounds were taken: **BIV-3** – 1-(3-butoxypropyl)-3-methylpiperidine 4-spiro 5'-imidazolidine-2',4'-dione, **BIV-4** – 1-(2-ethoxyethyl)-4-hydroxy-4-dimethoxyphosphorylpiperidine, **BIV-7** – complex of 3-(2-morpholinoethyl)-7-(3-isopropoxypropyl)-3,7-diazabicyclo [3.3.1] nonane with β-cyclodextrin. The comparison drug was methyluracil. Results of the studies are presented in this paper.
Key words: azaheterocyclic compounds, immunostimulating properties.

Introduction

In animals and humans, immune system performs an important function to maintain the constancy of the body internal environment, carried out by recognizing and eliminating alien substances of antigenic nature from the body. This immune system function is carried out with the congenital and acquired immunity factors. Different types of radiation, heavy metal salts, vitamin and micronutrient deficiency, stressful situations, age-related changes in the lympho-myeloid complex, therapy with anti-tuberculosis, antibacterial, hormonal, cytostatic drugs and a number of other factors lead to the development of immune diseases. These diseases can be treated with a set of immunotherapy methods; use of immunostimulants is one of them.

Today, immunostimulants are distinguished as of microbial, thymic, bone marrow, cytokine, nucleic, plant and synthetic origin. Many immunostimulants have a wide range of side effects. For example, a naturally occurring drug sodium nucleinate is widely used to stimulate the bone marrow cells proliferation [1]. Sodium nucleinate is able to stimulate both congenital and acquired immunity factors. All drugs from the group of nucleic acids are very effective inducers of interferon. Based on sodium nucleinate a number of synthetic drugs have been developed: poludan – polyadenylic-uridine acid complex; inosine pranobex (isoprinosine) – a complex of inosine with acetylamido-benzoic acid; methyluracil and riboxine – a complex compound consisting of hypoxanthine – riboside. Methyluracil is the most accessible and widely used synthetic immunostimulator [2]. We should remember that both synthetic and natural nucleic acid drugs containing precursors for the synthesis of DNA and RNA chains induce growth and multiplication of both eukaryotic and prokaryotic cells. Therefore, despite their strong immunostimulating properties, due to stimulation of growth and

reproduction of malignant, bacterial and other cells, many sodium nucleinate derivatives are prohibited in many countries of the world. Immunostimulants of bone marrow origin are known by high cost due to the unique ingredients and cause severe allergic diseases. Cytokine origin drugs can cause a non-controlled inflammatory reaction up to a fatal outcome. There is a continuous search for new effective immunostimulants. Among them, we should mention polyoxidonium, immunophane, immunomax and other. Laboratory of Pharmaceutical Chemistry of A.B. Bekturov Institute of Chemical Sciences monitors new synthetic immunostimulants in Kazakhstan. The laboratory staff has accumulated vast experience in the field of synthesis and chemical transformations of 4-oxopiperidines, have obtained new data, which allows making important conclusions about the relationship between the fine chemical structures of synthesized compounds and their reactivity, spectral characteristics and biological activities. Drugs with high anesthetic, antiarrhythmic, anti-allergic and other types of activity have been found, which have significant advantages over common medical products. In addition, the laboratory is engaged in the search for new immunostimulants. Stimulus for search among the piperidine derivatives was the manifestation of immunostimulating activity by prosedol drug, which is a derivative of piperidine and was obtained in this laboratory for the first time [3].

Thus, **the purpose** of our research was to study effect of BIV-3, BIV-4, BIV-7 on leukopoiesis and oxygen-dependent links of neutrophil defense reactions and adhesive properties of peritoneal macrophages.

Materials and methods

To study immunostimulating activity, the following compounds were taken: **BIV-3** – 1-(3-butoxypropyl)-3-methylpiperidine 4-spiro 5'-imidazolidine-2',4'-dione, **BIV-4** – 1-(2- ethoxyethyl)-4-hydroxy-4-dimethoxyphosphorylpiperidine, **BIV-7**-complex of 3-(2-morpholinoethyl)-7-(3-isopropoxypropyl)-3,7-diazabicyclo [3.3.1] nonane with β-cyclodextrin. The comparison drug was methyluracil [2]. Immunostimulating activity of the compounds was determined by ability of the test compounds to stimulate leukopoiesis to normal values of the blood leukogram and the phagocytic ability of the granulocytes were evaluated. Evaluation of the monocytes and granulocytes absorption function does not give an idea of the phagocytosis stages process peculiarities, which ensure the killing the of phagosome content. To assess the intracellular microbicidal nature of phagocytic cells, indirect methods are widely used to evaluate the production of superoxide radicals, in particular, the reduction test for nitro blue tetrazolium (NBT). It is also important to assess the adhesive ability of the phagocytic cells. The adhesion of a phagocyte to a foreign object serves as a trigger mechanism for the development of subsequent stages of the phagocytic process – antigen uptake, when the particle is captured and immersed in the cytoplasm of the phagocyte for intracellular disintegration of the absorbed particle.

Healthy adult laboratory mice of both sexes, 8-10 weeks of age, weighing 18-20 g were used to determine acute toxicity. The deviation in groups by the initial body weight did not exceed ± 10%. All experiments held at the same time of day (from 9:00 am). Immunostimulating activity was studied on laboratory mature adult albino rats of both sexes, 10-15 weeks of age with a body weight of 210-280 g, 48 individuals. All animals were obtained at the same time from the vivarium of laboratory animals at the Faculty of Biology and Biotechnology of the al-Farabi Kazakh National University. Studies were conducted in accordance with the current "Rules for preclinical (nonclinical) studies of biologically active substances" [4]. All animals were in the same habitat conditions (wood litter from sawdust, room temperature 22-24°C, 12-hour light) and feeding (standard briquetted food). Laboratory rats were divided into 6 groups of 8 individuals. The 6th group of animals was intact. No compounds were administered to animals of the intact group. All other experimental groups of animals were injected with sodium cyclophosphamide (OJSC "Kievmedpreparat", Ukraine, powder for solution for injection): intramuscularly at a dose of 30 mg/kg in saline solution of 0.5 ml, three times with a daily interval. On the 6^{th}, 8^{th} and 10^{th} day of the experiment the 1-5th group of animals was intramuscularly injected: 1st, 2nd, 3rd – at a dose of 1/10 LD_{50} of BIV-3, BIV-4, BIV-7 in saline in the volume of 0.5 ml intramuscularly, the fourth – in 0.5 ml (0.4 mg/kg) solution of methyluracil (control group), the 5th – saline 0.5 ml (placebo group). The test chemical compounds, the reference drug and saline were administered 3 times at a daily interval. Blood sampling was carried out from the orbital vein of rats on the 12^{th} day of the experiment, anesthetized with mild ether anesthesia at 09:00 am. The blood was tested on a hematological analyzer for laboratory animals "Abacus junior VET" (Diatron, Denmark). To ensure a double cytological control the blood smears were made to evaluate leukogram. Blood smears were

stained by Romanowsky-Giemsa, and the SA3300C microscope under the immersion (magnification 7x100) was counted on 100 cells per each smear, then the relative amount of each cell type was recalculated into an absolute value [5; 6]. The statistical processing of the data was carried out using Student's *t*-test.

Phagocytic, microbicidal and adhesive activity was done according to the generally accepted method of studying the spontaneous NBT test with the reduction of nitro blue tetrazolium in diformazan [7]. The reaction results were evaluated by an immersion objective (magnification 7x100) on a SA3300C microscope. The percentage of cells having diformazan in the form of granules or solid deposits was detected. The mean cytochemical coefficient (MCC) was calculated by G.Astaldi and L.Verg formula. Evaluation of adhesive properties was performed by a standard method on rat peritoneal mast cells. The index of adhesion of peritoneal macrophages (IA-PM) was equal to the percentage of cells attached to the glass Goryaev's chamber filled with Tyrode's solution in a Petri dish. The number of cells on the Goryaev's chamber was counted on a SA3300C microscope under an amplification of 7x10x40 [7].

The biological activity and acute toxicity of new compounds were compared with the data of the reference drug methyluracil.

Results and discussion

Results of chemical studies

Saturated azaheterocycles polyfunctional derivatives, especially piperidines, as one of the most promising families of chemical compounds because of their high pharmacological potential and simple synthesis, are subject of Research of the Pharmaceutical companies and Universities. Introduction into the piperidine molecule another pharmacophoric fragments leads to new biological activities. A functionalization of N-alkoxyalkyl piperidin-4-ones is carried out by us. For synthesis of spiro bicyclic having two-pharmacophore cycle – hydantoin and N-alkoxyalkylpiperidines Bucherer-Bergs reaction had been choosed. Interaction of N-alkoxyalkyl piperidin-4-ones with sodium cyanide and ammonium carbonate in an aqueous alcoholic solution is carried out in a single stage in sealed vials at 75°C for 4 hours. Target 1-(3-Butoxypropyl)-3-methylpiperidine hydantoin (I [8], BIV-3) was obtained in a yield of 40% yield, m.p.102-106°C.

Introduction of phosphate moiety leads to the appearance of new biological properties. α-Oxiphosphonates easily were obtained by interaction of N-alkoxyalkyl piperidin-4-ones with dimethylphosphite in the presence of sodium methylate in hexane. 1-(2-Ethoxyethyl)-4-(dimethylphosphoryl)-4-hydroxypiperidine (II [9], BIV-4) had been prepared, yield 93%, m.p. 112-113°S.

Simultaneous condensation of N-alkoxyalkyl piperidin-4-ones with paraformaldehyde and (2-morpholinoethyl) amine in methanol + acetic acid led to corresponding 3,7-diazabicyclo [3.3.1] nonane-9-ones with a yield of 40-60%. To search of potential BAS reduction of 3,7-diazabicyclo [3.3.1] nonane-9-one in a Wolff-Kishner reaction by hydrazine hydrate in triethylene glycol in the presence of KOH gave the corresponding 3,7-diazabicyclononane in a yield of 57%. Complex of 3-(3-i-propoxypropyl)-7-(2-morpholinoethyl)-3,7-diazabicyclo [3.3.1] nonan with β-cyclodextrin [10] is BIV-7.

Results of biological studies

1. New synthetic drugs acute toxicity indicators

In general, all compounds of the study series showed a very low acute toxicity index. In accordance with the received acute toxicity indicators, only one investigated BIV-3 compound can be attributed to the compounds of the first toxicity group. Its acute toxicity was 446.68 ± 3.24 mg/kg, but the BIV-3 compound was less toxic than the comparative drug methyluracil 1.12 times. The acute toxicity level of the BIV-7 compound was more than 500 mg/kg and this compound can be attributed to compounds with moderate acute toxicity. Acute toxicity of the BIV-7 compound was 790.68 ± 8.74 mg/kg and was less than that of the reference preparation in 1.99 times. The least acute toxicity was shown by BIV-4 compound. It can be attributed to low-toxic compounds. The acute toxicity of the BIV-4 compound was more than 1000 mg/kg and was 2.51 times less than the acute toxicity of the methyluracil comparative drug (Table 1). All test compounds were less toxic than the methyluracil [8].

2. Screening results of immunostimulating activity of new synthetic compounds

In order to investigate the immunostimulating activity of compounds in animals, it was necessary to induce an artificial immunosuppressive syndrome. The control values obtained from intact animals admitted to the experiment were within the physiological norm. The leukocyte count (9.83 ± 1.51) · 10^9/L blood, with lymphocyte (5.40 ± 1.1) · 10^9/L blood, which was (56.9 ± 0.9)%. Granulocytic leukocytes had a value (3.64 ± 0.9) · 10^9/L of blood with a percentage ratio in the blood leukogram of 37.0 ± 1.4%. The monocyte index (0.7 ± 0.0) · 10^9/L of blood was minimal, which according to the leukogram was (7.0

± 0.4)%. Also, the numbers of erythrocytes and platelets were normal. The erythrocyte index was (7.8 ± 1.4) · 10^{12}/L blood with a hemoglobin content (158.7 ± 1.2) g/L blood and accordingly a hematocrit (39.8 ± 1.9)%. The platelet score was also normal (350.6 ± 3.6) · 10^{9}/L of blood and thrombocrit was (12.6 ± 0.3)%. In general, the main blood indicators obtained from the animals during experiment were normal.

Table 1 – Acute toxicity of the compounds

No.	Compound name	Acute toxicity index (LD_{50}), mg/kg	The acute toxicity index (LD_{50}) relative to the methyluracil
1	Methyluracil	398.24 ± 0.52	1
2	BIV-3	446.68 ± 3.24	1.12
3	BIV-4	> 1000 mg / kg	>2.51
4	BIV-7	790.68 ± 8.74	1.99

Directed immunosuppressive effect of sodium cyclophosphamide led to a mielodepression effect with impairment of blood counts on the first day after injection. The total leukocyte count was (4.15 ± 1.2) · 10^{9}/L of blood, i.e. with a decrease of 2.19 times ($p \leq 0.05$) and on the 3rd day after injection, the level of leukocytes was (2.69 ± 0.54) · 10^{9}/L of blood, which was a 3.40-fold decrease in comparison with control ($p \leq 0.01$). According to the blood leukogram, significant negative changes can be noted in the cell pools of lymphocytes, granulocytes, and monocytes. The parameters of immunocompetent cells-lymphocytes from the control value (5.50 ± 1.1) · $10^{9/L}$ of blood decreased on the 1st day to (2.46 ± 0.75) · 10^{9}/L of blood and reached the 3rd day (1.99 ± 0.18) · 10^{9}/L of blood, i.e. in 2.74 times ($p \leq 0.05$) (Table 2).

Changes that are even more significant occurred in the cellular populations of granulocytes. The level of granulocytic leukocytes of blood decreased from 3.64 ± 0.9 ·10^{9}/L to (1.33 ± 0.18) · 10^{9}/L in 1st day, i.e. in 5.28 times ($p \leq 0.01$). Decrease in granulocytes in 3 days after injection of cyclophosphamide was (23.75 ± 8.55)%, i.e. in 1.68 times. A considerable decrease in the absolute granulocyte count (5.28 times) compared to a moderate decrease in the relative value of granulocytic leukocytes (1.68 times) can be explained by a substantial impairment in the overall leukocyte index, which affected the absolute values of the cells in the blood (Table 2).

A certain increase in monocytes was observed on the first day after the injection of cyclophosphamide, which can be explained by the mass death of cells and an increase in the functional load. The index of intact animals (7.0 ± 0.4)% on the first day after the injection of cyclophosphamide became (7.05 ± 4.6)%, but on the third day after injection it fell to (0.6 ± 0.0%), i.e. 10 times compared to control value ($p \leq 0.01$) (Table 2).

Table 2 – Animals blood leukogram after intoxication

Parameter	General leukocyte rate (WBC, · 10^{9}/L)	Abs. number of granulocytes (GRA, · 10^{9}/L) relative indicators granulocytes (GR, %)	Abs. number of lymphocytes (LYM, · 10^{9}/L) relative indicators lymphocytes (LY, %)	Abs. number of monocytes (MID, · 10^{9}/L) relative indicators monocytes (MI, %)
Intact animals	9.83±2.51	3.64±0.9 37.0±1.4	5.50±1.1 56.9±0.9	0.7±0.0 7.0±0.4
Immunodepression, 1st day	4.15±1.2	1.33±0.18 33.55±4.45	2.46±0.75 58.95±0.85	0.36±0.28 7.05±4.6
Immunodepression, 3rd day	2.69±0.54	0.685±0.355 23.75±8.55	1.99±0.18 75.65±8.55	0.015±0.005 0.6±0.0

No significant changes were observed in red blood cells as it was in the leukocyte cell populations. Some fluctuations of erythrocyte cells from (6.5 ± 1.4) · 10^{12}/L, decrease in the first day to (4.71 ± 1.37) · 10^{12}/L by 1.38 times and a slight increase to (5.80 ± 0.27) · 10^{12}/L on the third day after the injection of cyclophosphamide was noticed. Also, the same pattern of fluctuations on the first day and the third day after the injection of sodium cyclophosphamide was observed in the values of hemoglobin, hematocrit, the average volume of erythrocytes, the average hemoglobin content in erythrocyte cells, and

the erythrocytes distribution amplitude. Decrease in indices 1.2-1.6 times was observed on the 1st day. Significant changes were recorded in platelet counts, which naturally affects the values of platelet crit count, the average platelet count and the amplitude of platelet distribution. On the first day after the injection of sodium cyclophosphamide, platelet levels fell to (245.0 ± 126.0) · 10^9/L of blood, when the value for intact animals (350.0 ± 32.2) · 10^9/L of blood, i.e. 1.43 times (Table 3).

By the 3rd day after injection, the platelet count decreased to (74.5 ± 39.5) · 10^9/L of blood from the baseline value (350.0 ± 32.2) ·10^9/L of blood, i.e. 4.7 times ($p \leq 0.05$). This indicator is critical and characterized by spontaneous abdominal hemorrhage and other hemophilic disorders.

Thus, it shows that cyclophosphamide caused myelo suppression and the most sensitive cells were leukocyte cells and platelets. Lymphocytes, granulocytes and further monocytes were killed first among the leukocytic cells. Then animals having myelo depressive syndrome, were injected with azaheterocyclic compounds under the code "BIV". Based on the acute toxicity index, the therapeutic dose of the new compounds was calculated: TD_{50} (BIV-3) = 4.5 mg/kg; TD_{50} (BIV-4) = 10.0 mg/kg; TD_{50} (BIV-7) = 8.0 mg/kg, which was used. The therapeutic dose of the standard compound was TD_{50} (methyluracil) = 4.0 mg/kg.

After the treatment with the immunostimulating compound with methyluracil and new synthetic compounds of the BIV series, the following results were obtained. The BIV-3 compound showed the highest activity, it increased the total leukocyte count to (7.31 ± 1.54) ·10^9/L and exceeded the comparison drug 2.6 times. The overall leukocyte count returned to normal, the leukocyte formula was almost back to normal. The number of myelocytes decreased to 0.9%, metamyelocytes – 2.9%, stab neutrophils – 8.4%. There was intensive recovery of granulocytes. The next in immunostimulating activity scale was the BIV-7 compound. It was inferior in activity to the BIV-3 compound, but it was more active than BIV-4 and the reference drug 1.3 times. After the treatment, the BIV-7 compound increased the overall leukocyte count 1.9 times to 3.69 ± 0.31 × 10^9/L compared to the control group (Table 3).

Table 3 – Animals blood leukogram after injection of the test compounds, where: numerator is the total number of cells in 1μl of blood, while denominator is the relative content of cells in %

Parameter	General leukocyte index (WBC, ·10^9/L)	Abs. number of granulocytes (GRA, · 10^9/L) relative indicators granulocytes (GR, %)	Abs. number of lymphocytes (LYM, · 10^9/L) relative indicators lymphocytes (LY, %)	Abs. number of monocytes (MID, · 10^9/L) relative indicators monocytes (MI, %)
Intact group	9.83±2.51	3.64±0.93 37.01±1.43	5.50±1.10 56.9±0.98	0.70±0.00 7.0±0.41
Immunodepression	2.69±0.54	0.69±0.41 23.76±8.55	1.99±0.18 75.65±6.23	0.02±0.01 0.61±0.00
BIV-3	7.31±1.54	3.39±0.36 46.44±0.35	2.58±0.11 35.46±2.35	1.33±0.01 18.24±1.25
BIV-4	2.77±0.34	1.41±0.12 52.24±4.22	0.76±0.01 28.22±2.52	0.53±0.00 19.66±1.81
BIV-7	3.69±0.31	1.75±0.42 48.73±6.23	1.07±0.01 29.84±3.54	0.77±0.00 21.52±5.35
Control group	2.81±0.54	1.19±0.23 42.44±3.29	1.26±0.01 44.99±3.65	0.36±0.00 12.71±1.23
Placebo group	1.91±0.54	1.16±0.87 60.92±6.28	0.17±0.00 8.95±1.29	0.57±0.00 30.23±4.57

Similarly, as after treatment with the previous compound in the peripheral blood, a small amount of myelocytes and metamyelocytes was observed. BIV-4 compound showed activity comparable to the activity of the methyluracil. The overall leukocyte count was (2.77 ± 0.34) ·10^9/L. Thus, the newly synthesized BIV-3 compound exceeded the leucopoiesis stimulating activity of methyluracil. Cyclophosphamide intoxication led to the acquired immunosuppressive syndrome with a drop in the NBT-indicator to 1.09

± 0.01 assorted units; with an average cytochemical coefficient of 0.49 ± 0.01 conventional units, and the adhesion index of peritoneal macrophages 5.21 ± 0.04% [2].

NBT-test evaluates the functional state of neutrophils. It reflects the degree of activation of oxygen-dependent metabolism, primarily the hexomonophosphate shunt and the associated production of free oxygen radicals. When assessing the NST-test, the maximum index was for the BIV-7 compound, 7.02 ± 0.01 standard units, against the control 1.09 ± 0.01 conventional units ($p \leq 0.05$), exceeding methyluracil by 3.36 times and compound BIV-3 by 3.49 times. The compound showed a comparable high activity, but was inferior to the BIV-4 compound. The highly active BIV-4 compound exceeded the BIV-7, BIV-3 and methyluracil compounds in activity 1.73, 3.49 and 3.36 times, respectively (Figure 1, a).

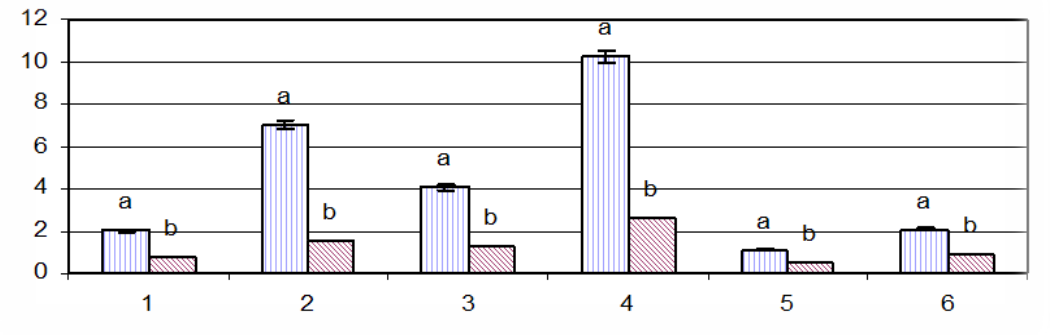

Figure 1 – Effect of compounds on the NST-indicator (a) and MCC-coefficient (b) neutrophils in peripheral blood of rats. On the abscissa axes – BIV-3 (1), BIV-4 (2), BIV-7 (3), intact (4), control (5), methyluracil (6); on the axes of ordinates – NBT-indicator and MCC-coefficient, standard units

To reflect the degree of activity of the enzyme systems of phagocytic neutrophils, the mean cytochemical coefficient (MCC) was calculated. MCC reflects the energy processes that ensure the production of bio-oxidants with bactericidal action. In this connection, the MCC in the spontaneous NBT test serves as an additional criterion for evaluating the bactericidal activity of neutrophils. According to the MCC, the BIV-4 compound had a maximum value of 1.53 ± 0.002 units, exceeding the metryluracil 1.66 times, BIV-3 compounds 1.91 times. A BIV-7 compound, comparable in value to the BIV-4 compound, was similar (Figure 1, b).

Effect of compounds on the adhesion index of peritoneal macrophages is presented on Figure 2.

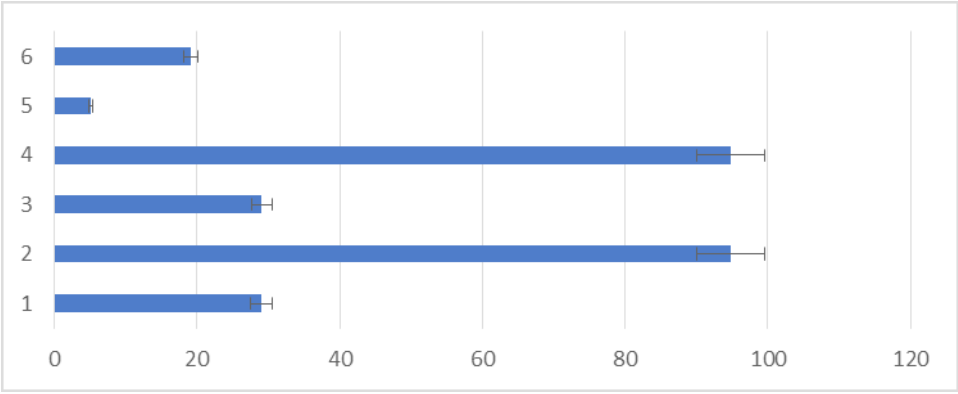

Figure 2 – Effect of compounds on the adhesion index of peritoneal macrophages. The ordinate is the BIV-3 (1), BIV-4 (2), BIV-7 (3), intact (4), placebo (5), control (6); on the axis of abscissa – the index of adhesion index, % of active cells

According to the adhesion index, the best result was shown by BIV-4 compound, 94.81 ± 0.07%, against the control 5.21 ± 0.04% ($p \leq 0.05$), which exceeded the control value 18.2 times and methyluracil 4.46 times. The IA-PM of the BIV-4 compound was almost identical to that of the intact animals, i.e. BIV-4 in a 10-day time interval restored the adhesive activity of cells of animals subjected to immunosuppressive stress.

Conclusion

1. Azaheterocyclic compounds with a piperidine nucleus are perspective for the search for new effective immunostimulating drugs. They have high immunostimulating activity and low acute toxicity.

2. The **BIV-3** – 1-(3-butoxypropyl)-3-methylpiperidine-4-spiro-5'-imidisolidine-2',4'-dione compound stimulates leukopoiesis and has low toxicity.

3. **BIV-4** – 1-(2-ethoxyethyl)-4-hydroxy-4-dimethoxyphosphorylpiperidine and **BIV-7** complexes of 3-(2-morpholinoethyl)-7-(3-isopropoxypropyl)-3,7-diazabicyclo [3.3.1] nonane with β-cyclodextrin stimulate intracellular microbicidal activity, the effectiveness of enzyme systems and the adhesive properties of phagocytic cells and are characterized by low toxicity.

References

1. Khaitov R.M., Pinegin B.V. (2003) Immunomodulators: the mechanism of action and clinical application. *Immunology*, vol. 24, no. 4, pp.196-203.

2. Mashkovsky M.D. (1993) Preparations, correcting the processes of immunity (immunomodulators, immunocorrectors). In the book: Medicines (Manual for doctors), Part II. pp. 192-209.

3. Praliev K.D., Yu V.K., Fomicheva E.E., Baktybayeva L.K., Svambaev E.A., Tuleukhanov S.T. (2007) Immunostimulants of the N-alkoxyalkyl piperidine series. *Chemical Journal of Kazakhstan*, no. 2, pp. 180-187.

4. Order of the Minister of Health of the Republic of Kazakhstan No. 745 from November 19, 2009 "On approval of the Rules for preclinical (non-clinical) studies of biologically active substances"

5. Giemsa G. (1904) Eine Vereinfachung und Vervollkommnung meiner Methylenazur-Methylenblau-Eosin-Färbemethode zur Erzielung der Romanowsky-Nochtschen Chromatinfärbung. *Centralbl f Bakt etc*., no. 37, pp. 308-311.

6. Bezrukov A.V. Coloring by Romanowsky: to the question of priority / To the 120th anniversary of the discovery of the Romanowsky effect, p. 12.

7. Khaitov R.M., Pinegin B.V., Latysheva T.V. (2002) Methodical instructions for testing new immunomodulating medications. *Herald of the Scientific center of expertise and state control of medicines*, no. 1, pp. 11-21.

8. Yu V.K., Praliev K.D., Fomicheva E.E., Baktybayeva L.K., Svambayev E.A., Tuleukhanov S.T. (2007) Immunostimulants based on N-alkoxypiperidines. *Chemical Journal of Kazakhstan*, no. 2, pp. 180-187.

9. Yu V.K., Praliyev K.D. (1997) Preliminary patent 5011 RK. 1-(2-Ethoxyethyl)-4-(dimethylphosphoryl)-4-hydroxypiperidine possess plant growth-stimulating activity. *Bull RK*, no. 3.

10. Praliyev K.D., Yu V.K., Zhaxibaeva Zh.M., Togyzbaeva N.A., Kemelbekob U.S., Baktybayeva L.K., Svambayev E.A. (2008) Preliminary patent 19832 RK. Complex of 3-(3-i-propoxypropyl)-7-(2-morpholinoethyl)-3,7-diazabicyclo[3.3.1]nonan with β-cyclodextrin and its precursors synthesis. *Bull RK*, no. 8.

11. Zimin Yu.S., Borisova N.S., Timerbaeva G.R., Gimadieva A.R., Mustafin A.G. (2016) Obtaining, toxicity and anti-inflammatory activity of complex compounds of uracil derivatives with polyfunctional acids. *Chemical-pharmaceutical journal*, vol. 50, no. 10, pp. 16-24.

12. Nozdrachev A.D. (2007) A large workshop on human and animal physiology of man and animals. Physiology of visceral systems. *M.: Publishing center* Academy, vol. 2.

13. Leskov V.P. (1999) Immunostimulants. *Allergy, asthma and clinical immunology*, no. 4, pp. 12-25.

14. Khaitov R.M., Pinegin B.V. (1996) Immunomodulators and some aspects of their clinical use. *Clinical medicine*, vol. 74, no. 8, pp. 7-12.

12. Kharkevich D.A. (2002) Pharmacology. Textbook for high schools. *M.: GEOTAR-MED*.

13. Hadden J.W. (1993) Immunostimulants. *Immunology Today*, vol. 14, pp. 275-280.

14. Werner G.H., Jolles P. (1996) Immunostimulating agents: what next? A review of their present and potential medical applications. *European Journal of Immunology*. vol. 242, pp. 1-19.

15. Mikhailova A.A. (1996) Individual myelopeptides are "new generation" drugs used for immunorehabilitation. *International Journal of Immunoreability*, no. 2. pp. 27-31.

16. Petrov RV, Khaitov RM, Nekrasov A.V. (1999) Polyoxidonium – immunomodulator of the last generation: results of a three-year clinical application. *Allergy, asthma and clinical immunology*, no. 3, pp. 3-6.

17. Ershov F.I. (1998) Antiviral drugs. Directory. *M.: Medicine*.

18. Petrov R.V. (1987) Immunological mobilization. *M.: Molodaja gvardija*.

19. Khaitov R.M., Pinegin B.V. (2000) Modern immunomodulators: the basic principles of their use. *Immunology*, no. 5, pp. 4-7.

20. Petrov R.V. (1994) Immunorehabilitation and strategy of medicine. *International Journal of Immunoreability*, Suppl. 1, pp. 5-6.

21. Khaitov P.M., Gushchin IS, Pinegin B.V., Zebrev A.I. (1999) Experimental study of the immunotropic activity of pharmacological preparations. *Herald of the Scientific center of expertise and state control of medicines*, no. 1, pp. 31-36.

22. Gaetke L.M., Chow C.K. (2003) Copper toxicity, oxidative stress and antioxidant nutrients. *Toxicology*, vol. 189, pp. 147-163.

IRSTI 34.29.15; 87.19.81

[1]Mursaleen, [1]Syed Zahir Shah, [1]Liaqat Ali, [2]Nadeem Ahmad,
[2]Izaz Kuram, [2*]S. Barinova

[1]University of Peshawar, Department of Botany, Islamia College University,
Peshawar, Khyber Pakhtunkhwa, Old Jamrud Road, Pakistan, PK-25120,
[2]University of Peshawar, Department of Botany, Khyber Pakhtunkhwa, Old Jamrud Road, Pakistan, PK-25120
[3]Institute of Evolution, University of Haifa, Mount Carmel, 199 Abba Khoushi Ave., Haifa 3498838, Israel
[*]e-mail: sophia@evo.haifa.ac.il

Bioindication of water quality by algal communities in the Mardan River, Pakistan

Abstract: The first results of ecological assessment of water quality in the Mardan River and its tributary Kaltang is representing as a results of implementation of bioindication methods and statistical approaches. Altogether 165 taxa-indicators of algae from six taxonomic Divisions were revealed for the communities of three sites in the Mardan River main stream and one site of its left tributary Kaltang. Diatom algae with subdominants of greens, charophytes and cyanobacteria mostly dominated algal communities. Species richness was higher in the lower part of studied river in site Mardan, but community structure was similar in all four studied sites. Water variables values were fluctuated in small range excluding temperature and turbidity, which dramatically increased down the river. Bioindicators distribution reflect pollution impact to the river ecosystem by toxicants and dissolved organic matters that start form the middle reaches of the river when it follow across the flatland. Statistical analysis of species-environmental variables relationships with 3D plots construction revealed that algal species grow is dependent mostly with water temperature, whereas impacted by turbidity. Nevertheless, the self-purification properties of the Mardan River ecosystem were in high level.
Key words: algae, bioindication, water quality, Mardan river, Pakistan.

Introduction

Pollution in the freshwater aquatic objects is complicated system. When water variables that reflect water quality can be measured directly, this need resources and expenses. Unfortunately, in the developing countries have not resources for full water quality monitoring whereas the water quality is decreasing year by year. In this situation can help the bioindication methods and indices that used for assessment of pollution impact on the natural water bodies and based on the ecological point of view to the water and biota relationships [1; 2]. The first level of the trophic pyramid, the algae, is define all processes in the aquatic ecosystems and therefore can be used for assessment of water properties with help of its community structure and species ecology [3]. Algae reflect all natural and anthropogenic processes occurring in water bodies with help of developed systems of indication [4]. A bioindication using algae community is inexpensive express-method as compared to chemical analysis. Up to now, the diversity of algae was used in bioindication methods as a tool to monitor water quality of the rivers and lakes in many countries of the southern Eurasia [5-17].

The major problem in the Mardan River as in all Pakistan rivers is of the water quality decreasing during recent years as a result of increasing of pollution in this settled area with increasing agriculture. There are water from municipalities and agriculture provides a continuous input of nutrient and suspended solids into the river water. In Pakistan, algae have been reported from various freshwater habitats to know their environmental role and ecological distribution [19-23] but bioindication methods were implemented effectively for only the Kabul River itself and its tributary Swat up to now [7-9; 24].

The aim of present work was to reveal algal species indicators in the Mardan River and its tributary and to assess water quality with bioindication methods and statistics.

District Mardan is a part of the Peshawar valley in Pakistan. It lies between 34° 05’ to 34° 32’ north latitudes and 71° 48’ to 72° 25’ east longitudes. It

 Printed in Kazakhstan

is bounded on the northeast by Buner district, on north and north-west by Malakand Agency, on the southeast by Swabi district, on the south by Nowshera district and on the west by Charsadda district. Total area of the district Mardan is 1632 square kilometers [25]. Generally, streams and rivers flow from north to the south and west to the east. Most of the streams falls into the River Kabul. An important stream (Kalpani) of the district comes out from Baizai and flows in northwards direction and falls into the River Kabul. The Mardan River start after narrow canal from the northern part of the Kabul River basin where the Swat River flow. So, practically the Mardan River is a second part of the lower reaches of the Swat River, the first part of it follow across the reservoir to the west and after it wriggles in the mountains with input to the Kabul River from the north. The river basin of the Mardan River is mostly placed on the flat territory with developed agriculture. The main city in the river basin is Mardan that very settled and take large place in the river basin surface. The left tributary of the Mardan River also start from foothill and later follow across the lowlands up to input to the River Mardan after the Mardan city and above the Mardan River input to the Kabul River (Figure 1).

Figure 1 – Sampling sites in the Mardan River basin (yellow buttons), the left tributary of the Kabul River (blue buttons) in Peshawar valley

Materials and methods

Four research sites in the Mardan River were selected for sampling (Figure 1) in purpose to assessment the water quality in the district Mardan. Sites Sher Gharh, Takht Bhai, and Mardan has been chosen in the Mardan River itself, but the site Katlang is represent upper part of the left tributary of the Mardan River. These sites were chosen as critical points of the river Mardan water quality changes in the results of pollution input of numerous pollutants from different sources to the water which flow down across agriculturally used areas. The sampling points were chosen during the field trips with help of visual assessment of pollution because sampling for ecological assessment of the Mardan River was doing in first time.

A total 35 algal and 35 water samples were collected from each the research sites at 120-meter radius in different seasons of 2016. Algal samples were collected from water by scooping, as well as by scratching of floating habitat, attached with stones, submerged plants, and on sidewalls of ponds, streams and river. The collected material was placed into plastic bottles of 25 ml and transported in icebox to the laboratory of Department of Botany, Islamia College, University of Peshawar. The specimens were preserved in 4% formaldehyde solution. Temperature and pH of the water were determine with the help of portable pH meter HANNA-8414 on the sampling point, while electrical conductivity (EC), turbidity, total dissolved solids (TDS) and total suspended solids (TSS) were measured in the laboratory by using standard techniques.

Algal species identification was doing with microscope Nikon Lambda E2000 viewed at ×10, ×40 and ×100 objectives. Images of the algal species were captured with help of digital camera. Micrometric measurement (length and width) for each algal species has taken with ocular micrometer. Standard references were used for algal taxonomical identification [26-31]. Modern taxonomy was adapted with algaebase.org [32]. Bioindication properties of each revealed species comes from our world database [33; 34]. Statistical analysis of the data for the species diversity, indicators and water variables relationships was doing by 3D Surface plots using the Statistica 12.0 Program.

Results and discussion

Water variables

Fluctuation of six physiochemical variables of the river water was revealed for four studied sites of the Mardan River basin in 2016 (Table 1). Water temperature increased from 18 °C in site 1-Sher Gharh to 27.7 °C in 3-Mardan. Water pH also increased down the river from 7.5 to 8.84. Turbidity was dramatically increase in lower sites 3-Mardan and 4-Katlang up to 98 NTU and 58 NTU respectively. Electrical conductivity (EC) also increased from 260 μS cm^{-1} in 1-Sher Gharh to 607 μS cm^{-1} in 3-Mardan. Site 4-Katlang electrical conductivity was similar of it in site 2-Takht Bhai. Total dissolved (TDS) and suspended solids (TSS) values were increase from upper to lower stations and confirm the fluctuation trend of EC, which also demonstrated low influence of dissolved solids to the water quality. Comparison of environmental variables fluctuation have demonstrated strong influence of water turbidity to EC, dissolved and suspended solids. Increasing of water temperature and turbidity in the lower sites can be result of flattened the landscape in the river basin as well as increasing of agricultural effluents down the river.

Table 1 – Mean of measured variables of the water in studied sites of the Mardan River (1-3) and its tributary Katlang (4) in 2016

Variable	Sher Gharh (1)	Takht Bhai (2)	Mardan (3)	Katlang (4)
Temperature, C°	18	21	27.7	26.4
pH	7.5	7.8	8.34	8.84
Turbidity	3.2	9.2	98	58
Electrical conductivity, μS cm^{-1}	260	365	607	306
Total dissolved solids, mg l^{-1}	108	210	236	246
Total suspended solids, mg l^{-1}	220	230	225	290

Bioindication

We revealed 165 taxa with known ecological preferences from total 201 species of algae of the Mardan River communities [24] that can be used as indicators of nine environmental variables (Table 2). Its taxonomic Divisional distribution over the studied sites can see in Figure 2. Diatoms prevail in all sites with maximal diversity in the site 3-Mardan. It can give the best opportunity for bioindication because the diatoms is mostly studied in regards of species ecological properties and have most developed bioindication properties as can be seen in Table 2. So, algae indicators prefer benthic and plankto-benthic lifestyle in the Mardan River (Figure 2). They are indicators of temperate water temperature and middle oxygenated slow streaming low-alkaline and low saline water (Figure 2, 3). Organic pollution diatom indicators according Watanabe and species-indicators from all Divisions according Sládeček reflects middle level of pollution corresponds to Class 2 and 3 of water quality (Figure 3). Trophic state indicators are diverse and related to six from seven known trophic groups. Indicators of mesotrophic state are increased down the river whereas oligotrophes decrease with the same contain in the sites 3-Mardan and 4-Kaltang (Figure 4). Indicators of the nutrition type for algal species can show toxic impact if present. But no, distribution of indicator groups of autotrophy-heterotrophy in Figure 4 show strongly prevalence of autotrophic organisms with photosynthetic way of proteins creation and therefore survived without sufficient toxic impact.

Table 2 – Algae indicator species in communities of the Mardan River basin sites, 2016. Sampling sites: (1) Sher Gharh; (2) Takht Bhai; (3) Mardan; (4) Katlang. Substrate preferences (P – planktonic, P-B – plankto-benthic, B – benthic, Ep – epiphyte, S – soil); Temperature preferences (cool – cool-water, temp – temperate, eterm – eurythermic, warm – warm-water); Oxygenation and streaming (st – standing water, str – streaming water, st-str – low streaming water, aer – aerophiles); Salinity ecological groups (hb – oligohalobes-halophobes, i – oligohalobes-indifferents, mh – mesohalobes, hl – halophiles); Saprobity groups of diatoms (sx – saproxenes, es – eurysaprobes, sp – saprophiles); pH preferences range (alb – alkalibiontes; alf – alkaliphiles, ind – indifferents; acf – acidophiles; neu – neutrophiles as a part of indifferents); Nitrogen uptake metabolism preferences (ats – nitrogen-autotrophic taxa, tolerating very small concentrations of organically bound nitrogen; ate – nitrogen-autotrophic taxa, tolerating elevated concentrations of organically bound nitrogen; hne – facultatively nitrogen-heterotrophic taxa, needing periodically elevated concentrations of organically bound nitrogen; hce – obligately nitrogen-heterotrophic taxa, needing continuously elevated concentrations of organically bound nitrogen); Trophic state indicators (ot – oligotraphentic; o-m – oligo-mesotraphentic; m – mesotraphentic; me – meso-eutraphentic; e – eutraphentic; o-e – oligo- to eutraphentic (hypereutraphentic)); S – Index saprobity S.

Taxa	1	2	3	4	Hab	T	Oxy	pH	Sal	D	Sap	S	Tro	Aut-Het
Cyanobacteria														
Anabaena cylindrica Lemmermann	1	1	1	1	P-B,S	-	aer	-	-	-	b-o	1.7	-	-
Aphanocapsa grevillei (Berkeley) Rabenhorst	0	1	1	1	P	-	-	-	hb	-	o-b	1.4	-	-
Chroococcus turgidus (Kützing) Nägeli	0	1	1	1	P-B,S	-	aer	alf	hl	-	x-b	0.8	-	-
Chroococcus prescottii Drouet & Daily	1	1	0	1	P	-	-	-	-	-	-	-	o	-
Dolichospermum sigmoideum (Nygaard) Wacklin, L.Hoffmann & Komárek	1	1	1	1	P	-	-	-	i	-	o-a	2	e	-
Gloeocapsa alpina Nägeli	0	0	1	1	Ep,S	-	aer	-	-	-	-	-	-	-
Gloeocapsa rupestris Kützing	1	1	1	1	Ep,S	-	aer	-	-	-	-	-	-	-
Kamptonema formosum (Bory ex Gomont) Strunecký, Komárek & J.Smarda	1	1	1	1	P-B,S	-	st	-	-	-	a	3.1	me	-
Limnococcus limneticus (Lemmermann) Komárková, Jezberová, O.Komárek & Zapomelová	1	1	1	0	P	-	-	-	i	-	b-o	1.7	om	-
Limnoraphis birgei (G.M.Smith) J.Komárek, E.Zapomelová, J.Smarda, J.Kopecky, E.Rejmánková, J.Woodhouse, B.A.Neilan & J.Komárková	0	1	0	1	P-B	-	st	-	-	-	-	-	-	-
Lyngbya lutea Gomont ex Gomont	0	1	1	1	P-B	-	-	-	mh	-	-	-	-	-
Merismopedia convoluta Brébisson ex Kützing	1	0	1	1	P-B	-	-	-	-	-	b-a	2.5	om	-
Merismopedia tenuissima Lemmermann	1	1	1	1	P-B	-	-	-	hl	-	b-a	2.4	e	-
Microcystis aeruginosa (Kützing) Kützing	1	1	0	0	P	-	-	-	hl	-	b	2.1	e	-
Nostoc paludosum Kützing ex Bornet & Flahault	0	1	1	1	P-B,S	-	st	-	-	-	b-o	1.6	m	-
Oscillatoria curviceps C.Agardh ex Gomont	1	1	1	1	P-B	-	st-str	-	i	-	x-a	1.6	me	-

Prolongation of Tables 2

Taxa	1	2	3	4	Hab	T	Oxy	pH	Sal	D	Sap	S	Tro	Aut-Het
Oscillatoria limosa C.Agardh ex Gomont	1	1	1	1	P-B	-	st-str	-	hl	-	a-o	2.6	e	-
Oscillatoria major Vaucher ex Forti	1	1	1	1	B,Ep	-	-	-	-	-	b	2.3	m	-
Oscillatoria ornata Kützing ex Gomont	0	0	1	1	P-B,S	-	st-str	-	i	-	o-b	1.5	om	-
Oscillatoria princeps Vaucher ex Gomont	1	1	1	0	P-B,S	-	st-str	-	-	-	a-o	2.8	om	-
Oscillatoria tenuis C.Agardh ex Gomont	1	1	1	1	P-B,S	-	st-str	-	hl	-	a-o	2.6	me	-
Phormidium ambiguum Gomont	1	1	0	1	B,S	eterm	st-str	ind	i	-	b	2.3	me	-
Phormidium irriguum (Kützing ex Gomont) Anagnostidis & Komárek	0	1	1	1	B,Ep	-	aer	-	-	-	-	-	me	-
Phormidium puteale (Montagne ex Gomont) Anagnostidis & Komárek	1	0	1	0	B,S	-	st-str	-	-	-	-	-	-	-
Phormidium retzii Kützing ex Gomont	1	1	1	1	B,S	-	st-str	-	-	-	o-b	1.4	o	-
Phormidium stagninum Anagnostidis	0	1	1	1	B,Ep	-	-	-	-	-	-	-	om	-
Scytonema ocellatum Lyngbye ex Bornet & Flahault	0	0	1	1	S	-	-	-	-	-	-	-	-	-
Spirulina major Kützing ex Gomont	1	1	1	0	P-B,S	warm	st	-	hl	-	a	3.4	-	-
Bacillariophyta														
Amphora ovalis (Kützing) Kützing	1	0	1	1	B	temp	st-str	alf	i	sx	o-b	1.5	me	ate
Asterionella formosa Hassall	1	1	1	1	P	-	st-str	alf	i	sx	o	1.4	om	ate
Aulacoseira granulata (Ehrenberg) Simonsen	0	1	1	0	P-B	temp	st-str	ind	i	es	b	2	me	ate
Brachysira vitrea (Grunow) R.Ross	1	1	1	1	B	-	st-str	alb	i	es	x-o	0.5	om	ats
Caloneis bacillum (Grunow) Cleve	1	1	1	1	B	temp	st-str	ind	i	es	o	1.3	me	ats
Cocconeis pediculus Ehrenberg	0	1	1	1	B	-	st-str	alf	i	sx	o-a	1.8	me	ate
Cocconeis placentula Ehrenberg	1	1	1	1	P-B	temp	st-str	alf	i	es	o	1.4	me	ate
Cocconeis scutellum Ehrenberg	1	1	1	1	B	-	-	-	hl	-	-	-	-	-
Craticula ambigua (Ehrenberg) D.G.Mann	1	1	1	1	B	warm	st	alf	i	es	b	2.3	me	-
Craticula cuspidata (Kutzing) D.G.Mann	0	1	1	1	B	temp	st-str	alf	i	es	b-a	2.5	me	-
Cymatopleura solea var. *vulgaris* Meister	0	1	1	1	B	-	-	ind	i	-	-	-	-	-
Cymbella affinis Kützing	1	1	1	1	B	temp	st-str	alf	i	sx	o	1.1	ot	ats

Prolongation of Tables 2

Taxa	1	2	3	4	Hab	T	Oxy	pH	Sal	D	Sap	S	Tro	Aut-Het
Cymbella tumida (Brébisson) Van Heurck	1	1	0	1	B	temp	str	alf	i	sx	b	2.2	me	ats
Cymbella vulgata Krammer	1	1	1	0	B	-	-	ind	-	-	o	1	ot	-
Cymbopleura cuspidata (Kützing) Krammer	1	1	1	1	P-B	temp	-	ind	i	-	o-a	1.8	om	-
Diatoma vulgaris Bory	0	1	1	0	P-B	-	st-str	ind	i	sx	b	2.2	me	ate
Fragilaria acus (Kützing) Lange-Bertalot	0	1	0	0	P	-	st-str	alb	i	es	o-a	1.8	-	-
Fragilaria capucina Desmazières	0	1	1	1	P-B	-	-	ind	i	es	b-o	1.6	m	-
Fragilaria crotonensis Kitton	1	0	1	1	P	-	st-str	alf	I	es	o-b	1.5	m	ate
Frustulia rhomboides (Ehrenberg) De Toni	1	1	1	1	B	-	st	acf	hb	es	x	0.3	ot	ats
Frustulia vulgaris (Thwaites) De Toni	1	1	1	1	P-B	-	st	alf	i	es	o-a	1.8	me	ate
Gomphonema angustum C.Agardh	1	1	1	1	B	-	st-str	ind	i	es	o	1.1	ot	ats
Gomphonema olivaceum (Hornemann) Brébisson	1	1	1	1	B	-	st-str	alf	i	es	o-b	1.5	e	ate
Gomphonema parvulum (Kützing) Kützing	1	0	1	0	B	temp	str	ind	i	es	b	2.4	om	hne
Gomphonema truncatum Ehrenberg	0	0	1	1	B	-	st-str	ind	i	es	o-b	1.4	me	ats
Gyrosigma acuminatum (Kützing) Rabenhorst	1	1	1	0	B	cool	st-str	alf	i	es	o-a	2	me	ate
Gyrosigma attenuatum (Kützing) Rabenhorst	1	1	1	1	P-B	-	st	alf	i	-	o-a	1.8	om	ate
Gyrosigma wormleyi (Sullivant) Boyer	1	1	0	1	B	-	-	alf	hl	-	b	2	om	-
Halamphora normanii (Rabenhorst) Levkov	0	1	1	1	B	-	ae	alf	hb	-	x	0.1	m	ats
Iconella robusta (Ehrenberg) Ruck & Nakov	1	1	1	0	P-B	-	st-str	ind	I	es	x-o	0.5	ot	-
Lindavia comta (Kützing) Nakov, Gullory, Julius, Theriot & Alverson	1	1	1	1	P	-	st	alf	i	sx	o	1.2	om	-
Mastogloia danseyi (Thwaites) Thwaites ex W.Smith	1	1	1	1	B	-	-	alf	mh	-	o	1	-	-
Mastogloia smithii Thwaites ex W.Smith	0	0	1	1	B	-	-	alf	mh	sx	o	1.3	me	-
Melosira varians C.Agardh	0	0	1	1	P-B	temp	st-str	ind	hl	es	b	2.1	me	hne
Meridion circulare (Greville) C.Agardh	1	1	0	1	B	-	str	ind	i	es	o	1.1	om	ate
Navicula cryptocephala Kützing	1	1	1	0	P-B	temp	st-str	ind	i	es	b	2.1	oe	ate
Navicula exilis Kützing	1	1	1	1	B	-	-	alb	hl	es	x-b	0.8	ot	-
Navicula radiosa Kützing	1	0	1	1	B	temp	st-str	ind	i	es	o	1.3	me	ate

Prolongation of Tables 2

Taxa	1	2	3	4	Hab	T	Oxy	pH	Sal	D	Sap	S	Tro	Aut-Het
Navicula rhynchocephala Kützing	1	1	0	1	B	-	-	alf	hl	-	o-a	2	om	ate
Navicula tripunctata (O.F.Müller) Bory	1	1	1	1	P-B	-	st-str	ind	i	es	b-o	1.7	e	ate
Navicula veneta Kützing	0	1	1	1	B	-	-	alf	hl	es	a-o	2.7	-	-
Neidium ampliatum (Ehrenberg) Krammer	0	1	1	1	B	-	st	ind	I	es	o-x	0.6	ot	-
Neidium dubium (Ehenberg) Cleve	1	1	1	1	B	-	str	alf	i	-	b-o	1.7	me	ats
Nitzschia commutata Grunow	0	1	1	1	P-B	-	-	alf	mh	-	b	2	-	-
Nitzschia filiformis (W.Smith) Van Heurck	1	1	1	1	P-B	-	st-str	alf	hl	es	b-a	2.5	e	hne
Nitzschia linearis W.Smith	1	1	1	1	B	temp	st-str	alf	i	es	b-o	1.7	me	ate
Nitzschia paleacea (Grunow) Grunow	1	1	1	1	P-B	-	st-str	alf	i	es	b	2.2	e	hce
Nitzschia scalpelliformis Grunow	0	0	1	1	B	-	-	alf	hl	sp	b	2	me	-
Nitzschia sigmoidea (Nitzsch) W.Smith	1	1	0	1	P-B	-	st-str	alf	i	-	b-a	2.5	e	ate
Odontidium anceps (Ehrenberg) Ralfs	1	1	1	1	P-B	cool	st-str	neu	hb	sx	o-x	0.6	ot	-
Pinnularia globiceps W.Gregory	0	0	1	1	B	-	-	acf	i	-	x	0.2	om	-
Pinnularia major (Kützing) Rabenhorst	0	1	1	0	B	temp	st-str	ind	i	-	o-x	0.6	me	ate
Pinnularia microstauron (Ehrenberg) Cleve	1	1	0	1	P-B	temp	st-str	ind	i	sp	o-x	0.7	ot	ate
Pinnularia viridis (Nitzsch) Ehrenberg	1	1	1	1	P-B	temp	st-str	ind	i	es	x	0.3	oe	ate
Placoneis gastrum (Ehrenberg) Mereschkowsky	1	1	1	1	B	-	st-str	ind	i	sx	o-b	1.4	e	ate
Sellaphora pupula (Kützing) Mereschkovsky	0	1	1	1	B	eterm	st	ind	hl	sx	o-a	1.9	me	ate
Stauroneis acuta W.Smith	1	0	1	1	B	-	st-str	alf	i	-	o	1	om	-
Stauroneis anceps Ehrenberg	0	1	1	1	P-B	-	st-str	ind	i	sx	o	1.3	om	ate
Surirella librile (Ehrenberg) Ehrenberg	1	1	1	0	B	-	st-str	alf	i	-	b	2.1	e	ate
Surirella ovalis Brébisson	1	0	1	1	P-B	-	st-str	alf	I	es	a	3	me	ate
Tryblionella hungarica (Grunow) Frenguelli	1	1	0	0	P-B	-	-	alf	mh	sp	a-o	2.9	e	ate
Ulnaria danica (Kützing) Compère & Bukhtiyarova	1	1	1	1	P-B	temp	-	alf	i	es	b-o	1.7	om	-
Ulnaria ulna (Nitzsch) Compère	0	1	1	1	P-B	temp	st-str	ind	i	es	b	2.3	oe	ate
Urosolenia longiseta (O.Zacharias) Edlund & Stoermer	1	0	1	1	P	-	-	-	hl	-	x-b	0.9	-	-

Prolongation of Tables 2

Taxa	1	2	3	4	Hab	T	Oxy	pH	Sal	D	Sap	S	Tro	Aut-Het
Ochrophyta														
Tribonema elegans Pascher	0	1	1	1	B	-	-	-	-	-	x	1	-	-
Tribonema minus (Wille) Hazen	0	1	1	1	B	-	-	-	i	-	x-b	0.9	-	-
Euglenozoa														
Euglena deses Ehrenberg	0	0	0	1	P-B,S	warm	st-str	ind	mh	-	b	2.2	-	-
Euglena elastica Prescott	1	0	1	0	P-B	-	st-str	-	-	-	b-a	2.5	-	-
Euglena gracilis G.A.Klebs	1	1	1	1	P-B	eterm	st	ind	oh	-	b	2.3	-	-
Euglena oblonga F.Schmitz	0	1	1	0	P	eterm	st-str	ind	-	-	b	2.1	-	-
Euglenaformis proxima (Dangeard) M.S.Bennett & Triemer	0	1	1	1	P-B	eterm	st-str	ind	mh	-	p-a	3.5	-	-
Monomorphina pyrum (Ehrenberg) Mereschkowsky	1	1	1	0	P-B	eterm	st-str	ind	mh	-	b	2.4	-	-
Phacus acuminatus Stokes	0	1	1	1	P-B	eterm	st-str	-	i	-	b-a	2.5	-	-
Phacus elegans Pochmann	0	1	1	0	-	-	-	-	-	-	o-a	1.9	-	-
Phacus triqueter (Ehrenberg) Perty	0	0	1	1	P-B	-	st-str	-	i	-	b-a	2.5	-	-
Trachelomonas superba Svirenko	1	0	1	1	P-B	-	st-str	-	-	-	o-a	1.8	-	-
Chlorophyta														
Acutodesmus acutiformis (Schröder) Tsarenko & D.M.John	0	1	1	1	P-B	-	st-str	-	-	-	o-a	1.8	-	-
Ankistrodesmus falcatus (Corda) Ralfs	1	1	1	1	P-B	-	st-str	-	hb	-	b	2.3	-	-
Chaetophora pisiformis (Roth) C.Agardh	1	1	1	1	B	-	-	-	-	-	o	1.3	-	-
Chlamydomonas angulosa O.Dill	1	1	1	1	P	-	st	-	-	-	o-a	1.8	-	-
Chlamydomonas debaryana Goroschankin	0	1	1	0	P	-	-	-	-	-	a	3	-	-
Chlamydomonas ehrenbergii Gorozhankin	1	1	1	1	P	-	-	-	-	-	p-a	3.5	-	-
Chlamydomonas globosa J.W.Snow	0	1	1	1	P,S	-	-	-	-	-	o-a	1.9	-	-
Chlorella vulgaris Beyerinck	1	1	1	1	P-B, pb,S	-	-	-	hl	-	a	3.1	-	-
Cladophora glomerata (Linnaeus) Kützing	1	1	1	1	P-B	-	st-str	alf	i	-	o-a	1.9	-	-
Coelastrum astroideum De Notaris	1	0	1	1	P	-	st-str	-	-	-	b	2.2	-	-
Coelastrum sphaericum Nägeli	1	1	1	1	P-B	-	st-str	-	i	-	o-b	1.4	-	-
Desmodesmus opoliensis (P.G.Richter) E.Hegewald	1	1	1	1	P-B	-	st-str	-	-	-	b	2.2	-	-

Prolongation of Tables 2

Taxa	1	2	3	4	Hab	T	Oxy	pH	Sal	D	Sap	S	Tro	Aut-Het
Geminella minor (Nägeli) Heering	1	1	1	1	-	-	-	-	-	-	o-a	1.8	-	-
Haematococcus lacustris (Girod-Chantrans) Rostafinski	1	0	1	1	P	-	st	-	-	-	o	1.3	-	-
Hydrodictyon reticulatum (Linnaeus) Bory	1	1	1	1	P-B	-	st	-	-	-	o-a	1.8	-	-
Kirchneriella obesa (West) West & G.S.West	1	1	1	1	P-B	-	st-str	-	i	-	o-a	1.8	-	-
Monactinus simplex (Meyen) Corda	1	1	1	1	P-B	-	st-str	-	-	-	b	2	-	-
Monoraphidium mirabile (West & G.S.West) Pankow	0	0	1	1	P-B	-	st	-	oh	-	b-a	2.5	-	-
Oedogonium cardiacum Wittrock ex Hirn	1	1	1	1	B	-	-	-	-	-	o-b	1.5	-	-
Pandorina morum (O.F.Müller) Bory	0	1	0	1	P	-	st	-	i	-	b	2.3	-	-
Protosiphon botryoides (Kützing) Klebs	0	1	1	1	S	-	-	-	-	-	o	1.1	-	-
Scenedesmus obtusus Meyen	0	1	1	0	P-B	-	st-str	-	-	-	o-a	1.8	-	-
Scenedesmus parisiensis Chodat	0	1	1	1	-	-	-	-	-	-	o-a	1.9	-	-
Schizomeris leibleinii Kützing	1	1	0	1	-	-	-	-	-	-	b-a	2.4	-	-
Selenastrum capricornutum Printz	1	1	1	1	-	-	-	-	-	-	o-b	1.5	-	-
Sphaerellocystis ampla (Kützing) Nováková	1	1	1	0	P-B	-	-	alf	-	-	b-o	1.7	-	-
Stigeoclonium lubricum (Dillwyn) Kützing	0	1	1	0	-	-	-	-	-	-	b-a	2.5	-	-
Tetradesmus dimorphus (Turpin) M.J.Wynne	1	1	1	0	-	-	-	-	-	-	b	2.3	-	-
Tetradesmus obliquus (Turpin) M.J.Wynne	1	0	0	1	P-B	-	st-str	ind	i	-	b	2.1	-	-
Ulothrix tenerrima (Kützing) Kützing	1	0	1	1	B	-	st	-	i	-	o-a	1.8	-	-
Ulothrix zonata (F.Weber & Mohr) Kützing	1	1	1	0	P-B	-	st-str	ind	i	-	o-a	1.8	-	-
Charophyta														
Chara aspera C.L.Willdenow	0	1	1	0	B	-	-	-	-	-	o	1.2	-	-
Chara braunii var. *schweinitzii* (A.Braun) Zaneveld	0	0	1	1	B	-	-	-	-	-	o	1.2	-	-
Chara globularis Thuiller	0	1	1	1	B	-	st	-	-	-	o	1.2	-	-
Chara vulgaris Linnaeus	1	1	1	1	B	-	st-str	-	-	-	o	1.1	-	-
Closterium acerosum Ehrenberg ex Ralfs	1	1	1	1	P-B	-	st-str	ind	i	-	a-o	2.6	e	-
Closterium angustatum Kützing ex Ralfs	0	1	1	1	B	-	-	acf	-	-	-	-	om	-
Closterium attenuatum Ralfs	0	1	1	1	B	-	-	ind	-	-	-	-	m	-

Prolongation of Tables 2

Taxa	1	2	3	4	Hab	T	Oxy	pH	Sal	D	Sap	S	Tro	Aut-Het
Closterium baillyanum (Brébisson ex Ralfs) Brébisson	0	1	1	1	B	-	-	ind	-	-	-	-	om	-
Closterium lunula Ehrenberg & Hemprich ex Ralfs	1	0	1	1	B	-	-	ind	-	-	x-b	0.8	m	-
Closterium parvulum Nägeli	1	0	1	0	P-B	-	-	ind	i	-	b	2	m	-
Closterium turgidum Ehrenberg ex Ralfs	1	1	1	1	B	-	-	acf	-	-	-	-	m	-
Cosmarium biretum Brébisson ex Ralfs	1	1	1	1	P-B	-	-	ind	-	-	-	-	me	-
Cosmarium botrytis Meneghini ex Ralfs	0	0	1	1	P-B	-	st-str	ind	i	-	o-a	1.9	m	-
Cosmarium formosulum Hoff	1	1	1	1	P-B	-	-	ind	-	-	o-a	1.8	me	-
Cosmarium granatum Brébisson ex Ralfs	1	1	1	1	B	-	st-str	ind	i	-	o	1.2	m	-
Cosmarium nitidulum De Notaris	1	0	1	1	-	-	-	acf	-	-	-	-	m	-
Cosmarium reniforme (Ralfs) W.Archer	0	1	0	1	P-B	-	st-str	ind	hb	-	o	1	me	-
Cosmarium subcrenatum Hantzsch	1	1	1	1	B,aer	-	aer	acf	-	-	o	1.1	m	-
Cosmarium undulatum Corda ex Ralfs	0	1	1	1	P-B	-	-	acf	i	-	-	-	m	-
Mougeotia robusta (De Bary) Wittrock	1	1	1	1	B	-	-	-	-	-	o	1	-	-
Mougeotia scalaris Hassall	1	1	1	0	B	-	-	-	i	-	o-b	1.5	-	-
Spirogyra crassa (Kützing) Kützing	0	1	1	0	B	-	-	-	-	-	o-b	1.5	-	-
Spirogyra daedalea Lagerheim	0	1	1	1	B	-	st-str	-	-	-	-	-	-	-
Spirogyra inflata (Vaucher) Dumortier	0	1	1	1	B	-	-	-	-	-	o	1.1	-	-
Spirogyra maxima (Hassall) Wittrock	1	1	1	1	B	-	-	-	-	-	o	1.1	-	-
Spirogyra parvula (Transeau) Czurda	0	1	1	1	B	-	st-str	-	-	-	-	-	-	-
Spirogyra porticalis (O.F.Müller) Dumortier	1	1	1	1	B	-	-	-	-	-	o-b	1.4	-	-
Spirogyra varians (Hassall) Kützing	1	1	1	1	P-B	-	-	-	oh	-	b	2.1	-	-
Spirogyra weberi var. *grevilleana* (Hassal) O.Kirchner	1	0	1	1	B	-	st	-	-	-	-	-	-	-
Zygnema vaginatum Klebs	0	1	1	0	B	-	-	-	-	-	o	1	-	-

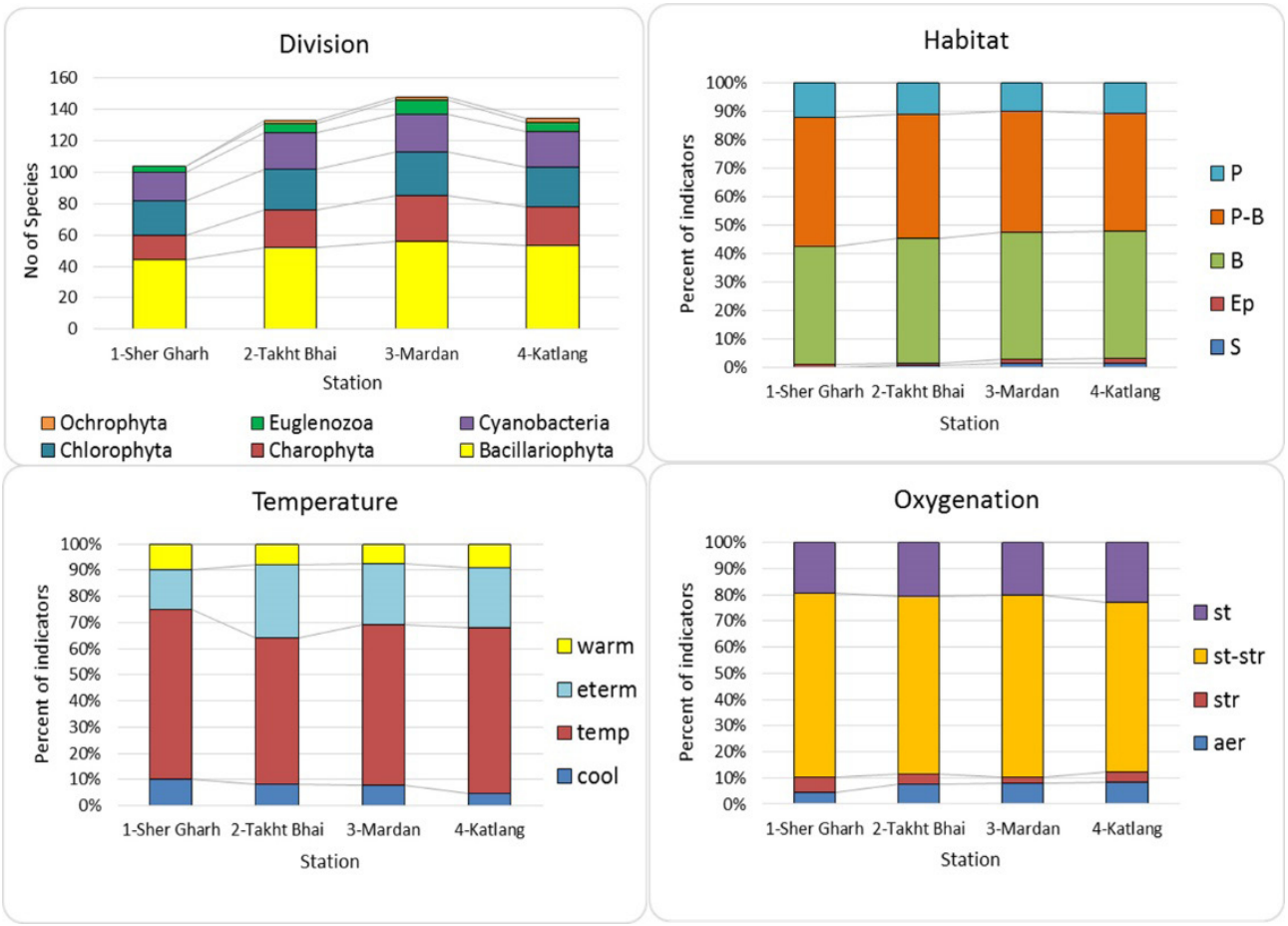

Figure 2 – Distribution of indicator species in Taxonomic divisions and in the ecological groups of habitat preferences, Water temperature, and Water streaming and oxygenation over the sampling sites of the Mardan River basin, 2016

Bioindicators give us great possibility to reveal the environmental variables that important to algal community grows because the primary producers are responsible o the self-purification process in the river ecosystem. By this, the 3D surface plots were constructed for revealing relationships between species groups and major environmental variables, which influenced it.

For this analysis, we choose the most fluctuated in the Mardan River environmental variables such as water pH, TDS, turbidity, and temperature for construction of 3D plots. Figure 5 show bioindicators and these variables relationships. The indicators of the lifestyle of algae in the Mardan River communities have two important groups of substrate preferences that defined self-purification process in the ecosystem of large rivers: planktonic and benthic species. Can be seen that planktonic group is preferred lower turbidity but indifferent to fluctuation of water temperature and TDS, and therefore, have better environment in the upper part of the river (Figure 5a, b). Benthic species preferred high temperature and TDS but indifferent to suspended solids (Figure 5c, d), and therefore can survive over all sites of studied river. Indicators of water fluidity and oxygenation distribution show preferences of high turbidity, pH and water temperature that are peculiarities of the lower sites of the river (Figure 5e, f). This distribution also demonstrate that turbidity is impacted factor for algal grows and indicators of this group are mostly reflected oxygenation than fluidity of water in the Mardan River.

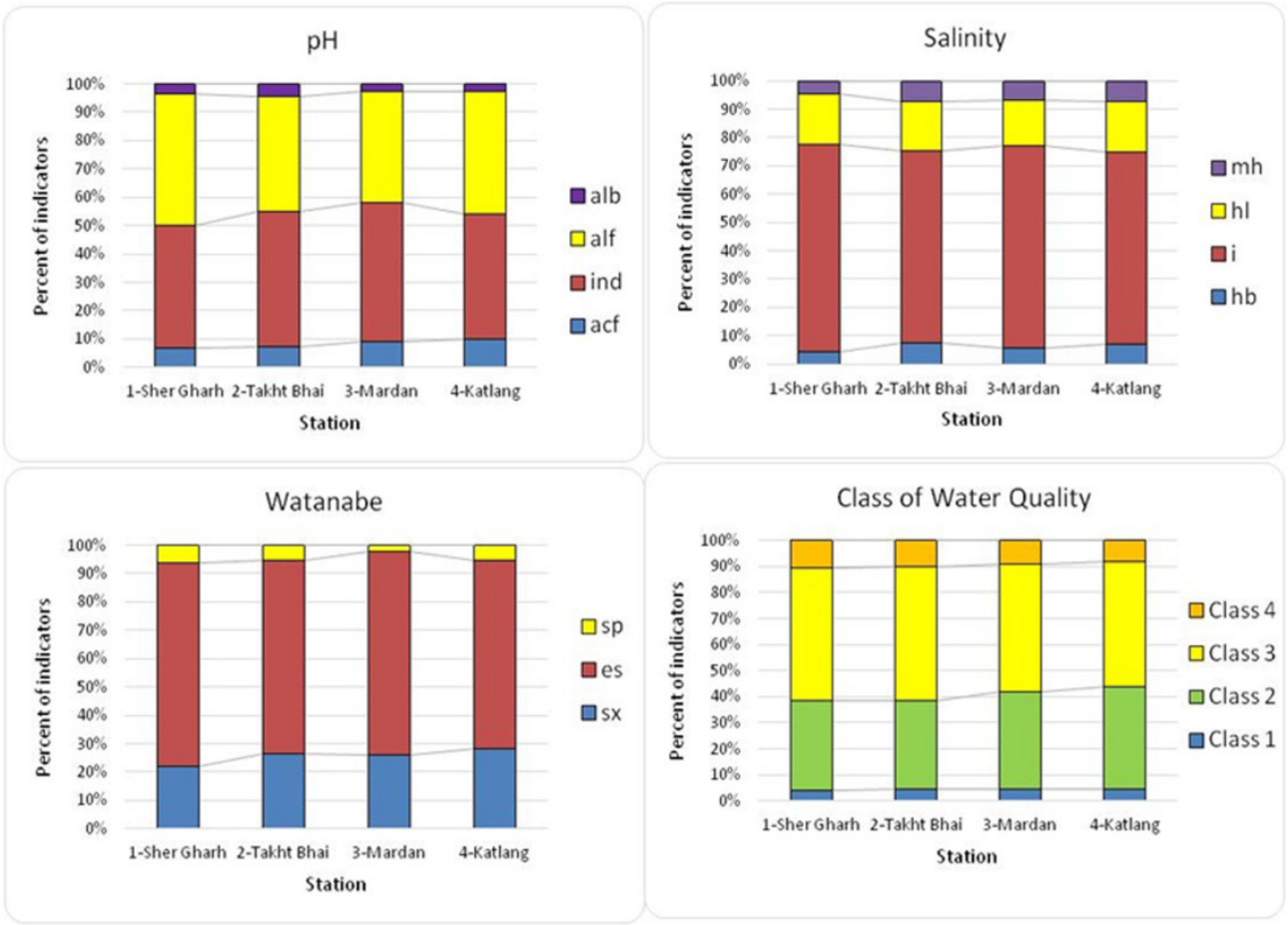

Figure 3 – Distribution of indicator species in the ecological groups of Water pH, Salinity, Organic pollution according Watanabe, and Class of Water quality according Sládeček self-purification ranks over the sampling sites of the Mardan River basin, 2016. Classes of Water Quality are in EU color code

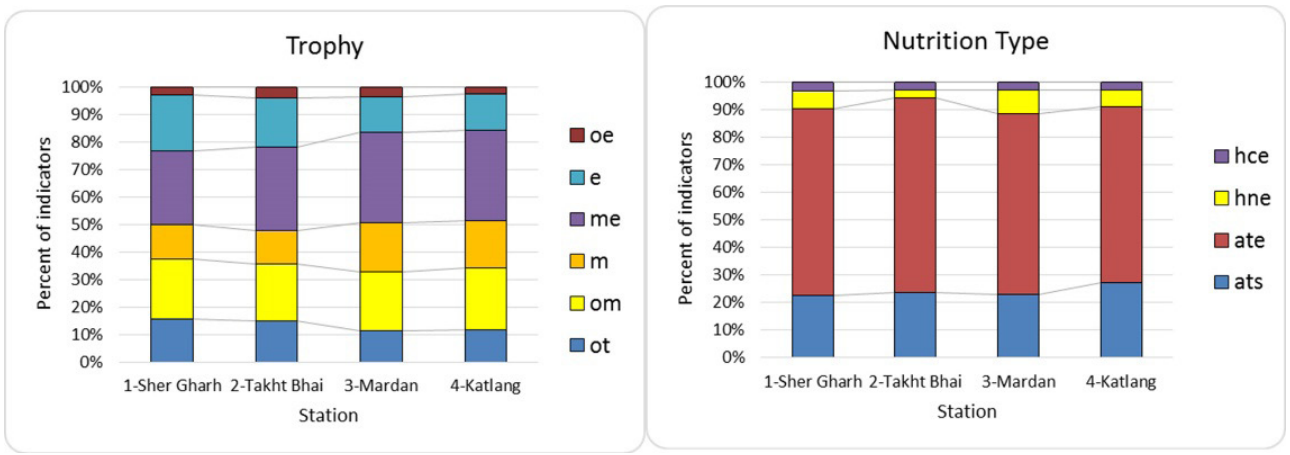

Figure 4 – Distribution of indicator species in the ecological groups of Trophic state and Type of nutrition over the sampling sites of the Mardan River basin, 2016

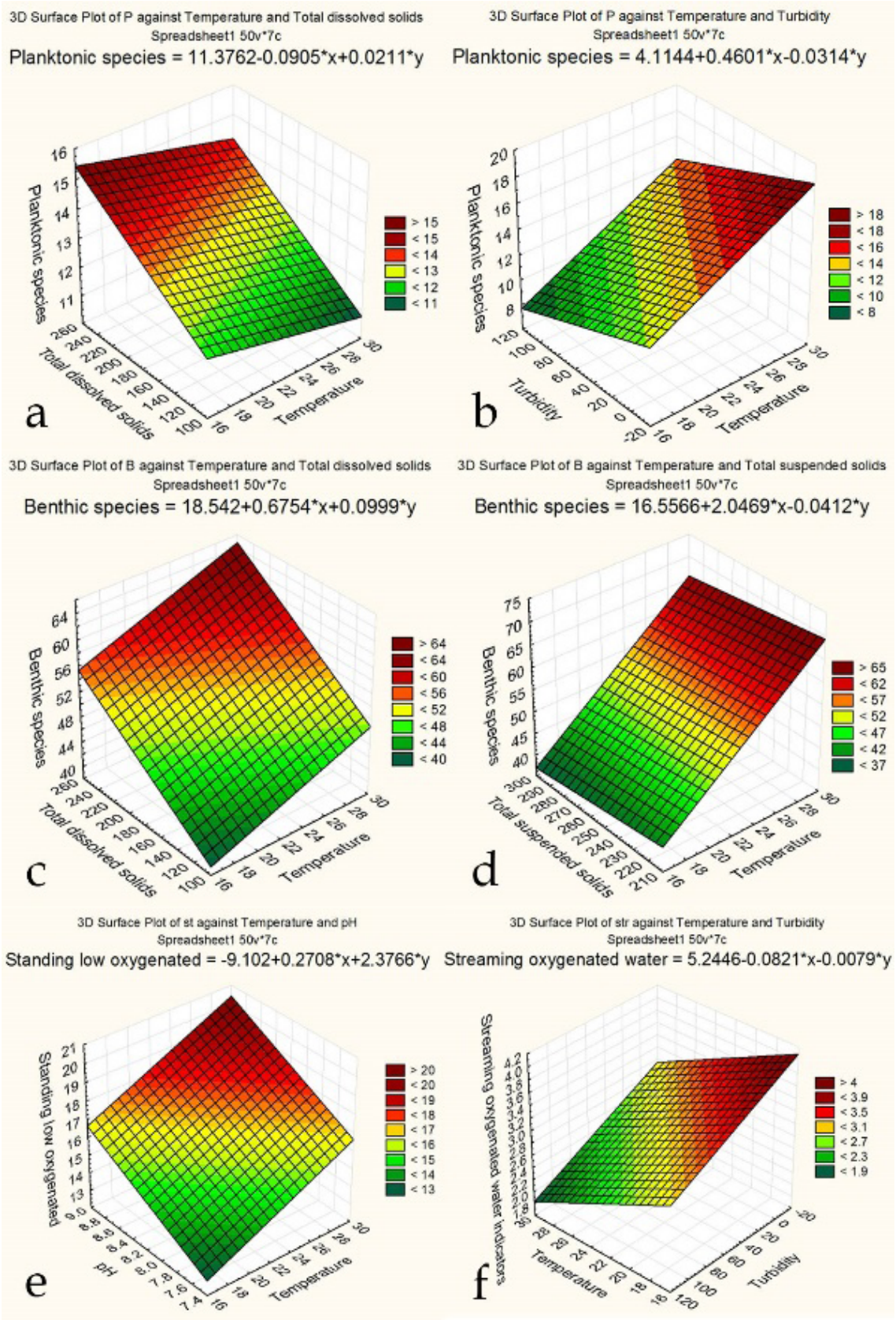

Figure 5 – Relationships of indicator species in the ecological groups of algal community habitat (a-d), water moving and oxygenation (e, f) and environmental variables: TDS, turbidity, temperature, and pH in the Mardan River basin, 2016

Distribution of salinity indicators show preference of its major groups of species for high water TDS but indifferent to water temperature (Figure 6a, b) and therefore marked the lower sites as source of salinity input. Indicators of acidification distribution (Figure 6c, d) demonstrated preference of high temperature but indifferent to turbidity that are water properties of the lower sites. Group of alkalibiontes, the indicators of high water pH, preferred lower temperature and high TDS that are in the upper site.

Figure 6e demonstrated organic pollution indicators preference of high temperature and TDS that are characteristics of lower sites, and marked it as polluted. The same preference can be recognized in Figure 6f where eutrophic state indicators mostly grows in the waters with high temperature and TDS that also marks lower sites 3-Mardam and 4-Kaltang as stay under eutrophication impact with organic pollution.

Indicators of nutrition type of algal species can clarify situation with toxic substances pollution [35]. So, Figure 7a show preference of autotrophic species the waters with high TDS but lower temperature (Figure 7a) which are in the upper part of the river. The facultative heterortophes, that used both types of nutrition, with chlorophyll and dissolved organics and can be a markers of some toxic influence, preferred wat

ers with high temperature and lower TDS (Figure 7b) that are the characteristic properties of water in the middle sites. Both this distributions (Figure 7a, b) can demonstrate that some pollution toxicants input is started from the middle part of the studied river, but ecosystem processes of self-purification still as rather high. Indicators of water quality of Class 2 preferred high temperature but water TDS was not so important for they grows (Figure 7c) that can be in the middle part of the river. The indicators of organically polluted waters of Class 4 preferred low temperature waters with high TDS (Figure 7d) that also is characteristics of the middle sites. It let us to conclude that organic pollution input start in the middle part of the Mardan River.

Our bioindication results demonstrated the similarity of studied Mardan River with the Swat River with differences of prevailing of autotrophic species and indicators of mesotrophic state in the Mardan River [14]. Similar distribution of species has been found for the Kabul River [9] but self-purification was mostly doing by charophytic algae in Kabul River. In any case, bioindication approach demonstrated peculiarities of the rivers in the Kabul River basin with prevailing of autotrophic algal species that preferred fresh middle oxygenated mesotrophic waters. These results are over than chemical analysis data [9] and can be received with help of bioindication only.

Conclusion

Bioindication of the Mardan River and its left tributary Katlang in 2016 was doing on the base of 165 species that were indicators of nine environmental variables. Bioindication methods were choose for the water quality assessment because the environmental variables were studied in the small quantity, only six due to limited opportunities for chemical analysis. In any case, the measured chemical water properties help us to reveal the water quality is fluctuated down the river with sharply increasing of temperature and turbidity in the lower site of the main river Mardan and its tributary Katlang. Water pH, dissolved and suspended solids were fluctuated in small range. We cannot define any other environmental variables but our aims were to describe situation with water pollution in the Mardan River basin because the water quality is very important for Pakistan. Biondication helps us to reveal that in self-purification processes in the studied river are mostly participated diatoms with followed by charophytes, greens and cyanobacteria. Temperature impact start from the site 2-Takht Bhai, whereas the measured variable show sharp increasing of this parameter only on the lower site 3-Mardan. Indicators are characterize the studied river as low saline, low alkaline and middle organically polluted where algae grows in plankton and periphyton and preferred low flowing middle oxygenated waters. More precision characteristics of water properties give us the statistical analysis of indicator species distribution over most fluctuated water variables – temperature, turbidity and pH. With helps of 3D surface plots, we revealed that turbidity is impacted factor for algal grows. Water temperature stimulated algal development in sites from middle reaches in site Takht Bhai and in the same site were started pollution effluents with organic and toxic components up to lower site Mardan and in tributary Katlang. Bioindication show also that this fluctuation of ecosystem properties can be related with flowing the river across the flatland with high agricultural activity. Nevertheless, algal community of the river is purify the river water mostly with help of photosynthetic processes. Therefore, we can to conclude that bioindication methods can help not only for characterize the water quality but also reveal early changes in pollution input and ecosystem trophic state when opportunities for chemical analysis is limited.

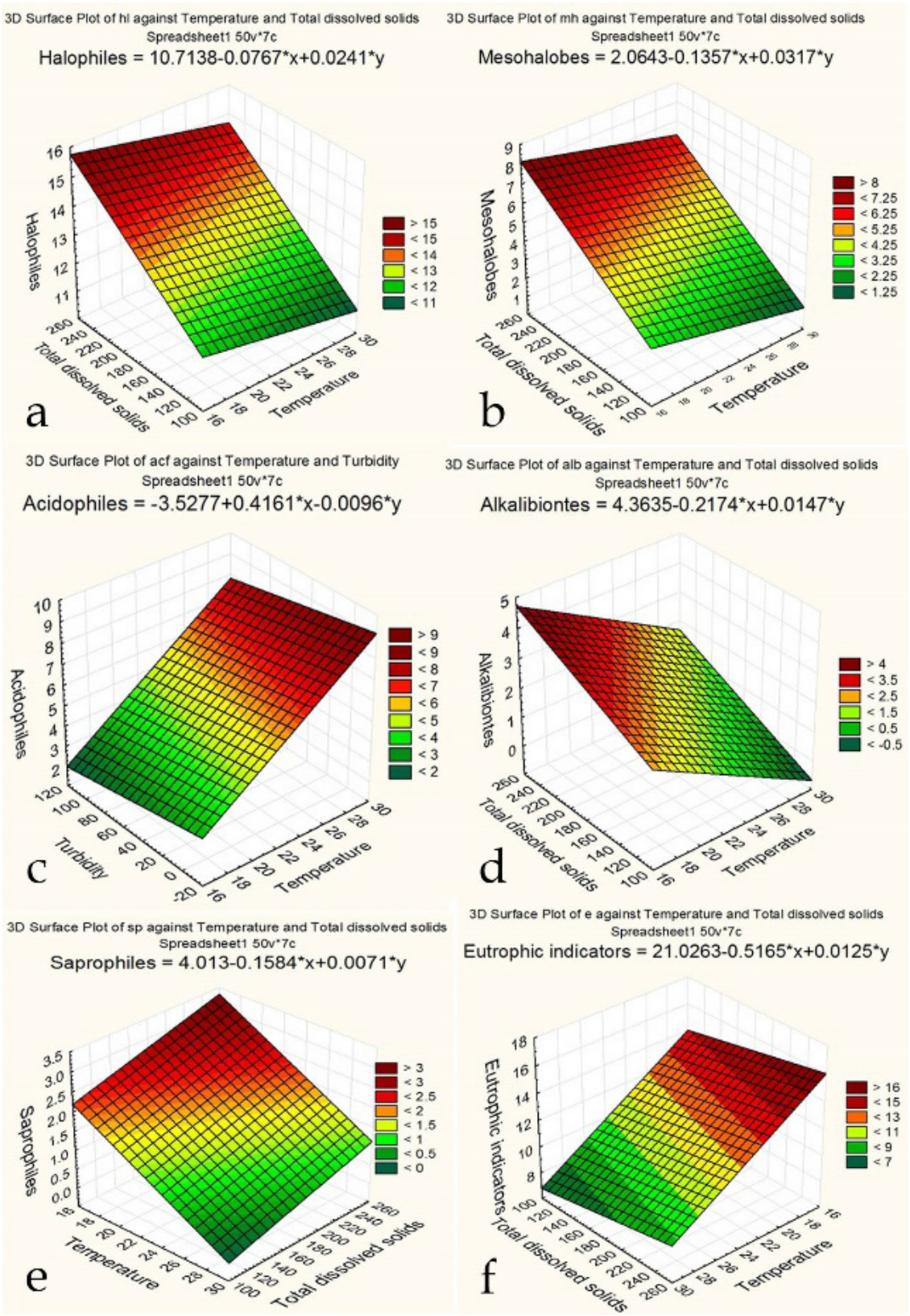

Figure 6 – Relationships of indicator species in the ecological groups of salinity (a, b), pH (c, d), organic pollution (e), and eutrophic state (f) and environmental variables: TDS, turbidity, temperature, and pH in the Mardan River basin, 2016

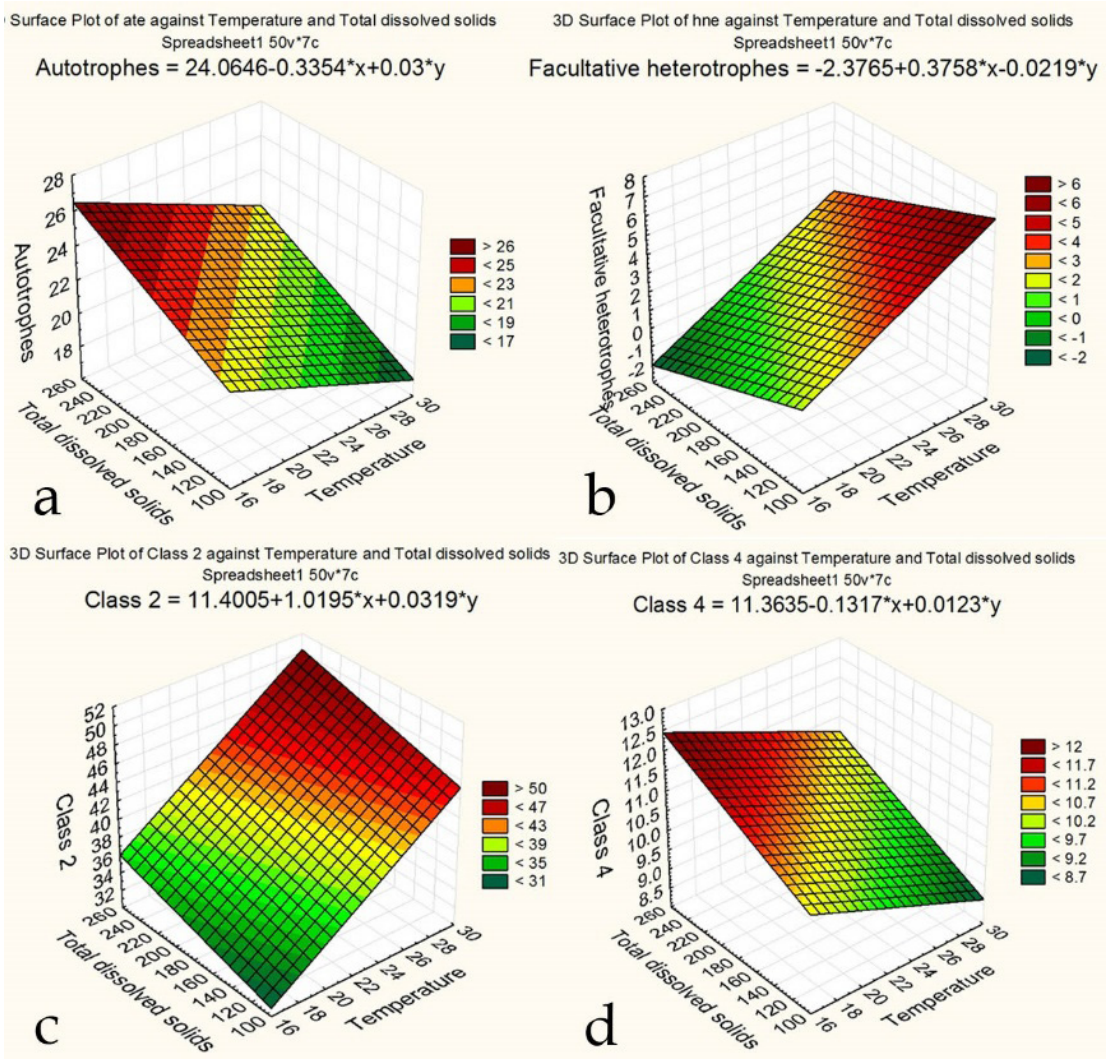

Figure 7 – Relationships of indicator species in the ecological groups of autotrophes (a), facultative heterotrophes (b), organic pollution indicators of Class 2 (c), and Class 4 (d), and environmental variables TDS and temperature in the Mardan River basin, 2016

Acknowledgements

We are thankful to the Department of Botany, Islamia College Peshawar, on providing us research facility to perform our research work in smooth environment. The work was partly supported by the Israeli Ministry of Aliyah and Integration.

References

1. Dokulil M.T. (2003) Algae as ecological bioindicators. In: Market B.A., Breure A.M., Zechmeister H.G. Bioindicators and Biomonitors. *Elsevier, Oxford*, pp. 285-327.

2. Bellinger E.G., Sigee D.C. (2015) Freshwater algae: identification and use as bioindicators. 2nd ed. *Chichester, UK: Wiley*. p. 296.

3. Barinova S. (2017) On the classification of water quality from an ecological point of view. *Int J Envir Sci Nat Res*., vol. 2, no. 2, pp. 1-8.

4. Barinova S. (2017) Essential and practical bioindication methods and systems for the water quality assessment. *Int J Envir Sci Nat Res*., vol. 2, no. 3, pp. 1-11.

5. Barinova S., Krassilov V.A. (2012) Algal diversity and bio-indication of water resources in Israel. *Int J Env Rec*., vol. 1, pp. 62-72.

6. Ghosh S., Barinova S., Keshri J.P. (2012) Diversity and seasonal variation of phytoplankton community in the Santragachi Lake, West Bengal, India. *Q-Science Connect*, vol.3, pp. 1-14.

7. Khuram I., Ahmad N., Jan S., Barinova S. (2014) Freshwater green algal biofouling of boats in the Kabul River, Pakistan. *Ocean Hydrobiol Stud*., vol. 43, no. 4, pp. 329-336.

8. Khuram I., Barinova S., Ahmad N., Ullah A., Siraj Ud Din, Jan S., Hamayun M. (2017) Ecological assessment of water quality in the Kabul River, Pakistan, using statistical methods. *Ocean Hydrobiol Stud*., vol. 46, no. 2, pp. 140-153.

9. Barinova S., Khuram I., Asadullah, Ahmad N., Jan S., Shin D.H. (2016) How water quality in the Kabul River, Pakistan, can be determined with algal bio-indication. *Adv Stud Biol*., vol. 8, no. 4, pp. 151-171.

10. Barinova S., Anissimova O.V., Nevo E., Jarygin M.M., Wasser S.P. (2004) Diversity and ecology of algae from the Nahal Qishon River, northern Israel. *Plant Biosys*., vol. 138, no. 3, pp. 245-259.

11. Barinova S., Tavassi M., Glassman H. (2009) Diversity and ecology of algae from the Lower Jordan River, Israel. *Plant Biosys*., vol. 143, no. 2, pp. 340-360.

12. Sarim F.M., Sultana N., Nisa K. (2009) Fresh water algae of river Sardaryab, district Charsadda, Pakistan. *Pak J Plant Sci*., vol. 15, pp. 69-74.

13. Barinova S. (2011) Algal diversity dynamics, ecological assessment, and monitoring in the river ecosystems of the eastern Mediterranean. *NY, USA: Nova Science Publishers*, p. 363

14. Barinova S., Ali N., Barkatullah (2013). Ecological adaptation to altitude of algal communities in the Swat Valley (Hindu Cush Mountains, Pakistan). *Exp Op Env Biol*., vol. 2, no. 2, pp. 1-15.

15. Barinova S., Krupa E., Tsoy V., Ponamareva L. (2018) The application of phytoplankton in ecological assessment of the Balkhash Lake (Kazakhstan). *Appl Ecol Env Res*., vol. 16, no. 3, pp. 2089-2111.

16. Niyatbekov T., Barinova S. (2018) Bioindication of water properties by algal communities in the Pamir high mountain mineral and thermal springs. *Transylv Rev Syst Ecol Res*., vol. 20, no. 3, pp. 1-30.

17. Barinova S., Krupa E. (2017) Bioindication of ecological state and water quality by phytoplankton in the Shardara Reservoir, Kazakhstan. *Env Ecol Res*., vol. 5, no. 2, pp. 73-92.

18. Barinova S., Keshri J. P., Ghosh S., Sikdar J. (2012) The influence of the monsoon climate on phytoplankton in the Shibpukur pool of Shiva temple in Burdwan. West Bengal, India. *Limnol Rev*., vol. 2, no. 2, pp. 47-63.

19. Khalid M.N., Mustafa S., Saleem S. (2010) Studies on bioactivities and phycochemistry of *Microcystis aeruginosa* (Cyanophycota) from Sindh. *Pak J Bot*., vol. 42, pp. 2635.

20. Ali S.T., Hasan M., Shameel M. (2008) Occurrence of the families Naviculaceae and Surirellaceae (Bacillariophyta) in the Punjab and NWFP, Pakistan. *Pak J Bot*., vol. 40, no. 5, pp.2143-2148.

21. Sarim F. M., Zaman A. (2005) Some freshwater algae of District Charsadda NWFP, Pakistan. *Pesh Uni Teach Assoc J. (PUTAJ)*, vol. 12, pp. P. 5-10.

22. Hussain F., Anjum G., Zaidi M. I., Faridi M.A.F. (1984) Fresh water algae of Hann Urak Valley Quetta. *Pak J Bot*., vol. 16, no. 1, pp. 81-84.

23. Anjum G., Hussain F. (1984) Two new algae from Peshawar valley. *Pak J Bot*., vol. 16, no. 1, pp. 85-86.

24. Mursaleen, Shah S.Z., Ali L., Ahmad N., Kuram I., Barinova S.S. (2018) Algal communities of the Mardan River in ecological assessment of water quality in district Mardan, Pakistan. *MOJ Ecol Env Sci*., vol. 3, no. 2, pp. 82-92.

25. District Sensus Report of Mardan District (DCR), 1998.

26. Prescott G.W. (1962) Algae of the Western Great Lakes area. *Dubuque, Iowa: Wm. C. Brown Co. Pub.*, p. 977.

27. Transeau E.N. (1951) The Zygnemataceae. *Columbus, Ohio: Ohio State Univ Press*, p.327.

28. Collins F.S. (1909) The green algae of North America. *Tufts College Studies*., vol. 2, pp. 79-480.

29. Lange-Bertalot H. (2001) Navicula sensu stricto. Diatoms of Europe. 2. *Ruggell: Gantner Verlag K.G*., p. 526.

30. https://westerndiatoms.colorado.edu/taxa/species/encyonema_pergracile. – Diatoms of the United States, 2017.

31. John D.M., Whitton B.A., Brook A.J. (2011) The freshwater algal flora of the British Isles: An identification guide to freshwater and terrestrial algae. *Cambridge, UK: Cambridge University Press*, p. 878.

32. Guiry M.D., Guiry G.M. (2017) AlgaeBase. World-wide electronic publication. Galway, National University of Ireland. http://www.algaebase.org.

33. Barinova S.S., Medvedeva L.A., Anissimova O.V. (2006) Diversity of algal indicators in environmental assessment. *Tel Aviv: Pilies Studio*, p. 498.

34. Barinova S., Fahima T. (2017) The development of the world database of freshwater algae-indicators. *J Env Ecol*., vol. 8, no. 1, pp. 1-7.

35. UNEP/IPCS. 2006. Training Module No. 3. Section C. Ecological Risk Assessment. Prepared by The Edinburgh Centre for Toxicology. http://www.chem.unep.ch/

IRSTI 34.39.27

[1*]G.D. Daulet, [1]G.K. Atanbaeva, [1]S.T. Tuleukhanov, [1]A. Ydyrys,
[2]A. Baishanbo, [3]S.N. Abdireshov

[1]Laboratory of Human and Animal Physiology, Almaty, Kazakhstan
[2]Basic medical college of Xinjiang medical university, Urumqi, China
[3]Institute of Human and Animal Physiology MES RK,
National Academy of Sciences, Almaty, Kazakhstan
[*]e-mail: daulet.guldana@mail.ru

Injection of sorbent and subsequent analysis of blood cells

Abstract: This article indicates the adaptive reaction of the blood and lymph system that is affected by the extreme factor which is toxic substance. Change of the viscosity and overall protein composition of the blood and lymph, the erythrocytes and leukocytes of the rats which were receiving toxic substance for a long period of time and small changes in concentration of ions were observed. SUMS-1 (1g/kg) was used as a detoxicant in the experiment. The impact of toxic substances has decreased and animal state has improved after intake of SUMS-1. Regarding the composition and flow of the lymph, physico-chemical and biochemical parameters of blood cells were positive. When using the organic compounds lymph flow declined and composition reduced, whereas application of enterosorbent detoxifiers resulted conversely. After introduction into abdominal cavity SUMS-1 displayed high sorption properties. Sorbents are characterized by their ability to absorb toxic substances. In recent years, sorbents are widely used in various diseases, so it has great importance in the treatment and prevention. It is noticed that the physical and chemical properties of the animals blood receiving the sorbent improved. As can be seen from these data, the excretion of toxic substances from the body during sorbent reception was significant higher. The data obtained during the experiment showed that the decrease in erythrocytes was observed simultaneously with the reduction of hematocrit, which showed that the plasma portion of the blood increased and the appearance of hydrobialysis. It should be noted that the addition of enterosorbent to rats leads to a restoration of the volume of plasma and blood cells. The results provide strong evidence that SUMS-1supplementation is beneficial in protecting the kidneys from CCl_4 toxicity. This kind work of research in this area should be continued.

Key words: composition of lymph, blood flow, SUMS-1, sorbent, biochemical parameters of blood, hematological parameters of blood, tetrachloromethane.

Introduction

According to the forecasts of the World Health Organization experts (WHO, Geneva, 2003), the XXI century faces the global spread of diseases of cardiovascular system, liver and kidneys [1]. Due to the impact of anthropogenic factors, the appearance of malfunction, disabilityes are constantly increasing, now they are on the first rank of social importance and will not lose urgency continue in future.

Heavy metal toxicity has proven to be a major threat and there are several health risks associated with it. The toxic effects of these metals, even though they do not have any biological role, remain present in some or the other form harmful for the human body and its proper functioning. They sometimes act as a pseudo element of the body while at certain times they may even interfere with metabolic processes [2]. Few metals, such as aluminum, can be removed through elimination activities, while some metals get accumulated in the body and food chain, exhibiting a chronic nature. Various public health measures have been undertaken to control, prevent and treat metal toxicity occurring at various levels, such as occupational exposure, accidents and environmental factors. Metal toxicity depends upon the absorbed dose, the route of exposure and duration of exposure, for example acute or chronic. This can lead to various disorders and can also result in excessive damage due to oxidative stress induced by free radical formation [3].

Metals are substances with high electrical conductivity, malleability, and luster, which voluntarily lose their electrons to form cations. Metals are found

 Printed in Kazakhstan

naturally in the earth's crust and their compositions vary among different localities, resulting in spatial variations of surrounding concentrations. Heavy metals are generally referred to as those metals which possess a specific density of more than 5 g/cm^3 and adversely affect the environment and living organisms. These metals are quintessential to maintain various biochemical and physiological functions in living organisms when in very low concentrations, however they become noxious when they exceed certain threshold concentrations. Although it is acknowledged that heavy metals have many adverse health effects and last for a long period of time, heavy metal exposure continues and is increasing in many parts of the world [4].

Carbon tetrachloride (CCl_4) is a potent nephrotoxin, as it causes acute as well as chronic toxicity in kidneys. CCl_4 is a toxic chemical, widely used in the dry cleaning industry, in filling fire extinguishers, in the fumigation of grains, and as an insecticide [5]. Recent studies have shown that CCl_4 is associated with advanced production of free radicals leading to dysfunction of several organs [6]. Chronic CCl_4 treatment is a common practice to induce hepatic fibrosis, renal, pulmonary and testicular injuries, and cardiac tissue damage in rats as an experimental model.

Tissue damage by CCl_4 depends on the amount of dosage and duration of exposure of the experimental animals to this toxicant. Its action is based on membrane lipid peroxidation and induction of trichloromethyl radical (•CCl3), resulting in severe cell damage [7-9]. It is evidenced that metabolic activation of CCl_4 by cytochrome P450 resulted in the production of trichloromethyl radical (•CCl3) and peroxy trichloromethyl radical (•OOCCl3) that, in turn, initiate subsequent lipid peroxidation, responsible for injuries in various organs such as liver and kidney [10]. Therefore, it can be stated that CCl_4 is the well-characterized tool for the study of oxidative stress trials as it consistently generates free radicals with the implication of pathological environment.

These free radicals damage the integrity of liver cell membranes by releasing the cytosolic enzymes such as alanine transaminase, aspartate transaminase, alkaline phosphatase, and lactate dehydrogenase into the blood stream and elevating thiobarbituric acid reactive substances (TBARS) level with subsequent necrosis and inflammatory cell infiltration; affect physical parameters of kidney such as urinary and serum profile; increase lysosomal enzymes activities of testis and kidney; and decrease the activity of a diagnostic marker enzyme creatinine phosphokinase (an enzyme responsible for ATP regeneration) in cardiac tissue [11].

Oral intake of magnesium also has beneficial effects on lipid metabolism and efficiency of insulin in maintaining glucose homeostasis in human subjects [12; 13]. Mg deficiency is known to decrease the level of GSH in erythrocytes and even inhibit its biosynthesis, and in agreement with these findings, magnesium supplementation was shown to induce a significant increase in GSH in kidney of mice treated with cadmium [14]. Magnesium intake is capable of decreasing the blood concentration of vanadate in rats and the cadmium level in blood, kidney, spleen, and bone marrow in rabbits. In addition, both oral and intraperitoneal supplementation of magnesium acetate were effective against cadmium toxicity.

Benzene is among the most widely used chemicals in the world. It is mainly used to make materials such as plastics, rubbers, dyes, detergents and pesticides. It can also be found in automobile and industrial fumes [15]. Its toxic effects on blood cells are well documented and it is known to cause different kinds of leukemia, multiple myeloma and non-Hodgkin lymphoma. However, the exact mechanisms involved in its toxicity are not yet understood [16].

Researchers from Universiti Kebangsaan Malaysia built on previous research that shows that benzene is metabolized in the liver, then its metabolites are further metabolized in the bone marrow to produce 1,4-benzoquinone (1,4-BQ), which is known for its toxic effects on blood cells. The team studied the effects of 1,4-BQ on haematopoietic stem cells (HSCs are stem cells found in the bone marrow that can give rise to any kind of blood cell) and haematopoietic progenitor cells (the bone marrow can differentiate into only one specific type of blood cell) in mic [17].

Adsorption at various interfaces has concerned scientists since the beginning of this century. This phenomenon underlies a number of extremely important processes of utilitarian significance. The technological, environmental and biological importance of adsorption can never be in doubt. Its practical applications in industry and environmental protection are of paramount importance. Crucial progress in theoretical description of the adsorption has been achieved, mainly through the development of new theoretical approaches formulated on a molecular level, by means of computer simulation methods and owing to new techniques which examine surface layers or interfacial regions [18; 19].

An effective method for removing dissolved organic substances that cause tastes, odours, or colours is adsorption by activated carbon. Adsorption is the

capacity of a solid particle to attract molecules to its surface. Powdered carbon mixed with water can adsorb and hold many different organic impurities. When the carbon is saturated with impurities, it is cleaned or reactivated by heating to a high temperature in a special furnace. The adsorbed molecules are usually referred to collectively as the adsorbate. An example of an excellent adsorbent is the charcoal used in gas masks to remove poisons [20-22].

During the study, the lymphatic system revealed the results of studies of toxic substances. During long-term use of organic poisons, one can notice changes in lymphatic flow, arterial pressure, total protein composition, lymphatic and viscous blood pressure, and changes in potassium ion concentrations in rats. In experiment we used sorbent SUMS-1 (1 gr/kg) as detoxicant. In generalit has positive effect on lymphatic and lymphatic components, on blood cells, on the physico-chemical and biochemical outcome.

The regeneration of blood cells after the action of sorbents significantly influenced the positive results in the lymphocyte counts in the blood cells. The use of entercorbents rapidly decreased the negative effects of organic poison to lymphodynamics and lymphatic structure. After thesorbents, the biochemical and physico-chemical properties of the plasmids and lymphsimproved. This determine the highest concentration of sorbent in SUMS-1 [23].

Materials and methods

55 laboratory rats with weight of 220-250 g served the objects of the study. They were divided into 4 groups. The first group was a control group (n=10), the second group (n=15) and the third group (n=15) were experimental group. Experiments were conducted after 10 and 30 days afterwards injecting intoxication, this group' rats received 0.3 mL of CCl_4, three times a week. The fourth group (n=15) obtained the SUMS – 1 sorbent (1/kg) after the injection of CCl_4.

Research work was carried out in the laboratory of physiology and lymphatic systems of the Institute of Human and Animal Physiology, MES RK and in the Laboratory of Human and Animal Physiology, Department of Biophysics and Biomedicine, Faculty of Biology and Biotechnology, Al-Farabi Kazakh National University. Morphology of the blood cells: erythrocyte, platelet, leukocyte indices were defined by using Sysmex KX-21 – hematological analyzer (HORIBA, Japan). Amount of blood oxygen and Ph index were defined with the help OSMETECH OPTI™ CCA-hematological analyzer (OPTI, USA). All animals were identified to have electrolytes from blood plasma, lymph and urine by ion analyzer. Experimental data was processed using the Microsoft Excel for Windows 2007 application, spreadsheet Excel 7.0.

Physical-chemical indicators of blood cells were determined by using the method of Sukharev, its viscosity is decided by the VK-4 viscosimeter and used well-known haemotoxic method. Total protein, urea, and creatinine concentrations in the lymph and plasma were measured by using Bio-Lachema-Test kits. Plasma activities of ALT and AST and bilirubin content were measured and thymol test was carried out by the Routine methods. The homeostasis disorders caused by CCl_4 were corrected by adsorbent (1 g/kg), shown on Figure 1.

Results and discussion

Also known by several other names, hematocrit is the most important determinant of the whole blood viscosity. It is the volume percentage of red blood cells in blood and normally counts 47±5% for men and 42±5% for women. It is considered an integral part of a person's complete blood count results, along with hemoglobin concentration, white blood cell count, and platelet count. Hematocrit levels can indicate possible disease. An abnormally low hematocrit may suggest anemia, a decrease in the total amount of red blood cells, while an abnormally high hematocrit is called polycythemia. Both are potentially life-threatening.

Blood viscosity and vascular resistance affect total peripheral resistance to blood flow, which is abnormally high in the established phase of primary hypertension. In accordance with hematocrit indices of plasma portion of the blood was decreased. When various changes appear, blood cells perform several functions in accordance with features (Figure 1).

According to the results, hematocrit indices that the amount of blood cells in poisoned rats has been decreased obviously and amounted to an average of 11-15%.

As can be seen from the Figure 2, 10 days since poisoning the number of the red blood cells decreased by 8.9%, and after 30 days, it rose to 17.14% (in the observation group 8.87 ± 0.1 mmol/L). Normally, the number of leukocytes 6.79 ± 0.2 mmol/L, after 10 days poisoning 4.62 ± 0.1 mmol/L, and after 30 days, the number of leukocytes rose considerably to 80.47% (Figure 2).

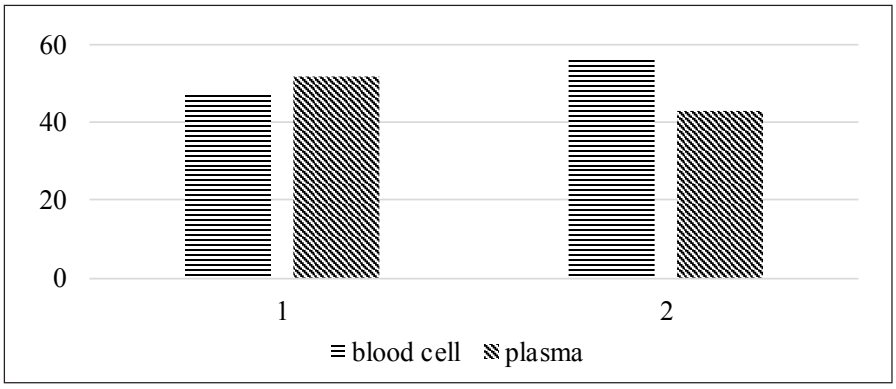

Figure 1 – Changes in hematocrit indices in normal rats and in rats poisoned with CCl_4, where: ordinate axis – the percentage of hematocrit; X–axis: 1 – normal group, 2 – after intoxication with CCl_4

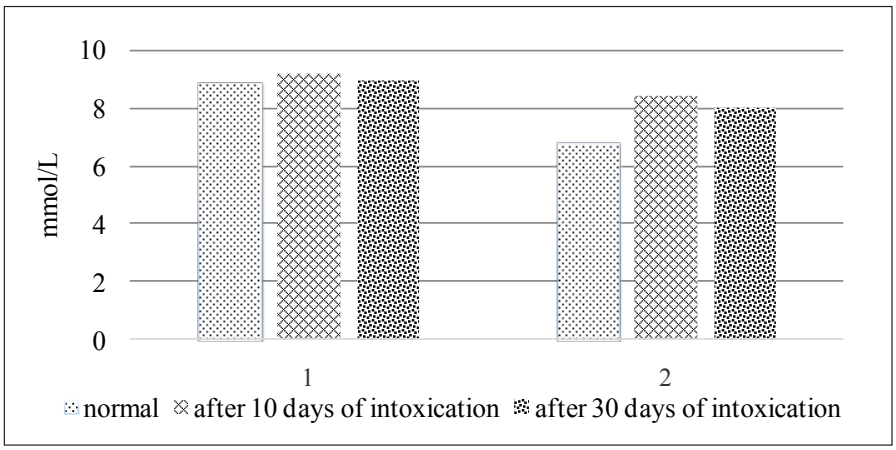

Figure 2 – Changes of erythrocytes and leukocytes after intoxication, where: ordinate axis – amount of blood cells, mmol/L; X–axis: 1 – red blood cells; 2 – white blood cells

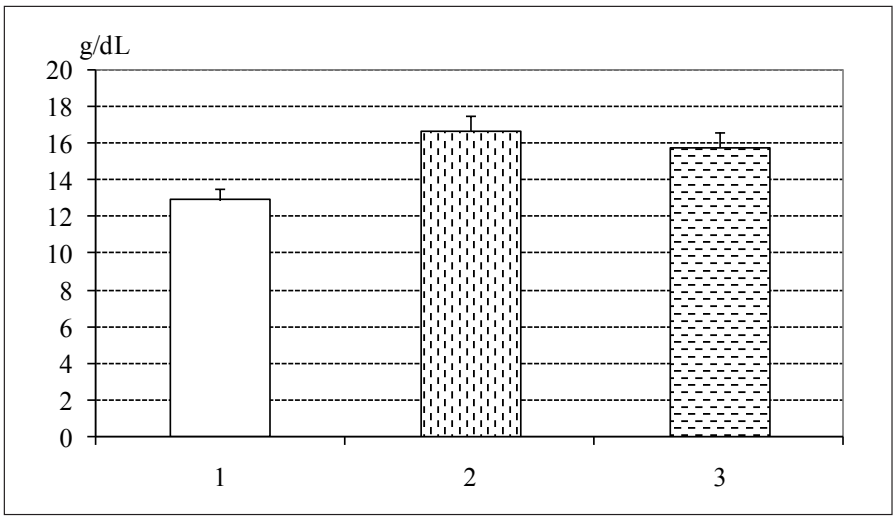

Figure 3 – The amount of blood hemoglobin of normal and poisoned rats, where: 1 – control (normal conditions), 2 – after 10 days of intoxication, and 3 – after 30 days of intoxication

Figure 3 shows that after 10 and 30 days of intoxication, hemoglobin and hematocrit level is climbing. The level of hemoglobin of rats during the observation period is 12.9, and in rats after 10 and 30 days of poisoning, it is equal to 16.7 and 15.8 g/dL (Figure 3).

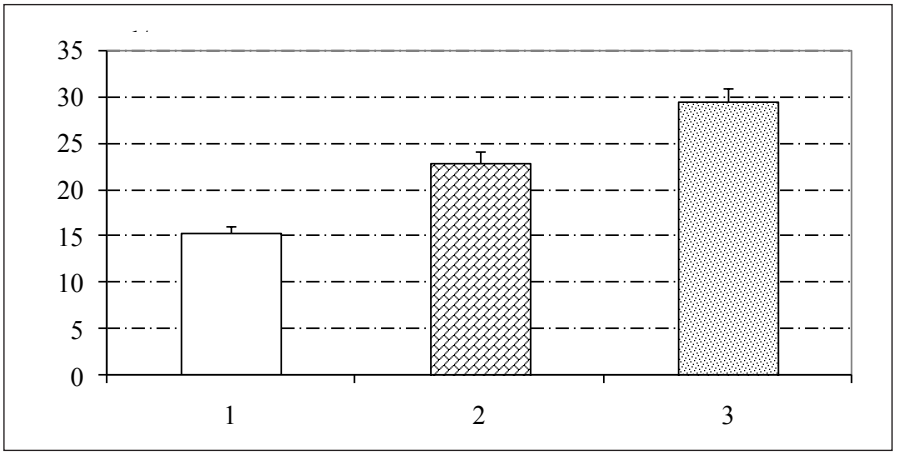

Figure 4 – Number of lymphocytes in the blood of rats, where: 1 – control (normal conditions), 2 – after 10 days of intoxication, and 3 – after 30 days of intoxication

As can be seen from the Figure 4, lymphocyte indices reach 59.08%, and rise up by 1.3 and 1.2 times after 10 and 30 days ($p<0.05$). Indices of blood monocytes in the normal state is 14.15%, after 10 and 30 days of intoxication, these numbers decrease to 35.8 and 47.9%. After 10 and 30 days of intoxication, platelets of the observation group increase by 2.3 times in compare to control.

The sorbents are different in nature, presented by natural betonies, such as clean soil consisting of minerals, as well as artificial synthetic sorbents. The method of absorption is called sorption therapy. Toxic substances from biological fluids might be removed with different sorbents, with enterosorption playing an important role in the reduction of the pathological condition of the body.

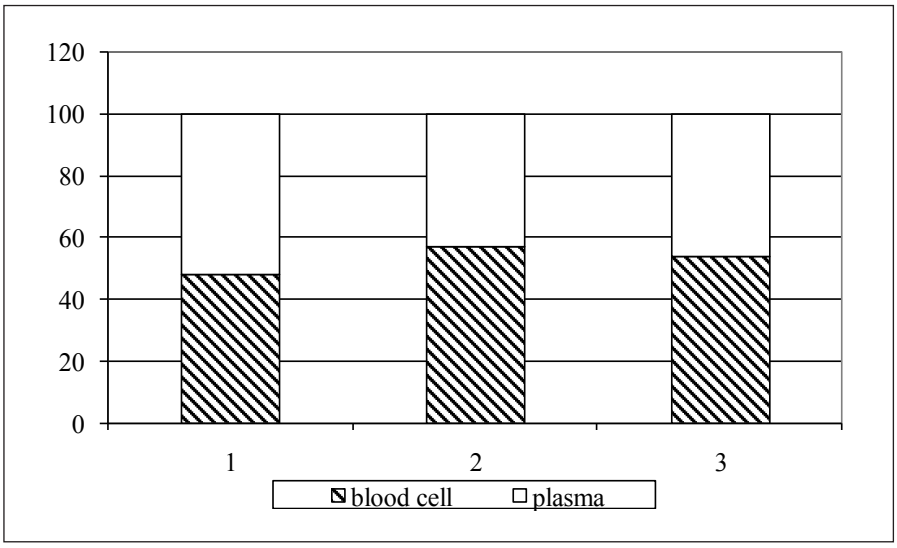

Figure 5 – Hematocrit indices of intoxication with dichloromethane and the perception of enterosorbent, where: ordinate axis: the percentage of hematocrit; X–axis: 1 – control (normal conditions), 2 – after intoxication, 3 – taking the sorbent with CCl_4

The experimental data shows that by hematocrit indices, levels of plasma part in the blood increased and decreasing volume of red blood cells shows the appearance of polyplasmia which can be seen simultaneously (Figure 5).

Improving the flow of lymph after taking enterosorbent accelerates the output of organic poisons from microcirculation zone. In experiment, sorbent SUMS-1 (1g/kg) was used as detoxicant. Influence of the sorbent blood cells restored, indices of lymphocytes in the blood is improved. Usage of enterosorbents immediately reduced the impact of organic poisons on lymph dynamics and lymph in the blood (Figure 7).

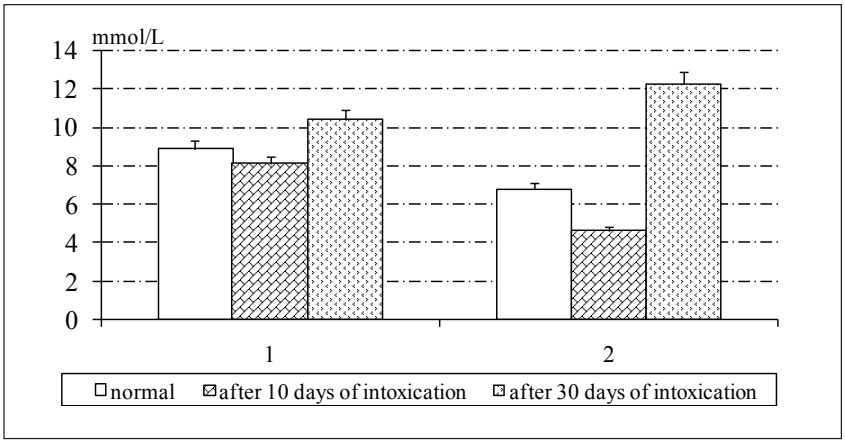

Figure 6 – The indices of erythrocytes and leukocytes in the perception of sorbent after intoxication with dichloromethane, where: 1 – red blood cells, 2 – white blood cells

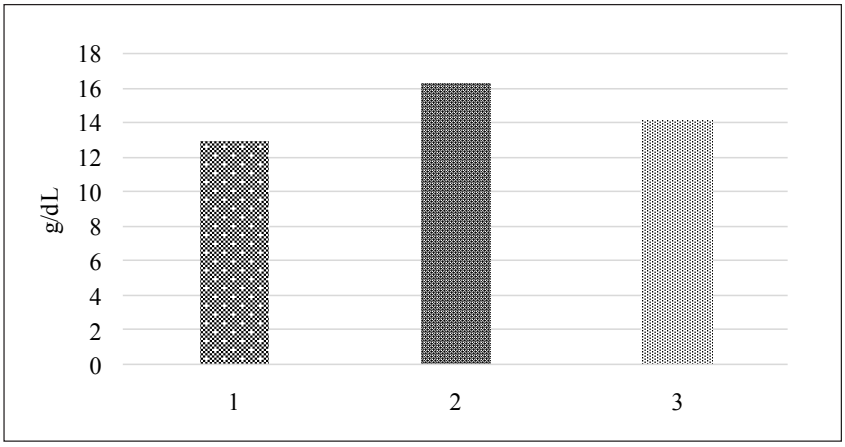

Figure 7 – Level of hemoglobin in animals after enterosorbent influence, where: 1 – control (normal conditions), 2 – after intoxication, 3 – taking the sorbent with CCl_4

Conclusion

1. During the poisoning of rats with organic toxicants, blood pH indicators change towards acidosis. The changes in the blood compared with the period of experiment shows that after 10 days erythrocytes number decreased by 8%, and after 30 days it increased by 17%, as well as the first 10 days the leukocytes number decreased by 31%, and after 30 days increased to 20%. From these result, we can see the more influence of CCl_4, the detrimental effect on the internal state of the animal, lymph dynamics and biochemical composition of blood and lymph. In addition, due to the influence of the sorbent blood cells restored, indexes of lymphocytes in the blood improved.

2. Usage of enterosorbents significantly reduced the adverse impact of organic poisons on lymph dynamics and composition of lymph. The regeneration of blood in rats after the injection of sorbents prove

that the sorbent SUMS-1 has a good quality of sorption. Sorbent SUMS-1 showed that it is possible to restore changes in the organism after intoxication. This shows that the work needs further researches. In experiment, applied sorbent SUMS-1 (1g/kg) as detoxicant which led to an improvement in the state of change which was the result of organic poisoning, in general terms – it became known that it has a positive effect on lymph flow, the cell lymph, blood cell elements, physical-chemical and biochemical parameters.

The regeneration of blood plasma in rats and renewal of biochemical and physical-chemical lymph indices after the applied of sorbents proves that the sorbent SUMS-1 has a good quality of sorption.

References

1. Jwai M., Morikowa T., Muramatsu A., Tanaka G. (2010) Biological significance of AFP expression in liver injury induced by CCl_4. *Acta. Histochem. et Cytochem.,* vol. 33, no. 1, pp. 17-22.

2. Morais S, Costa F, Pereira L. (2012) Heavy metals and human health. *Environ Health Perspect*., vol. 10, no. 2, pp. 227-246.

3. Basage H. (2016) Biochemical aspects of free radicals. *Biochem. Cell Biol.*, vol. 68, no. 7, pp. 989-998.

4. Linjen P., Staessen J., Fagard R., Amery A. (2001). Effect of cadmium on transmembrane Na^+ and K^+ transport systems in human erythrocytes. *Br. J. Ind. Med*., vol. 48, no. 6, pp. 392-398.

5. Shulka A., Shulka G.S., Srimal R.C. (2016). Cadmium-induced alterations in blood-brain barrier permeability and possible correlation with decreased micro vessel antioxidant potential in rat. *Human Exp Toxicol.*, vol. 15, no. 5, pp. 400-405.

6. Sarkar S., Jadov P., Bhatnagar D. (2014) Lipid per oxidative damage on cadmium exposure and alterations in antioxidant system in rat erythrocytes: a study with relation to time. *Biol.* vol. 11, no. 2, pp. 153-157.

7. Noonan C.W., Sarasua S.M., Campagna D., Kathman S.J., Lybarger J.A., Muller Patricia W. (2009) Effects of exposure to low levels of environmental cadmium on renal biomarkers. *Environ Health Perspect.*, vol. 10, no. 2, pp. 151-155.

8. Ozcaglar Hasan U., Agirdir B., Dinc O., Turhan M., Kilincarslan S., Oner G. (2011) Effects of cadmium on the hearing system. *Biochem Biophys Res Commun.*, vol. 121, no. 3, pp. 393-397.

9. Lodenius M., Soltanpour-Gargari A., Tulisalo E., Heattonen H. (2012) Effects of all application on cadmium concentration in small mamals. *J Environ Qual.*, vol. 31, no. 1, pp. 188-192.

10. Novelli Ethel L.B. Vieira Eliane P., Rodrigues Ney L., Ribas Bartolome O. (2016) Rick assessment of cadmium toxicity on hepatic and renal tissues of rats. *Environ Res J.*, vol *779,* no. 2, pp. 102-105.

11. Yang C.F., Shen H.M., Zhuang Z.X. (2017) Cadmium-induced oxidative cellular damage in Hyman fetal lung fibroblasts (MRC-5 cells). *Environ Hea Per.*, vol. 105, no. 3, pp. 712-716.

12. Boscolo P., Carmignany M. (2014) Mechanisms of cardiovascular regulation in male rats Cadmium as a factor of hypertension. *Brit J Industr Med.*, vol. 43, no. 986. pp. 605-610.

13. A., Perromat A., Deleris G. (2011) The *in vivo* toxity carbon tetrachloride and carrageenan on heart microcosms. *Physiol and Pharmacol.*, vol. 79, no. 9, pp. 799-804.

14. Nguen T.D., Villard P.H, Puyoou F. (2017) Pan ax vietnamenesis protects mice against carbon tetrachloride – induced hepatotoxity lack of modification if CYP2E1 gene expression. *Inter Sympos Micro*., vol. 3, no. 72, p. 186.

15. Padma P., Setty O.H. (1994) Studies on cytochrome oxidase in carbon tetrachloride treated rats. *Indian J Exp Biol*., vol. 37, no. 11, pp. 139-141.

16. Johnston M.J. (2001) New research development in understanding lymph venous Disorders. *Lymph Assoc of Ontario*, vol. 96, no. 34, p. 11.

17. Van Helden D.F., Weid P.Y., Crowe M.J. (2015) Electrophysiology of lymphatic smooth muscle. *Con Tis and Lymph*, vol. 56, no. 3, pp. 221-236.

18. Van Helden D.F., Weid P.Y., Crowe M.J. (2016) Intracellular Ca^{++} release: a basis for electrical peacemaking in lymphatic smooth muscle. *Smo Mus Exc*., vol. 1, no 2, pp. 355-373.

19. Zawieja D.C. (1996) Propagation and coordination of lymphatic contractile activity. *Ann Biomed Eng.*, vol. 24, no. 1, p. 31.

20. Crowe M.J., Weid P.Y., Brock J.A., Van Helden D.F. (2015). Coordination of contractile activity in guinea-pig mesenteric lymphatics. *J Physiol.*, vol. 500, no. 1, pp. 235-244.

21. Bulekbaeva L.E., Khanturin M.R., Alibaeva B.N., Demchenko G.A. (2016) Evolution of neurohumoral control of lymphatics. *Sci.*, vol. 5, no. 3, p. 197.

22. Assis D.N., Navarro V.J. (2001) Human drug hepatotoxicity: a contemporary clinical perspective. *Expert Opin Drug Metab Toxicol.*, vol. 5, no. 5, pp. 463-473.

23. Atanbaeva G.K., Toleuhanov S.T., Daulet G., Molsadykkyzy M., Ossikbayeva S.O., Orynbayeva Z.S. (2017) Study of the effect of cadmium, lead, zinc salts to the blood cells. *International Journal of Biology and Chemistry.* vol. 10, no. 1, pp. 9-14.

IRSTI 34.33.19/34.3323

[1*]K.S. Koshkimbayev, [2]E.M. Isakaev, [3]M.V. Kulemin,
[4]M.Zh. Halykova, [1]G.A. Utebayeva

[1]al-Farabi Kazakh National University, Almaty, Kazakhstan
[2]M.Kozybaev North Kazakhstan State University, Petropavlovsk, Kazakhstan
[3]Laboratory of epizootology and prevention of especially dangerous infections of the Chimkent anti-plague station, Chimkent, Kazakhstan
[4]Department of consumer protection of South Kazakhstan region, department of epidemiological surveillance for infectious and parasitic diseases, Shymkent, Kazakhstan
[*]e-mail: karshyga.kosh@gmail.com

Spring fauna of blackflies *(Diptera, Simuliidae)* of Syrdaria river middle reaches

Abstract: Starting from summer 2012, in the valley of the middle reaches of the Syrdaria river, from the Shardara reservoir to the level of the village of Shaulder, South Kazakhstan region, in some years to the railway station of the Tomenaryk, Kyzylorda region, as well as on the territories adjoining the valley massive attacks of blackflies (*Diptera, Simuliidae*) on people and agricultural animals are observed. This led to a number of economic, sanitary, epidemiological and social problems: it became difficult to conduct field agricultural work, grazing; cases of seeking medical assistance from persons who have been bitten by blackflies become more frequent; part of the population expresses the intention to move to another, more prosperous places. From March 31 to April 4, 2015 we conducted route studies from Shardara to the village of Shaulder in order to get familiar with the natural conditions of area being studied and obtain preliminary data on the species of attacking insects. From dry stems of plants growing in shallow water, from sunken snags, tree trunks, and other objects accidentally caught in water, about 800 cocoons and pupal exuvial pelts of the genus *Boophthora* were collected with about 200 mature pupae, more than 1000 cocoons and exuvia, one mature larva of the genus *Wilhelmia* and 1♂ of the same genus. Processing of the material made it possible to define them as *Boophthora erythrocephala De Geer* and *Wilhelmia turgaica Rubzov*. Probably, females of the same species attack in summer. Collection and processing of the material was carried out according to the well-known methods developed by I.A Rubcov (1956) and others. The insects were dissected using a stereomicroscope DM 143 with the Motic Images Plus 2.0 software, with x10 and x20 magnifications. Identification was carried out under a Leica DML B2 microscope with a digital camera Leica DFC 320 with magnifications x60 and x90. The above-mentioned species of *Simuliidae* were known from the valley of the middle reaches of the Syrdaria кiver in the 1970s and 1980s, but their numbers were low and the attacks were not of a mass nature. Current mass breeding of blackflies is linked with the changed, after the commissioning of the Koksarai water reservoir-counter regulator in 2011, hydrological regime of Syrdaria. Studies do not answer the question of specific factors favoring the mass reproduction of blackflies in the middle reaches of Syrdaria and point to the need for further detailed studies on the biology and ecology of blackflies in the Syrdaria Valley in order to develop measures to reduce the number of blackflies in this region.

Key words: Syrdaria river, Koksarai reservoir, *Diptera*, *Simuliidae*, spring fauna, massive attacks of blackflies.

Introduction

Blackflies (*Simuliidae*) are included in the group of bloodsucking dipterous insects, in the russian-language scientific literature united under the name "gnus". Preimaginal phases of blackflies develop in flowing, oxygen-rich water – from shallow streams to large rivers. Representatives of this family occur on all continents, with the exception of Antarctica, and most of the oceanic islands. According to the latest data, there are more than 2,200 species of blackflies in the world [1]. Females for ripening eggs need additional protein nutrition in the form of blood, which is obtained by attacking large vertebrates, including

 Printed in Kazakhstan

humans. They are specific or mechanical carriers of pathogens of a number of vector-borne diseases. Besides, injected saliva into the wound during blood-sucking, cause allergic reactions, with numerous bites develops a specific toxic-allergic disease known as "simulidotoksikoz" [2]. In connection with the above circumstances, representatives of the family are examined from a variety of positions and for different purposes: inventorying and studying the bioremediation of blackflies of a certain territory [3-5] spatial and biotopic species distribution [6], life cycles of mass economically important species [7], the impact of economic development of territories, changes in the hydrological regime of water courses and pollution on biodiversity and the habitat of blackflies [8]. Sometimes in the course of such studies, new species of blackflies are found for science [9].

In the past in Kazakhstan, blackflies had significance as ectoparasites of humans and agricultural animals mainly in mountainous areas. However, from the 60-70s of the XX century, after regulation of the runoff most rivers through the construction of reservoirs, they act as an important component of the "gnus" in the valleys of lowland rivers. This phenomenon was particularly clearly manifested in the Irtysh valley, where a cascade of reservoirs was built. In connection with the mass attacks of blackflies on people in the area of Pavlodar, measures were taken to reduce the number of blackflies in the Irtysh valley [10-12].

In spring of 2015, in connection with numerous complaints from the population of the Shardara and Otyrar districts, South Kazakhstan, on attack of *Simuliidae*, with an initiative of the regional administration the research group was established to study the situation on the place. The study carried reconnaissance character. In this paper, we present the results of the processing of materials collected during a routine survey conducted in 2015.

Materials and methods

Collection of material was conducted from March 31 to April 4, 2015 in the Syrdaria valley from the dam of the Shardara reservoir to the administrative boundary of the Kyzylorda region. The distance between the extreme points of selection sampling was, in a straight line, about 300 km. Study of the preimaginal phases of blackflies development was conducted at 13 points (Figure 1).

The geographical coordinates of selection sampling points were determined using the GPS navigator GARMIN GPSMAP 62s (Taiwan).

Point 1. Filtration streams in the floodplain of the river at the foot of the dam of the Shardara reservoir (Figure 2, A). Geographical coordinates: 41o14'15"/67o52'30". Water seeping through the body of the dam forms streams with a depth up to 20 cm, width up to 1 m. Before entering the river, the streams merge into one channel with a width of 2.0-2.5 meters. In streams are developed the vegetation. The aquatic phases of the development of blackflies were not detected, the attacks of imago were not observed.

Point 2. Syrdaria river in the vicinity of. Kosseit (Sunrise), left coast (Figure 2, B). Coordinates: 41°25'56"/68°05'09". Collected 549 cocoons with exuviae of departed blackflies and empty cocoons attached to dry, submerged stem of reed in water. Attacks of imago were not observed.

Point 3. Syrdaria river at the crossing of the main gas pipeline across the river, the left coast. Coordinates: 41°39'37"/68°02'20". Collected 592 cocoons with exuviae of departed blackflies and empty cocoons, 74 pupae attached to dry, submerged stem of reed in water. Attacks of imago were not observed.

Point 4. Syrdaria river in the vicinity of. Sutkent, at the confluence of the drainage collector into the river. Coordinates: 41°59'13.7"/68°09'56.2". Collected 569 cocoons with exuviae of departed blackflies and empty cocoons, 141 pupae, 1 mature larva of the 4th age with dry, submerged stem of reed and sunken branches. Attacks of imago were not observed.

Point 5. The floodplain of Syrdaria river in the vicinity of Sutkent, drainage collector (Figure 2, C). Coordinates: 41°59'42.5"/68°03'44.3". The aquatic phases of development of blackflies were not detected, attacks of imago were not observed.

Point 6. Syrdaria river, at the beginning of Koksaray, the right coast. Coordinates: 42°06'12.3"/68°12'52.7". The stones in the spillway were examined. The aquatic phases of blackflies development were not detected, attacks of imago were not observed.

Point 7. Syrdaria river, the channel 2 km below Koksaray, left coast. Coordinates: 42°07'36.5"/68°12'45.8". Various objects were examined immersed in water. The aquatic phases of blackflies development were not detected, attacks of imago were not observed.

Point 8. Syrdaria river in the vicinity of. Akkum, the left coast. The water level is high. Coordinates: 42°23'33.3"/68°14'41.5". Wrecked branches and stems of herbaceous plants, brought by the current, branches of willows were examined in shallow water. The aquatic phases of blackflies development were not detected, attacks of imago were not observed.

Figure 1 – Map of the valley of Syrdaria river within the South-Kazakhstan region with the designation of sampling points.
The names and coordinates of the points are indicated in the text

Point 9. Arys river, the right tributary of the Syrdaria, near the village of Shaulder. Coordinates: 42°46’45.5”/68°22’20.5”. The stems of coastal bushes were examined at the time of survey flooded with high water. The aquatic phases of blackflies development were not detected, attacks of imago were not observed.

Point 10. Syrdaria river at the confluence of the diverting channel from Koksarai. The water level is high. Coordinates: 42°24’21.3”/68°22’10.3”. The branches of willows were examined in shallow water, plant stems brought by the current. The aquatic phases of blackflies development were not detected, attacks of imago were not observed.

Point 11. Syrdaria river at the bridge in the area of Koksaray. The water level is high. Coordinates: 42^{0}35’15.3”/68^{0}14’30.5”. Wrecked branches and snags were examined, plant stems brought by the current. The aquatic phases of blackflies development were not detected, attacks of imago were not observed.

Point 12. Syrdaria river in the vicinity of Mayakum. The water level is high. Coordinates: 42°52’23.6”/68°05’24.2”. Sunken snags and plant stems were examined, brought by the current. The aquatic phases of blackflies development were not detected, attacks of imago were not observed.

a b c

Figure 2 – Some of the sampling points: filtration stream at the foot of the dam of Shardara reservoir (A), shore near Kosseit village (B) and drainage collector near Sutkent village (C)

Point 13. Syrdaria at the bridge in the village of Baltakol. The water level is high. Coordinates: 43º09'32.0"/67º51'65.8". Sunken snags and plant stems were examined, brought by the current. The aquatic phases of blackflies development were not detected. In the air, one adult male blackfly is caught.

In total, 1710 cocoons, left after the gab of adult, 215 mature, close-to-fly pupae, one mature larva of IV age were collected, and one male is caught in the air. The processing of the material showed that in the collection 2 species of blackflies are present: *B. erythrocephala* (779 empty cocoons) and *W. turgaica* (931 empty cocoons, 215 pupae, 1 larva, 1 imago).

Collection and processing of the material were conducted according to well-known methods [13]. To study the aquatic phases of blackflies, we collected dry stems of herbaceous plants, sunken branches, stones in shallow water, as well as other objects found in the water. Most part of collected material was placed in 96% ethanol for fixation. Part of the pupae was placed in large chemical tubes with filter paper to grow to the adult stage. Primary cameral processing of the collected material: purification from debris, counting of insects in each sample, clarification of accompanying labels was conducted in the laboratory of epizootology and prevention of especially dangerous infections of the Chimkent anti-plague station. After the cameral processing, the material was transferred to 70% ethanol. Production of microscopic preparations and identification of the species was conducted at the Department of Biophysics and Biomedicine, al-Farabi Kazakh National University.

Species belonging to insects were determined by the available determinants of blackflies of the fauna of the CIS and Russia [14]. All material collected during the expedition is stored at the Department of Biophysics and Biomedicine, al-Farabi Kazakh National University. Primary cameral processing of the material was conducted using a binocular magnifier MBS-10 manufactured by JSC "LOMO" with magnifications x6 and x10.

Dissection of insects and production of temporary micro-preparations was conducted using a stereomicroscope DM 143 (Motic, China), with the software Motic, Images Plus 2.0, with x2, x6 and x10 magnifications; the determination was conducted under a Leica DML B2 microscope (Germany) with a digital camera Leica DFC 320 with magnifications x60 and x90.

To determine the species temporary micro-preparations were prepared. Cocoons and pupae exuvia after 3-fold washing in 70% ethanol were consequently transferred to Petri dishes in a mixture of glycerin with alcohol, to a glass with drop of glycerin, covered with a slide glass, considered under magnifications of x2, x6, x20. Mature pupae with formed chitin structures of imago were fixed with 96% ethanol, dried and placed in a solution of potassium hydroxide for 24 hours. After that, they were washed in distilled water and transferred to glass with a drop of glycerin and cut according to a known scheme. The prepared parts of the head, wings, and sexual appendages were placed, in a drop of clove oil, and then transferred to glass in a drop of glycerin, covered with a slide glass. In this form, the prepared parts of the insect body were studied under a light microscope.

Results and discussion

A part of the middle and lower reaches of Syrdaria, one of the largest rivers of Central Asia, runs through Kazakhstan. In the valley of the Syrdaria,

as well as other rivers of Central Asia, bloodsucking dipterous insects have been numerous at all times.

In 1967, the construction of Shardarinskaya HPP was completed in the middle reaches of Syrdaria, in 1968 have finished the filling of the same reservoir with a capacity of 5 km^3. Before the construction of a reservoir in this part of the Syrdaria Valley, bloodsucking dipterous insects have not been studied. According to conducted studies in the mid-1970s in the lower reaches of the river in the Kyzylorda region, utmost importance among the components of "gnus" had mosquitoes (*Culicidae*) and horseflies (*Tabanidae*), single attacks of *Simuliidae* on domestic animals were observed [16]. At that time, from this part of the valley a new bloodsucking species of blackflies *Sulcicnephya syrdarienzis Rubzov* was described [17]. These data presents a certain value, to study the *Simuliidae* fauna of Syrdaria in general, but they do not fully reflect the situation in the middle reaches of the river.

In 1986 and 1987, we conducted faunistic studies in the middle reaches of the river from the Shardara reservoir to the village of Shaulder. 6 blackfly species were identified, including one new for science *Psilocnetha almae Yankovsky et Koshkymbaev* [18; 19]. By number *Wilhelmia turgaica Rubz.* dominated by the preimaginal phases of development, collected in the river and by imago. Females of this species attack mainly large domestic animals (horses, donkeys, cattle) getting to suck the blood in their ears [20]. They do not generally attack humans, although, within large numbers they can circle around people. The aquatic phases of *Boophthora erythrocephala De Geer* accounted for 3 to 5% of all collected larvae and pupae, and no imago was caught around human. At the same time, the aquatic phases of *Psilocnetha almae Yankovsky et Koshkymbaev*, accounted for 6-8% of the collected larvae and pupae and up to 10% of the imago was caught around human. Preimaginal phases of development of other species were found only in small streams below the dam of the Shardara reservoir and the overall pattern of the attack of *Simuliidae* in the Syrdaria valley did not exert any significant influence. Thus, the picture was very different from the one we observed in the spring of 2015.

The current mass reproduction and attacks of blackflies on the local population is associated with the construction and operation of the Koksarai reservoir-counter regulator. The reservoir is located on the right coast of the river, in the Otyrar district of the region in South Kazakhstan region, designed to solve a number of important economic and environmental problems, such as: protection of locality and economic objects located below the Shardara reservoir, including the regional center of Kyzylorda, from winter floods; uniform water supply in summer on irrigated fields of South Kazakhstan and Kyzylorda region; increase entrance of water into the lower reaches of the river and into the Small Aral. However, such a massive breeding of blackflies in the valley was not expected and it is not yet clear how the erection of the Koksarai reservoir contributed to the reproduction of representatives of this family of dipterous insects. The reservoir was partially filled in the winter of 2009-2010 and 2010-2011, and in the winter of 2011-2012 it was filled till the project capacity of 3 km^3.

For the first time, massive attacks of *Simuliidae* on people and domestic animals were noted in the river valley and adjacent territories in the summer of 2012. In subsequent years, attacks were repeated with some increase or decrease the intensity of attacks. This led to a number of economic, sanitary and epidemiological, social problems: it became difficult to conduct field agricultural work, grazing; cases of seeking medical assistance from persons who have been bitten by *Simuliidae* have become more frequent; a part of the population expresses the intention to move to another, more prosperous places [21].

We previously planned to study 5 types of potential habitats of breeding blackflies: the main channel and the major channels of the Syrdaria river; filtration streams below the dam of the Shardara reservoir; The Kyzylkum main canal and channels of the second-third order supply water directly to the fields; drainage collectors taking away ground and return-irrigation water from the fields of Kyzylkum irrigation array. In the filtration streams, despite the most thorough searches, the aquatic phases of blackflies were not found. The water began to flow into the main canal and channels of the second-third order 4-5 days before the beginning of our investigations, before that they remained dry, respectively, in them the aquatic phases of the blackflies could not be detected. The drainage collector functions throughout the year, but the water level in it is subject to considerable fluctuations. During our research, the level of water was high, the stems of large waterbirds and aquatic plants (cane, cattail, reed lake) that could serve as a substrate for the aquatic phases of *Simuliidae* were found at great depths and were practically inaccessible for survey. Thus, full-scale collections of larvae and pupae were made only in the river channel.

The Koksarai reservoir itself, as well as the inflow and outflow canals, cannot serve as biotopes for

the reproduction of blackflies: the reservoir is due to the lack of directional flow, the conditions necessary for the habitat of preimaginal phases of the blackflies, the canals, due to short-term functioning.

The inflow canal functions during the winter-spring period when the reservoir is filled, the outflow channel functions in the summer time for 2.5-3 months.

In autumn the reservoir is completely emptied and is preparing for re-filling. Consequently, the main mass of blackflies is melted in the Syrdaria river and its ducts. Some number of blackflies can produce artificial channels supplying water to the fields of the Kyzylkum irrigation array and channels of the drainage-collector system, but their significance as biotopes of the reproduction of the blackflies is difficult to estimate. The channel of Syrdaria can be divided into three segments, differing in the hydrological regime and according to their suitability for settling the aquatic phases of blackflies: the first section – from the Shardara reservoir to the water intake dam near the village Bayırkum; the second section – from the Bayyrkum dam to the mouth of the outflow channel when it flows into Syrdaria; the third is the river below the confluence of the outflow channel.

As can be seen from the study materials, the aquatic phases of blackflies were found only on the first stretch of the river – from Shardara to Bayırkum (points No. 2, 3, 4). In this case, in point No. 2 are collected only empty cocoons and pupae exuvia, in point No. 3 in 11.1% of the collected cocoons were mature pupae, in point No. 4 – in 19.8% – mature pupae, and was also found one larva of IV age. All found pupae and larvae belonged to *W. turgaica Rubz*., another species – *B.erythrocephala De Geer* had time to fly completely.

In spring of 2015 in the middle reaches of Syrdaria the found species of blackflies are defined as *B.erythrocephala De Geer* and *W. turgaica Rubz*. These species have been noted here and before [16; 18]. *B.erythrocephala* females actively attack both humans and domestic animals, while *W. turgaica* attack mainly large domestic animals (horses, donkeys, cattle) getting to suck the blood into their ears [20].

The collected material shows that local populations of these species hibernate in the phase of the larva, their pupation and emergence take place in the II – III decade of March. By this time *B. erythrocephala* managed to fly out completely – left empty cocoons and puffed skins- exuvia. Gab of *W. turgaica* finished in the southern, adjoining the reservoir are part of river channel (point No. 2) and continued in the more northern part of the length (points No. 3 and 4).

a b

Figure 3 – Pupae of *W.turgaica* in general view (A) and under x6 magnification (B)

During our research, there was not any attack of blackflies because of the unusually cold weather for this season of the year: the unstable rainy weather that has been standing since the beginning of the III decade of March has passed into a snowfall from 27 to 29 March, 2015. Then frosts followed up to -12°C [22]. This led to the death of those who had time to fly out of the adult. The imago of spring generation

of these species under more favorable weather conditions can attack people and domestic animals, but due to low numbers should not cause much concern. In our opinion, the contribution of insects of spring generation to the settling of aquatic phase of blackflies by existing waterways are more important, including artificial channels, into which water began to flow in the end of March-beginning of April. By the beginning of May in canals, as well as in the river itself, near-water and water vegetation are rapidly developing serving as a substratum for laying eggs and attaching larvae of blackflies, which greatly extends the area of biotopes of reproduction of blackflies. The presence of other bloodsucking species of *Simuliidae*, whose outbreaks of quantities have been observed in the past in the valley of Syrdaria should also be kept in mind. This years of their high numbers that the new species *Sulcicnephya syrdarienzis Rubzov* [17] and *Psilocnetha almae Yankovsky et Koshkymbaev* [19] were found and described.

Conclusion

Our study showed that in the middle reaches of the Syrdaria river, two species of blackflies – *Wilhelmia turgaica* and *Boophthora erythrocephala* – hibernate in the phase of the larva. By the beginning of April all the wintering individuals of *Boophthora erythrocephala* had time to fly out, flight of *Wilhelmia turgaica* still continued. These species were observed in valley of Syrdaria and before, but their numbers were insignificant and they did not show high aggression towards humans. It is known that female of *Wilhelmia turgaica* usually do not attack a person, although they can circle around people. Another species – *Boophthora erythrocephala* is known as a malicious bloodsucker attacking both animals and humans. Probably females of this species make main part of the insects attacking humans in summer periods. The spring of 2015 was anomalously cold for this season of year – the temperature decreased to -12.8^{0}C. In such conditions, all adults of blackflies, flying before cold snap are died. This can be explaint the absence of attacks of blackflies during research period. But, part of the flight females had time to lay eggs. Thus, the populations of these species plummeted into numbers, but were not completely destroyed. According to data received from settlements located in the valley of Syrdaria. in summer of 2015 there were no attacks of blackflies, in summer of 2016 there were isolated single attacks, and in summer of 2017 the number of attacking blackflies was again high, populations of these species regained their numbers. The absence of specialist-entomologists, who conduct account attacking blackflies to people does not allow us to judge about the number of insects more objectively. Judging by our collections, the highest density of overwintered blackfly was recorded in the channel of the Syrdaria, at a distance from a little below the dam of the Shardara reservoir to the water intake dam of the Koksarai reservoir. This does not exclude the reproduction of blackflies in other parts of the river, as well as in artificial channels: the Kyzylkum main irrigation canal and canals of II-III orders, drainage reservoirs. At the same time, the inflow and outflow canals of the Koksarai reservoir are of little use to inhabit the aquatic phases of blackflies, because of the short duration of their functioning. In order to clarify all the conditions that facilitate the mass reproduction of blackflies in the middle reaches of Syrdaria Valley, detailed studies on the ecology and biology of blackflies should be carried out, taking into account the hydrological regime of the river and the climatic features of each year.

References

1. Adler P.H., Crosskey R.W. (2016) World blackflies (*Diptera: Simuliidae*): a comprehensive revision of the taxonomic and geographical inventory. *http://entweb.clemson.edu/biomia/pdfs/blackflyinventory.pdf*, p. 109.

2. Hlyzova T.A., Fjodorova O.A., Sivkova E.I. (2017) Patologicheskoe vozdejstvie sljuny krovososushhih dvukrylyh nasekomyh na organizm cheloveka i zhivotnyh (Obzor) [Pathological effect of saliva of bloodsucking dipterous insects on the organism of human and animal (Review)]. *Vestnik Orenburgskogo gosudarstvennogo universiteta*, vol. 207, no. 7, pp. 90-96.

3. Hadi U.K., Takaoka H. (2018) The biodiversity of blackflies (*Diptera: Simuliidae*) in Indonesia. *Acta Tropica*, vol. 185, pp. 133-137.

4. Srisuka W., Takaoka H., Otsuka Y., Fukuda M. et. al. (2015) Seasonal biodiversity of blackflies (*Diptera: Simuliidae*) and evaluation of ecological factors influencing species distribution at Doi Pha Hom Pok National park, Thailand. *Acta Tropica*, vol. 149, pp. 212-219.

5. Cordoba-Lloria S., Serna-Mompeán J.P., Giménez-Gras O., Acosta-Aleixandre R., Bueno-Mari R. (2017) Notes on blackflies of the Jucar river and tributaries in Eastern Spain. *The Simuliid Bulletin*, no. 48, pp. 8-14.

6. Petrozhitskaya L.V., Rod'kina V.I. (2007) The fauna and distribution of blackflies (*Diptera, Simuli-*

idae) in rivers of the south-eastern Altai mountains. *Entomological Review*, vol. 87, no. 6, pp. 677-684.

7. Budaeva I.A., Khitsova L.N. (2010) The structure of the fauna and life cycles of blackflies (*Diptera, Simuliidae*) in streams of the forest-steppe in Central Russia. *Entomological Review*, vol. 90, no. 9, pp. 1192-1201.

8. Couceiro S.R.M., Hamada N., Sagot L.B., Pepinelli M. (2014) Black-fly assemblage distribution patterns in streams in disturbed areas in southern Brazil. *Acta Tropica*, vol. 140, pp. 26-33.

9. Jankovskij A.V., Isakaev E.M., Hasanova D.A. (2010) Novyj vid moshek *Montisimulium dirzhankolum Yankovsky, Isakaev, Khasanova, sp.n.* (*Diptera: Simuliidae*) iz Severo-Vostochnogo Kazahstana [A new species of blackflies *Montisimulium dirzhankolum Yankovsky, Isakaev, Khasanova, sp.n. (Diptera: Simuliidae)* from North-Eastern Kazakhstan]. *Parazitologija*, vol. 44, no 3, pp. 212-216.

10. Isakaev E.M., Shajmardanov Zh.K., Shajmardanova B.H., Ahmetov K.K., Lopatin O.E., Pakalnishkis S. (2002) O rezul'tatah ispytanija bakterial'nogo preparata «Vektobak 12AS» na r. Shiderty Pavlodarskoj oblasti [On the results of testing the bacterial preparation "Vektobak 12AS" on the Shiderti river of Pavlodar region]. *Biologicheskie nauki Kazahstana*, no. 3, pp. 62-72.

11. Koshkimbaev K.S., Shajmardanov Zh.K., Ahmetov K.K., Shajmardanova B.H., Isakaev E.M. (2005) Ob jekologicheskih predposylkah massovogo napadenija moshek (*Diptera, Simuliidae*) v Pavlodarskom Priirtysh'e [On the environmental prerequisites for a massive attack of blackflies (*Diptera, Simuliidae*) in Pavlodar Priirtyshye]. *Vestnik KazNU Serija jekologicheskaja*, vol. 16, no. 1, pp. 39-47.

12. Isakaev E.M., Koshkimbaev K.S. (2006) Sezonnaja dinamika napadenija krovososushhih moshek v okrestnostjah g. Pavlodara [Seasonal dynamics of attack of bloodsucking blackflies in the vicinity of Pavlodar city]. *Vestnik KazNU Serija jekologicheskaja*, vol. 18, no. 1, pp. 57-59.

13. Rubcov I.A. (1956) Metody izuchenija moshek. V pomoshh' rabotajushhim po zoologii v pole i v laboratorii [Methods for studying blackflies. To help those working in zoology in the field and in the laboratory]. *M., L.: Izd. Akademii nauk SSSR*, vol. 4, p. 55.

14. Rubcov I.A. (1962) Kratkij opredelitel' krovososushhih moshek fauny SSSR [A short determinant of the bloodsucking blackflies of the fauna USSR]. *M., L.: Izd. Akademii nauk SSSR*, p. 227.

15. Jankovskij A.V. (2002) Opredelitel' moshek (*Diptera: Simuliidae*) Rossii i sopredel'nyh territorij (byvshego SSSR) [The determinant of blackflies (*Diptera: Simuliidae*) of Russia and adjacent territories (former USSR)]. *S.-Pb*., p. 570.

16. Dautbaeva K.A. (1975) Krovososushhie dvukrylye (*Diptera: Phlebotomidae, Culicidae, Simuliidae, Ceratopogonidae, Tabanidae*) nizov'ja Syr-Dar'i (03.00.09 – jentomologija) [Bloodsucking Diptera (*Diptera: Phlebotomidae, Culicidae, Simuliidae, Ceratopogonidae, Tabanidae*) lower reaches of the Syrdariya (03.00.09 – entomology)]. *Avtoreferat dissertacija na soiskanie uchenoj stepeni kandidata biologicheskih nauk*. *Alma-Ata*, p. 24.

17. Rubcov I.A. (1976) Novyj krovososushhij vid moshek (*Diptera, Simulidae*) iz Juzhnogo Kazahstana [A new bloodsucking specie of blackfly (*Diptera, Simulidae*) from Southern Kazakhstan]. *Jentomol. obozr*., vol. 57, no. 3, pp. 666-667.

18. Koshkimbaev K.S. (1994) K faune i jekologii moshek (*Diptera: Simuliidae*) srednego i nizhnego techenija Syrdar'i [To the fauna and ecology of blackflies (*Diptera: Simuliidae*) of the middle and lower reaches of the Syrdariya]. *Izv. NAN Respubliki Kazahstan. Ser. Biologicheskaja*, no. 6, pp.70-72.

19. Jankovskij A.V., Koshkimbaev K.S. (1988) Novyj krovososushhij vid moshek *Psilocnetha almae sp. n.* iz Juzhnogo Kazahstana [A new bloodsucking specie of blackfly *Psilocnetha almae sp. n.* from Southern Kazakhstan]. *Parazitologija*, vol. 68, no. 1, pp. 351-354.

20. Shakirzjanova M.S. (1971) K biologii moshek *Wilhelmia turgaica Rubz.* (*Diptera, Simuliidae*) [To biology of blackflies *Wilhelmia turgaica Rubz.* (*Diptera, Simuliidae*)]. *Trudy Inst. zoologii AN Kaz SSR*, vol. 31, pp. 126-128.

21. Қajyrzhan Tөrezhan. (2015) Shirkej қaptap ketti. Nege? [The blackfly is increased. Why?]. *Gazeta Ajқyn*. 15 maja 2015g.

22. Meteostancija Shardara. Arhiv pogody v Shardare [Shardara wheather station], *mart-aprel' 2015 goda//http:www.pogodaiklimat.ru*

IRSTI 34.29.00

[1*]M.S. Kurmanbayeva, [1]N.M. Mukhitdinov, [1]A.D. Serbayeva,
[2]G. Sramko, [1]M.K. Makhambet

[1]Laboratory of plant ecomorphology, Almaty, Kazakhstan
[2]University of Debrecen, Debrecen, Hungary
[*]e-mail: Meruyert.Kurmanbayeva@kaznu.kz

Anatomical features of the rare species of *Erysimum croceum* M.Pop. from Trans-Ili Alatau

Abstract: *Erysimum croceum* M. Pop. (*Brassicaceae*) is an endemic species, growing only in Trans-Ili Alatau. It is included into Kazakhstan Red Data Book. The aim of this study is to compare two populations of *Erysimum croceum* M.Pop identified in Trans-Ili Alatau region, for which morphological and ecological analysis was undertaken. Plant communities of the 1st population growing in Small Almaty gorge (N43* 06.316', E077* 04.184') are dominated by indigenous plants with a significant proportion of endemic taxa, while the 2nd population from the Big Almaty gorge (N43* 04.790', E076* 59.512') is growing in subruderal positions with the presence of other plants. Statistical analysis of the morphological traits revealed significant differences between the two populations. In this article summary on comparative analysis of the main features of morphological and anatomical structures of endemic species *Erysimum croceum* is given. To identify the cause of its disappearance we studied seed germination and growth of seedlings. Seed germination is low and only reaches 18 %. Morphological structure of seedlings on the 45th day showed overall length of sprouts 6.67±3.84 cm, hypocotyl length 1.12±0.06 cm, root length 5.49±3.57 cm, leaves length 0.39±0.63 cm, and leaves width 0.2±0.2 cm. The anatomical features of *Erysimum croceum* were defined. Stem diameter in *Erysimum croceum* collected from the 1st population equals to 1052.92±11.7 μm, epidermis thickness – 25±0.9 μm, primary cortex thickness – 96.24±0.6 μm, core diameter – 796.51±5.9 μm. Stem diameter in *Erysimum croceum* collected from the 2nd population equals to 996.38±9.8 μm, epidermis thickness – 21±0.7 μm, primary cortex thickness – 80.98±0.4 μm, center circle diameter – 701.59±8.7 μm. Anatomical sections of rhizome and leaf were compared on virginal and generative stages, while the stem was studied only at generative stage. Main specification into the inner structure is designated by accumulation of sclerenchyma between conducting bundles in central cylinder and alternative location of small and large bundles.
Key words: *Erysimum croceum* M. Pop., seed, anatomy, stem, sclerenchyma, xylem.

Introduction

There are more than 13 thousand species of valuable plants in Kazakhstani flora, among which 5754 species are widely spread, 1820 species are endemic. *Erysimum* (*E.*) *croceum* plants are met in northeastern part of Trans-Ili Alatau, where its range is constantly reduced. For that reason, it was included into the Kazakhstan Red Data Book, containing rare species of cabbage samples, which needs special protection. The flowering period of this species is from April to May. It is propagated by seeds.

Erysimum is widespread at the Northern hemisphere, rich in morphological features and taxon complexity, with main distribution of *Erysimum* allied species in Europe, where 150-350 species are encountered. Several methods of phylogenetic relations were used for its study, including the patterns of morphologic evolutionary indicators and application of variability of the related genus.

Internal transcribed spacer DNA sequences from c. 85% of the species (117 for the first time), representing the full range of morphological variation and geographical distribution was performed with several approaches to reconstruct phylogenetic relationships, dating of diversification and patterns of evolution of morphological characters in the genus. Ancestral-state reconstructions of four morphological diagnostic characters were performed using maximum parsimony, maximum likelihood and Bayesian methods. This phylogenetic framework strongly supports the monophyly of *Erysimum* and recovers some well-

 Printed in Kazakhstan

supported clades that are geographically, rather than morphologically, correlated. The study confirms the placement of Erysimum in lineage I and reveals two *Malcolmia* (*M.*) spp. (*M.* maritima and *M.* orsiniana) as its sister taxa. The results suggest that the biennial duration and caespitose habit (vs. annual or perennial duration and herbaceous or woody habit) and large, yellow, glabrous (vs. small, non-yellow, pubescent) petals are ancestral in *Erysimum*. The ancestral-state reconstruction results show that annual vs. perennial and woody vs. herbaceous features have been independently derived several times. The dating analyses suggest an early radiation of Erysimum during the late Pliocene or early Pleistocene [1].

This tribe is distinguished by exclusively sessile, stellate and/or malpighiaceous (two-armed T-shaped) trichomes, yellow flowers and multi-seeds siliques [2]. Since it is extremely difficult to distinguish between morphological features, in 14 different Central European species of *Erysimum* relatives special attention was given to the study of the carotene and molecular volatility in the field, with largest differences observed in *E. cheiri* and *E. crepidifolium*. At the same time, it was noted that the exact set of taxon is quite similar to that of the cornea, only slightly different from *E. vergatum*. The molecular methods, including the total physical response, have increased the density of rDNA, while the genetic features of all *E.* relatives were established using random amplified polymorphic DNA. As a result, complexity of five out of six taxon problematic species: *E. hungaricurn, E. pieninicum, E. wahlenbergii, E. vergatum, E. durum* and *E. hieracifolium* was noted [3].

In order to examine the systematic application of seed-coat characters in *Erysimum (Brassicaceae)* distributed in Northeast of Iran, Khorassan province, the seeds of nine species with dense grain (14 populations) were examined with application of light (LM) and scanning electron microscopy (SEM). According to results of the LM, diagnostic signs include the shape of the seed, the width of the wing, epidermal cell-wall shape, and seed-surface sculpture. The SEM at high magnifications reveal seven types of seed-surface sculpture pattern, including: 1) reticulate, the basic type; 2) ocellate; 3) papillate; 4) reticulate-papillate; 5) scaliform; 6) ribbed; 7) reticulate-ocellate. The seed coat typically consists of four layers, including of the epidermis, subepidemis, sclerotic (or palisade) and the parenchymatous layer. Some species may not have some types of these layers [4].

E. capitatum seeds were planted alongside the alpine and low altitudes in order to study plants adaptability to location and climate. Plants exhibited home-size advantage in the form of higher survival at their native sites, especially for plants from high altitude. High- and low-altitude populations differed in seed germination, growth and morphology. Seeds from alpine *E. capitatum* tended to germinate to higher levels than those from low□altitude populations, especially under alpine conditions. The production of multiple rosettes, a characteristic morphology of alpine plants was negatively associated with survival at low altitude. Plants at low altitude suffered higher mortality, but showed faster growth and reproduction of those that survived. Thus, the differential plant performance observed in natural populations across altitude is attributable to direct environmental effects (plasticity) as well as population differentiation caused by genetic differentiation and/or maternal environmental effects [5].

Differences in the reproductive success of the two species *E. pieninicum* and *E. odoratum* can be considered among the potential causes for their contrasting distribution success, although their seed biological characteristics (preserved viability in seed gene banks for long time and sudden germination without the need of dormancy breaking treatments) show them as promising candidates for nature conservation and habitat restoration projects [6].

N, P and K concentration in aerial parts of *E. amasianum* is generally high in vegetative period. In generative period, however there is a decline. This situation can be explained with that in aerial parts of the plant, physiological actions are dense and elements are carried into the aerial parts of the plant. In generative phase the aerial parts comlete their development. The elements are carried into the underground parts in order that the plant can live until next vegetative period. The reason why N, P and K concentration increases in generative phase is this. Similar results can be seen in researches that were done to the plants such as *Asphodelus aestivus* Brot., *Iris sari* Schott ex Baker and *Alkanna haussknechtii* Bornm. [7].

Although establishing the adaptive significance of polyploidy to explain the geographic distribution of cytotypes is challenging, the occurrence of different cytotypes in different ecological niches may suggest an adaptive role of genome duplication. Climate variables, population elevation and soil properties to model ecological niches for the different cytotypes of *E. mediohispanicum* was used in order to study the effect that ploidy level has on the floral phenotype. A clear geographic pattern in the distribution of cytotypes, with diploid individuals occurring in the southernmost part of the distribution range was

noted, while tetraploids were found in the northern area. A contact (mosaic) zone between both cytotypes was identified, but diploids and tetraploids occur in sympatry in only one population (although in a highly unbalanced proportion). Gene flow between different cytotypes seems to be negligible, as evident from an almost complete absence of triploids and other minority cytotypes. Niches occupied by both cytotypes showed subtle, but significant differences, even in the contact zone. Precipitation was higher in regions occupied by tetraploid individuals, which present wider corolla tubes and thinner but taller stalks than diploids. Findings highlight the potential role of polyploidy in the ecological adaptation of *E. mediohispanicum* to both abiotic factors and biotic interactions [8].

With recent advances in genome sequencing, transcript profiling, plant transformation, transient expression assays, and plant metabolite analysis, another *Erysimum* representative, *E. cheiranthoides* (wormseed wallflower), a rapid-cycling, self-pollinating species with a relatively small, diploid genome, which characteristically produces cardiac glycosides as defensive metabolites, is proposed as a suitable model system to advance research on the biosynthesis of cardiac glycosides in plants [9].

In order to detect the cause of rare species of various populations encountered in Kazakhstan, the reproductive, morphological and anatomical structure of the seed requires a through investigation, and a comprehensive study is needed to preserve this species in nature.

Materials and methods

Study of morphological structure of *Erysimum croceum* M. Pop. (*E.croceum*) plants was carried out using the methods of common structural analysis. Morphological growth, germination, vegetation, diameter, root count, number of leaves, its shape, size were studied by the methodology of Serebryakov I.G. (1964), Fedorov A.A. (1956). Anatomical structure was studied using the generally accepted methodology, by methods of structural analysis and temporary preparations [12-16].

Measurements and microphotographs were produced by Micros MCx100 video microscope camera 519 CU5.0M CMOS.

Morphology-geographical method was used in carrying out the systematic analysis. Type determination was based on detection of the basic morphological features in a blossoming phase. For the purpose of a further morphologic-anatomic research of *E. croceum* plants were collected as herbarium during the expeditions to Trans-Ili Alatau. Stereoscopic binocular MBS-10 was used in the study of the objects morphological structure. Studies were conducted at the Laboratory of plant ecomorphology, Department of Biodiversity and Bioresources, al-Farabi Kazakh National University, Almaty, Kazakhstan.

Conservation of plant material was carried out by a technique of Strasburger and Fleming. Anatomic preparations were produced according to the standard techniques of Prozina M.N. (1960), Permyakov A.I. (1988) and Barykina R.P. (2004).

Possibility to use optic microscope Leica DM 6000 M with the high-resolution digital camera and software for the microscopic study of anatomic structure of reproductive organs of plants was kindly provided by our colleagues from the national nanotechnological laboratory of public type at al-Farabi Kazakh National University.

Results and discussion

The reason for the disappearance of endangered plant species is directly related to seed germination. In order to define sprout intensiveness 400 *E.croceum* plant seeds were placed into four Petri dishes (by 100 seeds in each).

Germinating capacity of seeds was defined on the 25th day according to the generally accepted international system. As can be seen from the Figure 1 *E.croceum* plant seeds did not germinate in noticed 25 days, germinating capacity 0%.

On the 30th-31st days, changes started appearing. On the 45th day plants got measured with overall length: 6.67 cm, hypocotyls overall length: 1.12 cm, roots overall length: 5.49 cm, overall length of leaves: 0.39 cm, leaves overall width: 0.2 cm (Figure 2).

According to the results from the Small Almaty and Big Almaty gorges *E. croceum* plants height is 30-60 cm, stem grows straightly. Leaves are long or like forage grasses, mitering corners; lowers are pedicellate, uppers are pliant. Flowers are reddish yelow or red, panicle settled in bouquet. They flower in May to July and give fruits in July to August. Fruit is tetrahedral pods. Plants can be used as decorative plants and may be grown in culture.

Study of morphological structures showed that *E. croceum* plants are biennial. No stem is developed during the 1st year (virginal period), only starting from 2nd year (generative period) stem will start growing, overall length in the 1st population is 45.9±18 cm, in the 2nd population is 49.8±3.6 cm, morphological structure published [16].

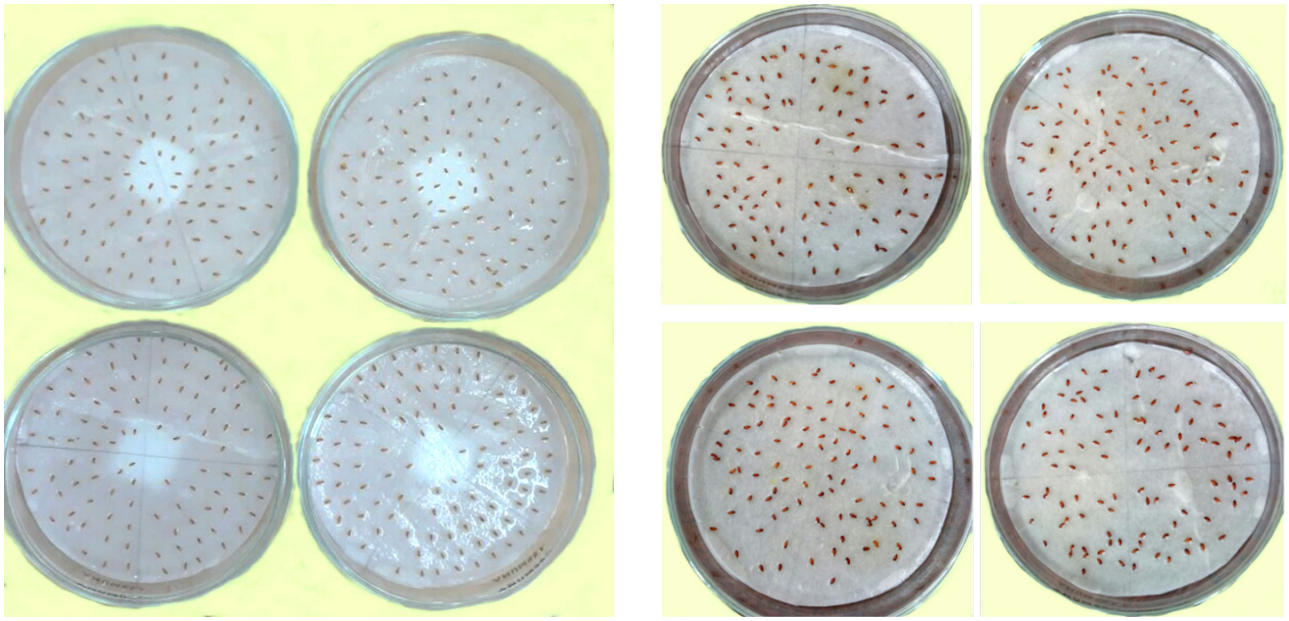

a b

Figure 1 – *E. croceum* plant seeds germinating capacity on the 1st (A) and 25th (B) day

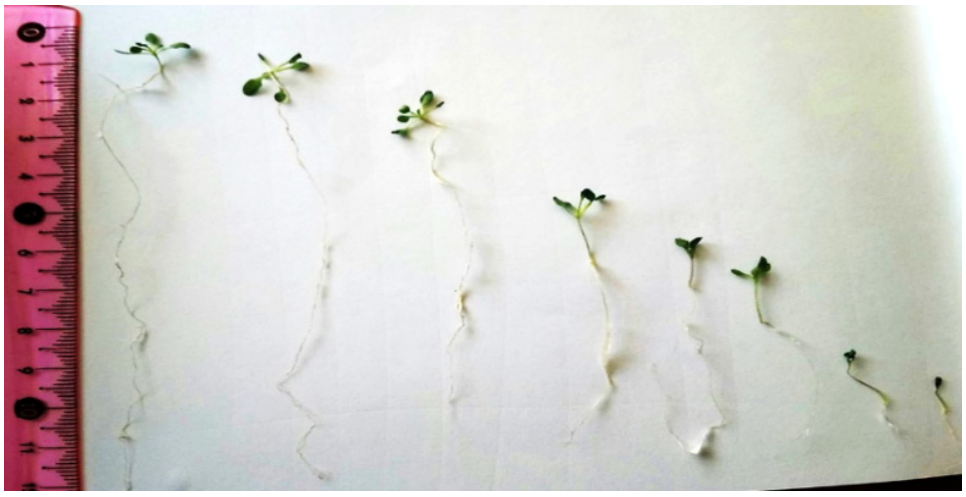

Figure 2 – *E.croceum* plant length, cm

The population structure of *E.croceum* plants is well defined in Small Almaty gorge, since this place is its growing areal; this species were found and characterized there for the first time.

Fixed material of *E.croceum* plants from Big and Small Almaty gorges of Trans-Ili Alatau was used in order to conduct comparable analysis of the index of anatomical structure.

Study of the anatomical structure of the stem of *E.croceum* plants from the 1st population (generative period) revealed its tetrahedral structure and well-developed trichomes in epidermis cells. Under epidermis primary cortex decreased. It consists from parenchyma and collenchyma. Primary cortex parenchyma cells located in 5-6 lines, conducting bundles in center circle located in a certain line, formed collateral open bundles. In center circle conducting bundles located over cambium circle located between collateral open xylem and phloem. Sclerenchyma is clearly developed and gathered in conducting bundles and in between two conducting bundles. Core expanded, parenchymas are consists of similar many-sided cells, which takes main part of stem. Core parenchyma is well developed (Figure 3).

Note: e – epidermis, p.c. – primary cortex; v.b. – vascular bundle, c – core, scl – sclerenchyma surrounding bundle; x – xylem, ph – phloem, s.t. – simple trichome

Figure 3 – Anatomical structure of *E.croceum* stem, generative period, 1st population

Study of the anatomical indexes of the stem of *E.croceum* plants from the 2nd population (generative period) reveals the tetrahedral structure of its trichomes, similarity of epidermis cells along the stem and emergence of glandular fibers. Hedrals expand and collenchyma decreases, primary cortex parenchyma consists of colorless cells. Well-defined growth of sclerenchyma located between each centered conducting bundle is revealed. Sclerenchyma located after large conducting bundle might be interchanged with small conducting bundle. In large bundle 10-15 lines of xylem are in row, and in small bundle, we can notice only one line of xylem. In large conducting bundle, sclerenchyma can be clearly observed. In core parenchyma, some unknown matters are present (Figure 4).

Comparative analysis of the morphometric specification of *E.croceum* stem shows higher index in the 1st population over the 2nd population (Table 1).

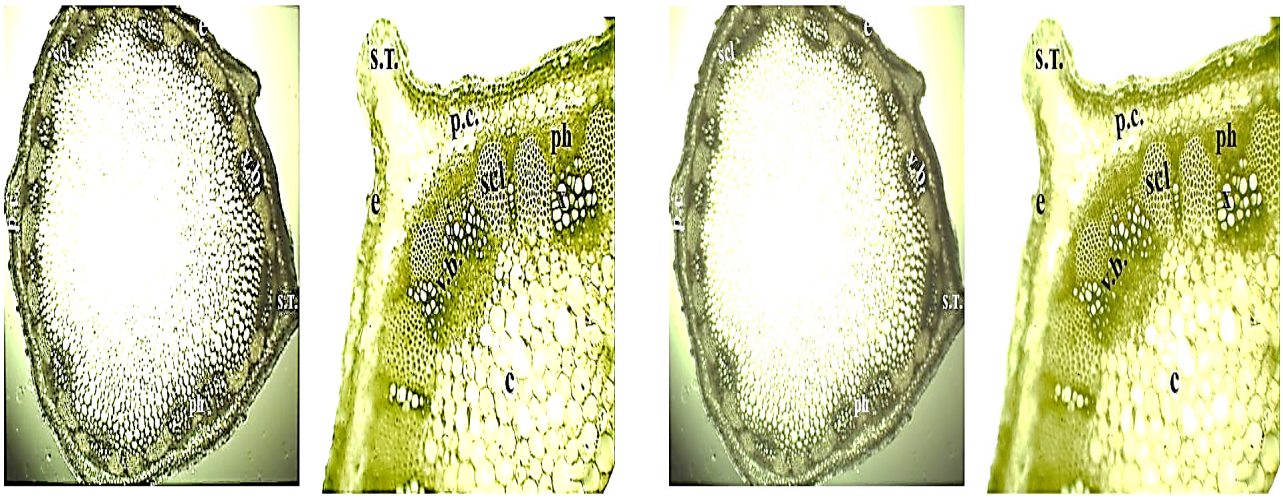

a b

Note: e – epidermis, p.c. – primary cortex; v.b. – vascular bundle, c – core, scl – sclerenchyma surrounding bundle; x – xylem, ph – phloem, s.t. – simple trichome

Figure 4 – Anatomical structure of *E.croceum* stem, generative period, 2nd population

Table 1 – Morphometric indexes in two populations of *E.croceum* plants

Generative period	Primary cortex thickness, μm	Center cylinder diameter, μm	Central conducting bundle diameter, μm
1st population	1280.62±13.9	932.55±9.4	96.00±0.7
2nd population	1125.53±12.4	856.24±8.3	72.11±0.4

In the 1st population stem diameter is 1052.92±11.7 μm, epidermis thickness is 25±0.9μm, primary cortex thickness is 96.24±0.6μm, and center circle diameter is 796.51±5.9μm. Morphometric index of the 2nd population is lower, with stem diameter of 996.38±9.8 μm, epidermis thickness of 21±0.7 μm, primary cortex thickness of 80.98±0.4 μm, center circle diameter of 701.59± 8.7 μm (Figure 5).

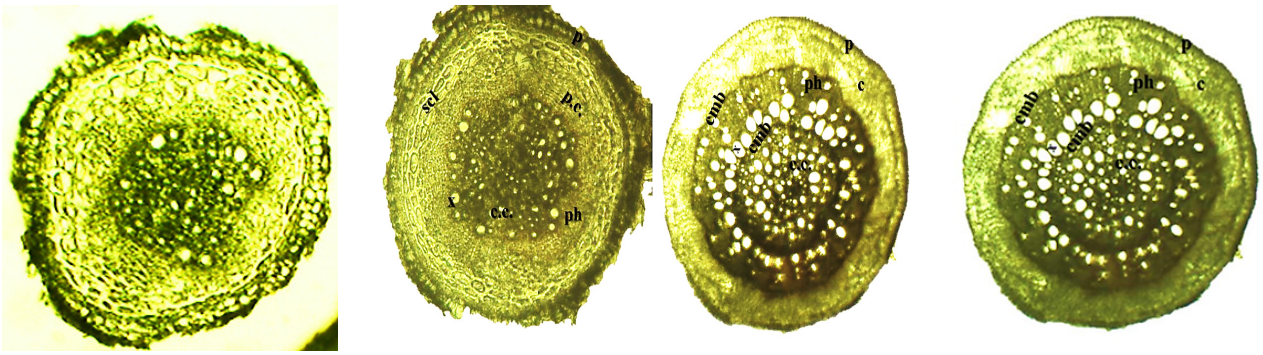

v g v-2p

Note: p – periderm, p.c. – primary cortex, c.c. – central cylinder, cmb – cambium, c – cortex, scl – sclerenchyma, ph – phloem, x – xylem

Figure 5 – Anatomical structure of *E. croceum* roots in virginal (v) and generative (g) periods, 1st population, and virginal period (v-2p), 2nd population

Anatomical structure of roots was studied in virginal and generative periods. In virginal period root is covered with second roofing tissue periderm. Consequent expansion of the core with enlarged xylem tubes along with decrease in primary cortex thickness is noticed in generative period (Figure 6).

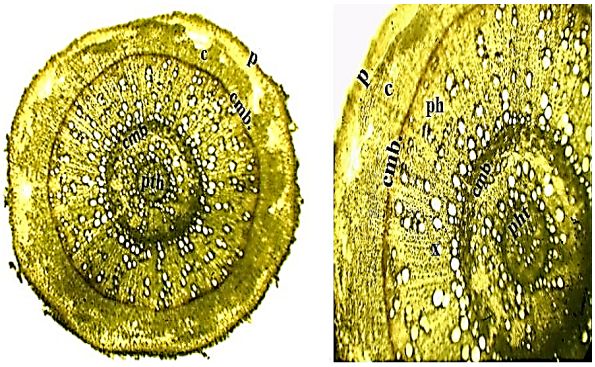

Note: p – periderm, p.c. – primary cortex, pth – pith, cmb – cambium, c – cortex, ph – phloem, x – xylem

Figure 6 – Anatomical structure of *E. croceum* rhizomes, virginal period, 2nd population, close-up

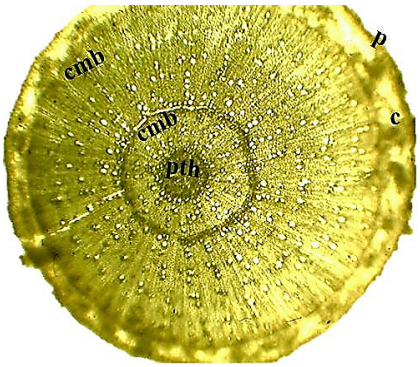

Note: p – periderm, pth – pith, cmb – cambium, c – cortex

Figure 7 – Anatomical structure of *E. croceum* rhizomes, generative period, 2nd population

Study on anatomical structure of root reveals rhizome; a two-year ring is clearly visible. Study of *E.croceum* plant rhizomes anatomical structure at virginal and generative periods reveals rhizome covered periderm, clearly defined lenticels (Figure 7).

Results of the comparative analysis of morphometric indexes of *E. croceum* rhizomes at virginal and generative periods are presented in Table 2, indicating higher general level defined at virginal period, even though diameter of central cylinder in generative period is larger.

Table 2 – Morphometric indexes of *E.croceum* rhizomes, virginal and generative periods, 2nd population

Virginal period		Generative period	
Measure the area	Length, μm	Measure the area	Length, μm
Overall rhizome diameter	625.89	Overall rhizome diameter	599.58
Primary cortex thickness	99.14	Primary cortex thickness	46.75
Diameter of central cylinder	427.61	Diameter of central cylinder	506.08

Morphometric indexes of *E. croceum* rhizomes in the 1st population are higher in comparison with the 2nd population.

Anatomical structure of *E.croceum* leaf at virginal period clearly shows that upper and lower epidermis cells consists from round shaped cells with defined trichomas. Conducting bundle consists directed to collateral upper epidermis xylem and directed to lower epidermis phloem. Large bundle is located at the core, over it small bundles are located; mesophyll is divided into column and lacunar cells. Core chlorenchyma is presented by clearly seen varying round shaped cells (Figures 8 and 9, Table 3).

Study of *E. croceum* leaf anatomical structure reveals larger conducting bundles in the 1st population in comparison with the 2nd population (Figure 8). In the 2nd population core is located under the upper epidermis, parenchyma is diffused. There is a defined air cavity at the core upper side of conducting bundle. In lower epidermis, trichomas are well developed.

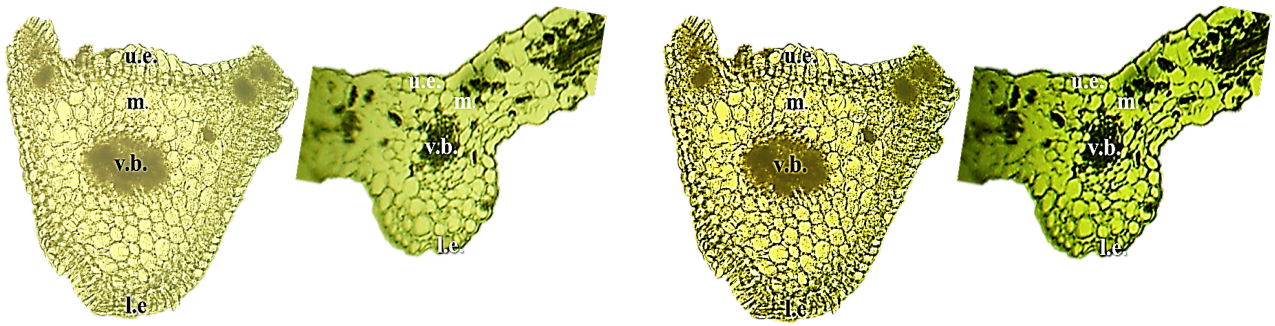

a b

Note: u.e. – upper epidermis, l.e. – lower epidermis, m. – leave mesophyll, v.b. – vascular bundle

Figure 8 – *E. croceum* leaf anatomical structure, virginal (A) and generative (B) periods, 1st population

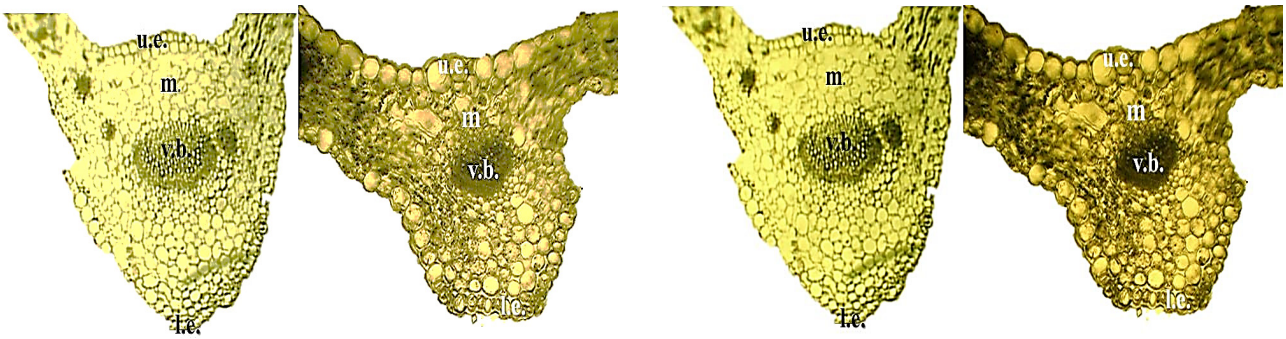

a b

Note: u.e. – upper epidermis, l.e. – lower epidermis, m. – leave mesophyll, v.b. – vascular bundle

Figure 9 – *E. croceum* leaf anatomical structure, virginal (A) and generative (B) periods, 2nd population

Results of the comparative analysis of *E.croceum* leaf morphometric indexes in the 1st and 2nd populations are presented in Table 3.

Plants from the 1st population were collected at the humid slopes of Trans-Ili Alatau, which had positive influence at *E. croceum* leaf morphometric indexes. For instance, core thickness in the 1st population is 689.08 μm, and in the 2nd population, it decreases to 601.79 μm.

Thus, comparative analysis of anatomical and morphometric parameters of two populations shows higher indexes of each part (stem, rhizome, leaf) of *E. croceum* in Big Almaty gorge of Trans-Ili Alatau.

Table 3 – Morphometric indexes of *E.croceum* leaf in the 1st and 2nd populations

1st population		2nd population	
Measured unit	Size, μm	Measured unit	Size, μm
Core thickness	689.08	Core thickness	601.79
Mesophyll thickness	259.75	Mesophyll thickness	209.38

Conclusion

Erysimum croceum M. Pop. plant seeds germination capacity is low, it comprises only 18%. In this regard, there is a risk of seed loss due to poor germination and measures should be taken in order to improve seeds germination. Plants do not form stem during the first year, stem started to grow only at the generative period of the second year.

Some features were defined during the study of anatomical structures. Stem is tetrahedral with well-developed trichomes in epidermis cells. Parenchyma cells stay only at sides of the primary cortex, in center circle, expanding conducting bundles are located in a certain order, and collateral open bundles are formed. The main noticed difference is that sclerenchyma formes bundles between the two bundles. Pith widenes, parenchyme is formed from the same cells, which define its basic position in the stem.

Comparative analysis of *E. croceum* M. Pop. plant rhizome morphometric indexes showed higher values at the virginal than in the generative period. In the structure of the rhizome, the biennial ring is clearly visible and in the center is the pith.

There is a defined air cavity at the core upper side of conducting bundle in leaves. In lower epidermis, trichomas are well defined.

References

1. Moazzeni H., Zarre S., Pfeil B.E., Bertrand J.K., German D.A., Al-Shehbaz I.A., Mummenhoff K., Oxelman B. (2014) Phylogenetic perspectives on diversification and character evolution in the species-rich genus Erysimum (Erysimeae; Brassicaceae) based on a densely sampled ITS approach. *Bot J Linn Soc*., vol. 175, no. 4, pp. 497-522.

2. Gostin I.N. (2009) Anatomical and micromorphological particularities of vegetative organs in endemic Erysimum wittmanii Zaw. ssp. Wittmanii. *Anal Univ Oradea, Fasc Biol*., vol. 16, no. 2, pp. 74-79.

3. Czarna A., Gawronska B., Nowinska R., Morozowska M., Kosinski P. (2016) Morphological and molecular variation in selected species of Erysimum (Brassicaceae) from Central Europe and their taxonomic significance. *Flora*, vol. 22, pp. 68-85.

4. Csontos P., Rucinska A., Puchalski J.T. (2010) Germination of Erysimum pieninicum and Erysimum odoratum seeds after various storage conditions. *Táj Lapok*, vol. 8, no. 3, pp. 389-394.

5. Ghaempanah S., Ejtehadi H., Vaezi J., Farsi M. (2013) Seed-coat anatomy and microsculpturing of the genus Erysimum (Brassicaceae) in Northeast of Iran. *Phytotaxa*, vol. 150, no. 1, pp. 41-53.

6. Kim E., Donohue K. (2013) Local adaptation and plasticity of Erysimum capitatum to altitude: its implications for responses to climate change. *J Ecol*., vol. 101, no. 3, pp. 796-805.

7. Cansaran A., Ergen Akçin Ö., Kandemir N. (2007) A study on the morphology, anatomy and autecology of Erysimum amasianum Hausskn. & Bornm. (Brassicaceae) distributed in Central Black sea region (Amasya-Turkey). *Int J Sci Tech*., vol. 2, no. 1, pp. 13-24.

8. Muñoz-Pajares A.J., Perfectti F., Loureiro J., Abdelaziz M., Biella P., Castro M., Castro S., Gómez J.M. (2018) Niche differences may explain the geographic distribution of cytotypes in Erysimum mediohispanicum. *Plant Biol*., suppl. 1, pp. 139-147.

9. Züst T., Mirzaei M., Jander G. (2018) Erysimum cheiranthoides, an ecological research system with potential as a genetic and genomic model for studying cardiac glycoside biosynthesis. *Phytochem Rev*., pp. 1-13.

10. Serebrjakov I.G. (1964) Zhiznennye formy vysshih rastenij i ih izuchenie // Polevaja geobotanika [Life forms of higher plants and their study // Field geobotany]. *L.: Nauka*, vol. 3, pp. 146-205.

11. Fedorov Al.A., Kirpichnikov M.Je., Artjushenko Z.T. (1956) Atlas po opisatel'noj morfologii vysshih rastenij [Atlas on descriptive morphology of higher plants]. *Izd-vo AN SSSR,* p. 303.

12. Prozina M.N. (1960) Botanicheskaja microtehnika [Botanical microtechnology]. *M.: Vyssh. shk.,* p. 206.

13. Permyakov A.I. (1988) Microtehnika [Microtechnology]. *M.: MGU*, p. 58.

14. Barykina R.P. et al. (2004) Spravochnik po botanicheskoj mikrotehnike, osnovy i metody [Reference book on botanical microtechnology, fundamentals and methods]. M.: MGU. p. 312.

15. Lakin G.F. (1990) Biometrija [Biometrics]. *M.: Vyssh. shk.,* p. 352.

16. Abidkulova K.T., Mukhitdinov N.M., A.A. Ivashchenko, A. Ametov, Serbayeva A.D. (2017) Morphological characteristics of a rare endemic species *Erysimum croceum* M. Pop. (*Brassicaceae*) from Trans-Ili Alatau, Kazakhstan. *Modern Phytomorph*., vol. 11, pp. 131-138.

IRSTI 34.17.39

[1]S.T. Tuleukhanov, [2]O.I. Salatova, [1]Z.Zh. Zhanabayev, [1*]A.N. Oralbek, [3]Iu.A. Kim

[1]Laboratory of Human and Animal Physiology, Almaty, Kazakhstan
[2]A.Baitursynov Kostanay State University, Kostanay, Kazakhstan
[3]Institute of Cell Biophysics, Russian Academy of Sciences, Pushchino, Russia
[*]e-mail: aiko-22.03.1993@mail.ru

Entropic index of diurnal dynamics of systolic and minute volumes of human blood before and after exercise stress

Abstract: The features of circadian dynamics of mean values of systolic and minute blood volumes of young people before and after the exercise stress have been recorded and analyzed. It is indicated that sizes of systolic and minute blood volumes after exercise stress increased with statistical significance of $p \leq 0.05$. Thus, the characteristics of systolic volume of human blood vary from 70.3±4.3 mL to 77.2±6.6 mL before exercise stress, and 92.6±8.8 mL up to 99.1 ±8.9 mL after the exercise stress. While for the minute volume, they vary from 5.00 ±0.50 L to 6.10 ±0.53 L and from 9.79 ±3.04 L to 11.19 ±2.53 L, correspondingly. The values of systolic volume of blood entropy before exercise stress are equal to 0.6208 and after exercise stress to 0.6438 and the value of minute volume of blood before exercise stress is equal to 0.6208 and after load is equal to 0.6438. The entropy characteristics of circadian dynamics with systolic and minute volumes of blood after the exercise stress has a tendency to increase. Despite numerous works on the study of percussive and minute cardiac output, there is yet no complete clarity about their relationship after the dosed physical exercises in the daily regime and nothing is known about their entropic parameters. Current work expounds the data on experimental material and the mathematical analysis on revealing the daily dynamics of systolic and minute volume of human blood before and after exercise stress and calculation of their entropic parameters.

Key words: circadian rhythms, systolic blood volume, minute blood volume, exercise stress, entropic parameters.

Introduction

Current stage in the development of biomedicine is consistent in that along with the knowledge of the spatial organization of the living systems, their temporal organization is intensively studied [1-4].

Rhythmicity is the basic property of a living organism and its inherent quality as a symphony of rhythms and temporalities underpin our development. The analysis of chronobiologic regularities on the evolutionary level promotes a deeper study of the biological mechanisms of human adaptation and the purposeful application of effective means (eg. physical culture and sport) increasing the resistance of the organism to various stress factors [5, 6].

In life, there is nothing more powerful than rhythm. Indeed, information about the rhythm of physiological processes is necessary for rational work and rest (chronohygiene), for diagnosis (chronodiagnosis) and for the effective treatment (chronotherapy). Chronobiological data is used for the scientific substantiation of dosage of the medicinal products (chronopharmacology), organizing the rational sports training, increasing the human capacity and preventing premature aging [7-10]. Thus, optimization of the parameters of biological rhythms facilitates increasing the duration of human life.

In 2017, the Nobel Prize in Physiology or Medicine was given jointly to Jeffrey C. Hall, Michael Rosbash and Michael W. Young for their discoveries of molecular mechanisms controlling the circadian rhythm. As stated on the official page of the Nobel Prize (https://www.nobelprize.org/nobel_prizes/medicine/laureates/2017/press.html): "Using fruit flies as a model organism, this year's Nobel laureates isolated a gene that controls the normal daily biological rhythm. They showed that this gene encodes a protein that accumulates in the cell during the night, and is then degraded during the day. Subsequently, they identified additional protein components of this machinery, exposing the mechanism governing the self-sustaining clockwork inside the cell. We now

 Printed in Kazakhstan

recognize that biological clocks function by the same principles in cells of other multicellular organisms, including humans". In this connection, continuous scientific interest to chronobiology, chronophysiology and chronomedicine becomes clear. Regardless of a huge amount of work in these areas, there is still a large field of activity for new research steps.

Materials and methods

1st-3rd year bachelor students, 19-20 years old, 68±5 kg in body weight, male were used as objects of the study. All subjects for health reasons were assigned to the main group (physical activity 2 hours per week). Physical exercise was performed with the help of a cycle ergometer (Proteus Cycle Pec 3000, 2012 y., Proteus, Taiwan) in the Laboratory of Human and Animal Physiology, Department of Biophysics and Biomedicine, Al-Farabi Kazakh National University. The methodology for determining the minute volume of the heart and for processing the analyzed parameters was developed on a computer based on the physiological idiogram "The Physiology of the Circulation" programs were created for the "Pentium-4" (Intel company, USA) computer to determine the physical performance and the functional state of the circulatory system. To characterize the functional state of the circulatory system, the following indices were used, obtained experimentally: arterial pressure (systolic and diastolic, mm mercury column); heart rate (beat/min); body weight (kg); age (years). In addition, based on the above indices, such important parameters as minute blood volume (MBV, L/min) and systolic (stroke) blood volume (SBV, L/min) were calculated. Statistical processing of the obtained results was carried out with the help of the Microsoft Excel program and the changes were considered reliable at $p \leq 0.05$. The entropic index of the daily dynamics of MBV and SBV before and after the physical exercise was calculated using program MATLAB (Matrix Laboratory, USA) [11].

Results and discussion

SBV is the volume of blood pumped from the left ventricle per beat. It is calculated using the measurements of ventricle volumes from an echocardiogram (ECG) and subtracting the volume of the blood in the ventricle at the end of a beat (called end-systolic volume) from the volume of blood just prior to the beat (called end-diastolic volume). The term stroke volume can apply to each of the two ventricles of the heart, although it usually refers to the left ventricle. The systolic volumes for each ventricle are generally equal, both being approximately 70 mL in a healthy 70-kg human. It is an important determinant of cardiac output, which is the product of systolic volume and heart rate, and is also used to calculate ejection fraction, which is systolic volume divided by end-diastolic volume. Because systolic volume increase in certain conditions and disease states, systolic volume itself correlates with cardiac function [12; 13].

Minute blood volume (MBV) and systolic or stroke blood volume (SBV) are the most important indicators of hemodynamics. With their help, it is possible to quantify the performance of the heart and its ability to increase the pump function with an increase in tissue metabolism leading to an increase in the oxygen demand of tissues. The values of cardiac output are also the basis for calculating a number of values that characterize the work of the heart and the entire circulatory system [14; 15]. For that reason, special attention should be given to these indicators.

Despite numerous works on the study of percussive and minute cardiac output, there is still no complete clarity about their relationship after the dosed physical exercise in the daily regime and nothing is known about their entropic parameters. Current work reflects the experimental material on daily dynamics of systolic and minute volume of blood of the person before and after the exercise stress and calculation of their entropic parameters (Table 1).

Judging by the averaged indices, SBV level before the exercise fluctuated by the type of a single-peak curve with a maximum at 8 pm and comparatively low values at the night (2 am).

SBV values in the norm during the day varied from 70.3 ±4.3 mL to 77.2 ±6.6 mL. The average SBV values after physical exercise during the day, both in rhythm configuration and in terms of SBV level, differed from the norm. While after the physical activity, the SBV values during the day varied from 92.6±8.8 mL to 99.1±8.9 mL, with a maximum at 4 pm and a minimum at 8 am. Averaged SBV indices before and after the physical exercise differ from each other both in level and in configuration of daily rhythms. SBV values after exercise are higher than in the norm.

The entropic parameters of SBV averaged values before and after the physical exercise are presented on Figures 1 and 2.

It can be seen from the Figure 1 that the values of the entropy of SBV in people before the physical exercise during the day vary from 70.5 to 77.3 mL and is equal to 0.6208 units.

Table 1 – Daily SBV dynamics before and after the exercise stress

t, hour	08	10	12	14	16	18	20	22	00	02	04	06	08
BE	77.2±6.6	76.4±6.9	74.3±5.6	74.9±6.0	75.3±3.7	75.0±3.7	74.8±3.9	74.6±4.0	74.1±3.5	70.3±4.3	71.1±4.4	75.5±4.2	76.5±4.5
AE	92.6±8.8	93.8±8.0	96.0±8.7	97.8±7.7	99.1±8.9	98.9±7.9	98.6±7.4	97.0±7.0	96.2±7.3	94.7±7.8	93.8±8.0	93.0±7.2	94.5±6.4

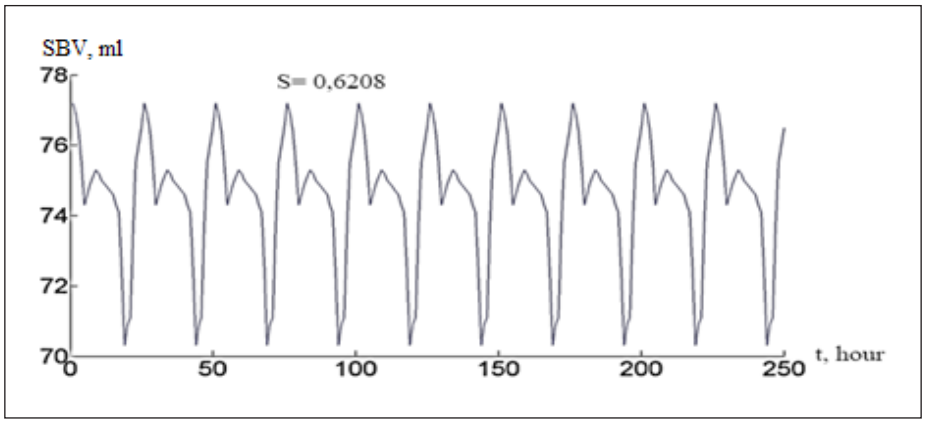

Figure 1 – Entropic parameters of daily SBV dynamics before the exercise stress

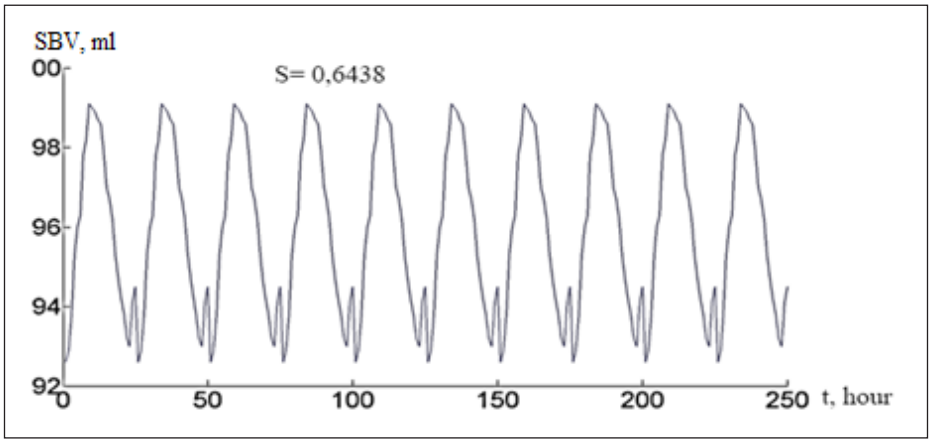

Figure 2 – Entropic parameters of daily SBV dynamics after the exercise stress

The values of entropy of SBV after the physical exercise during the day varies from 92.5 to 99.4 mL, and is equal to 0.6438 units.

It is established that the values of the entropy of SBV before exercise are lower than after physical exercise. Thus, for the first time we calculated the values of the entropy of SBV in humans before and after physical exercise and found an increase in the value of entropy of SBV after the exercise, which indicates activation of the cardiovascular system of the human body.

Normal values for a resting healthy individual would be approximately 60-100 mL. Patients undergoing surgery or in critical illness situations may require higher than normal SBV and it may be more appropriate to aim for optimal rather than normal SBV.

Considering the daily chromodynamics of MBV average, it was found that it is a subject to fluctuations both before and after the physical exercise (Table 2).

Results show that MBV values before the exercise vary from 5.37 ±0.69 to 6.10 ±0.53 within a day, with a minimum at 4 am and with a maximum in 10 am, and after the exercise from 9.79 ±3.04 to 11.19 ±2.53, with a maximum at 4 pm and a minimum of 4 am.

Table 2 – Daily dynamics of MBV mean values in students before and after the exercise stress

t, hour	08	10	12	14	16	18	20	22	00	02	04	06	08
BE	6.09 ± 0.49	6.10 ± 0.53	5.92 ± 0.71	5.77 ± 0.65	6.05 ± 0.54	6.07 ± 0.57	6.04 ± 0.43	5.89 ± 0.55	5.72 ± 0.68	5.55 ± 0.70	5.37 ± 0.69	5.90 ± 0.52	6.02 ± 0.56
AE	10.06 ± 3.23	10.17 ± 3.01	10.87 ± 2.7	10.01 ± 2.44	11.19 ± 2.53	11.03 ± 3.03	10.99 ± 2.98	9.97 ± 2.04	10.64 ± 3.33	9.92 ± 2.09	9.79 ± 3.04	10.22 ± 3.07	10.50 ± 3.08

Studies of MBV daily rhythm before and after the physical exercise show that daily MBV values after the exercise are higher than before PE, by almost 81%. Thus, we have established the values of daily dynamics of MBV in youngsters before and after the physical exercise. The results for the entropy of MBV daily dynamics calculation before and after the exercise are presented on Figures 3 and 4. The results show that MBV curves normally vary from 5.37 L to 6.1 L during the day and are clearly organized in time and the entropy values are 0.6208 (Figure 3).

Increase in minute blood volume after exercise stress is caused by the increasing need of an organism for oxygen. It can be seen that the daily MBV rhythm after the exercise varies from 9.8 L to 11.2 L and is clearly organized in time, however, the rhythm frequency is denser than normal and the entropy index is 0.6438 (Figure 4).

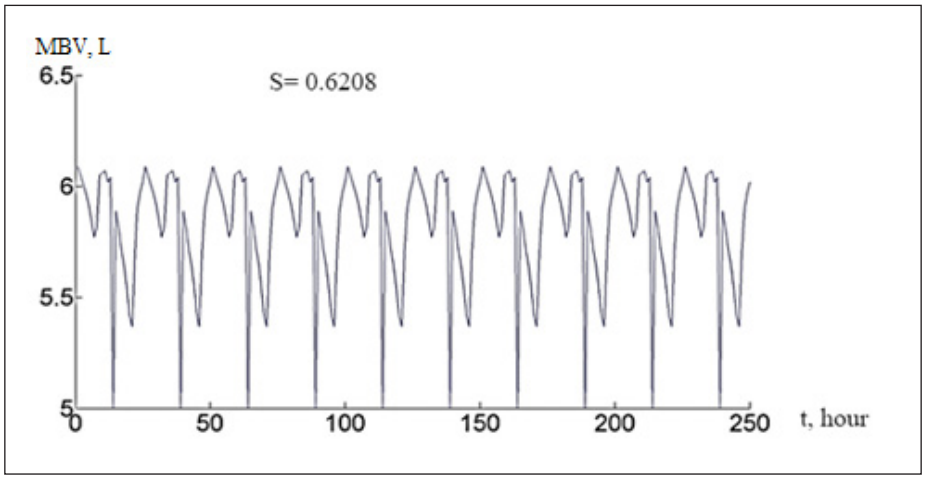

Figure 3 – MVB daily dynamics in students before exercise stress

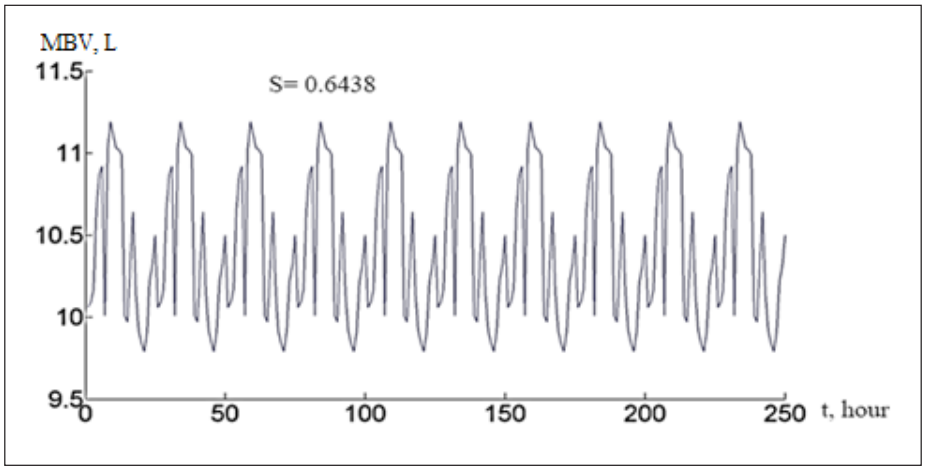

Figure 4 – MVB daily dynamics in students after exercise stress

Conclusion

Entropy is a well-defined quantity in physics, however its definition is fairly simple. The statement that entropy always increases can be derived from simple arguments, but it has dramatic consequences. In particular, this phenomenon explains occurrence of pathological processes [16-18].

Thus, for the first time we calculated the values of entropic indicators of the cumulative dynamics of systolic blood volume before and after the physical activity. It is established that the entropy values are lower in the norm than after the physical exercise, which indicates the energy stress in the cardiovascular system and increase of kinetic energy.

Proceeding from the above, we can draw the following conclusion: the minute volume of blood is a very sensitive and reliable indicator characterizing the reaction of the human body to the performance of a dosed physical load. All the test subjects experienced an increase in minute volume of blood values, which indicates the adequacy of adaptive processes. Between the level of activity of the cardiovascular system and the functional state of the organism, a certain statistically significant dependence is observed. It was established that the measured physical load caused the increase in the minute volume of blood value in the objects.

Ergo, it can be concluded that during the day, systolic blood volume is a subject to a slight vibrational rhythm (approximately 3-7%); the maximum values were observed at night (at 9 pm). The physical load causes an increase in the values of systolic blood volume (in the range of 11-15%). Physical activity stimulates the activity of the cardiovascular system, what in turn increases systolic blood volume leading to the rise of entropy. Similarly, in the course of the day, the minute volume of blood also changes. Entropy values for the systolic and minute blood volume.

References

1. Tuleukhanov S.T. (2002) Biologicheskie ritmy – fundamental'nyi zakon zhivoi prirody [Biological rhythms – the fundamental law of wildlife]. *Izvestija NAN RK: Serija Biolog i Med.*, vol. 6, no. 234, pp. 3-16.

2. Tuleukhanov S.T. (2002) Chronofiziologiya: dostizheniyz i perspektivy razvitiyz [Chronofiziology: achievements and prospects of development]. *Vestnik KazNU Biol series,* vol. 1, no. 16, pp. 94-101.

3. Rapoport S.I., Frolov V.A., Hetagurova L.G. (2012) Chronobiologiya and chronomedicina [Chronobiology and chronomedicine]. *M.: MIA*, p. 480.

4. Zhanabayev Z. Zh. (2013) Kriterii samopodobiya i samoaffinosti dinamicheskogo haosa [Criteria of self-similarity and self-affinity of dynamic chaos]. *Vestnik KazNU Phys series*, vol. 1, no. 44, pp. 58-66.

5. Zhanabaev Z. Zh, Kozhagulov Y.T., Khokhlov S.A. (2013). Scale invariance criteria of dynamical chaos. *Int J Math Phys*, vol. 4, no. 2, pp. 29-37.

6. Chaitun S.D. (2013) Traktovka entropii kak mery besporyadka i ee vozdeistvie na sovremennuiu nauchnuiu kartinu mira [Interpretation of entropy as measures of a disorder and her impact on a modern scientific picture of the world]. *Voprosy filosofii*, no. 2, pp. 62-74.

7. Cfasman A.Z., Alpaev D.V. (2010) Circadnaya ritmika arterial'nogo davleniya pri izmenennom sutochnom ritme zhizni [Circadian rhythmics of arterial blood pressure at the changed daily rhythm of life]. *Reprocentr.*, vol. 2, pp. 305-358.

8. Stepanova S.I. (1989) Sutochnye ritmy pokazatelei kardiorespiratornoi sistemy cheloveka [Daily rhythms of indicators of cardiorespiratory system of the person]. *Problemy kosmich biol*, vol. 64, pp. 34-60.

9. Haus E., Smolensky M. (2006) Biological clock and shift work: circadian dysregulation and potential long-term effects. *Cancer Causes and Control*, no. 5, pp. 489-500.

10. De Scalzi M, De Leonardis V., Calzolari F., Barchielli M., Cinelli P., Chiodi L., Fabiano F.S., Vergassola R. (1984) Heart rate and premature beats: a chronobiologic study. *Giornale Italiano di Cardiologia*, vol. 14, no. 7, pp. 465–470.

11. Ashirbaev Ch. K., Kabylbekov Ch. A., Abdrakhmanova A. I., Kydyrbekova Zh. B. (2017) Organizatciya komp'iuternoi laboratornoi raboty po issledivaniu elektricheskogo i magnitnogo polei s ispol'zovaniem paketa program MATLAB [The organization of computer laboratory work on a research electric and magnetic water with use of the software package of MATLAB]. *Izvestija NAN RK Phys Mat series*, no. 4, pp. 206-213.

12. Khalsa S.B., Jewett M.E., Duffy J.F. (2000) The timing of the human circadian clock is accurately represented by the core body temperature rhythm following phase shifts to a three-cycle light stimulus near the critical zone. *J Biol Rhythms,* vol. 15, no. 6, pp. 524-530.

13. Culic V. (2014) Chronobiological rhythms of acute cardiovascular events and underlying mechanisms. *Int J Cardiol,* no. 174, pp. 417-419.

14. Curtis A.M., Cheng Y., Kapoor S., Reilly D., Price T. S., Fitzgerald G. A. (2007) Circadian varia-

tion of blood pressure and the vascular response to asynchronous stress. *Proc Natl Acad Sci, USA, no. 104, pp. 3450-3455.*

15. Durgan D. J., Young M. E. (2010) The cardiomyocyte circadian clock: emerging roles in health and disease. *Circ Res, no. 106, pp. 647-658.*

16. Slomczynski W., Kwapier J., Zyczkowski K. (2000) Entropy Computing Via Integration over Fractal Measures. Chaos, vol.10, no. 1, pp. 180-188.

17. Costa M.D., Peng C.K., Goldberger A.L. (2012) Multiscale analysis of heart rate dynamics: Entropy and time irreversibility measures. *J Cardiovasc. Eng,* no. 8, pp. 88-93.

18. Valencia J.F., Porta A, Vallverdu M., Claria F., Baranowski R. (2009) Refined multiscale entropy: Application to 24-h holter recordings of heart period variability in healthy and aortic stenosis subjects. *J IEEE Trans Biomed Eng,* vol. 56, pp. 2202-2213.

IRSTI 34.39.55

[1*]A.A. Sazanova, [1]M.S. Kulbaeva, [1]S.T. Tuleukhanov, [2]Yu.A. Kim,
[1]A.I. Zhussupova, [1]G.K. Atanbaeva, [1]N.T. Ablaykhanova, [1]Zh.O. Oralkhanova

[1]Laboratory of Chronobiology and Ecological Physiology, Almaty, Kazakhstan
[2]Institute of Cell Biophysics, Russian Academy of Sciences, Pushchino, Moskovskaya obl., Russia
[*]e-mail: sazanova.aydana@mail.ru

Study of the influence of mobile phones on the functional condition of students' cardiovascular system during the examination period by Holter methods

Abstract: Excessive physical and mental discomfort, nervous breakdown work stress, inappropriate eating behavior accompanied with disproportionate use of mobile phones lead to various functional disorders and illnesses. Mobile phones, often used by the student community for examinations, social adaptation and self-identification in the future profession, can endanger human health, and might consequently lead to disorders of vegetative regulation of cardiovascular system, including the rising frequency of heart contraction, increase in arterial pressure, muscle and psycho-emotional stress. Holter monitoring based on electrocardiogram (ECG) methodology was used to study the physiological state of the heart within the period of 24 h in students with mobile phones overuse. This monitoring system consists of the MT-101 registry block and MT-200 computer-assisted analyzer. Nine students aged 20-21 years old served the objects of the study. ECG rates recorded in the pre-examination learning process were considered as control, and ECG indicators, recorded during the examination period, were considered as experimental. ECG was studied throughout the day during the learning process and in the examination period to esteem the effects of electromagnetic fields caused by stress situations and mobile phones and identify the frequency of ventricular depolarization (Q, R and S wave or QRS) and heart rate. Both in normal conditions and during the examination period the frequency of heart rate and QRS scores are higher in comparison with the nighttime, at night low values are registered depending on the body's relaxation period. Moreover, it was found that statistical reliability ($p<0.05$) during the period of examinations increased simultaneously in the nighttime in comparison to control.

Key words: examination period, mobile phones, Holter monitoring, frequency of heart contraction, QRS complex, electromagnetic field.

Introduction

The main purpose of higher education institutions is to help individual to become a well-educated, highly professional and cultured person. Education in higher education requires special attention to students' health. Frequent use of mobile phones by students has a significant impact on their academic progress and health [1; 2]. Mobile phones are the most frequently used devices for student communication with their friends and families. These devices are constantly kept "online" and it is hard to imagine whether they cannot be used in the library or at the university, in places where we eat, or in cars. Scientists from different countries are studying its effects on the body, including Dr. Magda Havas, Associate Professor of Environmental and Resource Studies at Trent University, Canada, who has proven that electromagnetic radiation from mobile phones has a profound effect on human brain and skin [3-5].

Students are a special social group with a certain age, life and working conditions. Excessive physical and mental stress, breakdown of work, rest, diet schedule, as well as over-use of mobile phones adapt the process that reduces the effectiveness of the learning process and leads to various functional disorders and illnesses. Frequent occurrence of nervous and psychological fatigue due to time scarcity in processing and receiving information and evening work co-occupancy affect their somatic health and mental conditions [6; 7]. Adaptation to a new set of factors is a complex multi-level social-psycho-physiological process accompanied by the system of compensatory formation in student bodies. Dur-

 Printed in Kazakhstan

ing the last 10-15 years, the flow of information load has increased significantly. During the examination period, due to the excessive load on the intellectual and emotional state of students it was found that the tendencies of excitation of the central nervous system were high [8; 9]. This can be particularly noted in students' learning as the features of neurovegetative regulation during the examination period roves the necessity to develop a strategy for strengthening students' health [10]. First steps in higher education are characterized by the influence of several new factors in student bodies, among them the features of educational process, new surroundings, living environment and nutrition are the main part of the educational process. At the same time, according to various literature sources, especially at the initial stages of study (earlier course) destruction of a high potential of psychosocial adaptation of students can be a consequence of examination, change of address and social relationships, chronic illnesses. Clearly psychosocial adaptation can adversely affect the ability of mind, memory and cognitive mental processes. At the same time, during the examination period, there was a decrease in short-term memories and long-term recurrence of the words in the background of the increased workload and attention of the earlier course students. This proves that adaptive reactions of earlier course students are much more complicated due to the information flow, where the adaptive nature should be directed to increase of general activity. However, stress situations for them are significantly different and characterized by increased brain capacity and long-term memory [12-14].

In recent years, studies have been conducted to study the effect of examination stress and mobile phones overuse on the nervous system, cardiovascular system and immune system. In recent years, the incidence of cardiovascular diseases in the Republic of Kazakhstan has risen by 5-7 times and our country takes one of the first places in terms of morbidity and mortality. We may say the main reason is that people do not pay attention to their health, though negative environmental impacts are also significant [16-23].

During the examinations period, disorders of vegetative regulation of cardiovascular system were registered among students in schools and universities along with increased frequency of heart contraction, increase of arterial pressure, rising of muscle strength and psychoemotional resilience [24; 25]. Being under the influence of continuous mobile phones use and the examination period stress makes a physiological load on the body; this load can cause any illness in the body as a whole. Investigating the consequences of this load on heart function, especially control of the heartbeat within 24 h, is a topical issue today [26-29].

Materials and methods

Study of the functional state of cardiac system in student bodies by Holter method during the examination period was completed at the scientific laboratory of Chronobiology and Ecological Physiology of the Department of Biophysics and Biomedicine at the Faculty of Biology and Biotechnology, Al-Farabi Kazakh National University. Mobile phones in the hands of each student are considered as sources of electromagnetic fields in the environment.

Nine students aged 20-21 years old served the objects of the study. ECG rates recorded in the pre-examination learning process were considered as control, and ECG indicators, recorded during the examination period, were considered as experimental. ECG was studied throughout the day during the learning process and in the examination period to esteem the effects of electromagnetic fields caused by stress situations and mobile phones and identify the frequency of ventricular depolarization and heart rate, for which the Holter monitoring was applied.

Electrocardiogram of cardiac work was registered with clinical and physiological methods of electrocardiography without interruption for 24 h at the SHILLER MT-200 HOLTER-ECG apparatus. Schiller Holter monitoring system consists of two parts: MT-101 registry block and MT-200 computer-assisted analyzer. Registrations provided by MT-101 registry block were transferred to the MT-200 computer-assisted analyzer, after which it was possible to save these signals and provide the complete analysis. In order to provide quality ECG registrations, it is necessary to check the quality of the ECG signals. Upon the completion of the registration, specially installed MT-200 computer-assisted analyzer provides the information transfer from the registry block to the personal computer and completes the ECG analysis [15].

Based on recorded electrocardiogram, FHC and QRS score were revealed. The results obtained were statistically calculated; Student's t-test was used to examine the validity of the data.

Results and discussion

During the learning process, the maximum heart rate – 101.0±2.8 beats/minute was registered at 03:00 pm, minimum rate – 61.0±4.2 beats/minute

registered at 5:00 am in the morning. Dynamics of the heart rhythm spectrum is observed within 24 hours with frequency of 77.0 – 101.0 beats/minute heart contraction in normal conditions, noticeably increasing during the period from 08:00 to 11:00 am. Heart rate decreases down to 75.0 beats/minute from 01:00 to 7:00 am. The decrease in heart rate depends on body rest. According to the results, a high intensity of heart rhythms depends on the activity of the organism in the daytime, and low intensity of the heart rate due to the rest of the body during the nighttime (Table 1).

Table 1 – Dynamics of the daily spectrum of heart contractions of students in normal conditions

Time, h	FHC, beats/minute	Time, h	FHC, beats/minute
12:00 pm	86.0±4.2	00:00 am	77.0±1.4
01:00 pm	89.0±1.4	01:00 am	68.5±3.5
02:00 pm	92.5±9.2	02:00 am	68.5±3.5
03:00 pm	101.0±2.8	03:00 am	66.0±2.8
04:00 pm	97.0±1.4	04:00 am	62.5±2.1
05:00 pm	87.5±9.2	05:00 am	61.0±4.2
06:00 pm	85.5±9.2	06:00 am	63.5±2.1
07:00 pm	89.0±1.4	07:00 am	64.5±4.9
08:00 pm	96.5±6.4	08:00 am	92.0±8.5
09:00 pm	88.5±6.4	09:00 am	95.5±4.9
10:00 pm	85.0±1.4	10:00 am	76.5±2.1
11:00 pm	82.0±1.4	11:00 am	83.5±3.5

During the examination period, the analysis of changes of heart rate fluctuations in students reveals the maximum frequency of heart contraction in students – 107.0±3.1 beats/minute registered at 5:00 pm, minimum rate – 75.0±5.6 beats/minute registered at 08:00 am. Fluctuations in dynamics of the daily spectrum of the student heart rhythm in normal conditions are observed in between 12:00 pm and 12:00 am with frequency of heart contractions of 77.0 – 101.0 beats/minute. During the daytime from 12:00 am to 12:00 pm and at 08:00 until 12:00 am of the next day the frequency of heart contraction increased and decreased. Of course, these changes can be attributed to the active body functions.

If we compare the frequency of heart contraction of students during their daily classes and examination period, anomalies in FHC are observed from normal conditions. During the daytime, high-low fluctuations are registered, while high values are determined at nighttime.

Compared to normal conditions, it was found that the relative increase in frequency of heart contractions is observed during the nighttime. Normally, it is equal to the minimum value between 01:00 and 07:00 am, and at the time of examinations, it was observed that there was a relative increase than the normal condition between 01:00 and 07:00 am. That is, the increase in the frequency of heart contraction depends not on the body's calmness (Table 2).

If we compare studied values of heart contractions during the examination period and in normal conditions, differences are observed within 24 h. From the time taken to study if at 05:00 pm – 107.0±3.1 beats/minute and at 06:00 pm – 106.0±9.2 beats/ minute, at 09:00 pm – 100.0±7.1 beats/minute, at 12:00 am – 85.0±2.1 beats/minute, at 01:00 – 84.0±4.2 beats/minute, at 02:00 am – 80.0±4.9 beats/minute, at 03:00 am – 79.0±5.1 beats/minute, at 04:00 am – 80.0±4.2 beats/minute, at 05:00 am – 82.0±4.5 beats/minute, at 06:00 am – 79.0±1.4 beats/minute, at 07:00 am–80.0±2.1beats/minute, at 08:00 am – 75.0±5.6 beats/minute, at 10:00 am – 107.0±8.1 beats/minute, at 11:00 am – 98.0±0.7 beats/minute with statistical accuracy ($p<0.05$) significantly higher than in normal conditions.

Table 2 – Dynamics of the daily spectrum of heart contractions of students during examinations

Time, h	FHC, beats/minute	Time, h	FHC, beats/minute
12:00 pm	96.0±6.4	00:00 am	85.0±2.1*
01:00 pm	94.0±71	01:00 am	84.0±4.2*
02:00 pm	101.0±1.4	02:00 am	80.0±4.9*
03:00 pm	103.0±3.5	03:00 am	79.0±5.1*
04:00 pm	101.0±7.3	04:00 am	80.0±4.2*
05:00 pm	107.0±3.1*	05:00 am	82.0±4.5*
06:00 pm	106.0±9.2*	06:00 am	79.0±1.4*
07:00 pm	89.0±7.1	07:00 am	80.0±2.1*
08:00 pm	88.0±4.2	08:00 am	75.0±5.6*
09:00 pm	100.0±7.1*	09:00 am	88.0±7.1
10:00 pm	86.0±2.8	10:00 am	107.0±8.1*
11:00 pm	83.0±2.8	11:00 am	98.0±0.7*

Note: * – statistical reliability in comparison to control, $p<0.05$

High FHC values of the active physiological state of the organism and its low values during the rest synchronously altered in terms of normal conditions.

The QRS set was studied as a chronostructural indicator of the cardiovascular system in normal conditions, that is, during the daily study. The QRS set represents the formation of the potential dynamics of the excitation in the abdominal muscle of the heart.

As can be seen from the Table 3 in the normal condition, QRS fluctuations are observed between 12:00 pm and 12:00 am with 5408.5±589.01 ÷ 4982.0±172.5 values registered in the period of 08:00–11:00 am.

QRS set results in maximum value of 6002.5±204.3 numeric unit registered at 03:00 pm and 5758.0±46.7 registered at 04:00 pm, and minimum value of 3798.5±130.8 registered at 04:00 and at 05:00 am with the value of 3687.0±213.5 (Table 3).

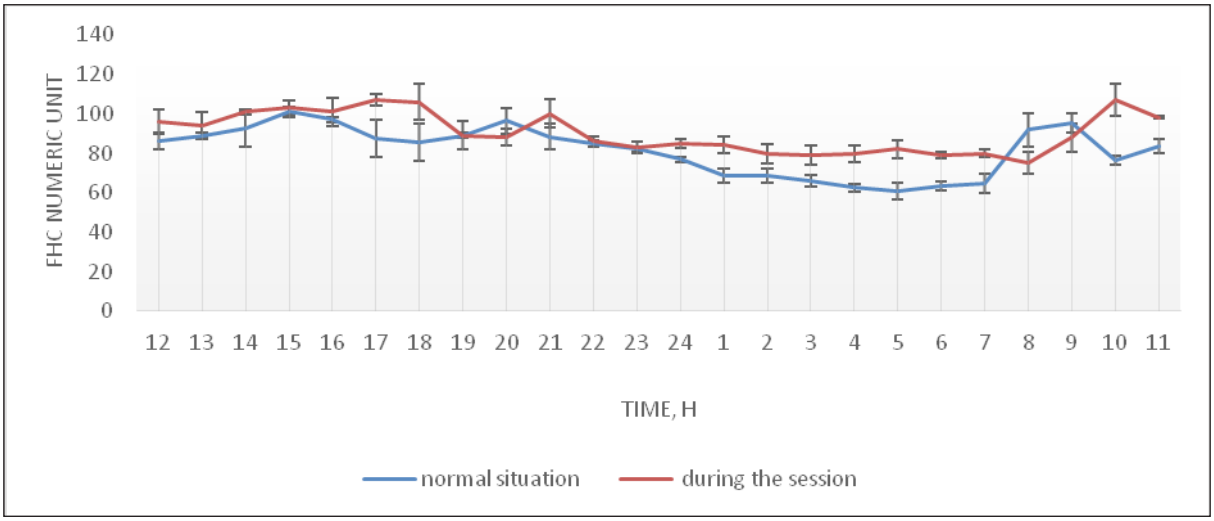

Figure 1 – FHC values in students during the examination period and in normal conditions

Table 3 – QRS set of students in the normal condition

Time, h	QRS	Time, h	QRS
12:00 pm	5156.0±227.7	00:00 am	4612.0±130.1
01:00 pm	5322.0±63.6	01:00 am	4137.0±216.4
02:00 pm	5548.5±539.5	02:00 am	4151.5±171.8
03:00 pm	6002.5±204.3	03:00 am	3987.0±162.6
04:00 pm	5758.0±46.7	04:00 am	3798.5±130.8
05:00 pm	5252.5±495.7	05:00 am	3687.0±213.5
06:00 pm	5139.5±536.7	06:00 am	3822.0±114.5
07:00 pm	5285.5±58.7	07:00 am	3877.5±273.6
08:00 pm	5801.5±403.7	08:00 am	5408.5±589.01
09:00 pm	5319.5±311.8	09:00 am	5627.0±288.5
10:00 pm	5129.0±113.1	10:00 am	4619.0±104.6
11:00 pm	4902.0±1.4	11:00 am	4982.0±172.5

Considering the QRS set of students during the examinations, maximum values from the received data are 6420.0±412.9 numeric unit at 03:00 pm and 5917.5±499.9 at 05:00 pm, but minimum values are 4197.5±272.2 at 08:00 am and 4321.0±406.5 at 03:00 am.

Table 4 – QRS set of students during the examination period

Time, h	QRS	Time, h	QRS
12:00 pm	5124.0±758.01	00:00 am	5340.0±115.2
01:00 pm	4968.5±740.3	01:00 am	4620.0±241.1
02:00 pm	5950.0±67.1	02:00 am	4500.0±271.5
03:00 pm	6420.0±412.9	03:00 am	4321.0±406.5
04:00 pm	5381.0±988.5	04:00 am	4430.0±239.7
05:00 pm	5917.5±499.9	05:00 am	4320.0±307.5*
06:00 pm	5148.5±1481.5	06:00 am	4410.0±88.3*
07:00 pm	4738.5±866.2	07:00 am	4800.0±66.4*
08:00 pm	5037.5±225.5*	08:00 am	4197.5±272.2*
09:00 pm	5363.5±825.2	09:00 am	4584.0±886.7*
10:00 pm	5250.0±172.5	10:00 am	5837.0±671.7*
11:00 pm	5120.0±181.01	11:00 am	5802.0±9.8

Note: * – statistical reliability compared to normal condition, $p< 0.05$

During the examination period, QRS set of students fluctuating anomalies are observed between 12:00 pm and 12:00 am, fluctuates between 5124.0±758.01 ÷ 5340.0±115.2 values. Meanwhile, from 01:00 to 09:00 am, decreased values 4620.0 ± 241.1 ÷ 4584.0 ± 886.7 were registered. At 10:00 – 11:00 am hours, the following values demonstrate a high return of 5837.0 ± 671.7 ÷ 5802.0 ± 9.8 QRS.

Compared with the normal situation, it was determined that the QRS aggregation, which displayed high and low values during the examination period, varies from time to time. At 08:00 pm – 5037.5±225.5 beats/ minute, at 05:00 am – 4320.0±307.5 beats/ minute, at 06:00 am – 4410.0±88.3 beats/ minute, at 07:00 am – 4800.0±66.4 beats/ minute, at 08:00 am – 4197.5±272.2 beats/ minute, at

09:00 am – 4584.0±886.7 beats/ minute, at 10:00 am – 5837.0±671.7 beats/ minute, at 11:00 am – 5802.0±9.8 beats/ minute with statistical accuracy ($p<0.05$) significantly higher than normal (Table 4).

In the first stage of stress, the heart of a person is often beated. In Europe, millions of people die each year due to stress from cardiovascular system disorders.

In normal days and during the examination period, there is an abnormality in total heart rate changes in the daytime compared to the FHS performance of students. From 12:00 pm-12:00 am and 07:00 am-12:00 pm the following day, when compared to the normal examination period, the value of both decreasing and higher values was observed. It is clear that during the examination period, at 12:00 am and 6:00 am, relative elevation was observed.

From normal to normal, the FHS in the normal examination period and at the sessions at 08:00, 09:00, 10:00 am on the following day at 05:00, 06:00, 09:00 pm with significant statistical reliability ($p\leq0.05$). At the same time, it can be seen that there are times when it is not reliable.

QRS reliability indicators correspond to the times when the FHS is subject to change. QRS is a rhythm of a moderately concave ventricle, taking the FHS as an indication of the overall heart rate.

Stress can lead to heart disease and stroke. This can lead to heart attacks if a person is experiencing a severe stress, an intense stress or a sad day. Stress also comes when a person is happy. If a person gets into some stress, first of all, heart rate changes, blood vessels tone is broken and other physiological changes. In severe stress, the tone of the heart muscle changes, which is called heart failure or cardiomyopathy.

Thus, in moderate daytime, i.e., when the body is active, it is equal to the higher values, and at night, low values are registered depending on the body's calmness. At night, during the examination period, it was higher than normal, but synchronously fluctuated values were registered.

During the examination period, the student body was not in the state of calmness; therefore, the values are higher than the normal one.

Conclusion

Dynamics of the daily spectrum of the heart rhythm of students with normal conditions there are anomalies are observed in the fluctuations from 12:00 pm to 12:00 am at night, the results of frequency of heart contraction during the examination period were different from the results of normal condition. During the examination period, QRS set of students fluctuating anomalies are observed between 12:00 pm and 12:00 am. Compared with the normal situation, it was determined that the QRS aggregation, which displayed high and low values during the examination period, varies from time to time. The data of the heart activity of students, which are accepted as a normal case, are consistent with standard accepted indicators. At the same time, during the examination period, students' thoughts along with psychosomatic stress, considering that as a physical load it does not remain inactive, as well as results of research work shows long-term effects on the electromagnetic field will also affect the heart function. The FHS and QRS concentration indicators are also characterized by moderate discontinuous changes in both calm and susceptible state (sleeping) identified synchronously increasing than normal times at night. Students during the examination period with the aim of focusing on heart function calming itself need to do training by exercises to overcome stress.

References

1. Aganyants E.K. (2005) Human physiology: the textbook for undergraduates and graduate students. *M.: Soviet sport*, p. 336

2. Amvros'eva V. (2004) Enterovirus infections of heart at patients with myocarditis and cardiomyopathies. *Vests NAN Belarus*, no. 3. p. 73-79.

3. Agadzhanyan N.A., Orayevsky V.N., Makarova I.I. (2001) Medico-biological effects of geomagnetic indignations. *M.: IZMIRAN*, p. 136.

4. Nikityuk B.A., Gladysheva A.A., Sudzilovsky F.V. (2003) Human anatomy: the textbook for institutes of physical culture. *M.: Terra-Sport*, p. 624.

5. Abzalov P.A. (2007) Regulation of functions of heart of a nepolovozrely organism at various motive modes. *Kazan*, p. 311.

6. Dudel Y., Ryuegg Y., Schmidt R. (2010) Human Physiology. *M.: Mir*, p. 323.

7. Elkin Yu.E., Moskalenko A.V. (2009) Basic mechanisms of arrhythmias of heart. *Clinical arrhythmology. Ed. by A.V. Ardashev. M.: Medpraktika-M*, p. 1220.

8. Sazanova A.A., Lespekova M.M., Oralkhanova Zh.O., Namys S.S. (2017) Study of the chrono-stroke performance of cardiac activity of young people suffering from pyelonephritis. *Proceedings of the International Scientific Conference of Students and Young Scientists "Farabi alemi" Almaty*, p. 46.

9. Sazanova A.A., Lespekova M.M., Oralkhanova Zh.O., Namys S.S. (2017) Research on the influence

of cardiac activity on cardiac activity by electromagnetic fields used by students in the learning process by Holter method. *Proceedings of the International Scientific Conference of Students and Young Scientists "Farabi alemi" Almaty*, p. 56.

10. Sazanova A.A., Kulbaeva M.S., Ablaikhanova N.T., Kulbaev T.T. (2018) Studying the functional state of the cardiac system in the body of the students during the examinations by Holter method. *Proceedings of the International Scientific-Practical Conference "Modern issues of ecological genetics and current biology" Almaty*, p. 115.

11. Makarov L.M. (2003) Holter Monitoring. 2 ed. *M.: Medpraktika-M*, p. 340.

12. Gerchikova T.N., Topolyansky A.V., Rybakova MK (2006) Diseases of the heart. *M.: Encyclopedia.* p. 543.

13. Grinshpuna L.D. (2011) Geriatric Hematology: diseases of the blood system in older age groups. *M.: Medium*. p. 312.

14. Shibkova D.Z. (2005) Workshop on human and animal physiology. *Chelyabinsk: CSPU Publishing House*, p. 279.

15. Makarov L.M. (2003) Holter monitoring. 2 ed. *M: Medpraktika-M*, p. 340.

16. Alter P., Rupp H., Maisch B. (2006) Activated nuclear transcription factor KB in patients with myocarditis and dilated cardiomyopathy relation to inflammation and cardiac function. *Biochem Biophys Res Comm*., vol. 339, no.1, pp. 180-187.

17. Barold S.S., Norman J. (2005) "Jeff" Holter – "Father" of ambulatory ECG monitoring. *J Intervent Cardias Electrophysiol.*, vol. 14, no. 2. pp. 117-118.

18. Braunwald E. (1997) Heart Disease: a textbook of cardiovascular medicine. *Philadelphia: W.B. Saunders Co.*, p. 108.

19. Bessisso M., Bener A., Elsaid M. (2005) Pattern of headache in school children in the State of Quatar. *Saudi Med J*., vol. 26, no. 4, pp. 566-570.

20. Bucheit M. (2007) Habitual activity, physical fitness and heart rate variability in preadolescents. *Int J Sports Med*., vol. 28, no. 3, pp. 204-210.

21. Coates A.L., Desmond K.J. et al. (1994) Sources of variation in FEV1. *Am J Respir Crit Care Med.*, no. 149, pp. 439-443.

22. Davignon A., Rautaharyn P., Davignon A., Boisselle E. (1980) Normal ECG standarts for unfant and children. *Ped. Cardiology*, vol. 1, pp. 123-131.

23. Doncheva N.I., Nicolova R.I., Danev S.G. (2003) Overweight, dislipoproteinemia, and heart rate variability measures. *Folia Med. (Plovdiv)*, vol. 45, no. 1, pp. 8-12.

24. Fujii H., Fukutomi O., Inoue R. (2000) Autonomic regulation after exercise evidenced by spectral analysis of heart rate variability in asthmatic children. *Annals of Allergy, Asthma & Immunology*, vol. 85, no. 3, pp. 233-237.

25. Guizar J. M. (2005) Heart autonomic function in overweight adolescents. J.M. Guizar R. Ahuatzin, N. Amador. *Indian Pediatr*., vol. 42, no. 5, pp. 464-469.

26. Helbig S., Lampert T., Klose M., Jacobi F. (2006) Is parenthood associated with mental health. *Soc. Psychical and Psychiatric Epidem*., vol. 41, no. 11, pp. 889-896.

27. Matturri L., Ottaviani G., Ramos S.G., Rossi L. (2000) Sudden infant death syndrome (SIDS): a study of cardiac conduction system. *Cardiovasc Path*., pp. 137-145.

29. Newby R. (2008) From Norman Jefferis "Jeff" Holter. A serendipitous life: an essay in biography. *Drumlummon Views*, pp. 224-256.

30. Sassone-Corsi Paolo. (1994) Rhythmic transcription and autoregulatory loops: winding up the biological clock. *Cell*, vol. 78, no. 3, pp. 361-364.

IRSTI 34.31.27

[1]G.I. Yernazarova, [1*]S.K. Turasheva, [2]A.A. Sartayeva, [1]S.B. Orazova,
[3]A.A. Bazargaliyeva, [2]E.M. Imanova, [2]G.K. Omarova, [4]S. Yancheva

[1]Laboratory of Environmental Biotechnology, Almaty, Kazakhstan
[2] Department of Biology, Kazakh State Women's Teacher Training University, Almaty, Kazakhstan
[3]Department of Biology, Aktobe Regional University named after K. Zhubanov, Aktobe, Kazakhstan
[4] Agricultural University-Plovdiv, Plovdiv, Bulgaria
[*]e-mail: svetlana.turasheva@kaznu.kz

Absorption of chromium by mono- and mixed cultures of microalgae

Abstract: In the article the sorption ability of microalgae cultures to chromium are discussed. The objects of the study were microalgae from the collection of the Department of Biotechnology of Al-Farabi Kazakh National University, related to cyanoprokaryotes (*Cyanoprocaryota/ Cyanobacteria*): *Anabaena flos-aquae, Anabaena arnoldii, Nostoc linckia, Calothrix pariethina* as well as their two-species mixtures *A. flos-aquae* x *C. pariethina, N. linckia* x *C. pariethina, A. flos- aquae* x *N. Linckia, A. flos-aquae* x *A. arnoldii* and *Scenedesmus quadricauda*. Also two green (*Scenedesmus quadricauda and Chlorhormidium sp.)* and one diatomaceous (*Nitzshia sp*.) algae were studied. The duration of cultivation was 20 days. Potassium bichromate was added to the nutrient medium at concentrations 0.01-0.2 mg/ml calculated per unit of chromium. The concentration of chromium in the filtrates of the studied cultures in some cases significantly decreased by the end of the cultivation period, which indicates the biosorption of this element by the microalgae cells. The investigated strains of microalgae absorb chromium from the medium in varying degrees. The most active biosorbents among the explored cultures were *A. flos-aquae, N. linckia* and *C. pariethina.* A microalgae *A. arnoldii* extracts chromium from the medium in smaller quantities. The listed strains refer to cyanoprokaryotes (cyanobacteria), from other cultures, the *Scenedesmus quadricauda* absorbs chromium quite actively. The highest intensity of chromium biosorption is characteristic of Nostoc (*N. linckia)*, which extracts from the medium 60.8-74.6% chromium at initial concentrations 0.05-0.1 mg/ml respectively. The most active biosorbents of chromium were four species of Cyanobacteria. In this regard, these strains have been selected by us for future study of the processes of sorption and metabolic activity in mono- and mixed cultures of microalgae.
Key words: microalgae, chromium, sorption, stability, antagonism, algoflora.

Introduction

The growth of cities and industrial production leads to environmental pollution by chemical elements. The consequence of this is the increasing spread of ecosystems, disturbed as a result of human technical activities. Pollution of the environment by potentially dangerous chemicals, especially various metal compounds, creates extreme conditions for living organisms, including humans [1].

The main sources of air, soil and water contamination with metals are fossil fuel combustion products and industrial emissions, especially mining, metallurgical and chemical. In the zones of influence of metallurgical and some other enterprises in water, soils and plants, a large number of metals can accumulate (Ag, Al, Be, Cd, Co, Cr, Cu, Fe, Mn, Mo, Ni, Pb, Sb, Sn, Ti, V, Zn and etc.) [2; 3]. Some of them cause death or inhibit the growth of plants, and when precipitated from the air, they are sucked from the surface of the soil by the roots of plants, impair the quality of vegetables and fruits, have harmful effects, plant animal feed resources and microorganisms involved in soil self-cleaning, with surface runoff in water and have a disastrous effect on fish and their food resources. They are filtered through the soil and at a low level of water in the reservoirs in winter with the groundwater enter rivers and lakes and have a harmful effect on aquatic organisms [4]. Heavy metals coming from anthropogenic sources of pollution have a great impact on aquatic ecosystems. In reservoirs that are testing the constantly increasing level of ecotoxicants in the water, they accumulate in the tissues and organs of plants and animals, a steady decrease in the number of individual components of the biocenosis, which can lead to a violation of the

 Printed in Kazakhstan

balance of biological processes and the death of the ecosystem [5-9].

Recently, the ability of microorganisms, including microalgae, to biosorbate heavy metals has been proven. The intensity of the process of metal sorption depends, first of all, on the physiological state of the culture. The actively metabolizing populations of microalgae store and macrophytes more intensively heavy metals than inactive cultures [1; 8].

Algae are an exceptionally convenient model object for studying the general patterns of the influence of toxicants on the cellular and population levels simultaneously [10-13].

Among the test objects of different trophic levels studied in the comparative toxicological experiment (seaweed *Phaeodactylum tricornutum* and *Coscinodiscus janishii A.S.*, the fusiform *Infusoria Euplotes patella lemani Dragesco*, the early nauplial stages of the trophic lobster crustaceans *Artemia salina L.,* the fertilized eggs of the bivalve mollusks *Mytilus galloprovincialis L.*) unicellular algae in general – the most sensitive to potassium dichromate group of organisms [14]. In this regard, algae, as one of the main test objects, are included in the methodological documents for the assessment of the toxicity of the polluted aquatic environment [11; 12]. In studies on the effects of harmful substances on aquatic organisms, potassium dichromate is used as a reference toxicant [13; 14].

Growth and development of microalgae in a certain range of concentrations of TM, due to genetic characteristics, can be characterized as tolerance. Resistance of microalgae populations to TM concentrations outside the tolerant zone is characterized as resistance. The concept of resistance is closely related to adaptation – the ability to experience unfavorable conditions that caused the death of a given organism.

It has been established that laboratory cultures of green microalgae *(Scenedesmus sp., Chlorella sp.)* are more resistant to chromium than diatomaceous algae cultures (*Fragillaria crotonensis)* [12; 15]. In natural populations of phytoplankton at elevated Cr^{2+} concentrations, dominance in some algal flora of some water bodies also changed from diatom and blue-green to green algae [16]. At the same time, the exceptional resistance of blue-green algae with gel-like mucous membranes on the surface of cells is also emphasized, and among others it performs the function of chelating many elements [17; 18].

Materials and methods

The microalgae species from the collection of the Department of Biotechnology of Al-Farabi Kazakh National University, related to Cyanoprokaryotes *A. flos-aquae, A. arnoldii, N. linckia, C. pariethina* as well as their two-species mixtures, two green (*Scenedesmus quadricauda and Chlorhormidium sp.)* and one diatomaceous (*Nitzshia sp*.) algae were used as the objects of investigation.

Microalgae in the form of monocultures and two-species mixtures were grown on Fitzgerald medium at 24-hour illumination. The duration of cultivation was 20 days. Potassium dichromate was added to the nutrient medium at concentrations of 0.01-0.2 mg/ml in terms of chromium.

The chromium content in the medium and the biomass of plant objects was determined on an AAS-IN atomic absorption spectrophotometer, Carl Zeiss, using a flame atomizer. The plant samples were kept in an oven for 1 hour at 130 °C. The samples were mineralized in a muffle furnace at 450 °C. The dish with the ash was cooled to room temperature and 1 ml of nitric acid solution was wetted with sulfur ashes. Then, the acid was evaporated to dryness on an electric cooker with a mild heating, and again a cup with a sample was placed in an electric oven at a temperature of 250 °C. The temperature was gradually brought to 450 °C and held for 1 hour. The mineralization was considered complete when the ash became white or slightly colored, without charred particles. In the presence of charred particles, the treatment of the ash was repeated with a solution of nitric acid or water. The metal concentration was determined by the following formula:

$$C\% = \frac{nVk100}{P},$$

where n is the determined concentration of metal in solution (μg/ml), is determined from the calibration curve; V is the volume of the solution (ml); P is the weight of the sample (g); k is the dilution factor [14].

The amount of metal in the medium was calculated by the formula:

$$C = \frac{nV_2}{V_1},$$

where n is the concentration of the element found in the solution (μg / ml), is determined from the calibration curve; V_1 – initial volume (ml); V_2 is the final volume (ml) [17]. To determine the dry mass of algae, several samples with 10 ml of medium were taken at the beginning and end of the experiment

and passed through a membrane filter. The weight of filters with algae and without algae was determined after repeated drying in bucks at 130 ° C. By the difference, a dry mass of algae was determined in each variant of the experiment at the beginning and end of the experiment.

The data were processed statistically and reliably at P> 0.95. The experimental data show the arithmetic mean values of the three experiments and their standard deviations.

Results and discussion

In this study were tested strains of microalgae from the collection of the Department of Biotechnology of Al-Farabi Kazakh National University. 9 strains of microalgae, belonging to the majority of Cyanoprokaryotes (6 strains), 2 green (*Scenedesmus quadricauda and Chlorhormidium sp.)* and 1 diatomaceous (*Nitzshia sp*.) were used in this investigation. The microalgae were cultured for 25 days on a Fitzgerald medium with a chromium content of 0,05 and 0.1 mg/ml. The concentration of chromium in the filtrates of the studied cultures in some cases significantly decreased by the end of the cultivation period, which indicates the biosorption of this element by the microalgae cells. In accordance with Figure 1, the investigated microalgae strains absorb chromium from the medium to some extent.

The most active biosorbents among the studied cultures were A. *flos-aquae, N. linckia and C. paryethina.* A little in smaller quantities extracts chromium from the environment of *A. arnoldii*. The listed strains refer to cyanoprokaryotes (cyanobacteria). Other cultures like *Scenedesmus quadricauda* is quite actively absorbed chromium and had the highest intensity of biosorption

Further follows *A. flos-aquae* (53.6-55.6%). It is interesting to note that the degree of extraction of chromium from the medium is not always directly proportional to its concentration in the medium. In *Calothrix pariethina*, the amount of absorbed chromium decreases slightly (from 53 to 51%) with an increase in its initial concentration in the medium. A decrease in the biosorption of chromium is also observed in the case of *A. arnoldii, Scenedesmus quadricauda, Anabaena variabilis, Chlorhormidium sp., Phormidium uncinatum*. The decrease in the intensity of metal absorption from the medium with increasing its concentration may be due to inhibition of growth processes and a decrease in the metabolic activity of the algae.

As noted above, the most active chromosome biosorbents have been shown to be 4 species of blue-green algae. In connection with this, these strains were chosen by us for the subsequent study of the processes of sorption and metabolic activity in mono- and mixed cultures of microalgae.

Some works indicate that mixed cultures of certain species of microalgae show higher growth activity than monocultures [3; 4]. This fact should be taken into account when selecting species that actively absorb heavy metals in mixed populations. To clarify the activity of chromium absorption, we studied not only the monocultures of the above four microalgae strains, but also their mixed two-species cultures. In cultures of 20 days of age, a growth curve appears on the plateau, which is the beginning of the stationary phase, when the metabolic processes are still quite active. It is known that there is some rhythm in the sorption-desorption-reabsorption processes. According to J. Fogg [4; 5], through the isolation of exometabolites, algae perform dissolution, complexation, reduction of various elements, as well as obtaining specific exogenous complexes ready for absorption.

In subsequent experiments, we studied the intensity of the processes of chromium sorption in correlation with the intensity of metabolic processes.

According to the Figure 2, where the results of the determination of chromium extraction from the medium at a greater concentration change (0.01-0.2 mg/ml) are presented, among the monocultures of the studied microalgae species, the most sorptive activity with respect to chromium was Nostoc, in the filtrate of which even at a very high initial concentration (0.2 mg / ml), only 19.5% of the initial amount of the element was found, which corresponds to an extraction of 80.6% (Figure 2). The value of the *A. flos-aquae* sorption activity at the maximum chromium concentration in the medium approaches the values determined for Nostoc, although at chromium concentrations from 0.01 to 0.05 mg/ml, the intensity of chromate absorption by anabenium was significantly lower than for Nostoc. Significantly less sorption activity was shown by *C. pariethina*. With an increase in the concentration of chromium from 0.05 to 0.2 mg/ml, the rate of its extraction from the medium decreases.

According to the intensity of biosorption of chromium, *A. arnoldii* showed the lowest activity in these experiments in comparison with the above species.

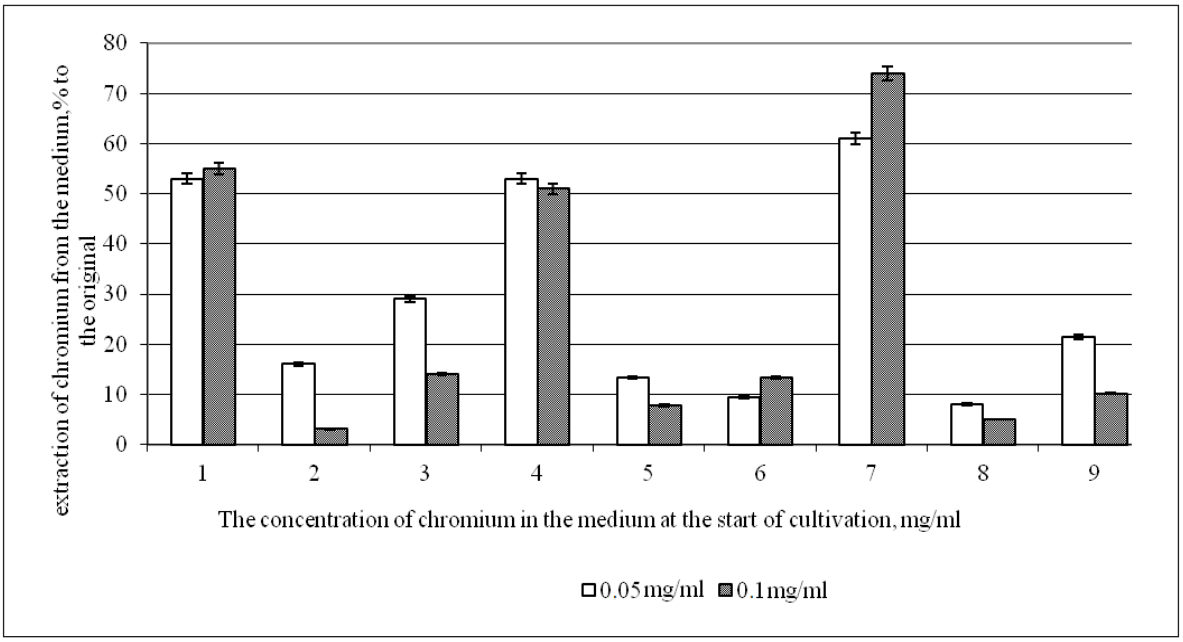

1 – *A. flos-aquae,* 2 – *Anabaena variabilis,* 3 – *A. arnoldii,* 4 – *C. pariethina,* 5 – *Chlorhormidium sp.,* 6 – *Nitzshia sp.,* 7 – *N. linckia,* 8 – *Phormidium uncinatum,* 9 – *Scenedesmus quadricauda*

Figure 1 – Screening of microalgae on the biosorption of chromium from the chromium environment is typical for nostoc, which extracts from the medium 60.8 – 74.6 % chromium at initial concentrations of 0.05 – 0.1 mg/ml, respectively

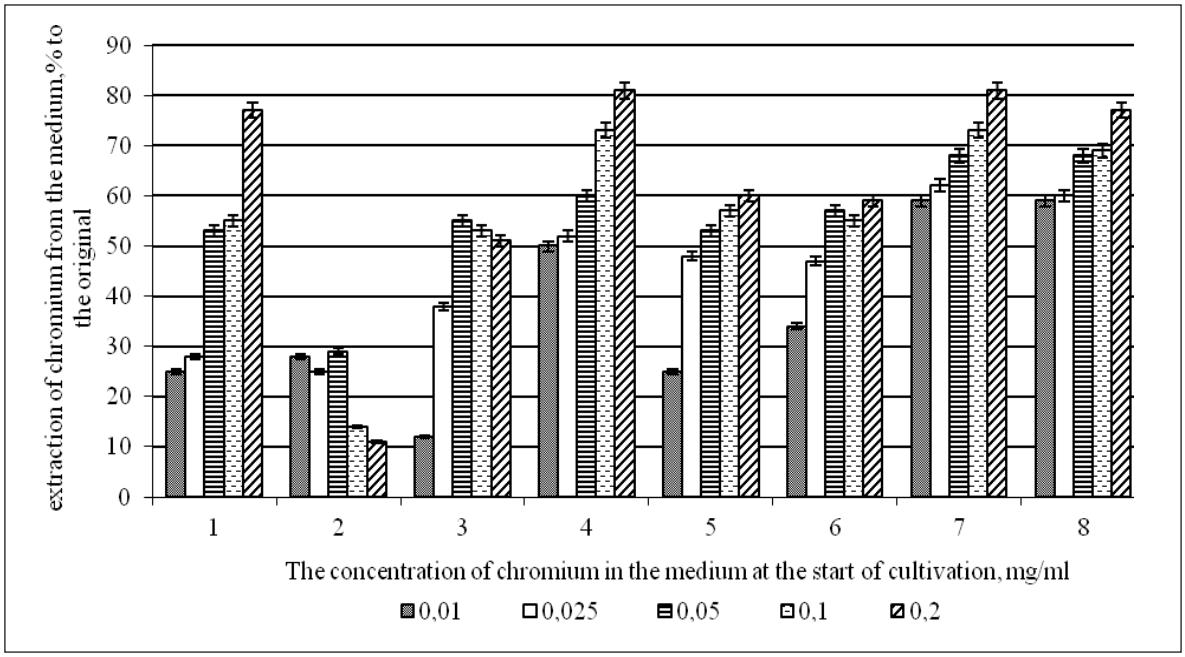

1 – *A. flos-aquae,* 2 – *A. arnoldii,* 3 – *C. pariethina*, 4 – *N. Linckia,* 5 – *A. flos- aquae* x *C. pariethina,* 6 – *N. linckia* x *C. pariethina*, 7 – *A. flos- aquae* x *N. Linckia,* 8 – *A. flos-aquae* x *A. arnoldii*

Figure 2 – Absorption of chromium by microalgae

In mixed cultures with negative allelopathy, the intensity of chromium uptake from the medium is, for the most part, comparable to the intensity of biosorption of one of the partners of the mixture or represents a certain average value between the extraction values in monocultures of both partners. At the same time, in mixtures with positive allelopathy, there is an increase in sorption activity in comparison with monocultures. In a mixture of *A. flos-aquae x N. linckia* as well as in a mixture of *A. flos-aquae x A. arnoldii*. a linear dependence of the extraction of chromium on its concentration in the medium is observed. The greatest amount of chromium was extracted at a concentration of 0.2 mg/ml of microalgae in the first 5 days of cultivation. The change in the intensity of sorption processes in the cultures of microalgae studied confirms this regularity. As an example, we give the results of analyzes carried out on the culture of *C. pariethina*. Table 1 shows the determination of chromium content in various fractions: 1) culture liquid, i.e. dissolved, residual chromium; 2) microalgae cells = absorbed chromium and 3) washings with a 5% solution of NH_4OH sediment of algal cells on the membrane filters (Table 1). The amount of chromium found in the wash solution was evaluated as adsorbed on the cell surface.

Data given in Table 1 show that at the first day of cultivation (24 hours) only 22% of the initial chromium content remains in the medium. 64% is absorbed by the cells, while a certain amount (14%) is adsorbed on the cell surface.

With the increase in the period of cultivation, gradual desorption of chromium from the cells into the medium is observed, which leads to an increase in the amount of dissolved metal to 66% by the 5th day of cultivation (120 hours). The amount of chromium adsorbed on the cell surface to 26% also increases. By this time of cultivation the chromium content in cells is reduced to 8%.

In accordance with Figure 3, where the accumulation of chromium is shown by the cells of the blue-green algae studied, a gradual increase in chromium content in the cells is observed in monocultures as the concentration of this element in the medium increases. The largest quantities were found in variants with a starting content of 0.2 mg/ml of chromium. Monocultures of blue-green algae in this variant of the experiment accumulate in the cells 15.0-25.0 mg of chromium per gram of dry mass.

Table 1 – Dynamics of chromium content in culture of *C. pariethina* in the initial period of cultivation (at an initial concentration 0.05 mg/ml)

Day	Dissolved chromium in the medium (residual)		Adsorbed chromium		Absorbed cells chromium	
	mg/ml	% to the original	mg/ml	% to the original	mg/ml	% to the original
1	0.011±0.003	22	0.007±0.001	14	0.032±0.002	64
2	0.016±0.002	32	0.007±0.001	14	0.027±0.003	54
4	0.019±0.002	38	0.008±0.002	16	0.023±0.004	46
5	0.026±0.001	52	0.014±0.003	28	0.010±0.003	20
6	0.033±0.003	66	0.013±0.003	26	0.004±0.001	8

In mixed cultures with negative allelopathy, the tendency to increase the chromium content in cells with an increase in its concentration in the medium does not persist. Thus, in a mixture of *A. flos-aquae x C. pariethina*, the maximum chromium content in cells was found in the variant 0.05 mg/ml, which is 17.2 mg/g. A further increase in the initial concentration of chromium in the medium leads to a decrease in the concentration of chromium in the cells, which is obviously explained by a decrease in the cell viability level in this mixture, as shown above. Cell death in another mixture with negative allelopathy (*N. linckia x C. pariethina*) leads to rather low values of chromium absorbed by the cells.

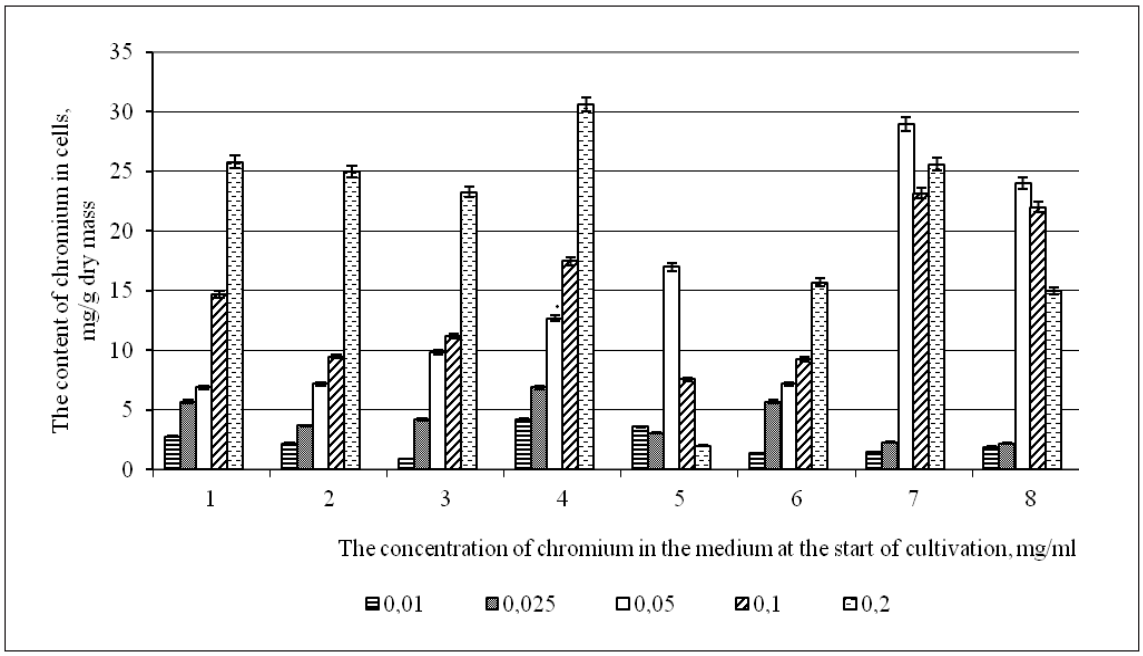

1 – *A. flos-aquae,* 2 – *A. arnoldii,* 3 – *C. pariethina*, 4 – *N. Linckia,* 5 – *A. flos- aquae* x *C. pariethina,* 6 – *N. linckia* x *C. pariethina*, 7 – *A. flos- aquae* x *N. Linckia,* 8 – *A. flos-aquae* x *A. arnoldii*

Figure 3 – Chromium content in cells of mono- and mixed cultures of microalgae

With an increase in the chromium concentration in the medium, the chromium content in the cells is further reduced. In the other two-species cultures, much higher amounts of chromium were detected in the cells. Allelopathy with positive interference of species, leading to active growth and division of cells of both partners, promotes intensive absorption of chromium from the environment. It can only be noted that at low chromium concentrations (0.01-0.025 mg/ml), the cells absorb rather small amounts of chromium. However, a further increase in chromium concentration in the medium leads to its accumulation in cells at sufficiently high concentrations. The highest chromium content in *A. flos-aquae x N. linckia* cells was found in variants with a starting content of 0.05 and 0.2 mg/ml. At a concentration of 0.1 mg/l decrease in the chromium content of the cells is observed, which is rather difficult to explain. According to some authors, the concentration absorption curves of metals can have several peaks, very often no linear dependence is observed. This character of metal absorption is explained by the biological specificity of the given object and the physicochemical features of the behavior of metal ions in solutions [1, p.84].

It is interesting to consider how the chromium extracted from the medium is distributed: whether it is absorbed by the cells. To do this, we used as an example to determine the chromium content in a 20-day mixed culture of *N. linckia x C. pariethina.* In Table 2 (similarly to Table 1), the determination of chromium content in different fractions is given: 1) culture liquid, i.e. dissolved, residual chromium; 2) microalgae cells = absorbed chromium and 3) washings with a 5% solution of NH_4OH sediment of algal cells on membrane filters (Table 2). The amount of chromium found in the wash solution was evaluated as adsorbed on the surface of the cells.

As can be seen from the data presented in Table 2, after a 20-day cultivation of chrome microalgae, the medium remains between 28 and 66%, depending on the initial concentration of chromium in the medium. The lowest degree of sorption is characteristic for both the minimum concentration (0.01 mg/ml) and its maximum concentration (0.02 mg/ml). Much more intensively, the cells absorb chromium in the 0.025 mg/l variant, reducing the amount of residual chromium in the medium to 28%. An increase in the chromium concentration to 0.05 and 0.1 mg/ml resulted in an increase in chromium content in the medium. The adsorption of chromium on the surface of cells increases in an abrupt way with increasing concentration. The greatest number was found in the variants with 0.025 mg/ml and 0.2 mg/ml of chromium. The chromium content in the cells decreased with increasing initial concentration in the medium, reaching a minimum of 9% at 0.2 mg/ml.

Table 2 – Distribution of chromium by fractions in a 20-day mixed culture *N. linckia x C. pariethina*

The initial concentration of chromium in the medium (mg/ l)	Chromium (residual) dissolved in the medium		Adsorbed chromium		Cell absorbed chrome	
	mg/l	% to the original	mg/l	% to the original	mg/l	% to the original
0.010	0.0062±0.0009	66.0	0.0010±0.0007	14.0	0.0042±0.0008	30
0.025	0.0071±0.0011	28.0	0.0081±0.0005	32.0	0.0120±0.0006	40
0.050	0.0210±0.0006	42.0	0.0141±0.0008	28.0	0.0153±0.0004	30
0.100	0.0520±0.0004	52.0	0.0192±0.0006	19.0	0.0291±0.0003	29
0.200	0.1270±0.0010	63.5	0.0552±0.0007	27.5	0.0182±0.0010	9

If we compare these data with those shown in Figure 1, the change in the intensity of chromium sorption from the medium by the cells of the studied mixed culture can be explained by the intensification and retardation of cell division. With the activation of growth processes at a concentration of 0.025 mg/ml, the uptake of chromium was increased to 72% (in total), with almost 45% of this amount adsorbed on the cell surface.

Inside the cells only 55% of the sorbed chromium penetrates. With increasing chromium concentration in the medium, the intensity of chromium uptake from the medium drops to 36.5%.

Conclusion

Most of this quantity (75.3%) remains adsorbed on the surface, and only 9% of sorbed chromium permeates the cells, which confirms the data of the researchers [6], who found that active metabolizing cells actively activate the biosorption of metals.

The obtained results indicate that the intensity of sorption is directly proportional to its concentration in the medium. Thus, as the results of studying of phytotoxicity tests, it has been established that cultivation in media with high concentrations of chromium, microalgae extract chromate ions from the medium from 25 to 80% of its original quantity. Up to 50 percent or more of the extracted chromium is adsorbed on the surface of the cells, while in chromium biomass chromium is detected in an amount not exceeding 30 mg/g dry weight. In the processes of intracellular absorption of chromium, mixtures with positive allelopathy are again leading. Perhaps, chromium binds to intracellular complexes such as polyphosphate bodies, designed to store substances and, thus, is rendered harmless.

References

1. Brigida D'Abrosca, Marina Dellagreca, Antonio Fiorentino, Marina Isidori, Pietro Monaco, Severina Pacifico (2006) Chemical constituents of aquatic plant Schoenoplectus lacustris. J Chem Ecol., vol. 32, no. 1, pp. 317-323.

2. Gadd G.M. (2010) Metals, minerals and microbes: geomicrobiology and bioremediation. Microbiol., vol. 156, pp. 609-643.

3. Adam S., Kumar Ps., Santhanam P., Kumar S.D., Prabhavathi (2015) Bioremediation of Tannery wastewater using immobilized marine microalga Tetraselmis sp.: experimental studies and pseudo-second order kinetics. Int conf Mar Biol Oceanogr., pp. 37-38.

4. Gadd G.M. (2009) Heavy metals pollutants: environmental and biotechnological aspects. In: Encyclopedia of microbiology. 3rd ed. Elsevier, Oxford, pp. 321-334.

5. Pratiush K.D. (2017) Microalgal technology for biosorption of hexavalent chromium in contaminated water bodies: opportunities and challenges. National Seminar on Role of microalgae in Waste Water treatment (RMWT)-2017, India.

6. Ghinwa Naja, Bohumil Volesky (2011) The Mechanism of metal cation and anion biosorption. In: Microbial biosorption of metals, Ch 3, pp. 19-38.

7. Muzichkina R.A., Korulkin D.J., Abilov Zh.A. (2012) Metodologia issledovania rastitelnih metabolitov. Monographiya [Methodology of investigation of plant metabolites. Monograph]. Almaty: MV-Print, p. 324.

8. Malathy R., Shaleesha A. Stanley (2015) Studies on the potential therapeutic effects on the aquatic macrophytes namely Cabomba aquatica, Ceratophyllum demersum and Hygrophila corymbosa. J Chem Pharmaceut Res, vol. 7, no. 4, pp. 479-483.

9. Gihan A. El Shoubaky, Essam A Salem (2014) Terpenes and sterols composition of marine brown algae Padina pavonica (dictyotales) and Hormophysa triquetra (fucales). Int J pharmacognosy phytochem res., vol. 15, no. 6, pp. 894-900.

10. Braginskiy L.P., Velichko M.M., Sherban E.P. (1987) Freshwater plankton in toxic environment, Kiev: Naukova dumka, p. 179.

11. Adam S., Kumar Ps., Santhanam P., Kumar S., Prabhavathi D. (2015) Bioremediation of Tannery wastewater using immobilized marine microalga Tetraselmis sp.: experimental studies and pseudo-second order kinetics. Int conf Mar Biol Oceanogr., p. 37.

12. Wallen D.G. (1996) Adaptation of the growth of the diatom Fragillaria crotonensis (Kitton) and the phytoplankton assemblage of Lake Eric to chromium. J Great Lakes Res., vol. 22, pp. 55-62.

13. Morsi H., Ebd-El-Monem, Corradi M.G. (1998) Toxicity of copper and zinc to two strains of Scenedesmus acutus having different sensitivity to chromium. Env and Exp Bot., vol. 40, pp. 59-66.

14. Ospanova A.K., Kaliyeva A.B., Anuarova L.E, Bazargaliyeva A.A., Yernazarova G.I., Ramazanova A.A., Sekenov I.E. (2017) Mildew of oleaster (Elaeagnus oxycarpa Schlecht.) registered in large industrial cities (Pavlodar, Aksu, Ekibastuz) of the Pavlodar region. Saudi J Biol Sci, in press, available at http://www.sciencedirect.com/science/article/pii/S1319562X16301152.

15. Eduardo Pérez-Rodríguez, José Aguilera, Félix L Figueroa (2003) Tissular localization of coumarins in the green alga Dasycladus vermicularis (Scopoli) Krasser: a photoprotective role. J Exp Bot., vol. 54, no. 384, pp. 1093-1100.

16. Dinesh S., Kumara Santhanama, Nandakumara P., Anantha R., Nithyac S., Dhanalakshmic P. (2016) An integrated approach. Desalination and Water Treatment, vol. 1, pp. 1-10.

17. Yernazarova G.I. (2016) Razrabotka effektivnoy mineralnoy pitatelnoy smesi dlya intensifikacii rosta diatomovih vodorosley presnovodnih vodoemov / Creation of the effective mineral nutrition medium for increasing growth of diatom algae from freshwater reservoirs. Science and Art, vol. 39, no. 4, pp. 95-103.

18. Dzhokebaeva S.A., Orazova S.B., Karpenyuk T.A., Goncharova A.V., Tsurkan Y.S., Kalbaeva A.M., Beisembaeva R.U. (2012) The use of microalgae and higher aquatic plants in the accumulation of chromium. 5th Int Symp Biosorp Bioremed. Prague, Czech Republic, pp. 9-13.

IRSTI 76.29.43

[1*]B.A. Ussipbek, [1]N.T. Ablaikhanova, [1]M.K. Murzakhmetova,
[2]V. Isachenko, [3]J.B. Ryskulova

[1]Al-Farabi Kazakh National University, Almaty, Kazakhstan
[2]University Maternal Hospital, Cologne University,Germany
[3]Clinic of ectopic fertilization "Nuray", Almaty, Kazakhstan
[*]e-mail: 119bota@gmail.com

Study of qualitative and quantitative indicators of the spermatogenesis for determination of the effectiveness of cryopreservation

Abstract: Semen or spermatozoa cryopreservation (commonly called sperm banking) is a procedure to preserve sperm cells. Semen can be used successfully indefinitely after cryopreservation and might be stored successfully over 20 years. It can be used for sperm donation where the recipient wants the treatment in a different time or place, or as a means of preserving fertility for men undergoing vasectomy or treatments that may compromise their fertility, such as chemotherapy, radiation therapy or surgery. However, before the cryopreservation, it is necessary to check the parameters of the ejaculate and treat the sperm in a special container (a small in diameter plastic box with information about the patient) to increase the concentration of spermatozoa. Put the container for storage into Dewar tube. In some cases, cryopreservation might worsen the quality of the ejaculate. After freezing, the mobility and morphology of the sperm can deteriorate. Thus, it is desirable to carry out freezing in test conditions to determine the need for the frozen material. Especially when spouses plan to use additional fertilization programs, this approach should be taken into account, since cryopreservation might cause a spontaneous change in the program of intracytoplasmic vaccination of the spouse. One of the methodological problems of cryopreservation is poor quality of the ejaculate, i.e. when freezing spermatozoa, their activity and function deteriorate from the norm. This reduces the possibility of using them in the future for artificial insemination. Results of the experiment show that cryopreservation is possible only in specialized centers with the highest professional standards.
Key words: spermatogenesis, infertility, ejaculate, cryopreservation.

Introduction

Further conservation of spermatozoa by cryopreservation method is a complex process, requiring special responsibilities and putting potential staff liabilities. It is advisable to evaluate the impediments to the researcher's work. In most cases, it is necessary to clarify the data on spermatozoa cryopreservation by evaluating the patient's psycho-emotional state. In the first place, this information may have a negative impact on the patient's psychological state [1-3].

In 1776, Spallancani, the first to maintain their mobility after dissolving spermatozoa. In the mid-nineteenth century, the idea of freezing spermatozoids was used to breed cattle. Apparently, the possibility of freezing army's sperm to allow their wives to have children when they were killed in the war began to be considered [4]. Successful fertilization and pregnancy induction for the first time with cryoconcentrated spermatozoids began in the first half of the 20th century. However, the decrease in spermatozoa concentration is not the most important factor in predicting the success of artificial insemination [5].

Cryopreservation of spermatozoids before the treatment, leading to the disorders of patients with oncological diseases, is a chance to preserve their reproductive capacity.

Ejaculators can be stored according to the following indicators:

– Potentially sterile chemotherapy and radiation therapy for malignant neoplasm and non-tumor diseases;

– Before operations that can cause a sharp decrease in men's fertility;

– The quality of ejaculate, which can lead to the appearance of azoospermia, in men with a decline in quality [6];

 Printed in Kazakhstan

– In men with non-obstructive azoospermia, the probability of separating spermatozoa using spermatozoa techniques is about 60-70% [7-12];

– Cryopreservation can also be used to preserve spermatozoids in intracytoplasmic doses in an amount that would prevent additional pairing of the super ovulation of the sperm (female);

– For insemination, the procedure is for the administration of intracytoplasmic vaccine with her sperm in the absence of a new ejaculate [13-19].

Materials and methods

60 healthy men aged 25-40 have voluntarily agreed to undertake the study by filling the special consent form. The results were obtained on three main indicators, i.e morphology, mobility, and quantitative index of sperm.Quantitative and qualitative indicators of the results of the spermogram were evaluated according to the criteria of the World Health Organization (WHO). We compared and analyzed quantitative and qualitative indicators of 3 types of environment for freezing the sperm.

The initial macroscopic evaluation of the ejaculate was performed visually under a microscope and calculated by the Laboratory Cell Calculator (Macler Method) with observation carried out in a special chamber with depth of only 10 microns (1/10 of the depth of the cell for counting blood cells) between two flat panes. With the computer method for assessing the motility of spermatozoa, the complex has the following configuration: a microscope, a television camera, a block for entering a television signal into a computer, a computer, special software. Using a television camera, a video of the movement of spermatozoa is recorded in the computer in real time. Then the computer, based on the analysis of individual frames of the video, calculates the motility of the spermatozoa.

In order to protect the frozen spermatozoa antioxidants (vitamine E), calcium ions-related substances (ethylenediaminetetraacetic acid), as well as phosphatyltillicoline (platelet activating factor) or methylxanthin were used.

Results and discussion

Men aged from 31 to 35 years old and older than 40 years were detected in order to determine the number of sperm in the ejaculate. Men were divided into three groups. In the study, the results of the difference in the number of sperm and men in the 1 mL ejaculate were shown (Figure 1).

According to the findings, the maximum concentration of sperm (56.21 million) identified in the group of men aged 31-35 years. The average value of these indicators depends on the age range of 26-30 years. They were found in men group 36-39 years and over 40 years. The concentration of spermatozoa in men aged between 26 and 30 years in 1 mL ejaculate is 55.62 million, respectively. The concentration of sperm in 1 mL of ejaculate in men between 31-35 years is 53.62 million and the concentration of sperm in 1 mL of ejaculate in the male group of 40 years is 51.65 million tons. However, as a result of the expertise, the group with the most promising concentration of spermatozoids was men under the age of 25. The mean concentration of spermatozoids in this group was 39.68 million times in 1 mL ejaculate.

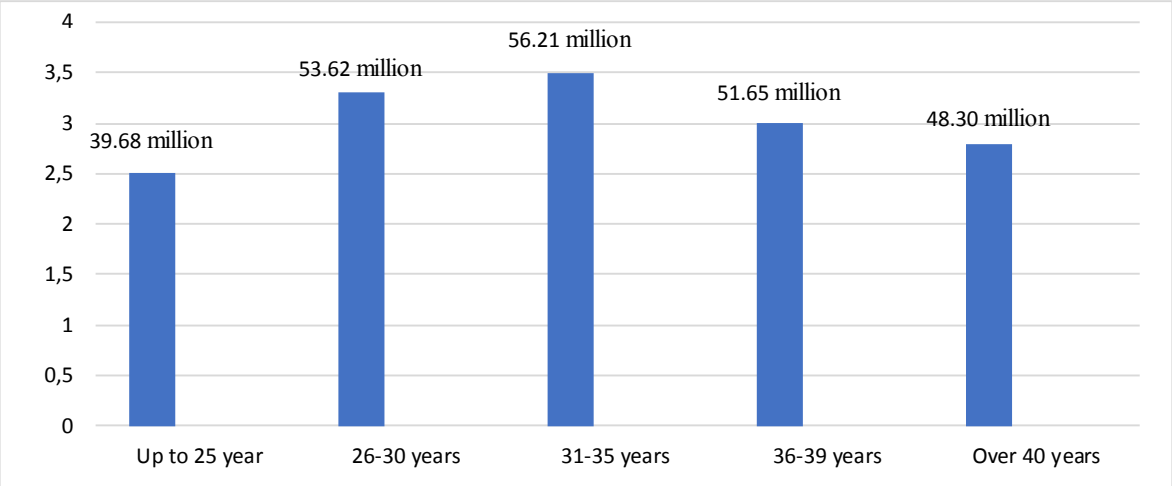

Figure 1 – The number of spermatozoids in 1 mL ejaculate of different ages of men

Similar results were obtained in the study of the share of active motion sperm in 1 mL ejaculation of men in different age groups. The best results were found in age groups between 36-39 and 31-35 (32.5% and 31.5% respectively), with a relatively small percentage of active motion spermatozoa fractions (18.4%) (Figure 2). The results of this series show that the lowest rates for sperm motions in active motion are typical for age groups up to 25 and 26-30 years (14.5% and 17.40%, respectively).

Morphologically normal spermatozoa were at lower WHO threshold levels in groups 31-35 and 36-39, respectively, and were 14.5% and 13.3%. The lowest results for the proportion of normal spermatozoa morphologically registered in the men's group over 40 years (8.6%).

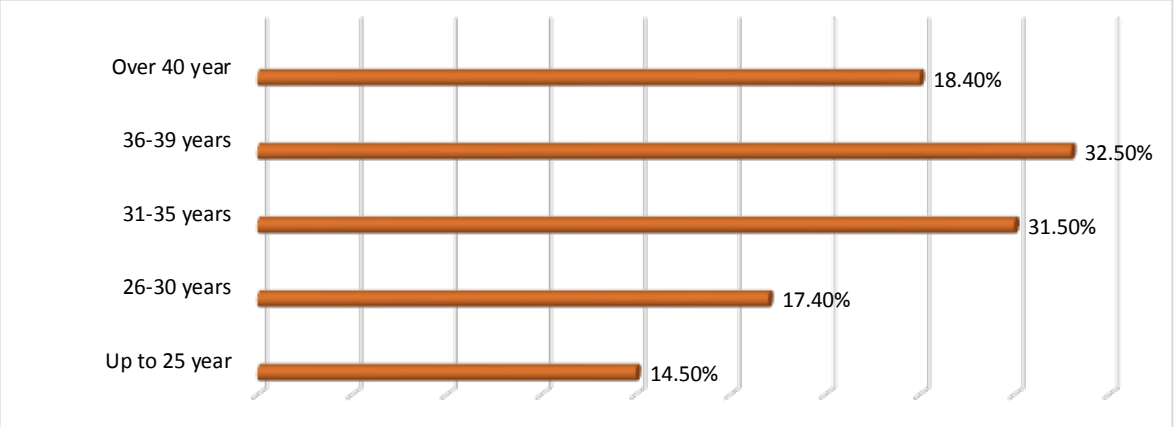

Figure 2 – The share of active motion spermatozoids in ejaculations of different ages of men

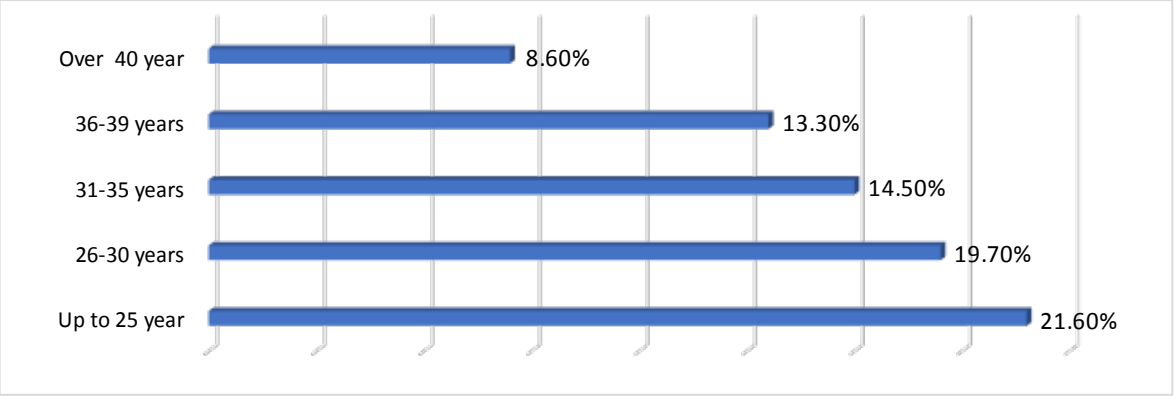

Figure 3 – Morphologically-moderate spermatozoa in ejaculations of different ages of men

In determining the morphologically-significant share of spermatozoa in the normal ejaculate, the group under 25 was the most promising group (21.6%) (Figure 3).

Comparably, the results of the group of young people between the ages of 26 and 30 were fairly high. The share of normal spermatozoa in the ejaculate in this group was 18.7%. Converting data from our study on the age-related male sperm relationships, genetic causes are the main cause of male relative malformation between 25 and 26-30 years on spermatozoa concentrations and active motion spermatozoa fraction.

The data presented show a sharp decline in the process of spermatogenic activity of male registered in the world since the second half of the twentieth century. This phenomenon is a manifestation of the daily environmental impact of the harmful factors on the human body. Many of the harmful factors (professional, natural, and domestic) can only cause

spermatogenesis only if it is sufficiently affected individually, but with long-term effects.

In order to effectively protect the human factor from the affect of spermatogenic activity, it is required to fully understand the mechanisms of their individual and joint harmful effects.

The fact that medical specialists and society pay serious attention to the problem of male spermatogenic activity only in the last decade may indicate a significant compensation stock of the reproductive system, which is observed only if the violations are only aggravated by serious cumulative effects.

In the third series of studies, quantitative and qualitative indicators were evaluated to assess the efficiency of the crusher. It was calculated using 3 types of cryoprotectors for the freezing of the obtained sperm. These analyzes have shown significant quantitative and qualitative results (Sperm Freeze – KITAZATO (Japan, 2012), Sperm Freezing – ORIGIO (Denmark, 2010), Sperm Freezing Medium – GLOBAL (Canada, 2008) (Figure 4).

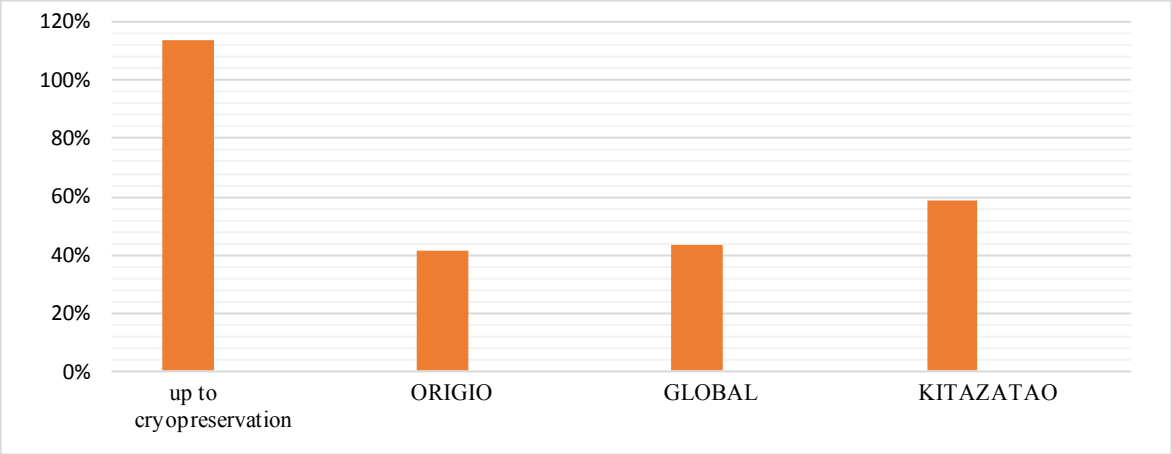

Figure 4 – Variations in quantitative indicators of spermatogenesis

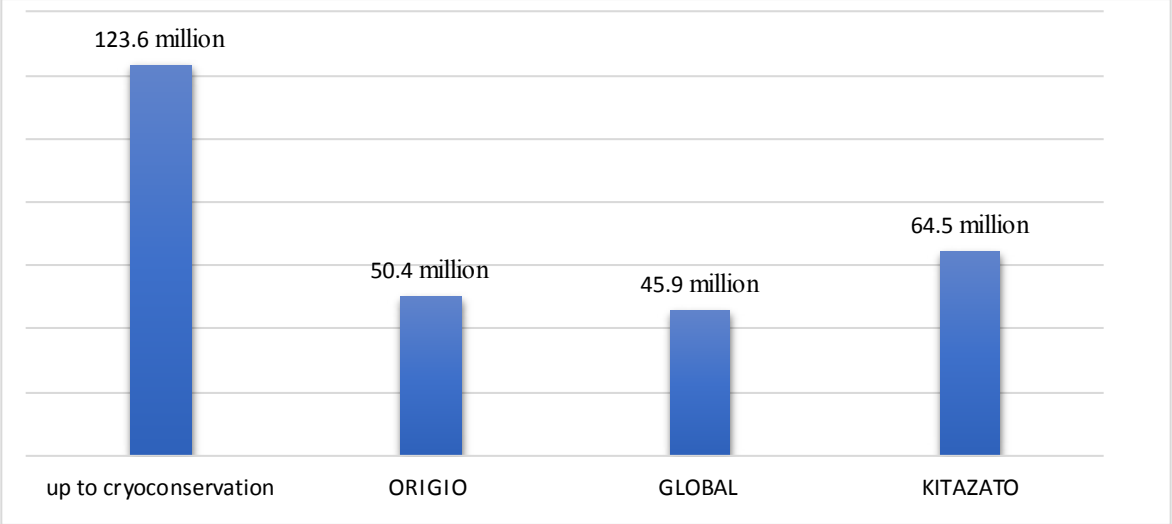

Figure 5 – Quantity of sperm in 1 mL of ejaculation and the efficacy of cryopreservation

The number of spermatozoids that are active in the total number of 60 men before cryopreservation is on the average – 114% – 123.6 million.is showed. After cryopreservation, sperm Freeze – KITAZATO – 58.8% – 64.5 million, Sperm Freezing – ORIGIO – 41.7% – 50.4 million; Sperm Freezing Medium – GLOBAL – 43.5% – 45.9 million (Figure 5).

The percentage of morphological spermatozoids in ejaculate has decreased by 73.80% compared to cryoconcentration, KITAZATO method – 54.50%, Sperm Freezing – ORIGIO-36.6%, Sperm Freezing Medium – GLOBAL method – 42.2% (Figure 6). Compared to Sperm Freeze – KITAZATO method for the freezing of sperm, 58.8% – 64.5 mL were the highest quantitative and qualitative indicators.

In addition, when the number of normal sperm motions required for fertilization is very small, their removal requires a great deal of effort and time. There is a need to keep the separated spermatozoids by cryopreservation when such risks are unlikely to occur again or physically impossible to obtain.

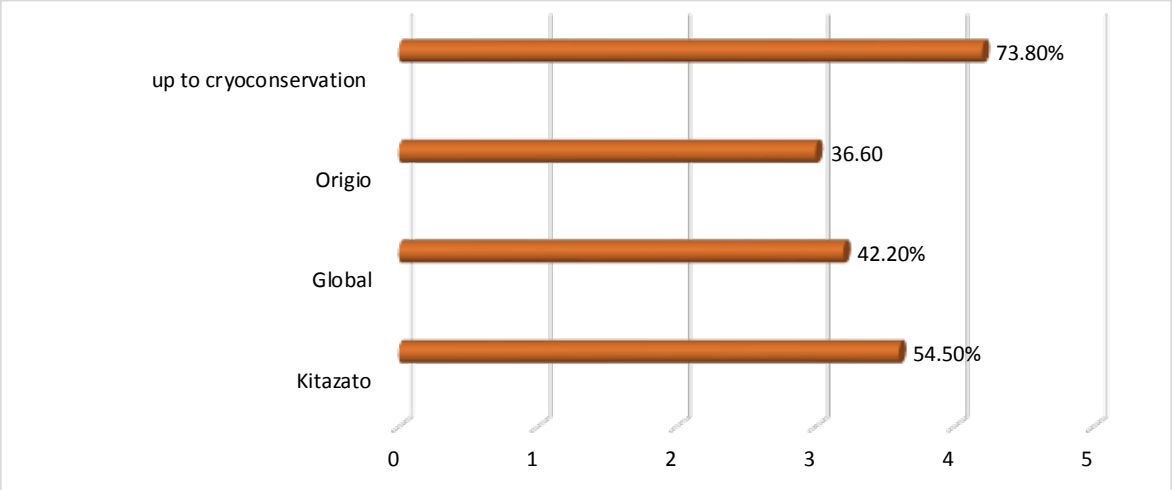

Figure 6 – Study on morphological parameters of spermatozoa ejaculate

Finally, it should be noted that the treatment of spermatozoa, which can be caused by the disorder of gonads, leads to the preservation of the ability to breed generations for patients suffering from oncological diseases. In the future, it is possible to freeze spermatozoa in patients who have been microsurgical for artificial insemination.

Conclusion

Semen or spermatozoa cryopreservation (commonly called sperm banking) can be used for sperm donation where the recipient wants the treatment in a different time or place, or as a means of preserving fertility for men undergoing vasectomy or treatments that may compromise their fertility, such as chemotherapy, radiation therapy or surgery. However, in some cases, cryopreservation might worsen the quality of the ejaculate. Thus, it is desirable to carry out freezing in test conditions to determine the need for the frozen material. One of the methodological problems of cryopreservation is poor quality of the ejaculate, i.e. when freezing spermatozoa, their activity and function deteriorate from the norm. This reduces the possibility of using them in the future for artificial insemination. Therefore, cryopreservation is possible only in specialized centers with the highest professional standards. As a result of the expertise, the group with the most promising concentration of spermatozoids was men under the age of 25. The mean concentration of spermatozoids in this group was 39.68 million times in 1 mL ejaculate. The lowest results for the proportion of normal spermatozoa morphologically registered in the men's group over 40 years (8.6%).

References

1. Fujita Y., Kubo S. (2006) Application of FTA technology to extraction of sperm DNA from mixed body fluids containing semen. *Legal Med*., vol. 8, pp. 43-47.

2. Gardner D.K., Weissman A., Howles C.M., Shoham Z. (2009) Textbook of assisted reproductive technologies laboratory and clinical perspectives. *Informa UK Ltd*., p. 944.

3. Horsman K.M., Barker S.L., Ferrance J.P., Forrest K.A., Koen K.A., Landers J.P. (2005) Separation of sperm and epithelial cells in a microfabricated device: potential application to forensic analysis of sexual assault evidence. *Anal. Chem*., vol.77, pp. 742-749.

4. Isachenko V., Alabart J.L., Dattena M., Cappai P., Nawroth F., Isachenko E., Cocero M.J., Olivera J., Roche A., Accardo C., Folch J. (2003) New technology for vitrification and field (microscope-free) thawing and transfer of the small ruminant embryos. *Theriogenology*, vol. 59, pp. 1209-1218.

5. Isachenko V., Montag M., Isachenko E., Nawroth F., Dessole S., Van der Ven H. (2004) Developmental rate and ultrastructure of vitrified human pronuclear oocytes after step-wise versus direct rehydration. *Hum Reprod*., vol.19, pp. 660-665.

6. Kuleshova L.L., Shaw J.M., Trounson A.O. (2001) Studies on replacing most of the penetrating cryoprotectant by polymers for embryo cryopreservation. *Cryobiology*, vol. 43, pp. 21-31.

7. Inyushin V.M., Chekurov P.R. (2017) Biostimulation with a laser beam and bioplasm. *Alma-Ata*, 404 p.

8. Kulakova V.I., Leonova B.V. (2016) Extracorporeal fertilization and its new directions in the treatment of female and male infertility. *M: Medicine*, p. 119.

9. Zagrebelnaya I.V. (2015) Modern aspects of pathogenesis and treatment of endocrine infertility. *Int Med J.*, vol. 1, pp. 178-196.

10. Best B.P. (2015) Cryoprotectant toxicity: facts, issues, and questions. Rejuvenation. *Res.*, vol. 18, pp. 422-436.

11. Lucena E., Bernal D.P., Lucena C. et al. (2006) Successful ongoing pregnancies after vitrification of oocytes. *Fertil Steril*., vol. 85, pp. 108-111.

12. Patist A., Zoerb H. (2005) Preservation mechanisms of trehalose in food and biosystems. *Colloids Surf. B Biointerfaces,* vol. 40, pp. 107-113.

13. Tucker M.J., Liebermann J. (2007) Vitrification in ART. *Informa UK Ltd*., p. 322.

14. Villarreal M.A., Diaz S.B., Disalvo E.A., Montich G.G. (2004) Molecular dynamics simulation study of the interaction of trehalose with lipid membranes. *Langmuir*, vol. 20, pp. 7844-7851.

15. Voorhees J.C., Ferrance J.P., Landers J.P. (2006) Enhanced elution of sperm from cottom swabs via enzymatic digestion for rape kit analysis. *J Forensic Sci*., vol. 51, pp. 574-579.

16. Saeednia S., Bahadoran H., Amidi F., Asadi M.H., Naji M., Fallahi P., Nejad N.A. (2015) Nerve growth factor in human semen: Effect of nerve growth factor on the normozoospermic men during cryopreservation process. *Iran J Basic Med Sci*., vol.18, pp. 292-299.

17. *Kopeika J., Thornhill A., Khalaf Y. (2015). The effect of cryopreservation on the genome of gametes and embryos: principles of cryobiology and critical appraisal of the evidence. Hum Repr Update., vol. 21, pp. 209-227.*

18. Patel M., Gandotra V. K., Cheema R. S., Bansal A. K., Kumar A. (2016) Seminal plasma heparin binding proteins improve semen quality by reducing oxidative stress during cryopreservation of cattle bull semen. *Asian-Austr J An Sci*., vol.29, pp. 1247-1255.

19. Thomson L.K., Fleming S.D., Barone K., Zieschang J.A., Clark A.M. The effect of repeated freezing and thawing on human sperm DNA fragmentation (2010). *Fertil Steril*, vol. 93, pp. 1147-1156.

IRSTI 31.19.29

[1*]A.B. Ibraimov, [1]M.M. Sergazina, [1]M.B. Alimzhanova, [2]M.B. Abilev

[1]Faculty of Chemistry and Chemical Technology, Al-Farabi Kazakh National University, Almaty, Kazakhstan
[2]Faculty of Chemistry, Amanzholov East Kazakhstan Government University, Ust-Kamenogorsk, Kazakhstan
[*]e-mail: a_bolatbekovich11@mail.ru

Analysis of tobacco products by chromatography methods: review

Abstract: Currently, the number of consumers of tobacco products in the world is growing rapidly. In this regard, the number of tobacco companies and varieties of tobacco is growing. Many tobacco companies write a small amount of components presented in the cigarette on the product box. But in fact, this information does not fully reflect the contents of the cigarette. This article presents methods for determining organic compounds in tobacco products, using gas chromatography-mass spectrometry, liquid chromatography, and liquid chromatography-tandem-mass spectrometry. Also the determination of heavy metals in tobacco products by extraction-absorption spectroscopy, atomic absorption spectroscopy, inversion voltammetry, inductively coupled plasma optical emission spectroscopy.
Key words: tobacco products, gas chromatography – mass spectrometry, liquid chromatography, liquid chromatography – mass spectrometry, heavy metals.

Introduction

According to the World Health Organization (WHO) reports in May 2017, about 7 million people die of cigarettes every year. More than 6 million deaths were caused by direct consumption of tobacco and more than 890,000 by tobacco smoke(passive smoking). More than 1.1 billion smokers report that 80% of them live in countries with a low or medium standard of living [1]. In June 2017, 400 people were interviewed in Almaty, among which 77% of participants reported that they do not smoke, and the remaining 23% replied oppositely. People who smoke only one box or more per day are 13%, several cigarettes a day are 8% and several cigarettes in a month are 2%. The reason for smoking cessation is that 40% of the participants refused to smoke by voluntary will, and 32% reported that their health is deteriorating, 8% are unhappy with smoking, and 6% have changed the social environment and 5% are pregnant [2]. But, despite this, the number of consumers of tobacco products has not decreased. That's why the consumption of tobacco products by residents of the 21st century causes environmental pollution.

The period of tobacco production begins mainly with the cultivation of tobacco leaves. The tobacco leaf contains nicotine and other alkaloids, proteins, amino acids, carbohydrates and fatty acids, resins, essential oils and pectin compounds. When smoking there are distinguished various chemical compounds in the atmosphere of the Earth [3]. To this end, it is important to assess the quality of tobacco products, identify toxic compounds, and investigate environmental safety through gas and liquid chromatographic methods.

Gas chromatography mass – spectrometry (GC-MS)

With the help of gas chromatography, the tobacco industry determines the water content [4], nicotine [5] in the smoke condensate (cigarette smoking can be carried out by standard or non-standard methods) [6; 7]. Also, chromatography methods help to establish the quality of tobacco products in accordance with State Standard (GOST). The analysis of residual amounts of organochlorine pesticides in tobacco products (including leaf tobacco) is also carried out using chromatographs [8].

Gas chromatography methods are widely used in the study of tobacco products:

– identification and quantification of alkaloids in tobacco products;

– quantitative determination of moisturizers in tobacco products;

– identification and quantitative determination of flavors in electronic cigarette liquids;

– identification and quantification of aromatic, carcinogenic volatile compounds in tobacco products;

– identification and quantification of toxic compounds in the tobacco filter, etc.

 Printed in Kazakhstan

By using the GC-MS method it is possible to determine the qualitative and quantitative composition of carcinogenic substances in tobacco smoke [9-11]. And as for the investigation of volatile organic substances, which are completely absorbed into the lungs of smokers, it was applied the GC-MS method [12]. British scientists have identified carbonyl compounds in tobacco smoke using GC-MS and HPLC. The GC-MS method proved to be more advantageous than HPLC [13]. Both GC-MS and HPLC methods were compared in the determination of phenolic compounds in tobacco smoke, after which the GC-MS method allowed to obtain a more precise and reliable result than HPLC. Using the GC-MS method, 24 types of phenolic derivatives in tobacco smoke were simultaneously identified, phenolic derivatives with a low concentration were also detected [14].

The gas chromatography-mass spectrometry method has a greater influence on the determination of chemical compounds in the smoke of electronic cigarettes than liquid chromatography. Scientists Goniewicz M.L, Knysak J, Gawron M having studied the smoke of 12 types of electronic cigarettes and ordinary cigarettes came to the conclusion that in tobacco smoke, 9.44 times less toxic substances [15]. Scientists Schober W, Szendrei K, Matzen W identified 7 polyaromatic hydrocarbons, propane-1-2-diol, a high amount of nicotine, carcinogenic glycerin and aluminum in the smoke of electronic cigarettes [16]. According to the authors of Schripp T, Markewitz D, Uhde E, the smoke of electronic cigarettes contains formaldehyde, acetaldehyde, isoprene, acetic acid, diacetyl, acetone, propanol, propylene glycol, diacetin (separated from flavorings), aromatic oils, nicotine [17]. By the studies of American scientists in the smoke of electronic cigarettes there are formaldehyde, acetaldehyde, propionaldehyde, acrolein, crotonaldehyde, methyl ethyl ketone, butyraldehyde, hydroquinone, resorcinol, catechol, phenol, m-cresol, p-cresol, o-cresol, 1,3-butadiene, isoprene, acrylonitrile, benzene, toluene, styrene, beryllium, cadmium, chromium, cobalt, lead, manganese, mercury, nickel, selenium, tin, N-nitrosonoricotine, N-nitrosoanatabine, N-nitrozoanabazine, 4- (methylnitrosamino) -1- (3-pyridyl) -1-butanone), 1-aminonaphthalene, 2-aminonaphthalene, 3-aminobiphenyl, 4-aminob phenyl, naphthalene, acenaphthylene, acenaphthene, ftorin, phenanthrene, anthracene, flyuranten, pyrene, benzanthracene, hrizon, benzo (b) fluoranthene, benzo (k) fluoranthene, benzo (g, h, i) perylene [18].

According to the above-mentioned study, GC and MS were able to replenish each other and demonstrated a number of advantages:

– increased separation efficiency (per connection);
– high efficiency and identification of separation;
– simultaneous identification of different samples by their nature;
– qualitative and rapid detection of various compounds (alkaloids, aromatic compounds, nitrogen compounds, etc.)

High performance liquid chromatography (HPLC)

HPLC along with GC-MS is also important in the investigation of tobacco products. The HPLC method has the following advantages:
– efficiency of separation
– high analysis speed
– highly accurate quantitative method
– high sensitivity
– lowest quantity of the sample to be penetrated.

Today, the "Cooperation Centre for Scientific Research Relative to Tobacco" has announced a residual amount and a list of 118 pesticides found in tobacco. In this connection, HPLC and LC-MS methods have a greater influence on the determination of pesticides in tobacco than GC-MS [19].

In 2016, Brazilian scientists Gabrieli Bernardi, Magali Kemmerich, Lucila C. Ribeiro, Martha B. Adaime, Renato Zanella, Osmar D. Prestes examined tobacco by HPLC and GC-MS. As a result, the HPLC method determined 55 pesticides, GC-MS method could not identify that amount of pesticides in tobacco [20].

The HPLC method and LC-MS make it possible to qualitatively and accurately determine the pesticides in tobacco products, as well as to isolate the analytes from the column well [21-25].

In 2017, scientists from the US Liqun Wang, Roberto Bravo Cardenas, Clifford Watson examined sucrose, aldose and humectants in cigarettes using HPLC. To determine the 11 types of sucrose, they used a HILIC column with a film thickness of 1.7 μm, and spent 15 minutes for sample preparation. The scientists came to the conclusion that the method is the most optimal, and by using the HILIC column all the peaks were accurately displayed, and it has a high sensitivity (1.2 ng/ml) [26].

Liquid chromatography mass – spectrometry (LC-MS)

The US "Food and Drug Administration" in 2012 introduced six primary amines to the list of especially dangerous carcinogens. This is o-toluidine, 2,6-dimethylaniline, o-anisidine, 1-naphthylamine, 2-naphthylamine and 4-aminobiphenyl. Also, the International Agency for Research on

Cancer reported that -toluidine, 2-naphthylamine, 4-aminobiphenyl lead to the development of cancer. These amines are in tobacco and while smoking they pass into tobacco smoke [27-28]. Chinese scientists using LC-MS method to determine six primary amines, concluded that this method is automated, fast, and very accurate (the sensitivity of the method is 0.04-0.58 ng / cigarette). The whole experiment was spent only 30 minutes and all 6 primary amines were determined simultaneously in the tobacco smoke [29].

The LC-MS method is most significant in the determination of amines and the mercapturic coupling of acrolein in the urine of smokers and non-smokers [30-33].

When using GC-MS and LC-MS methods, phthalates and tereflates were determined in liquids of electronic cigarettes. As a result, the LC-MS method showed a good separation for analytes such as diethyl, dibutyl, benzylbutyl, diphenyl, bis (2-ethylhexyl), di-n-octyl, diisoninyl and diisodecyl, dimethyl, bis-2-ethylhexyl. Has shown high sensitivity (100ng/ml) for the analytes. Since diphenyl, diisinyl and diisodecyl were non-volatile, they were not determined by GC-MS [34].

The LC-MS method proved to be the most suitable and allowed to obtain a more accurate and reliable result for the qualitative and quantitative determination of pyridine, 2-picoline, 4-picoline and quinoline in tobacco smoke [35].

Atomic absorption spectroscopy (AAS)

Tobacco smoke is toxic, and contains a large amount of carcinogenic substances. In the smoke there are both organic carcinogens and inorganic substances. This is cadmium, lead and other heavy metals [36]. In both tobacco and tobacco smoke, heavy metals such as Cd, Cr, Pb, Ni are found that penetrate the body through tobacco smoke [37-42]. Also tobacco smoke contains Cd and Hg, which are absorbed into the body, and lead to the development of cancer. Cd refers to the first group of carcinogenic substances, and Hg to the second [43; 44].

Table 1 – Methods for determining components in tobacco products

№	Method	Detectable component	Sample preparation	Methodological conditions	Reference
1	2	3	4	5	6
1	Extraction absorption spectroscopy	Cadmium	Tobacco was calcined in a corundum dish in a muffle furnace at a temperature of 600-700° C. Then, 5-7 ml of HNO_3 (ρ = 1.4) was added, again calcined for 10-15 minutes.	Spectrophotometer SF-16 λ = 585 nm ditch = 0.1 cm.	[50]
2	Atomic absorption spectroscopy	Heavy metal (Cu, Zn, Pb, Ag, Fe)	Samples were dried in an oven for 1 hour at a temperature of 105° C. Then 10 cm^3 of concentrated hydrochloric acid was added and the heating was continued for another 30 minutes.	Spectrometer Quantum-2A	[51]
3	Inversion voltammetry	Heavy metal (Cu, Zn, Pb, Cd, Hg)	Samples of tobacco weighing 0.2 g were collected, ashes were taken as a whole. The samples were treated with concentrated nitric acid.	Voltammeter TA-4 background electrolyte – 10 ml 0.45 M solution of formic acid	[52]
4	Inversion voltammetry	Heavy metal (Cu, Zn, Pb, Cd, Hg)	The tobacco smoke was extracted with an aqueous solution of 0.1 M formic acid	Voltammeter TA-4 background electrolyte – 10 ml 0.45 M solution of formic acid	[53]
5	Inversion voltammetry	Mercury (Hg)	The tobacco smoke was extracted with an aqueous solution of 0.1 M formic acid	Voltammeter AVA-3 background electrolyte – H_2SO_4 – 0.4 mol/l , KNO_3 – 0.1 mol/l , trilon B. – 0.001 mol/l	[53]

Continuation of table 1

№	Method	Detectable component	Sample preparation	Methodological conditions	Reference
1	2	3	4	5	6
6	Atomic absorption spectroscopy	Cadmium	The samples were dried in an oven at 80 ° C for 12 hours and allowed to cool in a desiccator. After that, it was treated, concentrated with HNO_3	Spectrophotometer UNICAM 969 λ = 228 nm	[54]
7	Atomic absorption spectroscopy	Heavy metal (Cu, Zn, Pb, Cd, Cr)	Cigarette smoke was collected in a conical flask which was filled with 50 ml of methanol and 2 drops of 1M nitric acid	Spectrometer Shimadzu 6200 graphite furnace	[55]
8	Inductively Coupled Plasma Optical Emission Spectrometry	Heavy metal (Al, Cd, Co, Cr, Mn, Ni, Pb, Sr)	1.5 g of tobacco was placed on a porcelain plate and 10 drops of 65% HNO_3 were added. The solution was then treated with 1.5% HNO_3.	Spectrometer iCAP 6300 Duo	[56]
9	Gas chromatography–mass spectrometry	Nicotine	0.1 g of the tobacco leaf powder was extracted 3 times with 5 ml of methanol and sonicated for 30 minutes.	Column: VF-5 (30 m × 0,25 mm × 0,25 μm); t_{oven}= 50 – 200°C (τ_{held}= 20 min); υ = 4°C/min; t_{oven}= 200 – 300°C; υ=10°C/min;	[57]
10	Liquid chromatography–tandem mass spectrometry	52 pesticides	2 g of ground tobacco were soaked with 6.25mL of 1% aqueous acetic acid for 5min	Column: Hydro RP-80 A (150 mm × 2,0 mm × 4μm); $t_{therm.}$=35°C; mobile phase A = methanol: water (10:90); mobile phase B = water: methanol (90:10);	[58]
11	Liquid chromatography–tandem mass spectrometry	Nitrosamines	0.5 mm of a e-cigarette liquid and 50 mL of phosphate buffer (pH 7.2) containing 0.2 g of ascorbic acid were placed in a 100-mL flask.	Column: Eclipse Plus C18 (50 mm × 2,1 mm × 1,8 μm); $t_{therm.}$=30°C; mobile phase A = 0.002% formic acid; mobile phase B = methanol;	[59]
12	Liquid chromatography-tandem mass spectrometry	Flavouring additives and nicotine	e-liquid samples were weighed in a 50 mL volumetric flask and diluted with a mixture of ACN:H_2O (1:9,v/v).	Column: Ace Ultracore Super C18 (100 mm × 2,1 mm × 0,25 μm); $t_{therm.}$=30°C; mobile phase A = water 0.05% v/v of formic acid; mobile phase B = acetonitrile 0.05% v/v of formic acid;	[60]
13	Gas chromatography–mass spectrometry	Caffeine	Tobacco from one cigarette was spiked with 10 ml of caffeine solution (100 mg/ml) and was shaken at 130 rpm by an orbital shaker in 25 ml of citrate buffer (5 mM ascorbic acid in 100 mM citrate–phosphate buffer, pH 4.5) at room temperature for 24 h.	Column: DB-5ms (30 m × 0,25 μm); $t_{oven.}$= 40°C ($\tau_{held.}$= 1 min) – 160°C ($\tau_{held.}$= 1 min); υ = 20°C/min; $t_{oven.}$= 160°C ($\tau_{held.}$= 1 min) – 200°C ($\tau_{held.}$= 1 min); υ = 4°C/min; $t_{oven.}$= 200 – 260°C ($\tau_{held.}$= 1 min); υ=15°C/min;	[61]
14	Gas chromatography–mass spectrometry	Diacetyl and acetylpropionyl	1g of each e-liquid sample was weighted into a 10ml brown flask and 500μl of internal standard was added. After that 300μl was transferred into a 10ml headspace vial to which 0.05g of sodium chloride was added.	Column: VF-5ms (60 m × 0,25 mm × 0,25 μm); $t_{oven.}$= 55°C ($\tau_{held.}$= 13 min) – 250°C; υ = 50°C/min;	[62]

Continuation of table 1

№	Method	Detectable component	Sample preparation	Methodological conditions	Reference
1	2	3	4	5	6
15	Gas chromatography–mass spectrometry	Free and bound aromatic compounds	10.0-g tobacco sample was extracted with 250 ml of dichloromethane.	Column: HP-5 (30 m × 0,25 m × 0,25 μm); $t_{oven.}$ = 40°C ($\tau_{held.}$ = 2 min) – 270°C ($\tau_{held.}$ = 10 min); υ = 2,5°C/min;	[63]
16	Gas chromatography–mass spectrometry	Glycosidically bound aroma compounds	2.0 g of dried tobacco was placed in a 100 mL cappedflask and 10μL of internal standard was added. The sample wasextracted by ultrasonic washer in twice with methanol (20 mL and 20 mL) for 30 min each..	Column: HP-5ms (60 m × 0,25 mm × 0,25 μm); $t_{oven.}$ = 60°C ($\tau_{held.}$ = 1 min) – 280°C ($\tau_{held.}$ = 5 min); υ = 2°C/min;	[64]
17	Liquid chromatography-tandem mass spectrometry	Trace amounts of nicotine	10 mg of an electronic cigarette liquid was transferred to a 10 ml flask and extracted with 50 μl of pyridoxine hydrochloride.	Column: Zorbax Eclipse XDB-C8; (150 mm × 4,6 mm × 5 μm); $t_{therm.}$=35°C; mobile phase A = acetonitrile with 0.01% of formic acid; mobile phase B= water with 10 mM of ammonium formate;	[65]
18	Gas chromatography–mass spectrometry	Humectants	4g of each tobacco product were extracted with 50 mL of methanol containing 2.0 mg/mL 1,3-butanediol and shaken for 1 hour After that extracts were filtered through Whatman 30 μm filter paper.	Column: DB-Wax (15 m × 0,53 mm × 1 μm); $t_{oven.}$ = 120°C ($\tau_{held.}$ = 2 min) – 180°C ($\tau_{held.}$ = 4 min); υ = 15°C/min;	[66]
19	Liquid chromatography	Eight polyphenols	0.25 g of tobacco powder was extracted with ultrasonic extraction for 30 min in 40 mL of methanol-water (70:30, v/v) solution and centrifuged at 10,000 rpm for 10 min.	Column: Zorbax Eclipse XDB-C18; (50 mm × 4,6 mm × 1,8 μm); $t_{therm.}$=30°C; mobile phase A = 0.01% formic acid mobile phase B= acetonitrile;	[67]
20	Gas chromatography–mass spectrometry	Benzene, toluene, ethylbenzene, and xylene	3.0 g of a 1 cm long tobacco filter was transferred to a 60 ml flask. After that, 50 ml of a 2-hexanone solution was added.	Column: TG-WaxMS (30 m × 0,25 mm × 0,25 μm); $t_{oven.}$ = 35°C ($\tau_{held.}$ = 2 min) – 100°C; υ = 15°C/min; $t_{oven.}$ = 100°C – 220°C ($\tau_{held.}$ = 3 min); υ = 20°C/min;	[68]

The atomic absorption spectroscopy method is usedto determine heavy metals in tobacco. During the research, a flame and electrothermal atomization is used. In general, a flame AAS [45; 46] and AAS with a graphite furnace [47-49] are used. After studying different literature, they came to the conclusion that AAS with a graphite furnace was the most widely applied.

In most cases, the GC-MS methodwas used for definition of organic components in tobacco products, such as nicotine, caffeine, aromatics, humectants, benzene derivatives. The GC-MS method gave a good possibility of isolating the components, as well as made it possible to determine unknown substances by their mass spectra. During the analysis, various columns were used, and all samples were dissolved in methanol. The techniques often used a gas chromatograph aglient from the United States. The method of atomic absorption spectroscopy was often used to determine heavy metals in tobacco products.

Conclusion

Chromatographic techniques for the determination of components in tobacco products were presented in this paper. The material can be used to control the quality of tobacco products in the market of Kazakhstan, as well as in the field of health and ecology.

References

1. http://www.who.int/mediacentre/factsheets/fs339/ru/

2. https://tengrinews.kz/kazakhstan_news/skolko-almatintsev-kuryat-issledovanie-322696/

3. http://www.bestreferat.ru/referat-118645.html#0

4. GOST 30622.1 – 2013. Determination of water content in the smoke condensate. Method of gas chromatography. – Enter. 2015–01–01. – M.: Standartinform, 2005. – P. 6.

5. GOST 30570 – 2015. Cigarettes. Determination of nicotine content in smoke condensate. Method of gas chromatography. – Enter. 2016–01–01. – M.: Standartinform, 2015. – P. 13.

6. GOST 31632 – 2016. Cigarettes. Sample selection. – Enter. 2017-01-01. – M.: Standartinform, 2016. – P. 19.

7. GOST 3308 – 2015. The machine is an ordinary laboratory for smoking cigarettes (smoking machine). – Enter. 2016–01–01. – M.: Standartinform, 2015. – P. 20.

8. GOST 32181 – 2013. Determination of residual amounts of organochlorine pesticides. Gas chromatography method. – Enter. 2014–07–01. – M.: Standartinform, 2014. – P. 18.

9. Noelia R., Vallecillos L., Lewis A.C., Borrull F., Marcé. M.R., Hamilton J.F. (2015) Comparative study of comprehensive gas chromatography-nitrogen chemiluminescence detection and gas chromatography-ion trap-tandem mass spectrometry for determining nicotine and carcinogen organic nitrogen compounds in third hand tobacco smoke. Journal of Chromatography A., vol. 1426, pp. 191 - 200.

10. Shi R., Yan L., Xu T., Liu D., Zhu Y., Zhou J. (2015) Graphene oxide bound silica for solid-phase extraction of 14 polycyclic aromatic hydrocarbons in mainstream cigarette smoke. Journal of Chromatography A.,vol. 1375, pp. 1 - 7.

11. Uchiyamaa S., Hayashidab H., Izub R., Inabaa Y., Nakagomeb H., Kunugita N. (2015) Determination of nicotine, tar, volatile organic compounds and carbonyls in mainstream cigarette smoke using a glass filter and absorbent cartridge followed by the two-phase/one-pot elution method with carbon disulfide and methanol. Journal of Chromatography A., vol. 1426, pp. 48 - 55.

12. Esther M., Joan O. G. (2015) A rapid method for the chromatographic analysis of volatile organic compounds in exhaled breath of tobacco cigarette and electronic cigarette smokers //Journal of Chromatography A., vol. 1410, pp. 51 - 59.

13. Pang X., Lewis A.C., Hamilton J.F. (2011) Determination of airborne carbonyls via pentafluorophenylhydrazinederivatisation by GC–MS and its comparison with HPLC method // Talanta., vol. 85, pp. 406 - 414.

14. Moldoveanu C.S., Kiser M. (2007) Gas chromatography/mass spectrometry versus liquid chromatography/fluorescence detection in the analysis of phenols in mainstream cigarette smoke. Journal of Chromatography A., vol. 1141, pp. 90 - 97.

15. Goniewicz M.L., Knysak J., Gawron M. (2014) Levels of selected carcinogens and toxicants in vapour from electronic cigarettes. Tobacco Control, vol. 23, pp. 133 - 139.

16. Schober W., Szendrei K., Matzen W. (2014) Use of electronic cigarettes (e-cigarettes) impairs indoor air qualityand increases FeNO levels of e-cigarette consumers. International Journal of Hygiene and Environmental Health, vol. 217, pp. 628 - 637.

17. Schripp T., Markewitz D., Uhde E., Salthammer T. (2013) Does e-cigarette consumption cause passive vaping. Indoor Air, vol. 1, pp. 25 - 31.

18. Tayyarah R., Long A.G. (2014) Comparison of select analytes in aerosol from e-cigarettes with smoke from conventional cigarettes and with ambient air. Regulatory Toxicology and Pharmacology. vol. 70, pp. 704 - 710.

19. Cooperation Centre for Scientific Research Relative to Tobacco. The concept and implementation of agrochemical guidance residue levels. – 2008. – Issue. 2.

20. Bernardi G., Kemmerich M., Ribeiro L.C., Adaime M.B., Zanella B., Prestes O.D. (2016) An effective method for pesticide residues determination in tobacco by GC-MS/MS and UHPLC-MS/MS employing acetonitrile extraction with low-temperature precipitation and d-SPE clean-up. Talanta, vol. 161, pp. 40 - 47.

21. .Li M., Jin Y., Li. H.F., Hashi Y., Ma Y., Lin J.M. (2015) Rapid determination of residual pesticides in tobacco by the quick, easy, cheap, effective, rugged and safe sample pretreatment method coupled with LC–MS. Journal of Separation Science, vol. 36, pp. 2522 - 2529.

22. Kwon H., Lehotay S.J., Geis-Asteggiante L. (2012) Variability of matrix effects in liquid and gas chromatography-mass spectrometry analysis of pesticide residues after QuEChERS sample preparation of different food crops. Journal of Chromatography A., vol. 1270, pp. 235 – 245.

23. Mayer-Helm B., Hofbauer., Muller J. (2008) Method development for the determination of selected pesticides on tobacco by high-performance liquid chromatography electrospray ionisation-tandem mass spectrometry. Talanta, vol. 74, pp. 1184 – 1190.

24. Ai D., Hu B., Pan L., Chen L., Liu H. (2014) Determination of 92 pesticide residues in tobacco by accelerated solvent extraction and liquid chromatography-tandem mass spectrometry. Tobacco Science & Technology, vol. 4, pp. 79 – 87.

25. Kemmerich M., Rizzetti T.M., Martins M.L., Prestes O.D., Adaime M.B., Zanella R. (2015) Optimization by central composite design of a modified QuEChERS method for extraction of pesticide multiresidue in sweet pepper and analysis by ultra-high-performance liquid chromatography-tandem mass spectrometry. Food Analytical Methods. vol. 8, pp. 728 - 739.

26. Wang L., Cardenas R.B., Watson C. (2017) An isotope dilution ultra high performance liquid chromatography-tandem mass spectrometry method for the simultaneous determination of sugars and humectants in tobacco products. Journal of Chromatography A., vol. 1514, pp. 95 – 102.

27. Irvine W.J., Saxby M.J. (1969) Steam volatile amines of Latakia tobacco leaf. Phytochemistry, vol. 8, pp. 473 – 476.

28. International Agency for Research on Cancer (IARC). (2010) IARC Monographs on the Evaluation of Carcinogenic Risk to Humans, vol. 1 – 100.

29. Bie Z., Lu W., Zhu Y., Chen Y., Ren H., Ji L. (2017) Rapid determination of six carcinogenic primary aromatic amines in mainstream cigarette smoke by two-dimensional online solid phase extraction combined with liquid chromatography tandem mass spectrometry. Journal of Chromatography A., vol. 1482, pp. 39 – 47.

30. Hongwei H.., Xiaotao Z., Yongfeng T., Gangling T., Yulan L., Qingyuan H. (2012) Development of a method for the determination of 4-(methylnitrosamino)-1-(3-pyridyl)-1-butanol in urine of nonsmokers and smokers using liquid chromatography tandem mass spectrometry. Journal of Pharmaceutical and Biomedical Analysis, vol. 63, pp. 17 - 22.

31. Yang J., Carmella S.G., Hecht S.S. (2017) Analysis of N′-nitrosonornicotine enantiomers in human urine by chiral stationary phase liquid chromatography–nanoelectrospray ionization–high resolution tandem mass spectrometry. Journal of Chromatography B., vol. 1044, pp. 127 - 131.

32. Carmella S.G., Chen M., Zarth A., Hecht S.S. (2013) High throughput liquid chromatography–tandem mass spectrometry assay for mercapturic acids of acrolein and crotonaldehyde in cigarette smokers' urine. Journal of Chromatography B., vol. 935, pp. 36 - 40.

33. Kotandeniya D., Carmella S.G., Pillsbury M.E., Hecht S.S. (2015) Combined analysis of N′-nitrosonornicotine and 4-(methylnitrosamino)-1-(3-pyridyl)-1-butanol in the urine of cigarette smokers and e-cigarette users. Journal of Chromatography B., vol. 1007, pp 121 - 126

34. Moldoveanu S.C., Yerabolu R. (2018) Critical evaluation of several techniques for the analysis of phthalates and terephthalates: Application to liquids used in electronic cigarettes. Journal of Chromatography A., vol. 1540, pp. 77 - 86.

35. Subhrakanti S., Rajib M., Ray B.C. (2010) Determination of pyridine, 2-picoline, 4-picoline and quinoline from mainstream cigarette smoke by solid-phase extraction liquid chromatography electrospray ionization tandem mass spectrometry. Journal of Chromatography A., vol. 1217, pp. 307 - 311.

36. International Agency for Research on Cancer (IARC). (1986) Tobacco Smoking. IARC Monograph, vol. 38.

37. Galazyn-Sidorczuk M., Brzóska M.M., Moniuszko-Jakoniuk J. (2008) Estimation of Polish cigarettes contamination with cadmium and lead, and exposure to these metals via smoking. Environmental Monitoring and Assessment, vol. 137, pp. 481-493.

38. Erzen I., Kragelj L. Z. (2006) Cadmium concentrations in blood in a group of male receruits in Solvenia related to smoking habits. Bulletin of Environmental Contamination and Toxicology, vol. 76, pp. 278 - 284.

39. Al-Bader A., Omu A. E., Dashti H. (1999) Chronic cadmium toxicity to sperm of heavy cigarette smokers: immunomodulation by zinc. Archives of Andrologyvol, vol. 43, pp. 135 - 140.

40. Rey M., Turcotte F., Lapointe C., Dewailly E. (1997) High blood cadmium levels are not associated with consumption of traditional food among the inuit of Nunavik. Journal of Toxicology and Environmental Health Part A, vol. 51, pp. 5 - 14.

41. Shaham J., Meltzer A., Ashkenazi R., Ribak J. (1996) Biological monitoring of exposure to cadmium, a human carcinogen, as a result of active and

passive smoking. Journal of Occupational and Environmental Medicine, vol. 38, pp. 1220 - 1228.

42. Paakko P., Anttila S., Kalliomaki P. L. (1989) Cadmium and chromium as markers of smoking in human lung tissue. Environmental Research, vol. 49, pp. 197 - 207.

43. Fowles J., Dybing E. (2003) Application of toxicological risk assessment principles to the chemical constituents of cigarette smoke. Tobacco Control, vol. 12, pp. 424 - 430.

44. International Agency for Research on Cancer (IARC) (2004). Inorganic and organic lead compounds. IARC monographs on the evaluation of carcinogenic risks to humans, vol. 87.

45. Muhammad O.A. (2014) Determination and assesment of heavy metals in tobacco sold and smoked in Palestinian Market. Thesis work.

46. Engida A.M., Chandravanshi B.S. (2017) Assessment of heavy metals in tobacco of cigarettes commonly sold in Ethiopia. Chemistry International, vol. 3, pp. 212 - 218.

47. Lazarević K., Nikolić D., Stošić L., Milutinović S., Videnović J., Bogdanović D. (2012) Determination of lead and arsenic in tobacco and cigarettes: an important issue of public health. Central European journal of public health, vol. 20, pp. 62-66.

48. Ren T., Chen X., Ge Y., Zhao L., Zhong R. (2017) Determination of heavy metals in cigarettes using high-resolution continuum source graphite furnace atomic absorption spectrometry. Analytical Method, vol. 9, p. 4033.

49. Ashraf M.W. (2012) Levels of heavy metals in popular cigarette brands and exposure to these metals via smoking. The Scientific World Journal, vol. 2012, p. 5.

50. Arstamyan Zh. M., Mkrtchyan S. V. (2009) Extraction-absorptiometric determination of cadmium by crystal violet in tobacco, milk and milk products. Proceedings of YSU, Chemistry and biology, vol. 1, pp. 29 – 33.

51. Vlasova A.S., Erokhina L.Yu. (2013) Determination of heavy metals in cigarettes. Scientific community of students of the XXI century. Natural Sciences, vol. 9, pp. 18 - 23.

52. Matveiko N. P., Braikova A. M., Sadovsky V. V. (2014) Determination of heavy metals in tobacco cigarettes and its combustion products. Bulletin of the Belarusian State Economic University, vol. 3, pp. 65 - 70.

53. Matveiko N. P., Braikova A. M., Sadovsky V. V. (2014) The content of heavy metals in cigarette smoke. Bulletin Vitebsk State Technological University, vol. 27, pp. 146 - 152.

54. Nnorom I. C., Osibanjo O., Oji-Nnorom C. G. (2005) Cadmium determination in cigarettes available in Nigeria. African Journal of Biotechnology. vol. 4, pp. 1128 – 1132.

55. Omari M.O., Kibet J.K., Cherutoi J.K., Bosire J.O., Rono N.K. (2015) Heavy metal content in mainstream cigarette smoke of common cigarettes sold in kenya, and their toxicological consequences. International Research Journal of Environment Sciences, vol. 4, pp. 75 – 79.

56. Armendáriz C.R, Garcia T., Soler A., Fernández A.J.G., Glez-Weller. D., González G.L., Torre A.H., Gironés C.R. (2015) Heavy metals in cigarettes for sale in Spain. Environmental Research, vol. 143, pp. 162 – 169.

57. Hossain A.M., Salehuddin S.M. (2015) Analytical determination of nicotine in tobacco leaves by gas chromatography–mass spectrometry. Arabian Journal of Chemistry, vol. 6, pp. 275 – 278.

58. Mayer-Helm B. (2009) Method development for the determination of 52 pesticides in tobacco by liquidchromatography–tandem mass spectrometry. Journal of Chromatography A., vol. 1216, pp. 8953 – 8959.

59. Hyun-Ji K., Ho-Sang S. (2013) Determination of tobacco-specific nitrosamines in replacement liquids of electronic cigarettes by liquid chromatography–tandem mass spectrometry. Journal of Chromatography A., vol. 1291, pp. 48 – 55.

60. Aszyk J., Kubica P., Kot-Wasik A., Namie´snik J., Wasik A. (2017) Comprehensive determination of flavouring additives and nicotine inecigarette refill solutions. Part I: Liquid chromatography-tandemmass spectrometry analysis. Journal of Chromatography A., vol. 1519, pp. 45 – 54.

61. Siqing S., David L. A. (1998) Sample purification for the analysis of caffeine in tobacco by gas chromatography–mass spectrometry. Journal of Chromatography A., vol. 814, pp. 171 – 180.

62. Barhdadi S., Canfyn M., Courselle P., Rogiers V., Vanhaecke T., Deconinck E. (2017) Development and validation of ahs/gc-ms method for the simultaneous analysis of diacetyl and acetylpropionyl in e-lectronic cigarette refills. Journal of Pharmaceutical and Biomedical Analysis, vol. 142, pp. 218-224.

63. Jibao C., Baizhan L., Ping L., Qingde S. (2002) Analysis of free and bound volatiles by gas chromatography and gas chromatography–mass spectrometry in uncased and cased tobaccos. Journal of Chromatography A., vol. 947, pp. 267 – 275.

64. Kai C., Zhangmin X., Wenjie P., Huina Zh., Zhu R., Bo L., Zhaoliang G. (2013) Identification

and quantitation of glycosidically bound aroma compounds in three tobacco types by gas chromatography–mass spectrometry. Journal of Chromatography A., vol. 1311, pp. 149 – 156.

65. Kubica P., Kot-Wasik A., Wasik A., Namie´snik J. (2013) "Dilute & Shoot" approach for rapid determination of trace amounts of nicotine in zero-level e-liquids by reversed phase liquid chromatography and hydrophilic interactions liquid chromatography coupled with tandem mass spectrometry-electrospray ionization. Journal of Chromatography A., vol. 1289, pp. 13 – 18.

66. . Rainey C.L., Shifflett J.R., Goodpaster J.V., Bezabeh D.Z. (2013) Quantitative analysis of humectants in tobacco products using gas chromatography (GC) with simultaneous mass spectrometry (MSD) and flame ionization detection (FID). Beiträge zur Tabak forschung International/Contributions to Tobacco Research, vol. 25, pp. 576 – 585.

67. Fuwei X., Ajuan Y., Dengke H., Huimin L., Li D., Shusheng Zh. (2011) Rapid and sensitive analysis of eight polyphenols in tobacco by rapid resolution liquid chromatography. American Journal of Analytical Chemistry, vol. 2, pp. 929 – 933.

68. Zhang X., Yu Ch., Liang L., Hans-Joachim H. (2014) Determination of BTEX in cigarette filter fibers using gc-ms with automated calibration. Handbook of GC-MS, vol. 3, pp. 491 – 493.

IRSTI 31.19.29

[1]A.M. Tuiebayeva, [2]M.M. Sergazina, [1*]M.B. Alimzhanova,
[3]Zh.S. Mukataeva

[1]Al-Farabi Kazakh National University, Almaty, Kazakhstan
[2]Center of Physico-Chemical Methods of Research and Analysis, Almaty, Kazakhstan
[3]Abai Kazakh National Pedagogical University, Almaty, Kazakhstan
[*]e-mail: mukhamiedinkyzy@mail.ru

Determination of the chemical composition of tea by modern physico-chemical methods: a review

Abstract. Tea is internationally one of the most favored and inexpensive beverages, next only to water. More than three billion cups of tea are consumed daily worldwide and considered to be a part of the huge beverage market, not to be seen in isolation just as a 'commodity'. Tea active ingredients are of interest to functional foods markets. Tea is a complex substance, which consists of many components and composition of tea has been researched in a wide range in the last few years. Most of the studies were performed by using chromatography methods. The review presents a summary of the latest information concerning the chemical composition of large variety of tea by different chromatographic methods, which has not previously been reviewed. Qualitative and quantitative analyses of volatile compounds, that contribute to flavor and aroma in tea composition were executed by gas chromatography (GC) and gas chromatography-mass spectrometry (GC/MS). Low volatility organic compounds were carried out by using high-performance liquid chromatography (HPLC) methods and GC/MS. Determination of catechins and coffein in different types of tea (green, black, oolong, pu-erh) were investigated by HPLC of the most current published researches. Exploration of tea chemical composition helps in evaluating its quality and helps to control and manage its growing, processing and storage conditions. Consequently, evaluation of tea quality does not only depend on subjective organoleptic appraisement, but also on objective physical and chemical methods with additional determination of tea components most beneficial to human health. The findings of this review are meaningful for the production of healthier teas and to help increase nutritional value of tea, ameliorate quality by supplying through developing of the growing, processing, and storage conditions.

Key words: tea, chemical composition, catechin, high-performance liquid chromatography, gas chromatography.

Introduction

Tea is the most widely consumed, popular beverage in the world next to water and prepared from Camellia sinensis plant. Composition of tea consists large amount of compounds, that significantly affect to human organism [1-2]. Tea is obtained by special treatment of evergreen tea tree leaves of Camellia sinensis. It has a very complex composition and tea leaves contain thousands of chemical compounds. Tea is typically divided into six subdivisions or types: white, green, yellow, oolong, black teas. The composition of ready-made tea depends on the origin, quality and types of fermentation. The main constituents of tea are catechins, hydroxyaromatic acids, flavonols, teaflavine, theogallins, pigments, alkaloids, sugars, amino acids, vitamins, dicarboxylic acids, cations, metal, and etc. [3].

Tea takes off fatigue and dizziness, enhances mental and physical activity, stimulates the brain, heart and breathing. Biological valuable substances in tea have a positive effect on the human body, creating a single complex. It also releases harmful substances (heavy metals, radionuclides) from the body through adsorption. The compounds of biological value in tea affect the counteracting effects on the metabolism of fats and cholesterol [5-6]. The benefits of tea, which we mentioned above, only apply to high-quality and properly maintained types of tea. And the tea we consume daily is not of high quality. Currently in our country there are 11 companies that supply tea. Due to the lack of production of tea in the country

 Printed in Kazakhstan

will be purchased about 2,500 tons of raw materials from abroad annually. The countries that import tea to Kazakhstan are India, Kenya and Russia. Almost all kinds of tea are imported from abroad and must be checked for compliance with standard requirements. Most people do not care about harmful substances contained in low-quality beverages, and consume them in large quantities. The most useful green tea become harmful and not healthy if it is made from poor quality raw materials and is not well processed. Proper collection of high quality raw materials ensures that the consumer receives the highest quality products. While collecting tea leaves, only top of the leaves is collected, leaves at the bottom are solid and can not be used as food. But over the past decades they are also being gathered. Tea of poor quality leaves is sold to third countries. Unfortunately, it is impossible to purchase tea from the best leaves in our country. A high price is not a measure of quality, on the contrary can be a source of substandard product sales at very high prices. An important part of tea leaves, as well as in finished tea, is a phenolic compound or called tannin. They not only reveal organoleptic qualities, but also show the physiological value of the drink. There are an approximately 30 000 polyphenolic compounds in tea, flavonoids are conceivably the most important group of polyphenols in tea and are the source of the many health claims surrounding tea, and specifically tea antioxidants [7; 8]. The most common flavonoids in the group are flavanols (or flavan-3-ols). Flavanoids are also referred tannins, and during oxidation are changed to theaflavins and thearubigins–the compounds responsible for the dark color and strong flavors notably present in black teas. The major flavanols in tea are: catechin, epicatechin, epicatechin gallate, gallocatechin, epigallocatechin, and epigallocatechin gallate [9-12]. Conventional tea brands have been shown to contain high levels of toxic substances such as fluoride and pesticides. Tea plants are capable of assembling large amounts of F in their mature leaves when grown on soils containing normal F concentrations, without showing toxicity symptoms. Therefore, older leaves contain a high content of fluorine, by contrast the amount of antioxidants, which increase its healing properties, decrease [13-16]. Low-priced tea products are made from such old tea leaves. It is known that a high content of fluoride in the human body can damage the bone, teeth and kidneys. Many tea leaves are not washed after leaf harvesting, thus pesticides remain in tea [17-19]. Also anthraquinone has been found in the composition of tea, which is used to protect tea plantation from birds. It was established that tea contains heavy metals such as Al, As, Pb, Cd. These metals can penetrate into tea from contaminated soil and depending on their concentrations, can have a wide range of effects on the human body.

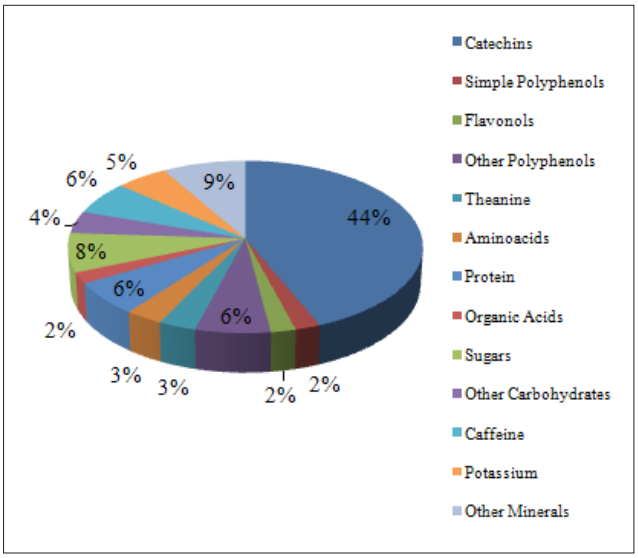

Figure 1 – The chart of chemical composition of tea [4]

Determination of some tea components, group of phenolic compounds – tannin and caffeine according with government standards, the method based on GOST 19885-74 allows to determine in the presence of an indoxin indicator, with an oxidizer potassium permanganate. In the caffeine separation process, the material is pretreated with an aqueous ammonia solution and then heated and separated with chloroform [20]. A method for determining caffeine with HPLC from tea is also shown in GOST 10727-2013. From tea samples, caffeine is extracted with water in the presence of magnesium oxide and filtered, then determined by HPLC method equipped with an ultraviolet detector [21].

Methods

High-performance liquid chromatography

High-performance liquid chromatography or high-pressure liquid chromatography is a perspective analytical version of modern classical colonial chromatographic devices. HPLC can simultaneously detect complex samples in components, detect several components and measure the concentration of one or

more compounds (depending on the specific analytical task and standard samples). The HPLC method is used in ecological quantitative chemical analysis, sanitary-hygienic and veterinary studies, control and certification of food products and agricultural products, medicine, pharmaceutics, petrochemistry and criminology. The determination of phenolic compounds in green tea was carried out by HPLC in less than 3 minutes by rapid gradient separation. Rapid chromatographic separation was used to determine the phenolic compound and catechins in green tea and tea infusions prepared by hot water at temperatures, respectively at 90 °C, 80 °C and 70 °C, and the influence of temperature on the reduction of the main compounds in tea was examined. Together with an HPLC/MS analysis, the antioxidant capacity and total polyphenol content were measured using spectrophotometric techniques. However, the spectrophotometric techniques did not expose the degradation of catechins during staying of infusion probably due to significant antioxidant properties of degradation products [22]. Advanced glycation end products such as N-ε-(carboxymethyl)lysine (CML) and N-ε-(carboxyethyl)lysine (CEL) in tea and tea infusions were determined by liquid chromatography-tandem mass spectrometry and the data showed that the levels of CML and CEL are related to the manufacturing processes. Withering, fermentation (oxidation), and pile fermentation may facilitate the formation of CML and CEL [23]. Caffeine and catechins in tea were absorbed by a montmorillonite clay mineral adsorbent, then the concentration was determined by HPLC. This work presented that the montmorillonite adsorbent is good for caffeine and is not effective for catechin [24]. Also caffeine and catechins were allocated by sequential supercritical fluid extraction and then the concentration was determined by HPLC. The experiment was conducted at different times, pressure, temperatures, and method was optimized. However, it is not good for caffein extraction from tea waste, but more promising for extraction of catechins [25]. Theophylline imprinted monolithic columns were designed and prepared for rapid separation of a homologous series of xanthine derivatives, caffeine, and theophylline by an in situ thermal-initiated copolymerization technique. Caffeine and theophylline were fully separated both under isocratic and gradient elutions on this kind of monolithic molecularly imprinted polymers column. Separation characteristic of monolithic MIP column was performed with a HPLC system [26]. The determination of putative chemical interactions between the milk fat globule membrane and green tea catechins was provided. In this study catechin concentrations were measured (in triplicate) by HPLC on a system equipped with a diode array detector [27]. more than 30 phenolics in tea were described by high-performance liquid chromatography-mass spectrometry methods for the rapid and routine analysis. Green and black tea infusions were injected directly onto a reversed phase HPLC column, and the phenolics eluted using two different mobile phase gradients, one optimized to resolve catechin derivatives and the other, flavonols and theaflavins [28]. 16 tea pesticides were found by the method based on matrix solid phase dispersion coupled with liquid chromatography-tandem mass spectrometry was established for the determination and the quantification of 16 pesticides in various tea [29]. Amino acids were also determined by high performance liquid chromatography with ultraviolet radiation for the rapid extraction of amino acids from tea. An accurate HPLC-UV method after derivatization using 9-fluorenylmethyloxycarbonyl chloride has been developed, validated and used to accurately and simultaneously determine 19 amino acids [30]. Green tea polyphenols extraction yield was determined using different extraction times from 10 to 60 min at 70°C, and also at different temperatures from 50°C to 100°C, keeping the extraction time constant. Also the aroma composition of different green tea samples was compared using the SPME/GC headspace methodology [31]. The effect of saccharides on sediment formation in green tea concentrate was investigated. The results show that the amount of tea sediment significantly decreased with the addition of fructose or sucrose and that the ratios of polyphenols and caffeine in the sediment sharply decreased while the proportion of total sugars markedly increased in the sediment [32].

Gas chromatography

Gas chromatography is used to separate several organic and inorganic gas mixtures, a very small number of components from the mixture can be detected and extracted. Due to the automation of the method and the shorter analysis time, gas chromatography is widely used in the continuous process in the chemical and petrochemical industries. Gas chromatography is also used in medicine, biochemistry, agrochemistry, geology, pharmacology, food production. Tea contains a large amount of volatile aromatic compounds, and the most effective way to detect these compounds are gas chromatography methods.

Phthalate esters (PAE), a group of environmental pollutants, in teas and tea infusions were quantitatively determined by a modified simultaneous distillation extraction (SDE) coupled with gas chromatography–mass spectrometry. SDE was employed as the proper extraction method for PAEs from tea samples and the extraction conditions had been optimized [33]. First information concerning (E)-nerolidol formation in tea leaves and (E)-nerolidol accumulation in oolong tea was provided [34]. A novel approach for the quantitative determination of nerolidol in teas has been developed using a headspace solid phase microextraction and a gas chromatography-flame ionization detector. The experimental parameters relating to the extraction efficiency of the HS-SPME such as fibre types, extraction temperature, extraction time, stirring rate were investigated and optimized [35]. Potent odorants in roasted stem tea was determined by using GC/MS and gas chromatography-olfactometry with aroma extract dilution analysis [36]. Various instant teas produced differently from black tea were compared for their differences in volatile compounds as well as descriptive sensory analysis. Volatile compounds in tea samples were analysed by HS/GC/MS [37]. Aroma compounds from the tea infusions were detected and quantified using HS-SPME coupled with GC/MS. Sensory evaluation was also made for characteristic tea flavor [38]. Volatile collection, identification and quantification were conducted using headspace solid-phase microextraction coupled with GC/MS with some minor modifications [39].

This method is a simple method of detecting vitamin K in green tea using SPME and a flame ionizing detector with a small amount of solvent and fast results. The best analytical conditions were obtained using polydimethylsiloxane fiber [40]. Also analysis of green tea aroma compounds has been performed using the SPME/GC methodology, on a polydimethylsiloxane-coated fibre [31]. Two extraction methods, namely, solid-phase microextraction (SPME) and simultaneous distillation–extraction both followed by gas chromatography–mass spectrometry were applied for the determination of a wide range of volatile compounds in pu-erh tea. The conditions of solid-phase microextraction including fiber selections and sampling condition optimization have been previously investigated. Qualitative and quantitative differences of pu-erh tea volatile profiles were observed by applying the two aforementioned extraction methods. SDE technique achieved higher percentages of high molecular weight alcohols, acids, and esters of low volatility, whereas SPME technique was found useful for analyzing low molecular weight alcohols, methoxy-phenolic compounds, aldehydes, ketones, and hydrocarbons of high volatility that were closely related to the characteristics of pu-erh tea aroma and its sensory perception. Therefore, SPME technique was a reliable extraction method for controlling pu-erh tea quality flavor [41]. A novel strategy for objective discrimination/classification of oolong tea varieties, based on potential volatile compounds analysed by HSSPME/ GC/MS was developed. [42]. Volatile compounds from Pu-erh tea were extracted using a headspace-solid phase microextraction (HS-SPME), and analysed with a GC/MS and a gas chromatography olfactometry. The most abundant aroma components in Pu-erh tea are 1,2,3-trimethoxybenzene, followed by a-terpineol, 1,2-dimethoxybenzene and linalool oxide II in order [43]. A method for determining eight pesticide residues in made green tea as well as a tea infusion (under various brewing water temperatures: 60, 80, and 100ºC) using gas chromatography (GC) microelectron capture detector was developed and validated. The extraction method adopted the relatively commonly used approach of solid sample hydration, with the green tea hydrated before being extracted through salting out with acetonitrile followed by a cleanup procedure. The analytes were confirmed using GC-coupled to tandem mass spectrometry (GC/MS/MS) with a triple quadrupole [44]. A method for analysis of 101 pesticide residues in tea leaves was developed and validated for the firsttime. Pure acetonitrile was used as extraction solvent rather than acetonitrile after matrix hydration basedon the amount of co-extracts and recoveries performance [45]. Linalool is a major volatile component of tea aroma was determined. A method based on HS-SPME combined with chiral GC wasdeveloped to determine R-(−)- and S-(+)-linalool in teas for thefirst time. To optimize the technique, the effects of various parameters on the extraction efficiency were studied comprehensively;the best extraction conditions were as follows: HS-SPME fiber, Car-boxen/divinylbenzene/polydimethylsiloxane CAR–DVB–PDMS, extraction time, 60 min; extractiontemperature, 60◦C. Under optimal conditions, the method showed satis-factory linearity, repeatability, detection limits, and recoveries [46].

Table

№	Analyte	Sample preparation	Equipment	Link to reference
1	Catechins	The extracts were prepared from one 1 g of tea bag + 200 ml hot water at: 70°C, 80°C, 90°C. The leaching time: 4 min.	HPLC/MS Column: C18, 50 mm x 2.1 mm x 2 μm; 40°C Solvents: 0.1% HCOOH in water + 0.1% HCOOH in methanol UV/VIS spectrophotometer 750 nm	22
2	N^{ε}-(carboxymethyl) lysine and N^{ε}-(carboxyethyl) lysine	40 mg of sample + n-hexane. Centrifuged at 5000g, 10 min and the n-hexane layer was removed. The residue was dried with N_2 and reduced overnight at 4 °C in a mixture of 1.5 mL of sodium borate buffer (0.2 M, pH 9.2) and 1 mL of sodium borohydride (1.0 M in 0.1 M NaOH).	LC–MS/MS Column: 2.1 x 100 mm, 3.5 μm; 35°C. Solvents:Acetonitrile+5 mM NFPA in Ultrapure water.	23
3	Caffeine, catechins	100 g of sample + 1000 mL water at 80°C extracted for 8 min.160-2000 mg of montmorillonite or 32-200mg of activated carbon was added to 40 mL of the diluted green tea extract. Suspension was centrifuged 10 min, and filtered.	HPLC Column: C18, 4.6 mm × 150 mm, 3 μm; 40 °C Solvents: water+acetonitrile+phosphoric acid and water+methanola+cetonitrile+ phosphoric acid+methanol+acetonitrile+ phosphoric acid	24
4	Caffeine, catechins	10 g of sample was placed in supercritical fluid extraction vessel (10, 20, 25, 30 MPa), (30, 40, 50, 60 °C) and extraction periods (1, 2, 3, 5 h) Supercritical CO_2 fluid contained different amount of ethanol as modifier (0.2; 0.3; 0.4 and 0.5 mL/min. flow rate) in 10 g/min.	HPLC Column: C18 5 mm, 4.6×250 mm; 35 °C Solvents :water+DMF-methanolacetic acid mixture, 20:1:0.5	25
5	Caffeine, theophylline	5g of green tea was extracted by 150mL doubly distilled water at 50 ◦C, 8 h. The obtained extraction was filtered with 0.2 mm,25mmsyringe filter, then it was stored in 4 °C for further work.	HPLC Column: 150mm×4.0mm	26
6	Catechins	Centrifugation of raw milk at 1030xg, 10 min, and 20 °. The raw cream was then washed three times with deionized water for 10 min, at 20 °C	HPLC Solvents: 0.1% trifluoroacetic acid in deionized water + methanol.	27
7	Catechins, flavonols, theaflavins	18 mL of boiling water + 1 g of leaves. After 3min, the brew was filtered to remove particulate matter prior to analysis of the filtrate.	HPLC Column: C12, 4 μm 250 mm×4.6 mm; 40 °C	28
8	16 pesticides	0.5 g tea +100μL 2μg/g TPP, D6-dimethoate, D10-chlorpyrifos and D6-trans-cypermethrin in methanol. Homogenized with a pestle with 0.75 g C18 and 0.75 g FLS for 5 min to obtain a homogeneous mixture.	LC–MS/MS Column: C18100 mm×2.1 mm Solvents : water+10 mmol/L ammonium acetate and methanol	29
9	Amino acids	100 mL boiling water + 1 g sample. Tea was brewed for 10 min on a magnetic stirrer and then filtered. For steeping time experiments, 1 g of ungrounded tea leaves was brewed up in 100 mL of hot water (90 °C) for 30, 60, 90, 120, 180, 240 and 300 s.	HPLC Column: C18, 2.6 μm, 100×2.10 mm, 100 A°, C18 pre-column 4×2 mm Solvents :M sodium acetate buffer 0.1 M + ACN/H2O (80:20, v/v)	30

Table continuation

№	Analyte	Sample preparation	Equipment	Link to reference
10	Catechins, aroma compounds	1 g of dried leaves was extracted with 20 ml of water at 70°C for 40 min. 100 mg of green tea was dissolved in 10 ml of hot water (70°C), and methylxanthines and pigments were extracted with 10 ml of chloroform.	HPLC Column: C18,4 μm 3.9 mm x 15 cm 2±3 μm 4.6 mm × 10 cm 35°C GC/MS Column: 25 m × 0.32 mm x 0.52 μm	31
11	Polyphenols, total sugar, catechins and caffeine	Green tea powder+ distilled water at 60 °C. Sugar (maltose, glucose, sucrose, or fructose) was added to the tea concentrate to a given concentration under magnetic stirring.	HPLC Column: C18, 250×4.6 mm 5 μm; 40 °C. Solvents: acetonitrile+acetic acid+water and acetonitrile+acetic acid+water	32
12	Phthalates	10 g sample + 500 mL ultrapure water at 100°C. After 5 min of infusion, the solution was filtered through a stainless steel filter.	GC/MS Column: 60 m × 0.32 mm x 0.25 μm	33
13	(E)-nerolidol	1 g of tea leaves were extracted with 4 mL of CH_2Cl_2 containing 5 nmol of ethyl ndecanoate as an internal standard for 8 h under dark condition. Then the solution was filtered.	GC/MS Column: 30 m × 0.25 mm × 0.25 μm	34
14	Nerolidol	Ground tea powder + 20 mL boiled. Commercial SPME fibres were used in the extraction.	HS-SPME–GC Column: 30 m × 0.25 mm x 0.25 μm	35
15	Odorants, amino acids and catechins	260 mL boiling distilled water +6 g of sample. After standing for 45 s, the mixture was filtered.	HPLC/MS Column: C18, 250 x 4.6 mm, 5 μm Solvents: 0.1% formic acid+water tetrahydro furan and acetonitrile.	36
16	Volatile Compounds	The operational conditions for continuous extractor were as follows: water inlet temperature (80-85°C), jacket temperature (80-85 ºC), tea feed rate (12 kg/h), water feed rate (42 L/h), and the slope of the extractor (3-5°).	HS/GC/MS Column: 60 m × 0.25 mm × 0.25 μm	37
17	Volatile Compounds	3 g tea + 150 mL distilled water for 5 min. By using a sieve, infused leaves were removed and tea infusions were transferred to glasses.	GC/MS Column:30m × 0.25 mm × 0.25 mm	38
18	Volatile Compounds	3 g tea + 150 mL distilled water for 5 min. By using a sieve, infused leaves were removed and tea infusions were transferred to glasses.	HPLC Column: C18, 5 μm × 4.6 mm × 250 mm Solvents: ethanoic acid+water and acetonitrile Column: 30 m x 0.25 mm x 0.25 μm	39
19	Vitamin K	1.5 g tea leaf + 250 mL of boiling bidistilleddeionized water. Then defined for 10 min. After this period, the tea infusions were filtered.	SPME–GC-FID	40
20	Volatile compounds	4 g pu-erh tea+4.8 g NaCl+16 mL of distilled water + a magnetic rotor into a 100 mL vial sealed with silicone septa, which was incubated at 60 °C.	GC/MS Column: 60 × 0.32 mm, 0.25 μm	41
21	Volatile compounds	10 g of dry tea sample was transferred to a 100 ml glass septum flask, and SPME fibre coated with 65 lmpolydimethylsiloxane/ divinylbenzene was rapidly inserted into the headspace of the flask.	GC/MS Column: 30 m × 0.25 mm × 0.25 μm	42
22	Volatile compounds	10.00 g of tea+ 30 ml boiling water, the vial was sealed with tetrafluoroethylene and immediately kept at 60°C to equilibrate for 5 min in a water bath.	GC/MS Column: 0.25 mm 0.25 μm	43

Table continuation

№	Analyte	Sample preparation	Equipment	Link to reference
23	8 pesticides	A 20 g samples + 20 ml of water. After 2 h, acetonitrile was added and the samples were homogenized at 10,000 rpm for 5 min. +20 g sodium chloride and shaken for 30 min. Then was centrifuged for 10 min at 3000 rpm.	GC/MS/MS Column: 30 m×0.25 mm	44
24	101 pesticides	5 g + 20 ml MeCN. The solution was then vortexed for 1 min. 4 g anhy-drous $MgSO_4$, 1 g NaCl, 1 g tri-sodium citrate dehydrate and disodium hydrogencitrate sesquihydrate was added, and the tube was vortexed to prevent coagulation of $MgSO_4$ for 1 min.	GC/MS/MS Column: 30 m × 0.25 mm x 0.25mm	45
25	Linalool	1 g of tea + 6 mL of boiling water + 10 μL of ethyl decanoate(0.2 mg/mL, IS). The vial was immediately placed in a water bath to equilibrate for 5 min at 60°C.	GC Column: 30 m × 0.25 mm × 0.12 μm	46
26	Polyphenols	0.5 g of tea + 50 ml of mineral water at 90°C and gently agitating under magnetic stirring for 7 min. Infusions were then filtered (43–38 lm) and diluted.	ABTS [2,20-azinobis-(3 ethylbenzothiazoline-6-sulphonic acid) diammonium salt] assay DMPD (N,N-dimethylp-phenylenediami nedihydrochloride)	47
27	As, Cd, Cr, Cu, Hg, Fe, Pb, Mn, Zn.	0.5 g samples were microwave-digested for 30 min in a closed quartz vessel with 4 mL of HNO_3, 2 mL of H_2O_2 and 1 mL of HCl mixture. The digested solution (7 ml) was then transferred to a 10 mL decontaminated tube for its later analysis.	Analyst 800 atomic absorption spectrometer	48
28	Polyphenols	2 g of sample + 100 ml boiling water and was filtered after1 min. using filter paper. 2 g tea + 4 g sugar +100 ml boiling water and boiling was continued for 2 min.	1,1-diphenyl-2-picryl hydrazyl radical (DPPH) used widely to evaluate the free radical scavenging ability of various extracts	49
29	Polyphenols	For sample preparations, dilutions of the samples were carried out using deionized water and phosphate buffer (50 mM, pH 6.8) for reconstituted milk (RS) and casein (Cn), respectively.	The fluorescent probe binding method (fluorimetry analysis) and isothermal titration calorimetry (ITC) analysis	50
30	Fluorine	2000-mg sample +200 ml deionized water, boiled for 15 min, filtered after cooling. An ion-selective electrode measured the fluorine content in the four filtrates separately with the standard curve method.	Ion-selective electrode standard curve technique	51
31	Mg, Ni, Rb, Sr, Cd, Cs, Ba, Pb, Al, Cu, U, Na, V, As, Se, Sn	Tea leaves were dried in oven at 70 °C for 12 h to constant weight. The dried samples were crushed to obtain fine powder using a mortar and pestle and sieved using a 75-μm nylon mesh.	ICP-MS	52
32	Catechins	10.0 g + 300 mL boiling water for 3 min. After filtering through the siliconetreated filter paper, the tea infusions were centrifuged at 10,000 g and 20 °C for 45 min.	FTIR spectroscopic measurements UV–vis spectroscopy analysis Fluorescence spectroscopy	53
33	Antioxidants, color parameters	1.00 g of +250 mL of boiling ultra-filtered water. Infusions were allowed to steep for 1 h with continuous swirling and thencooled. Subsequently, the infusions were filtered and stored at 4◦Cfor further analysis within 8 h.	ABTS [2,20-azinobis-(3 ethylbenzothiazoline-6-sulphonic acid) diammonium salt] assay DMPD (N,N-dimethylp-phenylenediamine dihydrochloride) ColorQuest XE	54

Table continuation

№	Analyte	Sample preparation	Equipment	Link to reference
34	Theophylline	2.0 g+100 ml of boiling water for 3 min. It was then diluted by a factor of 1:20.	Square-wave voltammetry	55
35	Tannins	0.5000 g of tea was heated for 10 min at 90 ◦C in about 50 mL of deionized water, the mixture was filtered.	Turbidimetric method Photometric method	56
36	Theophylline	5 g + 60 mL of boiling double distilled deionised water for 30 min. After filtration, the filtrate was collected into a 100 mL volumetric flask and diluted to marker.	Electrochemical method based on CdSe microparticles modified glassy carbon electrode	57
37	Fluoride	The method involves fusion of tea samples with 8 M NaOH at 600 °C for 30 min. The fused samples were extracted with boiling distilled water.	SPADNS colorimetric method USEPA Method 13A	58
38	Fluoride	2.000 g sample + 150 ml 100 °C deionized water and kept in a 100 °C bath for 10 min. After filtration, the volume was determined.	Fluoride ion selective electrode method	59
39	Fluoride	2 g of sample + 200 ml of de-ionized water (100 °C) and kept on water bath (100 °C) for 10 min, then cooled to room temperature,filtered, and the filtrate was brought back to 200 ml with de-ionized water.	Fluoride ion selective electrode and spectrometry.	60
40	Fluoride	Tea bag + 100 mL boiled water. After 5 min of infusion, tea bag was taken out and cooled to room temperature. 0.5 mL of total ionic strength adjustment buffer was pipetted per 5 mL standard fluoride solutions.	Fluoride ion selective electrode and spectrometry.	61
41	Amino acids, Na, K, P, Mg, Fe, Cu, Zn, Mn, Al, Ni, Cd, Pb	1 g of sample +hot distilled water(100 ml) was added to each beaker and the leaves were allowed to infuse for 10 min. The infusions were filtered.	Flame photometry Spectrophotometer AAS	62

All the scientific articles above are taken from the ScienceDirect database. Summarizing these scientific works, the composition of tea can be formed depending on the place of its cultivation (nature, climate, altitude, etc.). In the articles 80% of tea in the study was Asian tea. Identified important constant components of tea mass, product of secondary metabolism and constitutes the bulk of tea polyphenols – catechins and their types. Also types of caffeine and amino acids, natural or artificial types of volatile compounds that affect the smell and taste of tea were determined. Analyzed harmful compounds, that reduce the quality of tea, such as pesticides, fluorine, heavy metals. Several volatile compounds contribute to the aroma of tea beverages, and are identified by GC-MS in conjunction with head-space analysis or solid-phase microextraction (SPME). GC-MS was initially used for determining the difference in aromas of different tea grades. Volatile compounds of green, black, oolong and white teas by dispersive liquid-liquid microextraction coupled with GC have been reported. The aroma of Pu-erth tea characterized using headspace – solid phase microextraction, combined with GC-MS and GC-olfactometry. HPLC is the most frequently used methods to determine catechins, alkaloids, theaflavins, and thearubigins in teas. HPLC is also used to determine phenolic acids (such as gallic and caffeic acids, etc.), flavonols (such as quercetin, kaempferol, and myracetin), lignans, triterpenoid saponins, pigments (chlorophyll and carotenoids) in tea. The detection of heavy metals and fluorine was carried out using electrochemical methods and atomic absorption spectroscopy (AAS), flame AAS, inductively coupled plasma mass spectrometry. Methods for analytical analysis have been developed and optimized methods have been shown for sample preparation.

Conclusion

This paper presents chromatographic methods for determining the composition of the tea component and shows several useful aspects of this technique. New modern methods for studying the chemical composition of several species of tea were analyzed and generalized using various chromatographic methods. The review presents a summary of the latest information concerning the chemical composition of large variety of tea by different chromatographic methods, which has not previously been reviewed. Qualitative and quantitative analyses of volatile compounds, that contribute to flavor and aroma in tea composition were executed by gas chromatography and gas chromatography-mass spectrometry. Low volatility organic compounds were carried out by using high-performance liquid chromatography methods and GC/MS. Determination of catechins and coffein in different types of tea were investigated by HPLC of the most current published researches. In addition, the materials used in this article can be used in the field of tea research, determination of quality and evaluation of tea components.

References

1. Hicks A. (2008) Current Status and Future Development of Global Tea Production and Tea Products. FAO Committee on Commodity Problems – Intergovernmental Group on Tea, vol. 12, pp. 251-264.

2. Wan, X., Li, D., Zhang, Z. (2008) Green tea and black tea—manufacturing and consumption. Tea and tea products, pp. 1-8.

3. https://worldoftea.org/tea-chemistry/

4. http://mateasse.com/index.php?route=pavblog/blog&id=27

5. Oze I., Keitaro M. (2004) Coffee and green tea consumption is associated with upper aerodigestive tract cancer in Japan. International Journal of Cancer, vol. 135, pp. 391-400.

6. Chen D. (2004) Green tea and tea polyphenols in cancer prevention. Frontiers in Bioscience, vol.9, p. 2618.

7. Johnson R., Bryant S. (2012) Green tea and green tea catechin extracts: an overview of the clinical evidence. Maturitas, vol. 73, pp. 280-287.

8. Harold N. G. (1992) Green tea composition, consumption and polyphenol chemistry. Preventive Medicine, vol.21, pp. 334-350.

9. Baraboi V. A. Tea plant catechins: structure, activity, application [katekhiny chainogo rasteniia: struktura, aktivnost, primenenie] – 2008. – Vol. 3. – P. 25-36.

10. Wang H., Helliwell K. (2000) Epimerisation of catechins in green tea infusions. Food Chemistry, vol. 70, pp. 337-344.

11. Goh R., Jing G. (2015) Green tea catechins reduced the glycaemic potential of bread: an in vitro digestibility study. Food Chemistry, vol. 180, pp. 203-210.

12. Chen J., Jun X. (2015) Epigallocatechin-3-gallate attenuates lipopolysaccharide-induced mastitis in rats via suppressing MAPK mediated inflammatory responses and oxidative stress. International Immunopharmacology, vol. 26, pp. 147-152.

13. Wong, M.H., Fung K.F. (2003) Aluminium and fluoride contents of tea, with emphasis on brick tea and their health implications. Toxicology Letters, vol. 137, pp. 111-120.

14. Pehrsson P., Patterson, Y. (2011) The Fluoride Content Of Select Brewed And Microwave-Brewed Black Teas In The United States. Journal of Food Composition and Analysis, vol. 24, pp. 971-975.

15. Quock R., James X.G. Tea fluoride concentration and the pediatric patient. Food Chemistry, vol. 130, pp. 615-617.

16. Koblar A., Tavcˇar G. (2012) Fluoride in teas of different types and forms and the exposure of humans to fluoride with tea and diet. Food Chemistry, vol. 130, pp. 286-290.

17. http://deeprootsathome.com/tea-brands-pesticides/

18. https://www.drtaniadempsey.com/single-post/The-Truth-About-Pesticides-in-Tea-Tea-Toxicity-Chemicals-In-Tea

19. https://dailyhealthpost.com/pesticides-tea/

20. RMG 19885-74. Tea. Methods for determination of tannin and caffeine content [Chai. Metody opredeleniia soderzhaniia tanina i kofeina] Moscow, Russia, 2014

21. RMG 10727-2013. Tea and instant tea in solid form. Determination of caffeine content. Method using high-performance liquid chromatography [Chaj i bystrorastvorimyj chaj v tverdoj forme. Opredelenie soderzhaniya kofeina. Metod zhidkostnoj xromatografii vysokogo razresheniya] Moscow, Russia, 2014

22. Silarova P., Ceslova L. (2018) Fast gradient HPLC/MS separation of phenolics in green tea to monitor their degradation. Food Chemistry, vol. 237, pp. 471-480.

23. Jiao Y, Jialiang H. (2017) Nε -(carboxymethyl) lysine and Nε -(carboxyethyl)ysine in tea and the factors affecting their formation. Food Chemistry, vol. 232, pp. 683-688.

24. Shiono T., Yamamoto K. (2017) Selective decaffeination of tea extracts by montmorillonite. Journal of Food Engineering, vol. 200, pp. 13-21.

25. Sökmen M., Demir E. (2018) Optimization of sequential supercritical fluid extraction (SFE) of caffeine and catechins from green tea. The Journal Of Supercritical Fluids, vol. 133, pp. 171-176.

26. Sun H., Qiao F. (2006) Characteristic of theophylline imprinted monolithic column and its application for determination of xanthine terivatives caffeine and theophylline in green tea. Journal of Chromatography A., vol. 1134, pp. 194-200.

27. Rashidinejad A., Birch E.J. (2016) Interactions between milk fat globules and green tea catechins. Food Chemistry, vol. 199, pp. 347-355.

28. Del Rio D., Stewart J.A. (2004) HPLC-MSn analysis of phenolic compounds and purine alkaloids in green and black tea. Journal of Agricultural and Food Chemistry, vol. 52, pp. 2807-2815.

29. Cao Y., Tang H. (2015) A novel method based on MSPD for simultaneous determination of 16 pesticide residues in tea by LC–MS/MS. Journal of Chromatography B., vol. 998, pp 72-79.

30. Engelhardt R. (2013) Determination of amino acids in white, green, black, oolong, pu-erh teas and tea products. Journal of Food Composition and Analysis, vol. 31, pp. 94-100.

31. Baptista J. (1998) Comparison of catechins and aromas among different green teas using HPLC/SPME-GC. Food Research International, vol. 31, pp. 729-736.

32. Xu Y. (2017) Effect of saccharides on sediment formation in green tea concentrate. LWT - Food Science And Technology, vol. 78, pp. 352-360.

33. Du L., Ma L. (2016) Determination of phthalate esters in teas and tea infusions by gas chromatography–mass spectrometry. Food Chemistry, vol. 197, pp. 1200-1206.

34. Zhou Y., Zeng L. (2017) Formation of (E)-nerolidol in tea (Camellia sinensis) leaves exposed to multiple stresses during tea manufacturing. Food Chemistry, vol. 231, pp. 78-86.

35. Ma Ch., Qu Y. (2014) Determination of nerolidol in teas using headspace solid phase microextraction–gas chromatography. Food Chemistry, vol. 152, pp. 285-290.

36. Sasaki T., Koshi E. (2017) Characterisation of odorants in roasted stem tea using gas chromatography–mass spectrometry and gas chromatography-olfactometry analysis. Food Chemistry, vol. 220, pp. 177-183.

37. Kraujalytė V., Pelvan E. (2016) Volatile compounds and sensory characteristics of various instant teas produced from black tea. Food Chemistry, vol. 194, pp. 864-872.

38. Han Zh., Rana M. (2017) Data on green tea flavor determinantes as affected by cultivars and manufacturing processes. Data In Brief, vol. 10, pp. 492-498.

39. Han Zh., Rana M. (2016) Green tea flavour determinants and their changes over manufacturing processes. Food Chemistry, vol. 212, pp. 739-748.

40. Reto M. (2007) Analysis of vitamin K in green tea leafs and infusions by SPME–GC-FID. Food Chemistry, vol. 100, pp. 405-411.

41. Du L., Li J. (2014) Characterization of volatile compounds of pu-erh tea using solid-phase microextraction and simultaneous distillation–extraction coupled with gas chromatography–mass spectrometry. Food Research International, vol. 57, pp. 61-70.

42. Lin J., Zhang P. (2013) Discrimination of oolong tea (Camellia sinensis) varieties based on feature extraction and selection from aromatic profiles analysed by HS-SPME/GC/MS. Food Chemistry, vol. 141, pp. 259-265.

43. Lv H., Zhong Q. (2012) Aroma characterisation of pu-erh tea using headspace-solid phase microextraction combined with GC/MS and GC–olfactometry. Food Chemistry, vol. 130, pp. 1074-1081.

44. Cho S., Abd El-Aty A.M. (2014) Simultaneous multi-determination and transfer of eight pesticide residues from green tea leaves to infusion using gas chromatography. Food Chemistry, vol. 165, pp. 532-539.

45. Hou X., Lei. Sh. (2016) Optimization of a multi-residue method for 101 pesticides in green tea leaves using gas chromatography-tandem mass spectrometry. Revista Brasileira de Farmacognosia, vol. 26, pp. 401-407.

46. Yang T., Zhu Y. (2016) Enantiomeric analysis of linalool in teas using headspace solid-phase microextraction with chiral gas chromatography. Industrial Crops and Products, vol. 83, pp. 17-23.

47. Venditti E., Bacchetti T. (2010) Hot vs. cold water steeping of different teas: do they affect antioxidant activity? Food Chemistry, vol. 119, pp.1597-1604.

48. Martín-D. (2017) Determination of metalloid, metallic and mineral elements in herbal teas. Risk assessment for the consumers. Journal of Food Composition and Analysis, vol. 60, pp. 81-89.

49. Sharma V. (2008) Influence of milk and sugar on antioxidant potential of black tea. Food Research International, vol. 41, pp. 124-129.

50. Yuksel Z., Avci E. (2010) Characterization of binding Iinteractions between green tea flavanoids

and milk proteins. Food Chemistry, vol. 121, pp. 450-456.

51. Jin C. (2001) Processing procedures of brick tea and Their Influence On Fluorine Content. Food and Chemical Toxicology, vol. 39, pp. 959-962.

52. Zhao H.,Yu Ch. (2017) Effects of geographical origin, variety, season and their interactions on minerals in tea for traceability. Journal of Food Composition and Analysis, vol. 63, pp. 15-20.

53. Ye J., Fan F. (2013) Interactions of black and green tea polyphenols with whole milk. Food Research International, vol. 53, pp. 449-455.

54. Jin L. (2016) Antioxidant properties and color parameters of herbal teas in China. Industrial Crops and Products, vol. 87, pp. 198-209.

55. Zen J. (1999) Determination of theophylline in tea and drug formulation using a Nafion®/lead - ruthenium oxide pyrochlore chemically modified electrode. Talanta, vol. 50, pp. 635-640.

56. Marcelo B. L., Andrade S. (2012) Turbidimetric and photometric determination of total tannins in tea using a micro-flow-batch analyzer. Talanta, vol. 88, pp. 717-723.

57. Yin H., Meng X. (2012) Electrochemical determination of theophylline in foodstuff, tea and soft drinks based on urchin-like CdSe microparticles modified glassy carbon electrode. Food Chemistry, vol. 134, pp. 1225-1230.

58. Das S., Letuzia M. (2017) Fluoride concentrations in traditional and herbal teas: health risk assessment. Environmental Pollution, vol. 231, pp. 779-784.

59. Cao J. (2004) Safety evaluation on fluoride content in black tea. Food Chemistry, vol. 88, pp. 233-236.

60. Cao J., Zhao Y. (2006) Fluoride levels in various black tea commodities: measurement and safety evaluation. Food and Chemical Toxicology, vol. 44, pp. 1131-1137.

61. Emekli-Alturfan E., Yarat A. (2009) Fluoride levels in various black tea, herbal and fruit infusions consumed in Turkey. Food and Chemical Toxicology, vol.47, pp. 1495-1498.

62. Jabeen S., Alam S. (2015) Withering timings affect the total free amino acids and mineral contents of tea leaves during black tea manufacturing. Arabian Journal of Chemistry.

IRSTI 31.25.19

A.N. Azhkeyeva, R.K. Rakhmetullayeva, G.Zh. Yeligbayeva,
Ye.M. Shaikhutdynov, U. Nakan, M. Abutalip, K. Park

Institute of chemical and biological technologies, Satbayev Univesity, Almaty, Kazakhstan
*e-mail: ayganym_90@mail.ru

Synthesis of novel thermosensitive copolymers based on ethylacrylate

Abstract. New thermo-sensitive copolymers (CPL) based on 2-hydroxyethylacrylate (HEA) and ethylacrylate (EA) were synthesized by radical copolymerization method. The composition of CPL, copolymerization activity were calculated. Physicochemical properties of new water-soluble CPL with composition of initial monomer mixture 90:10%; 80:20%; 70:30; 60:40%; 30:70%; 20:80%; 10:90% were investigated. The main regularities of the thermo-sensitive behavior of CPL were studied.

We found the compositions of copolymers and calculated the relative activities of comonomers the values of which evidence the higher reactivity of ethylacrylate compared with the reactivity of hydroxyethylacrylate. The study of phase diagrams of aqueous solutions of copolymers allowed identifying the presence of lower critical solution temperature (LCST).

As the main physicochemical methods of investigation, in work are used: IR-, ^{1}H NMR-, UV- spectroscopy, thermogravimetric analysis (TGA), differential scanning calorimetry (DSC), turbidimetry.

Key words: Radical copolymerization, 2-hydroxyethylacrylate, ethylacrylate, interpolymer complexes, lower critical solution temperature.

Introduction

More and more attention of scientists of the world community is attracted by materials possessing a certain "memory" and capable of reacting to changing the parameters of the external environment according to a pre-programmed scheme. Such materials include water-soluble hydrophilic polymers [1] and, especially, their mesh analogs–polymer hydrogels, which are capable of retaining significant amounts of water in their structure. Researchers particular interest is stimulus-sensitive hydrogels capable of swelling and contracting when changing environmental parameters [2], such as temperature [3], pH [4], electric field, etc. Synthesis and investigation of the physico-chemical properties of stimulus-sensitive polymers appear to be important both from the point of view of understanding the features of structure formation and in terms of creating polymer reagents for various purposes. Areas of practical application of hydrophilic polymers are very numerous and diverse: medicine (controlled injection and isolation systems, dressings, contact lenses, construction materials for endoprosthetics, contraceptives, transplantation in cell therapy, etc.) [5-7], agriculture (hydroabsorbents for regulation of water regime of soils) [8], biotechnology (concentration, purification, utilization of biological objects) [9], robotics (artificial muscles), etc.

The development of the fundamental foundations for the creation of such polymers is very relevant in connection with the broad prospects of their practical application. The thermo- and pH-sensitivity of the swelling polymer networks can be realized with a certain hydrophilic-hydrophobic balance of the macrochains of the nets. The given balance, in turn, is provided by the ratio of hydrophilic and hydrophobic monomers participating in the copolymerization reaction in the synthesis of the copolymer. The hydrophobicity is generally the hydrocarbon chains of alkenes, dienes, alkyl methacrylates, hydrophilicity–sections of macrochains containing heteroatoms, hydrophilic or ionogenic groups. The most investigated hydrophilic polymers include, for example, ethylene glycol monomethacrylate, 2-hydroxyethylacrylate (HEA)-VBE [10], HEA- butylacrylate [11], hydroxyethylacrylate (HEA)-hydroxyethylmethacrylate [12] (2-hydroxyethyl acrylate). A similar ester of acrylic

 Printed in Kazakhstan

acid in the creation of stimulus-sensitive nets was not investigated. Although, in this monomer, the absence of a β-methyl group makes it possible to reduce hydrophobicity.

In the recent years the researchers have showed a special interest in thermosensitive copolymers the aqueous solutions of which possess lower critical solution temperature among water-soluble polymers. Currently, most of them have already been used in biomedicine to provide the controlled delivery of drugs, in tissue engineering, food industry, electronics and etc.

However, the range of available thermosensitive polymers is quite limited and besides the main part of papers is devoted to poly-N-isopropylacrylamide and polymers of polyethylacrylate are investigated to a much lesser extent [13]. In the present paper the approach based on radical copolymerization of monomers with a significant difference in the hydrophobic-hydrophilic balance of chemical structure was used to synthesize novel thermosentitive polymers. It allows regulating the ratio of hydrophobic and hydrophilic components in macrochains, and respectively, the temperature of phase transitions in polymer-water system in wide ranges [14]. The important thing is that monomers, homopolymers, which do not have LCST in aqueous solutions can be used starting materials for such copolymers. In the present paper to synthesize stimulus-sensitive copolymers we used 2-hydroxyethyl acrylate as a hydrophilic monomers and ethylacrylate was as a hydrophobic monomer.

Materials and methods

2-hydroxyethylacrylate (HEA) (Sigma Aldrich (UK)) contained 96% of basic product. It was purified by double vacuum distillation in argon flow (b.p.=91^0/12 mm. sec., n_D^{20}=1.4500).

Ethylacrylate (EA) (Fisher Scientific (UK) contained 96% of basic product. It was washed by 10 % water KOH solution from inhibitor, was dried above potash and was purified by double vacuum distillation (b.p.=99^0C, T_i=71^0C, n_D^{20}=0.9405).

Azo-bis-iso-butyric acid dinitrile (ABAD) of "c" grade (Acros (USA) was twice recrystallized from absolute methanol, m.p.=103°C.

Ethanol (absolute with m.p.=78°C/760 mm. Hg, n_D^{20}=1.3612-1.3618) was produced by Sigma-Aldrich Co. (USA).

To prepare solutions the distilled water was used.

Synthesis of HEA-EA copolymers of linear and crosslinked structure.

Water-soluble linear (co)polymers of HEA-EA with composition 90:10%; 80:20%; 70:30%; 60:40%; 30:70%; 20:80%; 10:90% were synthesized using the method of radical copolymerization of 50% solution of HEA:EA mixture of various compositions in ethanol at 60°C. Copolymerization was carried out in the ampoules of molybdenum glass. Reaction mixtures were blown off by argon for 20 minutes to remove oxygen from reaction mixture. The substance radical polymerization of liner EA and HEA monomers was initiated by thermal decomposition of azo-bis-iso-butyric acid dinitrile. The resulting linear copolymers were poured into the dialysis membrane to purify from unreated monomers. The samples obtained were dried by liophylization up to a constant weight and then aqueous solutions were prepared.

Physico–chemical methods of investigation of polymers.

The composition of the HEA-EA copolymers was determined by ^{1}H NMR spectroscopy in deuterated dimethylsulfoxide (DMSO-d_6) using NMR spectrometer (Bruker DPX-400 (400 MHz) (UK) at 293 K. All chemical shifts were recorded as δ in parts per million (ppm), and references to the residual solvent signal (CD_3) SO: ^{1}H, δ=2.50 ppm) were recorded too.

IR spectra of initial samples of polymers was recorded on a spectrophotometer (Perkin-Elmer FTIR Spectrum Two (UK) in the region of 400-4000 cm^{-1}. Samples were prepared in the form of tablets with KBr.

The optical density of solutions of polymers was determined on the UV spectrophotometer (Shimadzu UV/ VIS-2401 PC (Japan)) at a wavelength of 400 nm.

The effect of the temperature on aggregation behavior and phase diagrams of the solutions of polymers were investigated by determining the cloud points on UV-spectrometer with the help of thermostat cell using thermo-electronic cuvette regulator (CPS-240A Shimadzu (Japan)).

Thermal analysis of (co) polymers was carried out using a thermogravimetric analyzer on the instrument (Perkin Elmer Pyris 1 TGA (Perkin Elmer Instruments (UK) at a heating rate of 10°C/min in a dry nitrogen atmosphere (99.99%, flow rate 20 ml/min). The mass of polymer samples in isopoly acid was about 10-12 mg. The experiments on differential–scanning calorimetry of the samples were carried out on the instrument (Perkin Elmer Diamond DSC by Perkin Elmer Instruments (UK) at scanning rate of 10°C/min in the atmosphere of dry nitrogen. As the parameters of thermoanalysis, particularly glass point, are sufficiently sensitive to the conditions of the experiment and the presence of moisture inside the polymers the system together with the samples were pre-heated up to 210°C at the rate of 10°C/min and then cooled at a rate of 10°C/min. The second scanning was made as experimental data.

Liophylization. The samples were liophylized using Heto PowerDry® LL3000 connected to rotor lubricating pump (Edwards RV3) at -53°C.

The dialysis membranes (molecular mass of 12-14 kDa) were supplied by MediCell International Ltd company (UK).

Results and discussion

In the present paper to synthesize novel thermosensitive copolymers based on copolymerization of monomers with a significant difference in hydrophilic-hydrophobic balance of chemical structure was used. It allows regulating the ratio of hydrophilic and hydrophobic components in macrochains and, respectively, temperature of phase transitions in polymer-water system in wide ranges. Earlier Nurkeeva Z.S. et.al. effectively used this procedure when creating a wide range of novel thermosensitive polymers [14; 15]. Importantly, monomers, homopolymers, which do not have LCST can be used as starting materials. In the paper, for the first time, the synthesis of novel copolymers based on 2-hydroxyethylacrylate (HEA) and ethylacrylate (EA) was made by radical copolymerization. HEA–EA copolymerization was carried out in the presence of azo-bis-isobutyric acid dinitrile as an initiator.

To determine the chemical composition of the resulting copolymers ^{1}H NMR–spectroscopy was used. DMSO–d_6 was used as a solvent. The Figures 1 and 2 show ^{1}H NMR – spectra of poly-2-hydroxyethylacrylate (PHEA) and polyethylacrylate (PEA) for comparison. PEA: protons–CH_3 group of the basic chain (a and d) show resonance in the range of 1.1-1.2 ppm. Resonance signals of the protons of –CH- and –CH_2- groups of the basic chain (a and b) of 1.35-1.85 ppm and –CH_2- (c) methylene protons of homopolymer are observed at 2.1-2.3 ppm, 3.9-4.1 ppm, respectively. These data are well–correlated with PHEA NMR spectra data.

For PHEA (Figure 1) in NMR spectrum protons of -CH- and -CH_2- (a and b) groups of the basic chain exhibit resonance at 1.4-1.8 ppm and 2.15-2.3 ppm, respectively. The signals at 3.5-3.6 ppm and 3.9-4.1 ppm relate to -CH_2- protons of hydroxyethyl group (d and c) and resonance at 4.7-4.8 ppm corresponds to OH (f) of the group given above. These data are well-agreed with PHEA NMR spectrum data obtained by Coca et al. [16].

For copolymers obtained during the initial stages of conversion the composition was identified by ^{1}H NMR–spectroscopy. The composition was determined by the ratio of the integral intensities of NMR spectrum signals in the region of 4.70-4.81 ppm belonging to the position to protons of HEA hydroxyl group and also the intensity of the signals observed in the region of chemical shifts at 1.1-1.2 ppm typical of the protons of EA (Figure 3) end methyl group (DMSO–d_6 was used as a solvent).

As ^{1}H NMR spectra show (Figure 3) integration and account of the ratio of the intensity of signals observed in the region of chemical shifts at 3.6 ppm characteristic of PHEA methylene group and the signal in the region of 1.2 ppm relating to the protons of PEA –CH_3- group allowed determining the composition of copolymers (table 1) and calculating copolymerization constants *(r_1* and *r_2)* for monomers during copolymerization. Initial monomer mixtures, compositions of copolymers, their molecular–mass characteristics are shown in table1.

The processing of these data by Feynman-Ross (Figure 4) and Kelen Turdosa equations (Figure 5) has showed constants of copolymerization r_1(HEA)=0,46-0,3 and r_2(EA)=0,62-0,72 which indicate the higher reactivity of EA compared with the reactivity of HEA.

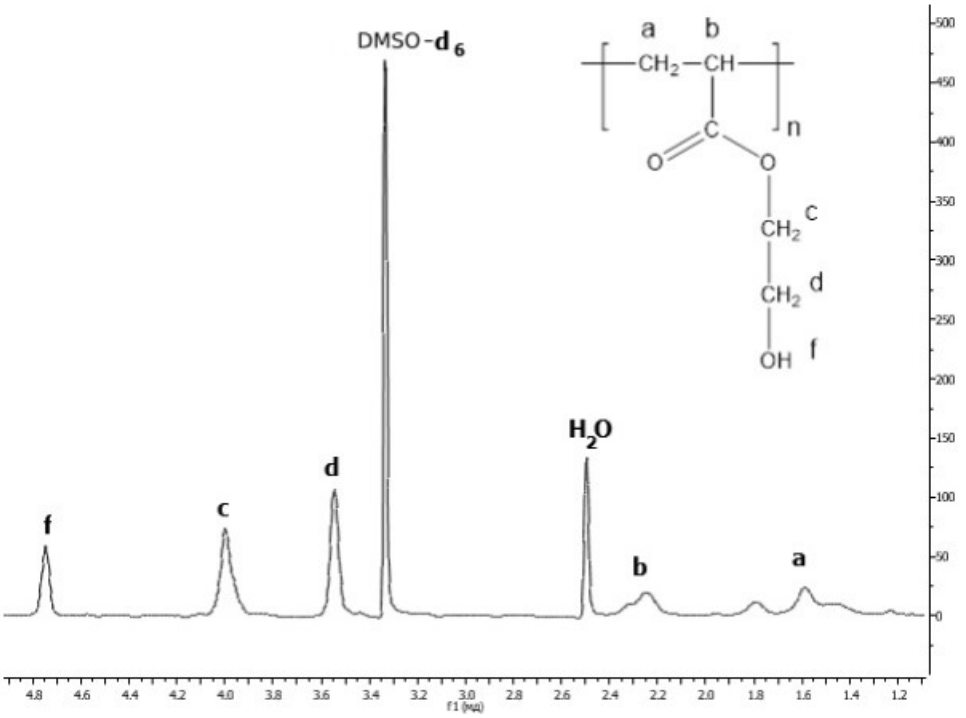

Figure 1 – [1]H NMR–spectra of poly-2-hydroxyethylacrylate (PHEA)

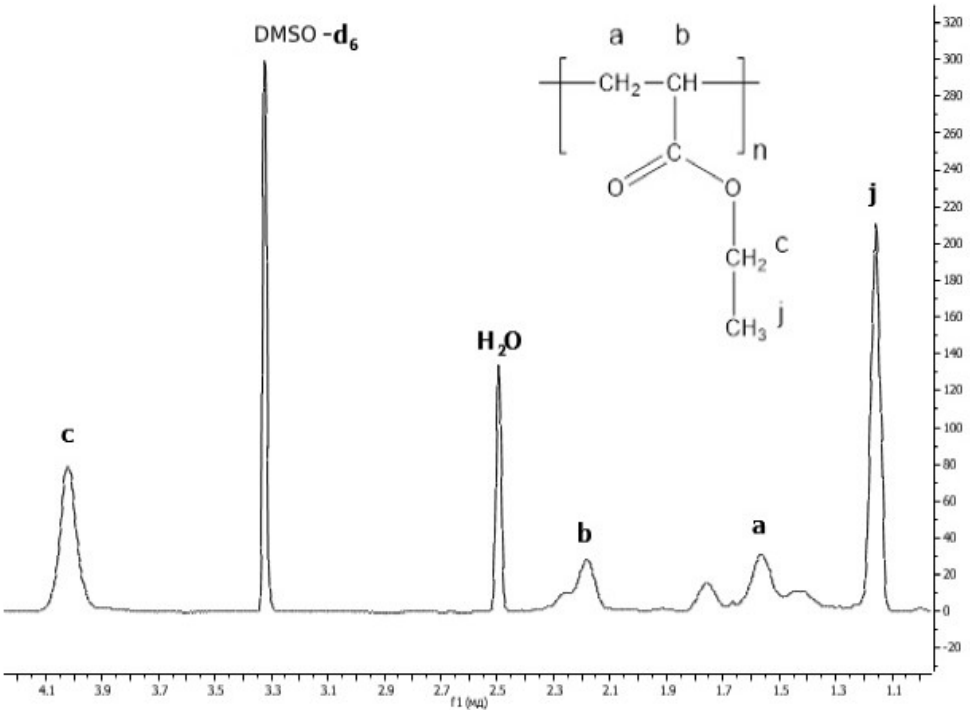

Figure 2 – [1] H NMR–spectra of polyethylacrylate (PEA)

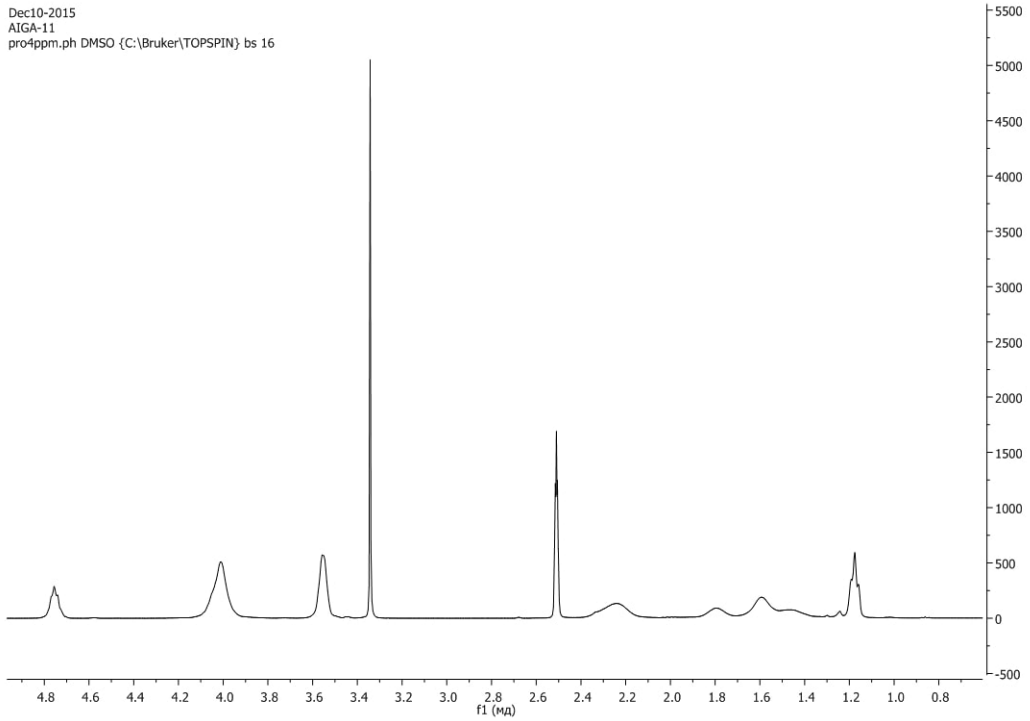

a)

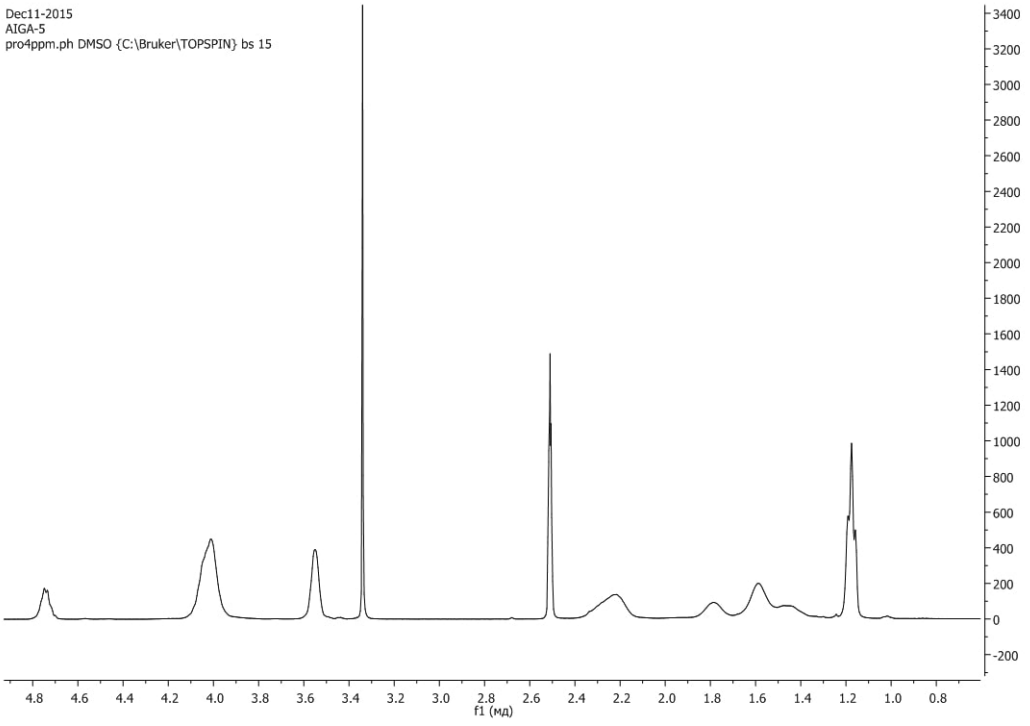

b)

IMM [HEA]:[EA]=70:30 (a); 30:70 (b) mol.%

Figure 3 – ^{1}H NMR–spectra of copolymers HEA:EA

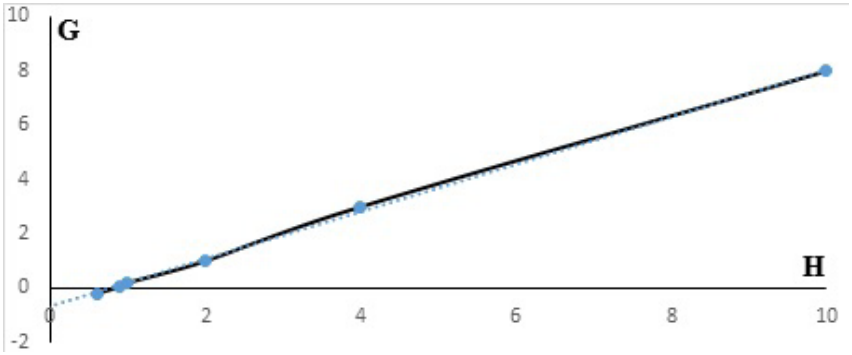

Figure 4 – Determination of the copolymerization constant by the Fayman-Ross method

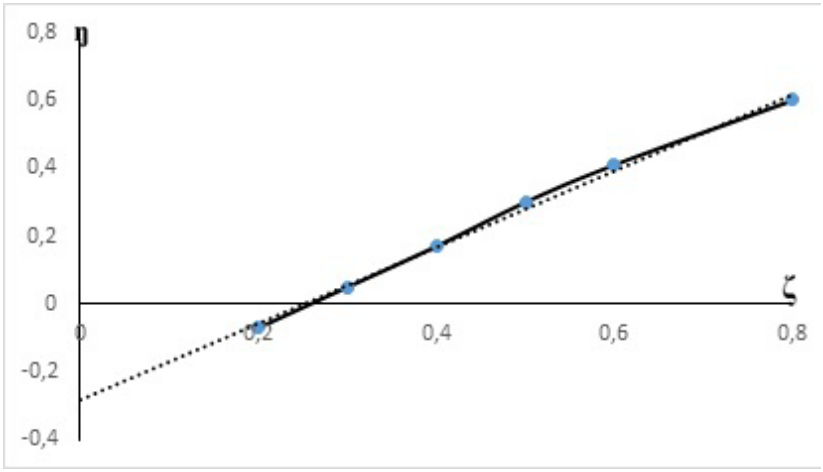

Figure 5 – Determination of the copolymerization constant by the Kelen Turdos method

Table 1 – Determination of constant of copolymerization based on HEA-EA with Feynman-Ross and Kelen-Turdosa method

IMM [HEA]:[EA] mol.%		Composition of the copolymer [HEA]:[EA] мол.%		F= M_1 / M_2	f= m_1 / m_2	G=F(f-1) /f	H=F^2/f	η=G/(α+H)	ζ=H/(α+H)	The copolymerization constant	Fineman-Ross(FR)	Kelen-Turdos(KT)
M_1	M_2	m_1	m_2									
90	10	88,78	11,22	9	7,913	7,863	10,237	0,619	0,806	r_1	0,46	0,3
80	20	80,12	19,88	4	4,030	3,008	3,970	0,468	0,617			
70	30	69,72	30,28	2,33	2,303	1,318	2,358	0,273	0,489	r_2	0,62	0,72
60	40	63,33	36,67	1,5	1,727	0,631	1,303	0,168	0,346			
50	50	51,47	48,53	1	1,061	0,057	0,943	0,017	0,277			
40	60	43,10	56,90	0,67	0,758	-0,214	0,593	-0,070	0,194	r_1*r_2	0,29	0,22

$$\alpha(H_{max}H_{min})^{1/2}=2.463$$

For synthesized copolymers based on HEA and EA IR-spectra (400-4000 cm^{-1}) were recorded. Figure 6 shows IR-spectra of HEA-EA copolymers of a various composition. The following signals allowed identifying functional groups of HEA-EA copolymers of $–CH_3$- group 1019-1078 cm^{-1}, $–CH_2$- group (1165-1256 cm^{-1}), –CH- group (1395-1450 cm^{-1}), C=O (1729 cm^{-1}) and HEA components of $–CH_2$- (2850cm^{-1}) which are next to hydroxyl group 3417 cm^{-1} respectively.

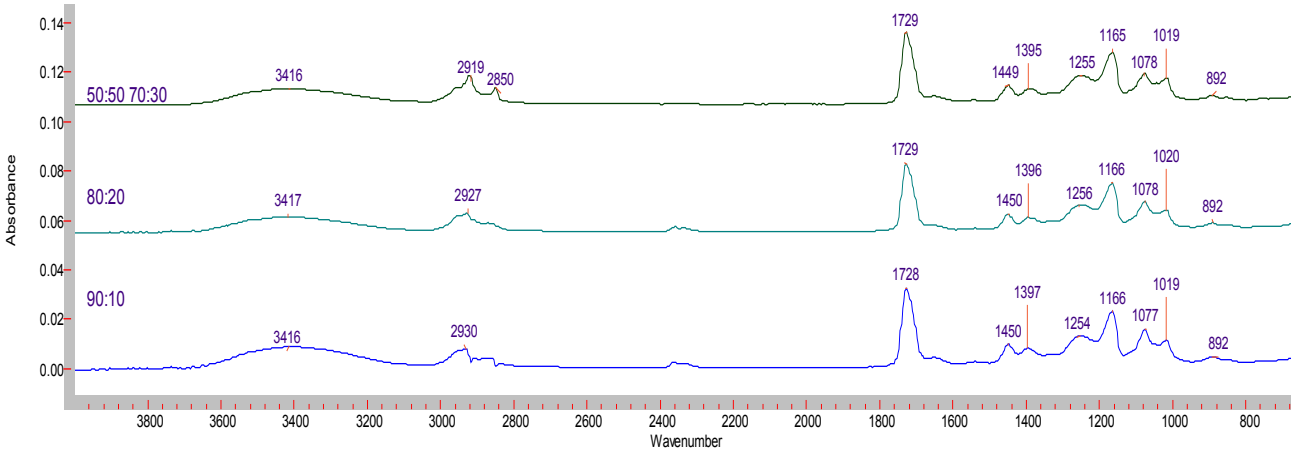

IMM [HEA]:[EA] = 90:10; 80:20; 70:30 mol.%

Figure 6 – IR spectra of copolymers of HEA-EA

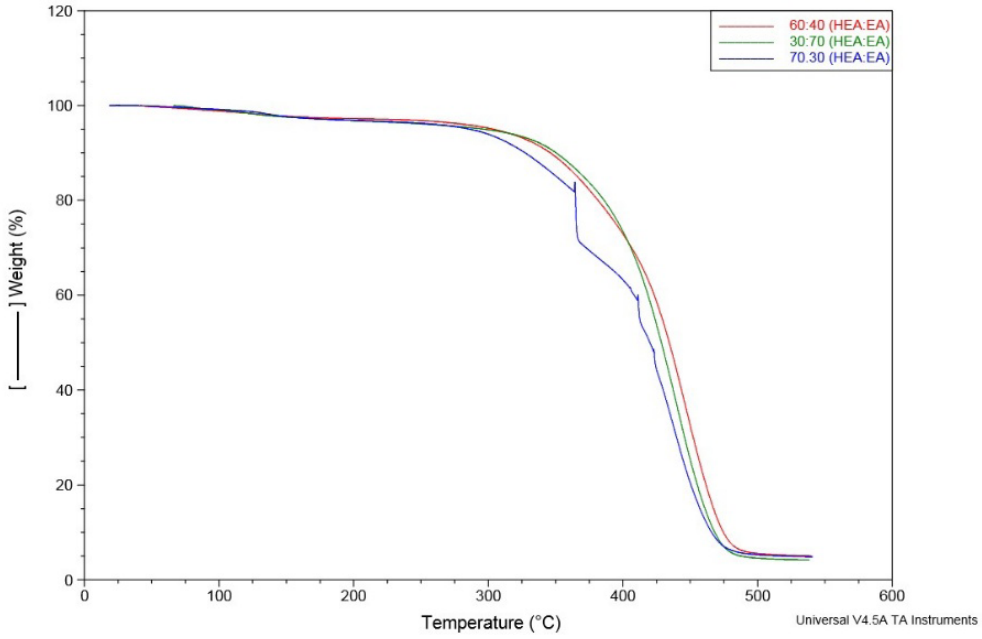

IMM [HEA]:[EA]=70:30 (1); 60:40 (2); 30:70 (3) mol.%

Figure 7 – TGA curves for HEA-EA copolymers

Figure 7 shows the data of thermogravimetric analysis (TGA) of the samples of HEA-EA copolymers of a various composition. Destruction of copolymers consists of two stages. The initial loss of weight is observed at about 50-225°C. It is conditioned by releasing air moisture absorbed. The final

and complete loss of the weight of copolymers up to 90% starts at about 470°C and reaches maximum at 482°C that causes the complete degradation of copolymers. In general, the absence of apparent inflections evidence that the samples don't contain low-molecular impurities including solvent of oligomer.

To study the compatibility of HEA-EA copolymers in details their *standard temperatures were determined using the instrument of differential-scanning calorimetry (DSC)*. Figure 8 shows DSC analysis results of HEA-EA copolymers, respectively. These figures show that there is one transition from glass state to high-elasticity in thermographs at that standard temperature shifts to the region of lower values with decreasing HEA content in the copolymer composition. The data of standard temperatures obtained by theoretical and experimental calculations are given in table 2. DSC analysis data confirm the value of standard temperature for copolymers with theoretically-calculated data.

For novel linear HEA and EA copolymers hydrodynamic behavior in the solution at temperature variation was studied using turbidimetry (Figure 9-11). It is seen that when temperature increases the solutions of HEA-EA copolymers grow turbid in a narrow range. It indicates their thermosensitive properties i.e. Lower critical solution temperature (LCST) is typical of copolymers (CPL) above of which layer separation occurs. At that when the concentration of the solutions increases phase transition shifts to the region of low values which is obviously connected with worsening the thermodynamic quality of a solvent due to the destruction of hydrogen polymer-solvent bonds and also to the enhancement of hydrophobic interactions of EA components.

In the paper temperature of phase transition of the solution of copolymers based on HEA-EA was found not to exhibit thermosensitivity when the content of EA components decrease (figure 10) by 10% mol. The data obtained are well-agreed with the results of the paper [17] which shows that when the content of the components of NIPAAM monomer increases in the copolymer composition temperature of phase transition of the solutions of copolymers based on HEA-EA decreases.

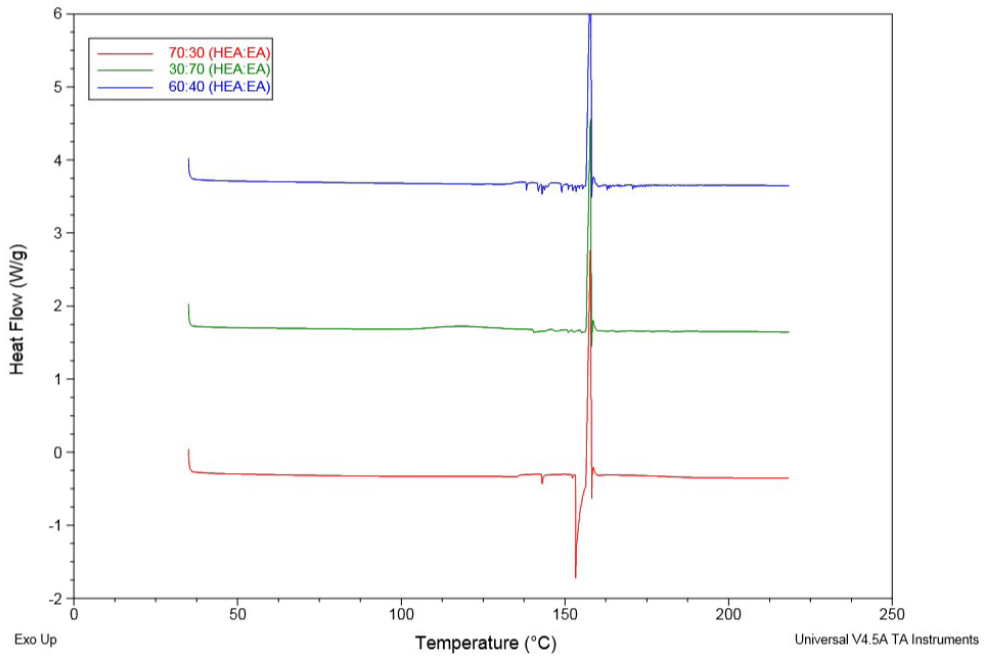

IMM [HEA]:[EA]=70:30 (1); 60:40 (2); 30:70 (3) mol.%

Figure 8 – DSC curves for HEA-EA copolymer

Table 2 – Thermal characteristics based on HEA-EA

[HEA-EA] мол.%.	T_{st}, °C	Temperature, °C	Loss of mass, %	The remainder of the mass, %	PDT_{max}, °C
30:70	158	90-175 345-600	1.98 93	98.02 5,02	482
60:40	156	50-200 340-600	4.99 92	95.01 3	477
70:30	152	130-225 341-600	5.98 91.5	94.02 2.52	470

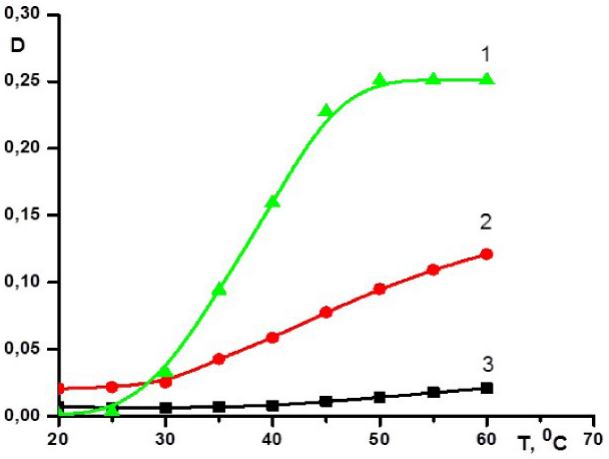

IMM [HEA]:[EA]=70:30 mol.%;
[HEA:EA]=0.05 (1); 0.025 (2); 0.01% (3)

Figure 9 – Dependence of optical density of aqueous solutions of linear copolymers of HEA-EA on temperature

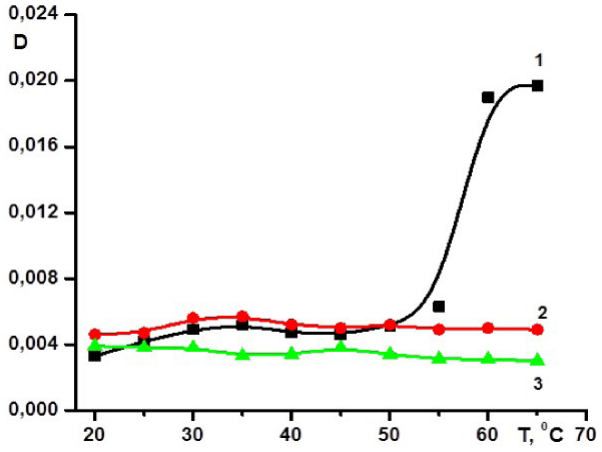

IMM [HEA]:[EA]=90:10 mol.%;
[HEA:EA]=0.05 (1); 0.025 (2); 0.01% (3)

Figure 11 – Dependence of optical density of aqueous solutions of linear copolymers of HEA-EA on temperature

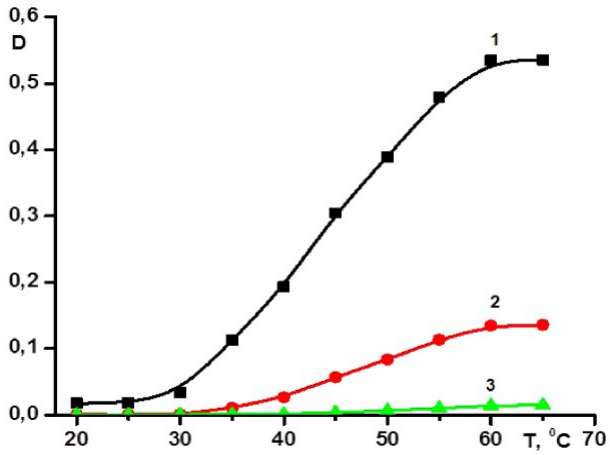

IMM [HEA]:[EA]=80:20 mol.%;
[HEA:EA]=0.05 (1); 0.025 (2); 0.01% (3).

Figure 10 – Dependence of optical density of aqueous solutions of linear copolymers of HEA-EA on temperature

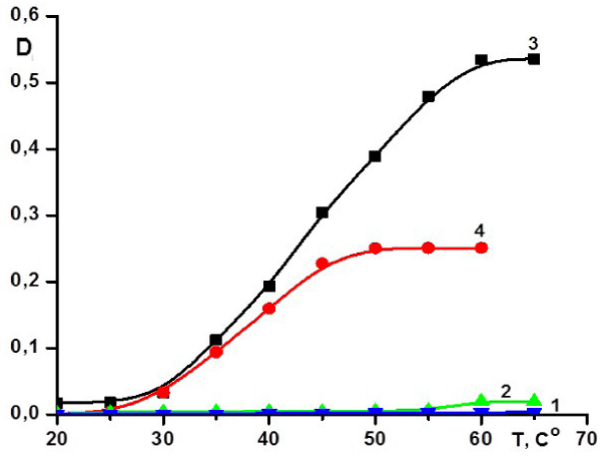

PHEA (1); IMM [HEA]:[EA]=90:10 (2);
80:20 (3); 70:30 (4) мол.%;
[HEA:EA]= 0.05%

Figure 12 – Dependence of optical density of aqueous solutions of linear copolymers of HEA-EA on temperature

In the paper the effect of the composition of copolymers on temperature was also studied (figure 12). When the content of EA fragments increases in copolymer composition phase transition of the aqueous solutions of copolymers from a globule to a coil occurs within a lower temperature range and the aqueous solution of homoHEA doesn't exhibit thermosensitivity [18].

Conclusion

For the first time, thermosensitive polymers hydrogels based on 2-hydroxyethyl acrylate (HEA) and ethyl acrylate (EA) have been synthesized by radical copolymerization.

To determine the physicomechanical properties of a copolymer IR-, ^{1}H NMR-, UV- spectroscopy, thermogravimetric analysis (TGA), differential scanning calorimetry (DSC), turbidimetry was used.

To determine the compositions of copolymers and relative activities of comonomers were calculated. The study of phase diagrams of the aqueous copolymer solutions showed LCST presence the value of which rises with increasing the content of HEA components in the composition of copolymers.

References

1 Safrany A. (1999) Synthesis and characterization of superclean thermoreversible copolymer hydrogels. Radiation Physics and Chemistry, vol. 55, pp. 121-126.

2 Jeong B., Gutowska A. (2002) Lessons from nature: stimuli-responsive polymers and their biomedical applications. TRENDS in Biotechnology, vol.20, №7, pp.305-311.

3 Peng T., Cheng Y.L. (1988) Temperature-responsive permeability of porous PNIPAAm-g-PE membranes. J. Appl. Polym. Sci., vol. 70, pp. 2133-2142.

4 Hester J.F., Olugebefola S.C., Mayes A.M. (2002) Preparation of pH-responsive polymer membranes by self-organization. J. Membr. Sci., vol. 208, pp.375-388.

5 Park, K., Mrsny, R. (2000) Eds.: Controlled Drug Delivery: Designing Technologies for the Future (ACS Symposium Series 752). American Chemical Society, Washington, DC, p. 459.

6 Dong L. C., Yan Q., Hoffman A. S. (1992) Controlled release of amylase from a thermal and pH-sensitive, macroporous hydrogel. J. Controlled Release, vol .19, p. 171.

7 Peppas N.A. (1991) Physiological responsive gels. J. Bioact. Compat. Polym., vol. 6, pp. 241-246.

8 Okano T., Kikuchi A., Sakurai Y., Takei Y., Ogata N. (1995) Polymeric drug delivery systems for treatment of cardiovascular calcification, arrhythmias and restenosis. Controlled Release, vol. 36, p. 125.

9 Galaev I.Yu., Mattiasson B. (1993) Enzyme and Microb. Technol., vol. 15, pp. 354–366.

10 Gillies E. R., Jonsson T. B., Fréchet J. M. J. (2004). J. Am. Chem. Soc., vol. 126, p. 11936.

11 Schilli C. M., Zhang M. F., Rizzardo E., Thang S. H., Chong Y. K., Edwards K., Karlsson G., Müller H. E. A. (2004). Macromolecules, vol. 37, p. 7861.

12 Rzaev Z. M. O., Dincer S., Piskin E. (2007), Prog. Polym. Sci., vol. 32, pp. 534–595.

13 Rabinovich V.A., Khavin V.Ya. (1991) A brief chemical handbook. L.: Chemistry, p. 432.

14 Khutoriansky V.V. (2000) Interpolymer complexes of polymers of simple vinyl ethers and composite materials on their basis. Abstract of candidate of chemical sciences: 02.06.00, p. 26.

15 Mun G.A., Nurkeeva Z.S., Khutoryanskiy V.V., Sergaziyev A.D., Rosiak J.M. (2002) Radiation synthesis of temperature-responsive hydrogels by copolymerization of [2-(methacryloyloxy)ethyl]-trimethylammonium chloride with N- isopropylacrylamide. Radiat. Phys. Chem., vol. 65, №1, pp. 67-70.

16 Coca S., Jasieczek C.B., Beers K.L., Matyjaszewski K. (1998) Polymerization of acrylates by atom transfer radical polymerization. Homopolymerization of 2- hydroxyethyl acrylate. J. Polym. Sci. Part A, Polym. Chem., vol. 36., pp.1417-1424.

17 Rakhmetullayeva R.K., Mun G.A.., Shaikhutdinov E.M., Nakan U., Bagitova Zh.K. (2013) Semi-interpenetrating network based on N-isopropylacrylamide. Chemical Bulletin of Kazakh National University, chemical series, vol. 2, pp. 49–57.

18 Bekturov E.A., Bimendina L.A. (1981) Interpolymer complexes. Adv. Polym. Sci., vol. 43, pp. 100-147.

IRSTI 31.25.15

A.N. Azhkeyeva, R.K. Rakhmetullayeva, G.Zh. Yeligbayeva,
Ye.M. Shaikhutdynov, M. Abutalip

Institute of chemical and biological technologies, Satbayev Univesity, Almaty, Kazakhstan,
*e-mail: ayganym_90@mail.ru

Complexation of new linear copolymers based on ethyl acrylate

Abstract. The processes of complexation of diphilic macromolecules with high molecular acids in recent years have moved into a separate and rapidly developing direction of the chemistry of polymers. Of particular interest are complexes based on nonionic thermosensitive copolymers and polycarboxylic acids, which acquire properties significantly different from those of the original components. In this regard, studies related to the establishment of complex-forming and surface-active behavior of non-ionic polymers with thermoregulated characteristics, acquires a particular urgency, both scientifically and in practice.

In the preparation of copolymers of a linear structure by the radical polymerization method, the samples were crosslinked after traditional planting and drying, and for this reason the method for the first time used the method of removal from unreacted monomers and oligomers by a dialysis membrane and dried samples by the lyophilic dryer.

The study also investigated the establishment of the main regularities of synthesis and intermacromolecular reactions of heat-sensitive, proton acceptor copolymers based on 2-hydroxyethyl acrylate (HEA) and ethyl acrylate (EA) with proton-donor polycarboxylic acids. Using the turbidimetry method, it was possible to show that the mutual transition of the hydrophobic complex-hydrophilic associate can be initiated not only by changing the pH, but also by varying the concentration of the solution. A whole layer of new interesting data has been obtained on the features of the effect of complexation on the thermosensitive properties of diphilic macromolecules. The set of the obtained data allowed to describe in more detail and demonstrate the scheme of mutual transitions hydrophobic complex-hydrophilic associate-noninteracting macromolecule depending on pH.

Key words: Radical copolymerization, 2-hydroxyethylacrylate, ethylacrylate, polyacrylic acid, interpolymer complexes.

Introduction

During the last several decades, there has been an intensive study of the issues concerning intermacromolecular interactions underlying the changes in the physicochemical characteristics and behavior of polymer systems. To date, there is a fairly large number of publications devoted to this area, which points to the special significance of products of interactions-IPC [1-4]. IPC are insoluble high-molecular structures formed due to the association of repeating units of various macromolecular chains. That is, macromolecules interact with each other through the forces of physical nature of a different nature and intensity. These links are most often Van der Waals forces, hydrogen bonds, hydrophobic and electrostatic interactions [1; 2]. In addition, such an interaction is accompanied by a change in the conformations of the links and individual segments of the macromolecular chain. Chemical and steric complementarity is a condition for effective interaction of polymers with the formation of IPC [2]. Complementary are such macromolecules, the functional groups of which can interact in a specific way, and the structure of these molecules should not create obstacles for the formation of the number of bonds necessary for the stability of the complex. By the type of dominant interaction, IPC are divided into stereocomplexes, polyelectrolyte complexes and complexes formed by hydrogen bonds [1; 5].

It should be noted that polycomplexes are formed in acidic media, therefore, the stability of the complex is highly dependent on pH as well as ionic strength. In addition, complexation is stabilized by cooperative nature, hydrophobic interactions, and is usually enhanced by decreasing ambient temperature [2; 6].

The interaction of polymeric acids with proton-acceptor nonionic polymers leads to the formation

 Printed in Kazakhstan

of polycomplexes stabilized by hydrogen bonds with precipitation. In this case, IPC have a strictly defined composition and their physicochemical, mechanical and other properties in most cases do not depend on the properties of the initial components of the components. Such IPC are of considerable interest from a practical point of view. The products of intermolecular interaction through hydrogen bonds are already widely used as medical materials [7-9], biomaterials [10], emulsifiers [11], sorbents for the recovery of heavy metals [12], etc. In this regard, the expansion of the range of IPC with the use of available polymers, as well as the creation of new composite materials on their basis, is a very urgent task.

The composition of IPC stabilized by hydrogen bonds can be determined by the number of proton acceptor centers in the non-ionic polymer. Thus, as the oxygen content of the non-ionic polymer increases, the number of polycarboxylic acid units bound to the polycomplex increases. For most systems in dilute solutions, the formation of complexes of stoichiometric composition is characteristic [1].

For the new copolymers (CPL) based on HEA and EA, the processes of their complexation with polycarboxylic acids were first studied. The critical value of complexation (pH_c) was fruitfully used as a criterion for the complexing ability of systems, which made it possible to establish a number of regularities on the influence of factors of different nature on the stability of the generated IPC. When studying the complexation of linear copolymers of HEA-EA with linear polyacrylic acid in solutions, the formation of polycomplexes of stoichiometric composition stabilized by hydrogen bonds and hydrophobic interactions has been established. As the basic physicochemical methods of investigation, we used: IR spectroscopy with Fourier transducer, UV spectroscopy, turbidimetry.

Materials and methods

2-hydroxyethylacrylate (HEA) (Sigma Aldrich (UK)) contained 96% of basic product. It was purified by double vacuum distillation in argon flow (b.p.=91^0/12 mm. sec., n_D^{20}=1.4500).

Ethylacrylate (EA) (Fisher Scientific (UK)) contained 96% of basic product. It was washed by 10 % water KOH solution from inhibitor, was dried above potash and was purified by double vacuum distillation (b.p.=99^0C, T_i=71^0C, n_D^{20}=0,9405).

Polyacrylic acid (PAA) with a molecular mass of 250000 (Sigma-Aldrich Co. (the USA)) was used without additional purification.

Azo-bis-iso-butyric acid dinitrile (ABAD) of "c" grade (Acros (the USA)) was twice recrystallized from absolute methanol, m.p.=103°C.

Ethanol (absolute with m.p.=78°C/760 mm. Hg, n_D^{20}=1.3612-1.3618) was produced by Sigma-Aldrich Co." (USA).

The solutions of isopoly acid were prepared by mixing the solutions of starting components. They were allowed to stand for 5 minutes. The measurements were made.

To prepare solutions distilled water was used.

Synthesis of HEA-EA copolymers of linear and grid-typed structure

Water-soluble linear (co) polymers of PHEEA, PEA, HEA-EA of composition 90:10%; 80:20%; 70:30%; were synthesized using the method of radical copolymerization of a 50% solution of a mixture of HEA-EA of various compositions in an ethanol solvent at 60°C. Copolymerization was carried out in the ampoules of molybdenum glass. The content of ampoules was blown off by argon for 20 minutes to remove oxygen from reaction mixture. The substance radical polymerization of liner EA and HEA monomers was initiated by thermal decomposition of azo-bis-iso-butyric acid dinitrile. The resulting linear copolymers were poured into the dialysis membrane to purify from unreated monomers. The samples obtained were dried by liophylization up to a constant weight and then aqueous solutions were prepared.

Physico–chemical methods of investigation of polymers and their intermolecular complexes.

IR spectra of initial samples of polymers and their interpolymer complexes (IPK) were recorded on a spectrophotometer (Perkin-Elmer FTIR Spectrum Two (UK)) in the region of 400-4000 cm^{-1}. Samples were prepared in the form of tablets with KBr.

The optical density of solutions of polymers and their interpolymer complexes (IPC) were determined on the UV spectrophotometer (Shimadzu UV / VIS-2401 PC (Japan)) at a wavelength of 400 nm.

pH of polymer solutions and their mixtures were determined at a constant temperature of 25°C on the digital ionomer (Hanna Instrument pH 211 meter (Hanna Ltd., Portugal)) with a precision of +0.01 units of pH.

pH of the solutions were regulated by adding small amounts of 0.1 M HCl and 0.1 M NaOH

Liophylization. The samples were liophylized using Heto PowerDry® LL3000 connected to rotor lubricating pump (Edwards RV3) at -53°C.

The dialysis membranes (molecular mass of 12-14 kDa) were supplied by MediCell International Ltd company (UK).

Results and discussion

A special class is the IPC formed by polycarboxylic acids with non-ionic polymers and stabilized by the hydrogen bond system. IPC possess a unique set of physico-chemical properties, different from those of the initial components.

In the present paper the complex formation of HEA-EA copolymer with polyacrylic acid (PAA) in aqueous solutions was studied using turbidimetry. The addition of the solutions of HEA-EA copolymers to PAA solutions is accompanied by increasing optical density which evidences the formation of hydrogen bonds formed by the system with the involvement of PAA carboxyl groups with hydroxyl and carbonyl groups of HEA-EA components in isopoly acid system (Figure 1, Scheme 1) [13, 14]. The curbes of turbidimetric titration obtained evidences stoichiometricity of the composition of polycomplexes.

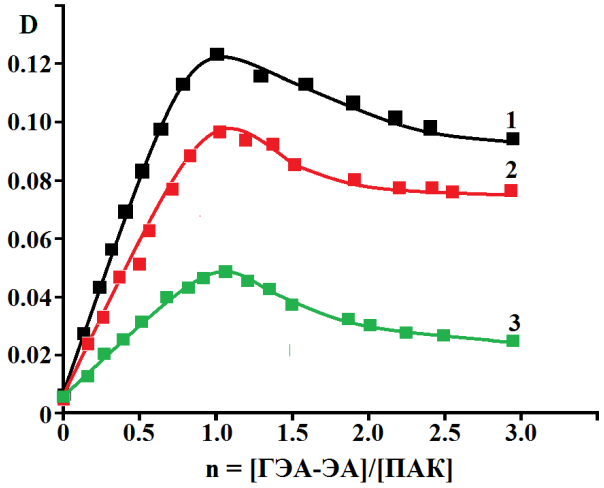

IMM [HEA]:[EA]=70:30 (1); 80:20 (2) mol.%;
PHEA(3); T=298 K;
MM (PAA)=250000; [HEA:EA]= [PAA]=0,01 M

Figure 1 – Turbidimetric titration of PAA solution with solutions of copolymers HEA-EA

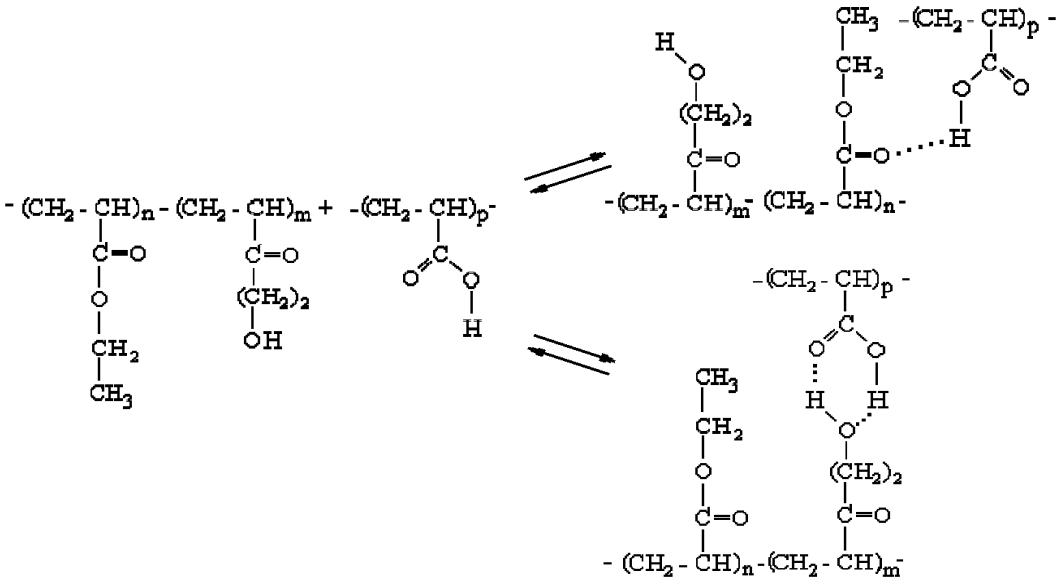

Scheme 1 – Scheme of interaction of linear copolymers based on HEA-EA with PAA

To confirm the formation of a hydrogen bond between the interacting polymers, IR spectra of polycomplexes and initial polymer components were recorded.

Figure 2 shows the IR spectra of the CPL HEA-EA, PAA and IPC on their basis. It can be seen from these figures that the characteristic bands in the IPC spectra are clearly related to the initial polymer components. In this case, a shift to the short-wavelength region (λ= 1731.7 cm^{-1}) is observed for the band belonging to the valence vibrations of the carbonyl group of PAA (λ = 1715.6 cm^{-1}), which is obviously due to the formation of a hydrogen bond between C = O carboxyl PAA and hydroxyl group of monomer units of HEA. Complexation of polymers by hydrogen bonding in aqueous solutions is accompanied by compacting of macromolecules with the precipitation of IPC.

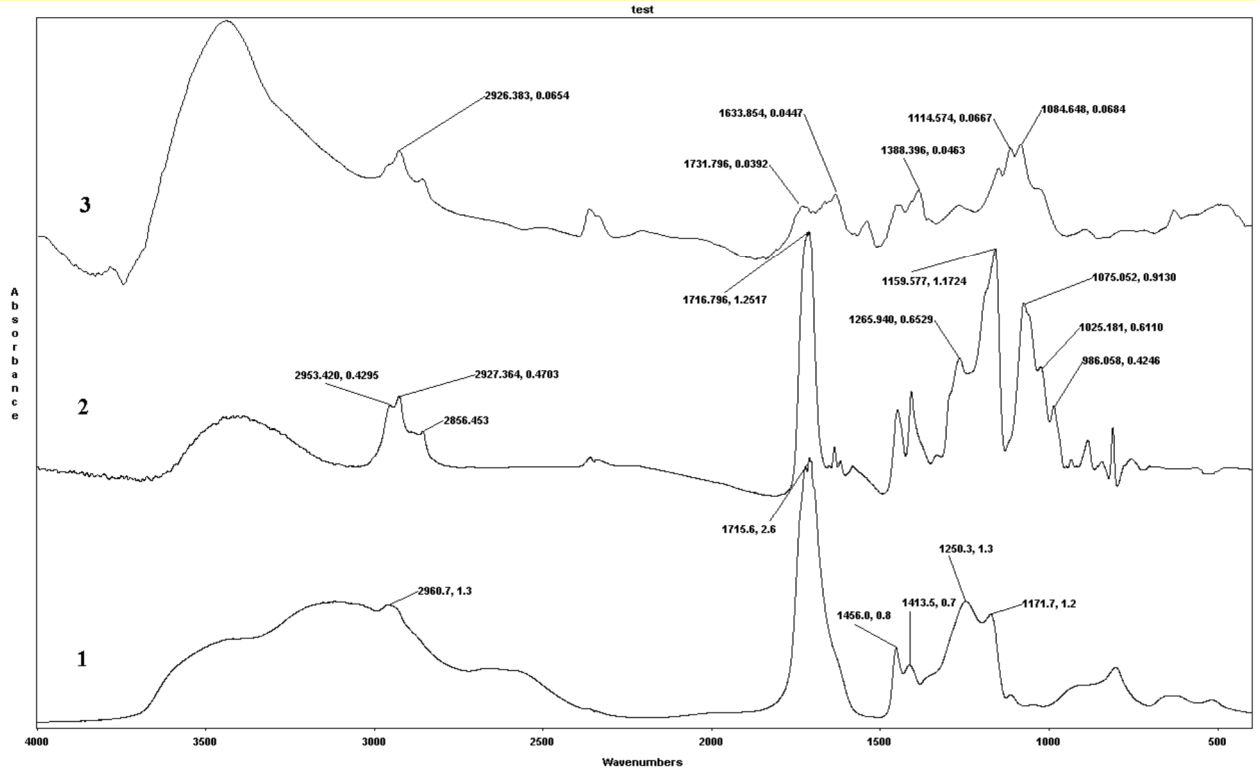

IR spectra: PAA (1); CPL HEA-EA (2); complex CPL HEA-EA – PAA (3).

Figure 2 – IR spectra of PAA, CPL HEA-EA и HEA-EA copolymers with PAA

The processes of formation of IPCs are characterized by critical phenomena. Significant changes in various parameters of the environment depend on the properties of the system. In addition, to form a polymer-polymer complex, the polymer must have a minimum critical size of functional groups in order to provide the required level of hydrogen bonding density between complementary macromolecules.

The critical pH of complex formation depends on the nature, concentration and ionic strength of the macromolecules that act, as well as the presence of various substances in the solution. The critical pH_c value is used as a quantitative criterion for the complex formation ability of a polycarboxylic acid-nonionic polymer system, in aqueous solutions. Its increase indicates that the interpolymer complex formation of macromolecules is enhanced. The cooperative nature of the process and, consequently, a sharp increase in the turbidity of the medium is observed below the critical pH of complexation (pH_c), first mentioned in the works of Tsuchida et al. [15] and a certain gravimetric method from the analysis of dry IPC samples of some polycarboxylic acids with polyethylene oxide.

For the quantitative evaluation of the complexing ability of HEA-EA copolymers with PAA we determined critical pH of complex formation (pH_c) (Figure 3-4). The sharp increase in optical density was found to be observed for the mixtures of the solutions of HEA-EA copolymers with PAA when reaching pH_c. It evidences the complex formation between polymers. At that when HEA content increases in the copolymer composition the value pH_c shifts to the region of lower values (from 2.8 to 3.2) which evidences the decrease in the system complexing ability conditioned by decreasing the contribution of hydrophobic interactions of EA components to the stabilization of polycomplexes. If the component of ethyl acrylate is increased in the copolymer, then the pH_c increases. This increases the process of the complex and creates high-strength complexes. (figure 5). The data obtained are well-agreed with the results of the paper [16-18].

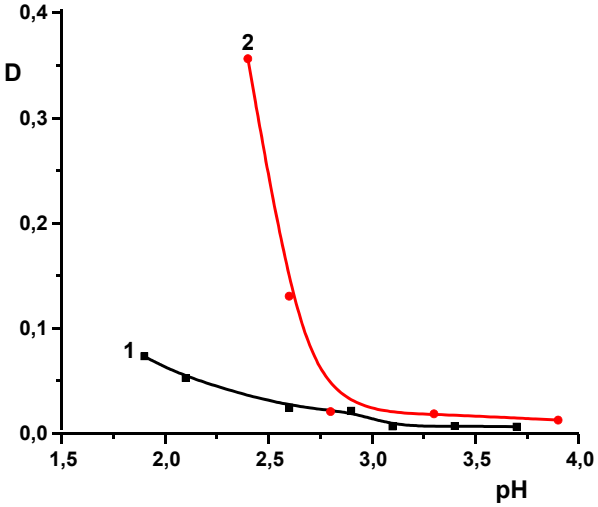

IMM [HEA]:[EA]=90:10 mol.%;
[PAA]=[HEA-EA]= 0.01 (1); 0.05% (2);
MM (PAA)=250000; [PAA]/[HEA-EA]=1:1

Figure 3 – Dependence of the optical density of aqueous solutions of mixtures CPL [HEA-EA]/ [PAA] on pH

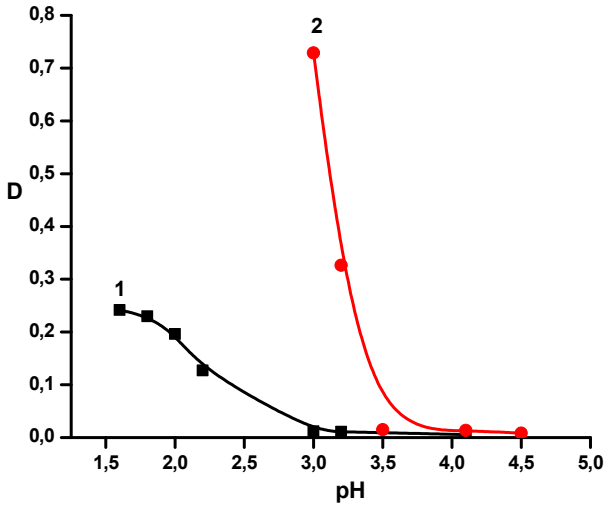

IMM [HEA]:[EA]=80:20 mol.%;
[PAA]=[HEA-EA]= 0.01 (1); 0.05% (2);
MM (PAA) = 250000; [PAA]/ [HEA-EA]= 1:1

Figure 4 – Dependence of the optical density of aqueous solutions of mixtures CPL [HEA-EA]/ [PAA] on pH

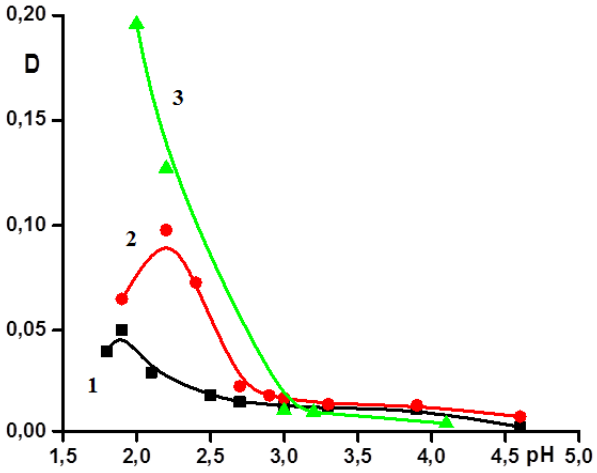

PHEA(1); IMM [HEA]:[EA]=90:10 (2); 80:20 (3) mol.%;
MM (PAA)=250000;
[PAA]/[HEA-EA]=1:1. [HEA-EA]=0.01%

Figure 5 – Dependence of the optical density of aqueous solutions of mixtures CPL [HEA-EA]/ [PAA] on pH

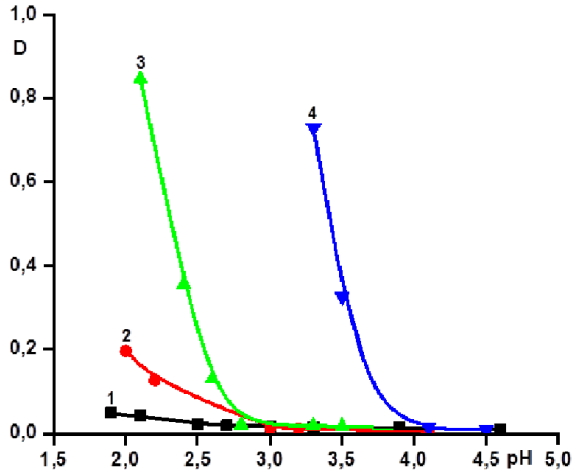

IMM [HEA]:[EA]=80:20 mol.%;
MM (PAA)=2000 (1); 100000 (2); 250000 (3); 750000 (4);
CPL [HEA-EA]/ [PAA]=1/1; [HEA-EA]= [PAA]=0.01%

Figure 6 – Dependence of the optical density of aqueous solutions of mixtures CPL [HEA-EA]/ [PAA] on pH

In the paper the influence of the molecular mass of polyacrylic acid on the interaction in HEA-EA copolymers–polycarboxylic acid was studied (Figure 6). The formation of isopoly was shown not be observed in the solution of copolymers when adding PAA with a macromolecule of 2000 which is well-agreed with the ideas of existing the lower limit of macrochain length during isopoly acid formation [17; 18]. When PAA macromolecule grows in the range of 100000-750000 the critical value of complex formation increases. This can be explained by an increase in the proportion of non-ionized carboxyl

groups, an increase in the effect of cooperativity, and an increase in the length of the macrochain, a decrease in the degree of ionization of the polyacid, and the formation of hydrogen bonds with nonionic polymers.

Conclusion

For the first time, complex formation of linear HEA-EA copolymer with linear PAA in the solutions was studied, the formation of polycomplxes stabilized by hydrogen bonds and hydrophobic interactions was identified. The efficiency of complex formation was shown to increase with rising the content of ethylacrylate in the composition of copolymers and PAA macromolecule mass.

References

1 Bekturov E.A., Bimendina L.A. (1981) Interpolymer Complexes. Adv. Polym. Sci., vol. 41, pp.99-147.

2 Tsuchida E., Abe K. (1982) Interactions Between Macromolecules in Solution and Intermacromolecular Complexes. Adv. Polym. Sci., vol. 45, pp.1-119.

3 Jiang M., Li M., Xiang M., Zhou H. (1999) Interpolymer Complexation and Miscibility Enhancement by Hydrogen Bonding. Adv. Polym. Sci., vol. 146, pp.121-196.

4 Nurkeeva Z.S., Mun G.A., Khutoryanskiy V.V. (2003) Interpolymer complexes of water-soluble nonionic polysaccharides with polycarboxylic acids and their applications. Macromol. Bioscience, vol. 3, pp.283-295.

5 Kabanov V.A., Papisov I.M. (1979) Complexation between complementary synthetically polymers and oligomers in dilute solutions. Polym. Sci., vol. 21, pp.243-281.

6 Bimendina L.A., Roganov V.V., Bekturov Ye.A. (1974) Hydrodynamic properties of complexes of polymethacrylic acid – polyvinylpyrrolidone in solutions. Polym. Sci. USSR., vol. 16, pp. 3274-3279.

7 Tirosh B., Baluom M., Nassar T., Friedman M., Rubinstein A. (1997) The effect of Eudragit RL-100 on the mechanical and mucoadhesion properties of polycarbophil dosage forms. J. Contr. Rel., vol. 45, pp.57-64.

8 Ozeki T., Yuasa H., Kanaya Y. (2000) Controlled release from solid dispersion composed of poly(ethylene oxide)–Carbopol® interpolymer complex with various cross-linking degrees of Carbopol®. J. Contr. Rel., vol. 63, pp.287-295.

9 Lele B.S., Hoffman A.S. (2000) Mucoadhesive drug carriers based on complexes of poly(acrylic acid) and PEGylated drugs having hydrolysable PEG-anhydride-drug linkages. J. Contr. Rel., vol. 69, pp.237-248.

10 Shojaei A.H., Li X. (1997) Mechanisms of buccal mucoadhesion of novel copolymers of acrylic acid and polyethylene glycol monomethylether monomethacrylate. J. Contr. Rel., vol. 47, pp.151-161.

11 Mun G.A., Khutoryanskiy V.V., Nurkeeva Z.S., Urkimbaeva P.I., Zhunuspaev D. (2004) Stabilization of water/n-hexane emulsions by amphiphilic copolymers based on vinyl ethers and their polycomplexes with poly(acrylic acid). J. Polym. Sci. Part B, Polym. Phys., vol. 42, pp. 2625-2632.

12 Rivas B.L., Moreno-Villoslada I. (1998) Chelation properties of polymer complexes of poly(acrylic acid) with poly(acrylamide), and poly(acrylic acid) with poly(N,N-dimethylacrylamide). Macromol. Chem. Phys., vol. 199, pp.1153-1160.

13 Rakhmetullayeva R.K., Mun G.A.., Shaikhutdinov E.M., Nakan U., Bagitova Zh.K. (2013) Semi-interpenetrating network based on N-isopropylacrylamide. Chemical Bulletin of Kazakh National University, chemical series, vol. 2, pp. 49–57.

14 Nakan U., Rakhmetullayeve R.K., Urkimbaeva P.I., Shaikhutdinov E.M., Mun G.A., Yeligbayeva G. Zh., Negim E.S.M. (2014) The Effect of Nanoparticle Silver on the Thermal Stability of N-isopropylacrylamide (NIPAAm). World Applied Sciences Journal., vol. 29, pp. 359-364.

15 Tsuchida E., Abe K. (1982) Interactions between macromolecules in solution andintermolecular complexes. Adv. Polym. Sci., vol. 45, pp. 1-125.

16 Bagitova Zh.K.., Rakhmetullayeva R.K., Nakan U., Mun G.A.., Shaikhutdinov E.M. (2014) Polycomplex based on copolymers of N-isopropylacrylamide and polyacrylic acid. The Sixth All-Russia Kargin Conference “Polymers -2014”, p.874.

17 Khutoryanskiy V.V., Maria G. C., Luigi L., Nicoletta B., Nurkeeva Z.S., Mun G.A., Dubolazov A.V. (2004) Morphological and thermal characterization of interpolymer complexes and blends based on poly(acrylic acid) and hydroxypropylcellulose. Polym. Int., vol. 53, pp.307-311.

18 Khutoryanskiy V.V., Mun G.A., Nurkeeva Z.S., Dubolazov A.V. (2004) pH and salt effects on interpolymer complexation via hydrogen bonding in aqueous solutions. Polym. Int., vol. 53, pp.1382-1387.

IRSTI 31.21.15

[1]Zh.Zh. Akzhigitova, [1]A.M. Baiseitova, [2]Yang Ye, [1]J. Jenis

[1]Division of Applied Life Science (BK21 plus), Gyeongsang National University, Jinju, Korea
[2]Shanghai Institute of Materia Medica, Chinese Academy of Science, Shanghai, China
*e-mail: janarjenis@mail.ru

Investigation of chemical constituents of *Artemisia absinthium*

Abstract: The aerial part of *Artemisia absinthium,* collected in Almaty region of Kazakhstan, investigated for chemical constituent with sufficiently completed quantitative and qualitative analysis. Biological active constituents such as organic acid (1.08%) and flavonoids (0.52%) together with the moisture content (7.14%), total ash (6.4%), and extractives (12.82%) of plant *A. absinthium* were determined. In the ash of the plant was found 8 macro-micro elements, main of them was K (417.930 μg/ml), Ca (116.0225 μg/ml), Mg (26.2250 μg/ml), Na (15.9825 μg/ml) by using the method of multi-element atomic emission spectral analysis at the Institute of Combustion Problems. Additionally, twenty amino acids and eight fatty acids were identified from *A. absinthium.* As the results showed that the major contents of amino acids were glutamate (2380 mg/100g), aspartate (1200 mg/100g) and alanine (712 mg/100g), and main contents of fatty acids were linoleic (44.8%) and oleic (30%) acids, relatively.
Key words: *Artemisia absinthium,* bioactive constituents, macro-micro elements, amino and fatty acids.

Introduction

The tribe Anthemideae of the family Compositae includes about sixty genera and over nine hundred species. The largest and most widely spread through the world of these is the genus *Artemisia*, also known as wormwood, comprising four hundred species [1]. *Artemisia* species is described in pharmacopoeia books in many countries around the world [2]. *A. absinthium* L. is used for the treatment of various inflammatory diseases, including chronic bronchitis, asthma, gastroenteritis and pruritus [3]. The aerial part of *A. absinthium* L. has shown to possess anti snake venom activity [4]. Antimalarial and anticancer activities are among the prominent biological effects reported for different species of the genus *Artemisia* [5]. For instance, a Chinese researcher, Tu Youyou, won her Nobel prize in Medicine for a drug, which she developed to treat malaria from herb plant *Artemisia annua*, or sweet wormwood [6].

Compounds of absinthin, artabsin and guainolides *are* main constituents of *A. absinthium* which is bitter tonic, aromatic, anthelmintic, stomachic, antiparasitic, antiseptic and choleretic, carminative medicinal plant and also possessing anti-inflammatory and mild antidepressant activities. The effectiveness of wormwood as an aromatic bitter and its antimicrobial properties come from the bitter compounds and its essential oil. The oil of the plant can be used as a cardiac stimulant to improve blood circulation. Pure wormwood oil is very poisonous, but with proper dosage poses little or no danger [7].

In the present study, the quantitative and qualitative analysis of phytochemical constituents of medicinal plant *A. absinthium* which grown in Almaty region of Kazakhstan have been made for the first time.

Materials and methods

Plant material

The aerial part of plant material *A. absinthium* was collected in Almaty region Kazakhstan in September, 2017. The botanical identification was made by Dr. Alibek Ydyrys, The Herbarium of Laboratory Plant Biomorphology, Faculty of Biology and Biotechnology, Al-Farabi Kazakh National University, Almaty, Kazakhstan. The air dried aerial part of *A. absinthium* was cutted into small pieces and stored at room temperature.

Quantitative and qualitative analysis

The quantitative and qualitative analysis of biologically active constituents of the plant were made

according to methods reported in the State Pharmacopeia XI edition techniques of RK.

Macro-micro elemental composition

In The Institute of Combustion Problems using the method of multi-element atomic emission spectral analysis in the ash of *A. absinthium* was analyzed elemental constituents. To determine the mineral composition of ashes was used Shimadzu 6200 series spectrometer.

Fatty acid composition

Determination of fatty acid composition of the plant *A. absinthium* extracted with a chloroform-methanol mixture (2:1) for 5 minutes, the extract is filtered through a paper filter and concentrated to dryness. Then, to taked extract add 10 ml of methanol and 2-3 drops of acetyl chloride and further methylation at 60-70° C in a special system for 30 minutes. The methanol is removed by rotary evaporation and the samples are extracted with 5 ml of hexane and analyzed using a gas chromatograph "CARLO-ERBA-420" allocated the Kazakh Academy of Nutrition for 1 hour. As a result, chromatograms of methyl esters of fatty acids were obtained. By comparison with reliable samples by the time of exit from the column, eight fatty acids were identified.

Amino acid composition

To determine the amino acids composition was made erenow [14] of the raw material used GS/MS device. GS/MS analysis: of *A. absinthium* were analyzed by Gas Chromatograph coupled to Mass Spectrometer using polar mixture of 0.31% carbowax 20 m, 0.28% silar 5 CP and 0.06% lexan in chromosorb WA-W-120-140 mesh, column (400x3 mm). The column temperature was programmed from 110°C (held for 20 min), at 6°C/min from 110°C to 180°C, at 32°C/min from 185°C to 290°C. When it reaches to 250°C, it should stay constant till fishing of exit of all amino acids. The chromatogram is counted according to an external standard.

Results and discussion

Quantitative and qualitative analysis

The quantitative and qualitative analysis of biologically active constituents itemizing moisture content, total ash, extractives contents were determined from aerial part of *A. absinthium.*The results shown in Table-1.

The amount of ash in plant raw materials varies within certain limits and depends on the specific nature of the raw material itself, the way it is collected and the drying conditions. Significant deviations usually indicate the contamination of raw materials with a mineral admixture or the untimely collection of raw materials and etc.

The complex of organic and inorganic substances extracted from plant raw materials by an appropriate solvent and quantitatively determined as a dry residue is conventionally called the extractive substances of medicinal plant matter. The content of extractive substances in medicinal plant raw materials is an important numerical indicator that determines its good quality for the content of biological metabolites. Typically, a solvent is used for a tincture or extract from this raw material that is more advantageous in preparation.

Organic acids play an important role in maintaining the acid-base balance of the human body. Organic substances increase the pH level of the medium, which improves the absorption of nutrients by internal organs and the excretion of slags.

Flavonoids – a group of useful plant substances, when ingested in human body with food, has an effect on the activity of enzymes. As medicines are very widespread in both traditional and traditional medicine. The therapeutic value of these unique biologically active substances is difficult to assess. They have an antioxidant effect, due to this, the body recovers. It has been scientifically proven that there is a direct correlation between cardiovascular diseases and daily consumption of flavonoids – the mortality rate is 5 times less.

Table 1 – Quantitative analysis of bioactive constituents of aerial part of *A. absinthium*

Content, %				
Moisture content	Ash	Extractives	Organic acids	Flavonoids
7.14	6.4	12.82	1.08	0.52

Macro-micro elemental composition

In the ash of *A. absinthium* were determined eight macro- and microelements, showed in Table 2 and Figure 1.

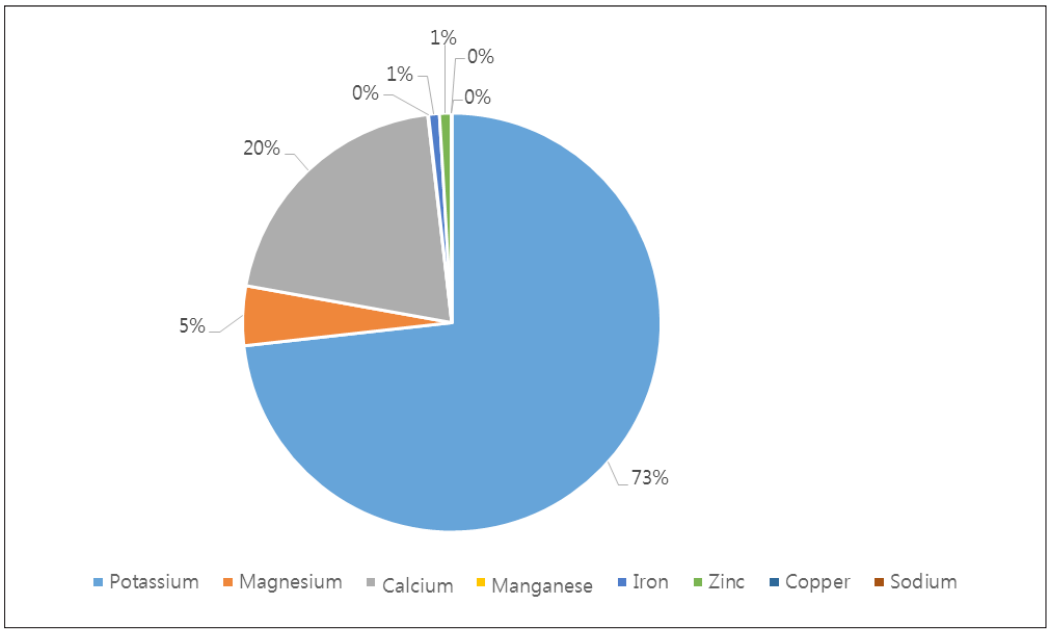

Figure 1 – Percentage contents of macro- and micro elements in ash of *A. absinthium*

Table 2 – Composition of macro-micro elements in the ash of plant *A. absinthium*

Element	K	Mg	Ca	Mn	Fe	Zn	Cu	Na
µg/ml	417.930	26.2250	116.0225	0.3317	4.7662	5.2564	0.1471	15.825

Trace elements are necessary for living organisms to ensure normal life activity. With a lack of potassium, there are disruptions in the work of the heart and skeletal musculature. Prolonged potassium deficiency can cause acute neuralgia. Prolonged deficiency of calcium and vitamin D in the diet leads to an increased risk of osteoporosis, and in infancy causes rickets. In living organisms, iron is an important microelement that catalyzes the processes of oxygen exchange (respiration). The main intracellular depot of iron is the globular protein complex – ferritin. Lack of iron is manifested as a disease of the body: chlorosis in plants and anemia in animals. Zinc is essential for the production of sperm and male hormones, is essential for the metabolism of vitamin E, is important for the normal functioning of the prostate, is involved in the synthesis of various anabolic hormones in the body, including insulin, testosterone and growth hormone, is necessary for the breakdown of alcohol in the body, alcohol dehydrogenase. Magnesium is necessary in maintaining the normal function of the nervous system and heart muscle, has a vasodilating effect, stimulates bile secretion, and increases the motor activity of the intestines, which helps to eliminate cholesterol from the body.

Fatty acid composition

The major fatty acids which is contained in *A. absinthium* were linoleic acid (44.8%) and Oleic acid (30%).

Table 3 – Fatty acids from *A. absinthium*

№	Fatty acids	Molecular formula	Structure	MW	Amount in plant, %
1	Meristic acid $C_{14:0}$	$C_{14}H_{28}O_2$	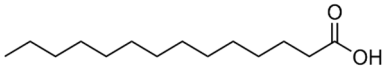	228	2.3

Continuation of table 3

№	Fatty acids	Molecular formula	Structure	MW	Amount in plant, %
2	Pentadecanoic acid $C_{15:0}$	$C_{15}H_{30}O_2$	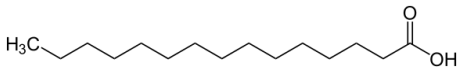	242	2.1
3	Palmitic acid $C_{16:0}$	$C_{16}H_{32}O_2$	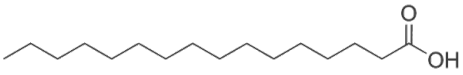	256	14.3
4	Palmitoleic acid $C_{16:1}$	$C_{16}H_{30}O_2$	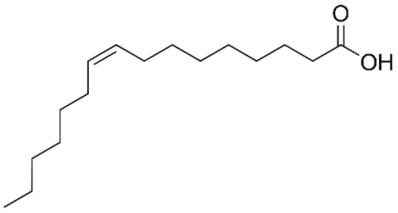	254	1.2
5	Stearin acid $C_{18:0}$	$C_{18}H_{36}O_2$	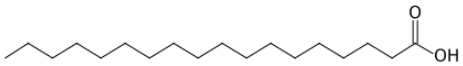	284	4.6
6	Oleic acid $C_{18:1}$	$C_{18}H_{34}O_2$	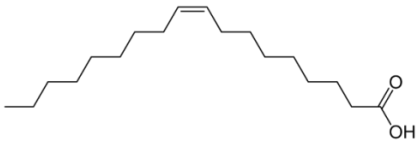	282	30
7	Linoleic acid $C_{18:2}$	$C_{18}H_{32}O_2$	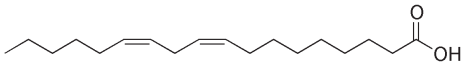	280	44.8
8	Linolenic acid $C_{18:}3$	$C_{18}H_{30}O_2$	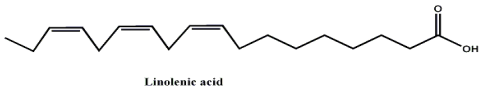 Linolenic acid	278	0.7

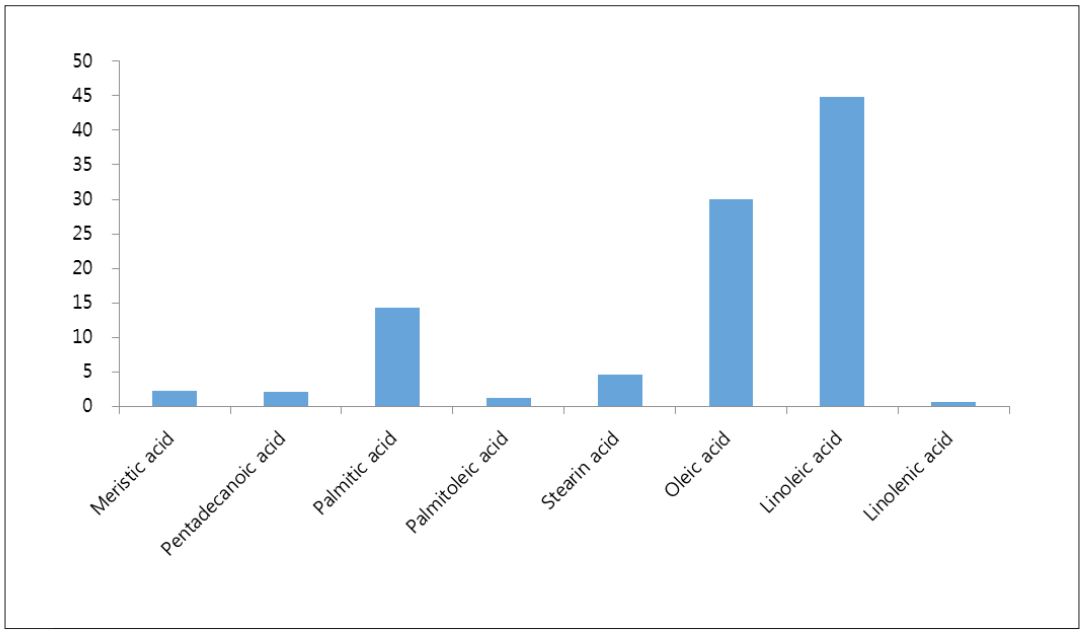

Figure 2 – Fatty acid contents of *A. absinthium*

Linoleic acid has received much attention in recent years because of its interesting biological benefits. The main health effects described for linoleic acid include reduction of carcinogenesis, atherosclerosis, inflammation, obesity, diabetes, as well as growth promoting and bone formation-promoting properties [9]. Oleic acid can inhibit the progression of diseases affecting the brain and adrenal glands, as well as improve memory and reduce blood pressure, but there is evidence that the substance can provoke cancer, in particular breast cancer [10].

Amino acid composition

In the composition of amino acids mainly were glutamate (2380 mg/100g), aspartate (12 mg/100g) and alanine (712 mg/100g).

Table 4 – Amino acid contents of from *A. absinthium*

№	Amino acids	Molecular formula	Structure	MW	Amount in plant, mg/100g
1	Alanine	$C_3H_7NO_2$	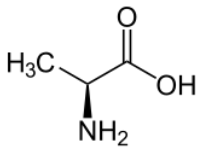	89	712
2	Glycine	$C_2H_5NO_2$	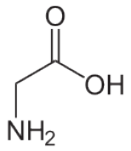	75	340
3	Leucine	$C_6H_{13}NO_2$	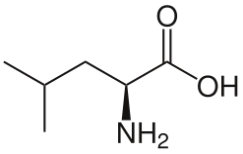	131	326
4	Isoleucine	$C_6H_{13}NO_2$	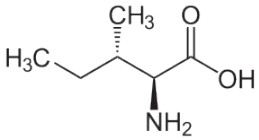	131	315
5	Valine	$C_5H_{11}NO_2$	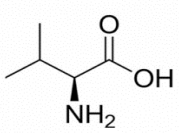	117	286
6	Glutamate	$C_5H_9NO_4$	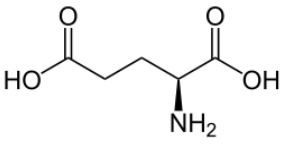	147	2380
7	Threonine	$C_4H_9NO_3$	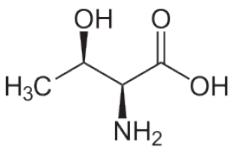	119	280

Continuation of table 3

№	Amino acids	Molecular formula	Structure	MW	Amount in plant, mg/100g
8	Proline	$C_5H_9NO_2$	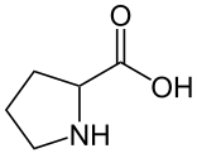	115	596
9	Methionine	$C_5H_{11}NO_2S$	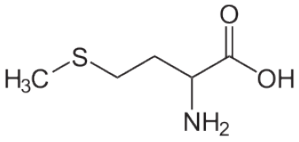	149	60
10	Serine	$C_3H_7NO_3$	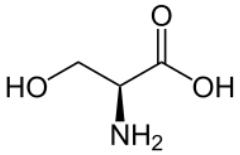	105	406
11	Aspartate	$C_4H_7NO_4$	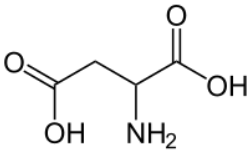	133	1200
12	Cysteine	$C_3H_7NO_2S$	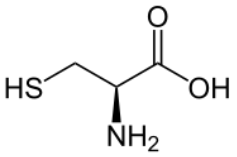	121	1
13	Oxyproline	$C_5H_9NO_3$	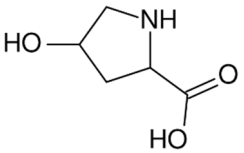	131	1
14	Phenylalanine	$C_9H_{11}NO_2$	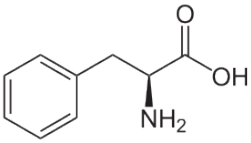	165	328
15	Tyrosine	$C_9H_{11}NO_3$	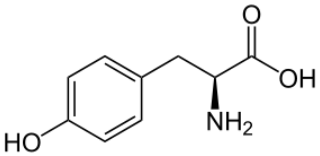	181	364
16	Histidine	$C_6H_9N_3O_2$	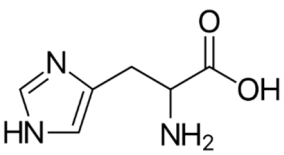	155	188

Continuation of table 3

№	Amino acids	Molecular formula	Structure	MW	Amount in plant, mg/100g
17	Ornithine	$C_5H_{12}N_2O_2$	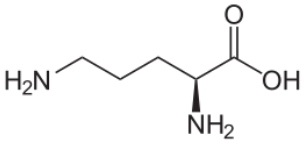	132	1
18	Arginine	$C_6H_{14}N_4O_2$	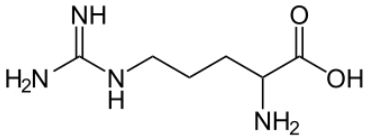	174	505
19	Lysine	$C_6H_{14}N_2O_2$	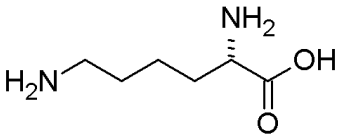	146	140
20	Tryptophan	$C_{11}H_{12}N_2O_2$	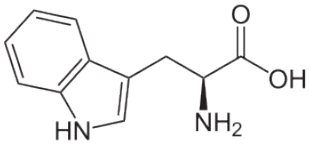	204	80

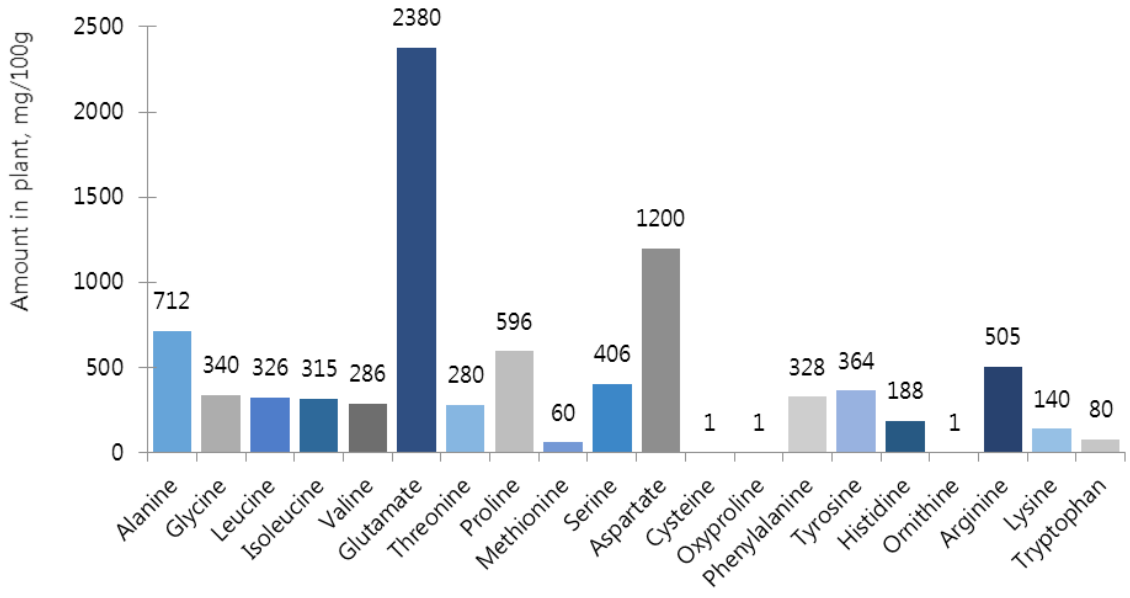

Figure 3 – Amino acid contents of plant *A. absinthium*

Glutamate is a nonessential amino acid, a major bioenergetic substrate for proliferating normal and neoplastic cells, and an excitatory neurotransmitter that is actively involved in biosynthetic, bioenergetic, metabolic, and oncogenic signaling pathways [11]. Aspartic acid increases immunity, metabolism, deactivates ammonia, participates in the formation of ribonucleic acids, promotes the removal of chemicals, including drugs, restores working capacity. Studies conducted by scientists have proved the effectiveness of taking asparaginic acid preparations for increasing testosterone levels. Aspartic acid is taken as an additive by bodybuilding athletes to improve strength, increase libido and testosterone in the blood [12]. Alanine plays a significant role in metabolic processes, as well as to regulate the level of sugar in the bloodstream. This amino acid protects against the development of cancer of the pancreas and prostate gland, it is an important part of sports nutrition, increases physical endurance and allows to build muscle mass [13].

Conclusion

In conclusion, quantitative and qualitative analysis of total bioactive constituents and the moisture, total ash, and extractives contents of *A. absinthium* were determined. Besides, macro-micro elements in the ash of the medicinal plant were investigated, and total eight macro-micro elements were identified by the method of multi-element atomic emission spectral analysis. Meanwhile, twenty amino and eight fatty acids were determined from *A. absinthium*. The results showed that the major contents of amino acids were glutamate (2380 mg/100g), aspartate (1200 mg/100g) and alanine (712 mg/100g), and main contents of fatty acids were linoleic (44.8%) and oleic (30%) acids, relatively.

A. absinthium has lots of medicinal properties and main of them are killing cancer cells, getting rid of parasites and treating Crohn's disease and SIBO (Small intestinal bacterial overgrowth). In addition, it has antimicrobial and antifungal abilities. Absinthin, an extract isolated from wormwood, is the most powerful antimalarial available and by this activity was invented as a drug.

Acknowledgements

The work was supported by grants from Ministry of Education and Science of the Republic of Kazakhstan (0118PK00458).

References

1 Geissman T. A., lrwin M. A. (2000) Chemical contributions to taxonomy and phylogeny in the genus Artemisia, pp.167-180.

2 Omera B., Krebsb S., Omerc H., Noord T.O. (2007) Steroid-sparing effect of wormwood (Artemisia absinthium) in Crohn's disease:A double-blind placebo-controlled study. Phytomedicine, pp.87-95.

3 Ke W. Z., Li X. L., Xiao M. S., Hai N. L., Fang J. S., Qian Y., Xin D., Yong J., Peng F. (2015) Caruifolin D from artemisia absinthium L. inhibits neuroinflammation via reactive oxygen species-dependent c-jun N-terminal kinase and protein kinase c/NF-κB signaling pathways. European Journal of Pharmacology, pp.82-93.

4 Nalbantsoy A., Erel S.B., Köksal C., Göcmen B., Yıldız M.Z., Karabay Y.N. (2013) Viper Venom induced inflammation with Montivipera xanthina (Gray, 1849) and theanti-snake venom activities of Artemisia absinthium L. in Rat. Toxicon, vol. 65, pp. 34–40

5 Mohammad A., Bilal H. A., Ihsan-ul-haq. (2013) Department. Production of commercially important secondary metabolitesand antioxidant activity in cell suspension cultures of Artemisia absinthium L. Industrial Crops and Products, pp. 400-406

6 "The Nobel Prize in Physiology or Medicine 2015" (PDF). Nobel Foundation. Retrieved 7 October 2015.

7 Mahboubeh T. (2014) Mutagenic and antimutagenic activities of Artemisia absinthium volatile oil by the bacterial reverse mutation assay in Salmonella typhimurium strains TA98 and TA100. Asian Pacific Journal of Tropical Disease, pp. S840-S844

8 Szymczycha-Madeja A, Welna M, Pohl P. (2012) Elemental analysis of teas and their infusions by spectrometric methods. TrAC Trends in Analytical Chemistry, vol. 5, pp. 165-181.

9 Yang B, Chen H, Stanton C, Ross RP, Zhang H, Chen YQ, Chen W. (2015) Review of the roles of conjugated linoleic acid in health and disease. Journal of Functional Foods, vol. 15, p. 314-325.

10 Bowen K.J., Kris-Ethertona P.M., Shearera G.S., Westa Sh.G., Reddivaric L., Jones P.J. (2017) Oleic acid-derived oleoylethanolamide: A nutritional science perspective. Progress in Lipid Research, vol. 67, pp. 1-15.

11 Stacey S. W., Shahriar K. G. (2013) Glutamate Receptors, and Downstream Signaling Path-

ways. International Journal of Biological Sciences, pp .948-959

12 Katane M, Kanazawa R, Kobayashi R, Oishi M, Nakayama K, Saitoh Y, Miyamoto T, Sekine M, Homma H. (2017) Structure–function relationships in human D-aspartate oxidase: characterisation of variants corresponding to known single nucleotide polymorphisms . BBA - Proteins and Proteomics, vol. 1865, pp. 1129-1140.

13 Liu L, Chen Y, Yang L. (2014) Inhibition study of alanine aminotransferase enzyme using sequential online capillary electrophoresis analysis. Analytical Biochemistry, vol. 467, pp. 28-30.

IRSTI 31.19.29

[1*]A.A. Kapar, [1]M.B. Alimzhanova, [2]M.M. Sergazina, [3]A.P. Abdykarimova

[1]Department of analytical chemistry, al-Farabi Kazakh National University, Almaty, Kazakhstan
[2]Kazakh National Pedagogical University named after Abay, Almaty, Kazakhstan
[3]Almaty Technical University, Almaty, Kazakhstan
[*]e-mail: anelyakapar@gmail.com

Determination of hazardous components in dairy products by chromatographic methods: a review

Abstract: Milk and dairy products takes an important place in human nutrition, being indispensable source of favorably balanced and easily digestible proteins, fats, carbohydrates, minerals and vitamins. Furthermore, it is a raw material for many dairy products, such as yoghurt, cheese, kefir and etc. Before the consuming of ready milk, it goes through production, circulation and processing. Each step reaches potentially unsafe factors, influencing to its chemical contamination that can affect milk quality. For the present time methods of determination the consistency of milk and milk products are sufficient. However not all methods are convenient and economically available to analyze dairy products with a high accuracy and expressively. During the research was collected the most effective analyzes of milk production due to the international sources data and it was approved that chromatography methods allow identifying hazardous components in dairy products through sensitive, less time-consuming and cheap analysis, than traditional methods that is particularly important for milk, which is a highly perishable food. It was established that according to complex compound of dairy products, 80 percent approximately of all researches were provided by gas chromatography and high performance of liquid chromatography methods which are highly sensible. This article reviews the essential chromatographic methods for the determination of harmful components in milk and dairy products approaching a special focus on sample preparation.
Key words: milk products, chromatography, gas chromatography, high performance of liquid chromatography.

Introduction

Milk and dairy products contribute an important role to human body. They are considered as the source of variety of nutrients, and influence on the exchange of calcium and phosphorus. Due to its medical properties, Avicenna used milk to treat many people and he had proved that cow's milk is the most suitable in treatment of humans [1]. Calcium in milk strengthens our bones and teeth; vitamins such as B2 and B12 cause effective metabolism and nerve function [2].

Demand for dairy products growth every year with the increasing population, and production of dairy products is increased respectively. But there is a great responsibility and resources are needed to produce a high qualitative milk product in big quantities. For example, with the aim of increasing the production rate of milk, all female ruminants are often treated with various kinds of medicines (e.g., antibiotics, urea, and hormones). In addition, animal feed is also subject to contamination, that source is considered to be different pesticide sprays that are used on the same farm. Thereby, bovines are endangered by various types and sources of anthropogenic contaminants, which, consequently, have a high possibility to remove to the milk [3].

The rations of ruminants usually consist of roughage, juicy and concentrated fodder, receiving by the technology of conservation of wet forage. Ruminant animals that consume plant food are more likely to be at the danger from exposure of mycotoxins, compared to animals that do not consume fodder grasses and their derivatives. Physiological and anatomical features of the digestive tract of ruminants determine the active metabolism of mycotoxins that transfers with feeds. It should also be taken into account that mycotoxin metabolites formed in the rumen can be more toxic in comparison with the original contaminants. For example, metabolite aflatoxin B1, such as aflatoxicol and aflatoxin M1 (AFM1) can be detected in milk after a few hours. The maximum concentra-

 Printed in Kazakhstan

tion in milk is observed after 24 hours. These results confirm the rapid absorption and metabolism of aflatoxins in the body of ruminants [4].

Other sources that decrease the quality of milk and may effect on the human body negatively: condition of technology of milk production. The process of technology is valuable part where all steps and additives are responsible for the quality of milk [12]. For instance, common hazardous materials may be assumed as unhygienic water, salt, blotting paper, melamine, caustic soda, urea, hydrogen peroxide, formalin, and others. In addition, in cattle farming a large amount of stimulus chemicals are injected routinely into the body of the ruminants to promote more milk production. These chemicals are then secreted along with the milk and may not be removed during pasteurization [5].

Also the harmful things in contamination of milk that transform it into cheap and available products can be chemicals such as emulsifiers, flavorings, colorants preservatives that are able to replace the natural products [3].

The milk market reaches in Kazakhstan today, the variety and quantity of production of milk products grows year by year [6]. However not all dairy contamination is detailed completely that concern scientists.

Many scientists consider the method of chromatography detection is the most suitable for the analysis of dairy products. In this review variety chromatography methods are presented with consideration of different sample preparation.

The analyzes of dairy products by chromatographic methods are given in Tables 1-6.

Table 1 – Determination of melamine in dairy products by chromatographic methods

№	Techniques	Products analyzed	Condition of analysis	Sample preparation	Reference
1	LPME-HPLC	Milk	2.0-5.8 ng mL−1 42 ., YL 9120 UV-Vis detector, column C18 (Hector, 5 μm, 250 mm × 4.6 mm	All the samples were dissolved in hot (40 °C)	[7]
2	HPLC	Milk, milk products	column 5 μm, 250 mm×4.6 mm	0.5 g sample + diethyl-water-ACN 10:40:50, t = 30 min, 200 mcl al., t=70°C + Sylon-BFT solution	[8]
3	HPLC	Milk, milk products	5 μm, 250 mm × 4.6 mm column	10 g sample + water, t = 10 min ultrasonic bath	[9]
4	C-gel fitation	Milk	Superdex 75 10/300GL column 10 × 300 mm and Superdex 200 10/300GL column 10 × 300 mm	10 g sample + 1.0 mL 0.1 M NaOH + water 100 mL, filtration	[10]
5	HPLC – derivatization by LLME	Milk	Supelcosil LC-18: 25cm × 146 4.6 mm, 5μm column	8.0 ml of 5% (w/v) trichloroacetic acid + 1.0 ml of 2.2% (w/v) lead acetate + 1.0 g of each homogenized raw milk, the mixed solution was centrifuged 163 for 10 min at 10,000 rpm	[49]
6	HPLC-FD	Milk	A Zorbax SB-C18 (150 mm× 4.6 mm, 5 mm) column connected to a Zorbax ODS (12.5mm×4.6 mm, 5 mm) pre-column	70 ml glacial acetic acid (HOAc) + 10 ml sample + 3 ml of ultrapure water. The resulting mixture (pH ¼ 4.6) was vortex-mixed for 3 min, centrifuged at 6000 rpm (2.012 g) for 10 min	[50]

Table 2 – Determination of antibiotics in dairy products by chromatographic methods

№	Techniques	Products analyzed	Analyte	Condition of analysis	Sample preparation	Reference
1	UHPLC-MS	Milk	β-lactam, macrolide, amide alcohol, forest amine	HSS T3 column (2.1 mm × 100 mm × 1.8 μm), scan range was m/z 100-1000.	1 ml sample + 4 ml CAN t=30 sec 3000 rpm t=10 min was centrifuged + 4,5 ml supernatant on SPE.	[11]

Continuation of table 2

№	Techniques	Products analyzed	Analyte	Condition of analysis	Sample preparation	Reference
2	LC-MS	Milk, cheese	Dicecyldimethyl, ammonium, chloride	Fusion-RP 80A column (75 mm × 2.00 mm, 4 m), cal: 5, 10, 20, 50, 100 and 150 g kg^{-1}	1 g sample + 10 ml deuterated solution + 20 ml (98-100%) HCOOH + 9 ml ACN / EtAc – 50:50 + 2 g $MgSO_4$	[12]
3	UHPLC-MS	Milk	Neomycin, genemycin, hygromycin, gouromycin	HILIC column, flow rate of 0.5 mL min^{-1} .	2 g sample + 250 µL CH_3OOH (15%) t=5 min was centrifuged +3.5 mL of 50 mM potassium phosphate buffer at pH 7.0	[13]
4	UHPLC	Milk	Theophylline, paracetamol	C18 column (250 mm x 4 mm; particle size 5 µm) and C18 pre-column (4 mm x 4 mm; particle size 5 µm)	0,1 g sample 2000 rpm t=10 min was centrifuged + 20 µL supernatant on SPE	[14]
5	GC-MS UHPLC	Milk	Diethyl phthalate bis(2-butoxyethyl) phthalate bis (2-ethylhexyl) phthalate	30 m × 0.32 mm i.d., 0.25-µm film DB-5 fused-silica capillary column	5,0 g sample +1,0 ml 10% CH_3OOH, t=10 min sand heating, 0,45 µm nylon filter. 5 ml filtrate + 1.0 ml ethylacetate by 3 times extracted + 0.5 ml methanol	[15]
6	LC-Q-Orbitrap-MS	Milk	Diethyl phthalate bis(2-butoxyethyl) phthalate bis (2-ethylhexyl) phthalate	C-18 aQ connected to a 10 mm × 2.1 mm, Accucore C-18 aQ guard column	15 f sample + 1% CH_3OOH + 10 ml MeCN + MgSO4 (6 g), + NaAc (1,45 g) t=5 min 4000 rpm was centrifuged + 1,2 g $MgSO_4$, 405 mg PSA and 95 mg C_{18}	[16]
7	LC-FD	Milk	CIP, LOM, DAN, FLE, OFL, ENR, NOR, MAR, LEV, ORB, FLU	C18 column (150 × 4.6 mm i.d., 6 µm) with gradient elution.	4.0 g sample into 10 ml polypropylene centrifuge tube + standard working solution. Then, the samples stand in the dark for 30 min at room temperature before centrifugation for 10 min at 10000 rpm	[51]
8	LC-MS	Milk	Enrofloxacin, Ciprofloxacin, Difloxacin, Danofloxacin, Sarafloxacin	C18 column (75 mm 4.6 mm; 3.5 mm particle diameter) from Waters. A Phenomenex C18 column (4.0 mm 3.0 mm)	5 ml sample + 6 ml ACN (0.1% formic acid). The mixture was vortexed again and kept at low temperature (20°C) for 30 min, tubes were centrifuged for 30 min at 12,000 rpm	[52]
9	SPME-GC-MS	Milk, milk products	NPX, KPF, TLF	J&W DB-5MS capillary column with dimensions of 30 m × 0.25 mm i.d., 0.25 m film thickness	To all samples 10 mL of ACN and 2 g of NaCl were added. The tubes were shaken in a vortex-mixer for 60 s and centrifuged at 5000 rpm for 15 min, at 5 ◦C	[56]
10	UHPLC-MS	Milk products	Nitroimidazoles, benzimidazoles, and chloramphenicol	C18 column (50 mm 2.1 mm i.d., 1.7 lm particle size)	1 g of sample + 3 ml of acetonitrile + 2 g NaCl were added and vortexed for 1 min. The mixture was centrifuged for 5 min at 10000 rpm, 4 C.	[61]

Table 3 – Determination of amino acids in dairy products by chromatographic methods

№	Techniques	Products analyzed	Analyte	Condition of analysis	Sample preparation	Reference
1	LC-Q-TOF-MS/MS	Milk	Glycinin G1 / G2, glycinin G20, glycinin G4 – allergic proteins	QTrap 4000 LC-MS/ MS system	Washed samples with ethanol were homogenized in 0.1 mol/L of aqueous ammonium 158 bicarbonate at 9500 rpm 159 for 2 × 20 s, followed by 13,500 rpm for 30 s and then, vacuum-dried using a CentriVap 160 micro IR.	[17]
2	LC-MS	Yoghurt	β-casomorphin	C18 column 100 mm × 2.1 mm, 100Å, 2.6 µm particle diameter with a guard column (2.1 mm x 10 mm)	Ph = 4,5 -20^{0}C	[18]
3	LC-MS	Cacao kefir. cheese	Tryptophan-2,3-thioxogenase (TDO), indolamine-2,3-22-dioxygenase-1 (IDO-1) and indolamine-2,3-dioxygenase-2 (IDO-2)	column (100 x 2.1 106 mm i.d., 1.9 µm) and Acquity UPLC HSS C18 column (150 x 2.1 mm i.d., 1.8 µm	Sample + methanol/water (60:40)	[19]
4	GC	Kefir	D, L-alanine, D- and L-valine, methionine and cysteine	column 25 m x250 µm	100 ml sample t=10 min was centrifuged pH=4,25 +7 M NH_3H_2O +3 M HCl	[20]

Table 4 – Determination of fatty acids in dairy products by chromatographic methods

№	Techniques	Products analyzed	Condition of analysis	Sample preparation	Reference
1	GC	Milk, cheese	column, 25 m x 0.32 mm	10 ml sample + 10 ml ethanol + 1 ml H_2SO_4 (2,5 mol/l t=10 min was centrifuged + 1 g Na_2SO_4 + 0,3 ml $MgSO_4$ (2,5 mol/l) + C_7H_{16} (1:1)	[21]
2	GC	Milk, cheese	Six-meter (0.25 mm i.d.)-fused silica capillary columns with chemically bonded DB-5 (0.1 pm coating thicknes	10 ml sample +10 ml ethanol + 1 ml H_2SO_4 2,5 mol/l t=10 min was centrifuged +1 g Na_2SO_4 + C_7H_{16} (1:1)	[22]
3	GC-MS	Milk	column coated with polyimide 60 mm x250 mm i.d., 0.25 mm film thickness column	1000 ml sample + 100 ml SS + 1180 ml ethanol + 200 ml pyridine pH = 5	[23]
4	GC	Milk, yoghurt	column (30 m × 250 µm i.d., 0.32-µm phase thickness;	All samples at -18 ° C was frosted.	[24]
5	GC-MS	Butter	C18 column (5 lm, 150 4.6 mm i.d.)	400 g sample to 500 ml was transffered t=75±2^{o}C + sediment, the precipitate was filtered and + Na_2SO_4	[25]
6	SPME-GC-MS	Milk	SLB-IL111 capillary column (100 m 0.25 mm i.d., 0.20 lm film thickness	25 mg of sample was derivatized to fatty acid methyl esters (FAME) by base-catalyzed methanolysis of the glycerides with KOH in methanol according to ISO-IDF procedure	[57]

Table 5 – Determination of hormones in dairy products by chromatographic methods

№	Techniques	Products analyzed	Analyte	Condition of analysis	Sample preparation	Refer-ence
1	UHPLC	Yoghurt, cheese	17-Estradiol	(10, 25, 50, 75 and 100 lmol L1, MIPs and NIPs were packed into 50x4.6 mm	500g sample + 150 ml methanol/acetone 1:1 t=5 min mix, + 15 ml water	[26]
2	UHPLC-MS	Cheese, kefir	β-zearalanol, β-zearalenol α-zearalanol,ethinyl estradiol, 17α-estradiol	Agilent 1909/S capillary column (30 m × 0.25 mm	3,1-12 g sample + 5 ml ethanol	[27]
3	GC	Cheese, kefir	formononetin, daidzein, entero-diol, Genistein	X-Bridge C18 column (50 mm x 2.1 mm, 1.7 µm)	100 g sample	[28]
4	GC-MS	kefir, yoghurt	Melatonin	SB-C18 column (50 4.6 mm i.d., 3.5 lm)	5 g sample t=3 min 20 000 rpm was centrifuged	[29]
5	GC-MS	Cheese, milk, yoghurt	17b-estradiol (17b-E2), 17a-ethynylestradiol (EE2), estrone (E1), estriol (E3)	MWCNTs (8–15 nm outer diameter (o.d.), 50 lm length) and MWCNTs (10–20 nm o.d., 10–30 lm length), and packed in a column	Sample +10 ml n-hexane + 10 MeOH + water, + 10 ml MeCN t=10 min was centrifuged	[30]

Table 6 – Determination of mycotoxins, preservatives, colorants and metal in dairy products by chromatographic methods

№	Techniques	Products analyzed	Analyte	Condition of analysis	Sample preparation	Refer-ence
1	GC-MS	Milk, yoghurt	Aflatoxin M1, aflatoxin G2, gliothoxin	100 mm × 2.1 mm, i.d., 2.6 m, Thermo Accucore C-18 aQ connected to a 10 mm × 2.1 mm	15 g sample + CH_3COOH + 10 ml MeCN/water (84:16)	[31]
2	UHPLC	Yoghurt	Aflatoxin M1	LiChrospher 100 RP-18, 5 Am column 25 4.6 mm	10 g sample + 10 ml CH_2Cl heated and + 5 ml water to dissolve.	[32]
3	SPE-UPLC-MS	Milk	Zarolenone, aflatoxin M1, Aflotoxin B1	C18 column (150 mm × 2.1 mm i.d., Thermo Fisher Scientific)	5 g sample + 25 ml water + t=10 min magnetic stirrer.	[33]
4	HPLC-MS	Milk	Oxystrerol	column Synergi Hydro, 4 µm, 250 162 x 2.0 mm	0,5 g sample + 40 µL CH_3OH + 5 ml 2 M KOH, t=30 sec mix, left on 16-18 hours.	[34]
5	UHPC	Milk	Phosphatidylserine	PS by the analytical column	0,75 g sample + 1,5 ml water + 9 ml methanol + 10 ml chloroform	[35]
6	UHPLC-MS	Yoghurt, cheese	Cr(III)	column (250 × 4 mm internal diameter (i.d.), 9 µm particles diameter) as well as an IonPac CG5A guard column	Ph = 8,5 + 6 ml 0,05 M EDTA 10000 rpm t =15 min was centrifuged.	[36]
7	SPME-GC-MS	Yoghurt	Acetaldehyde, 2-butanone, 2,3-butadione, hexanal	(Titanium alloy Ti-6Al-4V, length: 136 mm, tip diameter: 13 mm)	Sample was heated to 45 ° C	[37]

Continuation of table 6

№	Techniques	Products analyzed	Analyte	Condition of analysis	Sample preparation	Reference
8	HPLC	Yoghurt	Colorants: Y1 INS 110 NI MD2, NI MD3, MD4, E122, MD6, MD12, MD13 E102, E110, MD14, E123, E124	column oven CTO-20AC	5 g sample + 10 ml ethanol	[38]
10	HPLC	Milk	Kestosis, nystosis, fructofuranosyl nystosis	Atlantis dC18 (150 3 mm, 5 μm particle size	0,5 g sample + 1 g sediment t=5 min was centrifuged, 0,22 mm nylon filter.	[39]
11	HPLC	Cheese, milk, yoghurt	Benzoic, sorbic, propionic acids	Optimal wavelength 235 nm	10 g sample transfer into 250 ml + 100 ml extragent, t=10 min ultrasound bath + 5 ml Carrez I, Carrez II solutions + water	[40]
12	UHPLC	Yoghurt	Biogenic amines: cadaverine, spermidine, spermine, tyramine, putrescine	C18 column (150 mm length x 4.6 mm inner diameter, 5 μm particle size)	5 g sample + 10 ml $HClO_4$ Whatman n ° 1 was filtered(pH> 8, 12) + 2,5 ml NaOH 2 M t=10 min was centrifuged	[41]
13	HPLC-MS	Milk	Lactose	Carbohydrates NH2 (5 μm, 250 × 4.6 mm) and Luna NH2 (5 μm, 250 × 4.6 mm)	1 ml phosphotungstic acid + 5 mL of milk. shaking for 30 s and reacting for 15 min, the mixture was centrifuged at 4500 rpm (1920g) for 5 min	[46]
14	LC-FD	Milk	Drugs: NOR, OFL, FLE, CIP, DAN, LOM, ENR, ORB	C18 column (5 μm, 100 Å, 4.6 × 150 mm)	The sample was kept in the dark for 30 min and then centrifuged at 10,000 rpm (6950 g) at 20°C for 10 min.	[47]
15	HPLC–UV	Milk	formaldehyde	C-18 (250 X 4.6 mm; 5 μm; Supelco) column	2.5 ml + .0 mL of 0.1 g L-1 DNPH solution in ACN, pH = 4.0 + 0.2 and was vortex-mixed for 1 min and centrifuged at 6000 rpm (2.012 g) for 20 min.	[48]
16	SPME-GC-MS	Milk	NA, AcPY, AcP, FL, PHEN	HP-5MS capillary column (30 m × 0.25 mm i.d., 0.25m film thickness)	5 mL of a liquid sample or 5 g of a solid sample were placed into a 15 mL SPME-vial. The vial was filled with water in order to avoid the headspace	[54]
17	SPME-GC-MS	Milk, milk products	Volatile compounds:	HP-5MS column (30 m length, 0.25 mm inside diameter, 0.25 μm film thickness	Sterile milk was prepared by reconstituting 10% (wt/ vol) skimmed milk powder in distilled water and autoclaving at 95°C for 5 min	[53]
18	SPME-GC-MS	Milk, milk products	Ink photo-initiators	Column (PDMS, 100 m film thickness), polyacrylate (PA, 85 m film thickness), Carboxen–PDMS (CAR–PDMS, 75 m film thickness)	All samples were homogenized and transferred into 20 ml vials	[55]

Continuation of table 6

№	Techniques	Products analyzed	Analyte	Condition of analysis	Sample preparation	Reference
19	GC-MS	Milk products	Dimethyl phthalate, diethyl phthalate, diallyl phthalate, diisobutyl phthalate, benzyl butyl phthalate	30 m × 0.32 mm i.d., 0.25-μm film DB-5 fused-silica capillary column	5 ml of sample was pipetted into a 10-mL glass centrifuge tube + 1.0 mL of 10% (vol/vol) acetic acid was added, mixed well, and heated in a sand bath at 70°C for 10 min and centrifuged for 10 min	[58]
20	GC-MS-AED	Milk products	Dimethylselenide, dimethyldiselenide	Capillary column DB-624 (30 m × 0.32 mm I.D. × 1.8 m) with G2350A microwave-induced plasma atomic emission detector	2 mL of sample were placed into a 15 mL SPME–vial, into which 0.6 g NaCl had been previously weighed.	[59]
21	HPLC	Milk, yogurt	Formaldehyde	5 μm particle sized octadecylsilyl (ODS) column (250 mm × 4.6 mm i.d.)	samples were pastoralized before the analyses and added 5 ml of acetonitrile	[60]

Sample preparation

Sample preparation takes almost 70% of all time of analysis, and has a great responsibility on the next step of analysis. Therefore in any process sample preparation is the important part to confirm components and identify quantities of them. The main products of the contamination of milk are included lactose (4.6%), proteins (3.2%), and lipids (3.9%). Even if these components are the homogeneous system, they are different in another animal's milk.

During the analysis protein and lipids complicate the treatment, substituting the ions of another component. Generally, it is suitable to use Mass-spectrometry method for purification of these components. However, in Mass-spectrometry method the water volume can disturb the extraction of analytes, affecting on their diffusion. Therefore, many scientists subjected the samples to sublimatic drying before the analysis [42]. As a result, Solid Phase Extraction (SPE) is used effectively in removal system components from the samples. But depending on the sorbents Liquid-Liquid Extraction (LLE) also can be useful [43]. As the sorbents were used acetonitrile, ammonium acetate, complex agent Na_2EDTA, and methanol, selecting suitable reagent by their organic class. For example, β-lactam is very sensible for methanol whereas tetracycline is able to be extracted only at pH=4, at another pH index it can participate for epimerization, dehydration, isomerization processes. Moreover, many antibiotics produce chelated complexes with metal ions and disturb the analysis of protein system [44].

High performance of liquid chromatography

HPLC analysis depends on the chromatography column, used sorbent and eluent. Due to its efficiency and time expressing HPLC method is highly demanded in the analysis of milk and dairy products. According to Governmental Standard no. 31504-2012 the optimum pH=4.5 to identify the preservatives in dairy products at 230-260 nm range. Analyzing all other researches, acetonitrile is the acceptable sorbent due to its non-selectivity to other components and easily accessible reagent that allows identifying analytes in 5-10 minutes. Moreover, for instance in Methodological instruction no.4.1.2420-08 was provided analysis where the rate of concentrations of melamine in milk compounds were 1,0-100 mg/kg. However, determination of melamine by Chromato-Mass-Spectrometry method consists of 2 parts: extraction of melamine and its derivatization. Mass spectrometry method allows determining the quantity of melamine even in very low concentration ranges undoubtedly, but it takes a lot of time for sample preparation, in addition, for derivatization is used t trimethylsilyl that interrupt the determination of other components [44].

Ultra high performance of liquid chromatography

The advantage of this method is highly sensitive column, as a rule it usually 50x4,6 mm with 1,7 μm size particles and expressive separation of components occurs within less than 2 minutes. In the tables provided above for the determination of components in milk products UHPLC method was used mostly. For example, in determination of estrogens Waters

Symmetry C18, 500 nm, 150 × 4.6 mm column was used, analyze time = 5 minutes, as a result 0.116–0.461 nmol/kg concentration rate – which is very small identified in 500 g sample [26]. However, in identification of synthetic colorants in yoghurt using special column and providing expressive time of analysis, pH of the analyzing solution should be equal to 7 which is not completely appropriate for us [30]. Also this method was used in amines detection [46]. The disadvantage of this method is expensive and inaccessible devices. In addition, this method is directed on the selectivity more not efficiency. Therefore UHPLC is appropriate to use only as combined method, for instance UHPLC-MS [30].

Gas Chromatography

Gas chromatography was used for analysis of dairy products, especially in identification of fatty acids. Gas chromatography is characterized by high selectivity, accuracy and also by its automated [45]. According to Governmental Standard no. 32915-2014, there was provided standard preparation of methyl ester, carrier gas was nitrogen, time of analysis was 50 minute. The main minus of this method is long duration of time for sample preparation. However the time of preparation and analyzing depends on analyte that is going to be tested, according to cognitive structure of dairy products [27]. For example, when amino acids were analyzed in dairy products with HP 6890 gas chromatograph the time of analysis was less than in previous research and as a result 3 amino acids were detected in kefir [38].

Quantitative determinations were provided by using the standard addition method. The identification of amino acid derivatization method by using chloroform in aqueous medium has been proceeding to the use of different alkyl chloroform and alcohols. These reactions provide an extremely fast and simple route for derivatization carrying out from aqueous samples in only one step [21].

Other procedures

LC–MS/MS method was optimized for determination of ammoniums in cheese and milk products at concentration levels in full obtains with the preliminary MRL setting as 100 g kg−1. In this method used 50:50 (v/v) proportion of ACN/EtAc defining it as the best sensitivity for. Because ACN is known to be a poor solvent for polar compounds otherwise increasing the volume of EtAc promotes the extraction of long-chain alkyl substances (especially DDAC C16 and C18) [13]. The similiar method was used for quantifying qualifiers of amino acids such as β-casomorphin in milk and yoghurts. The advantage of this method was useful sample preparation using SPE cartridges followed by LC–MS for the identification of low molecular weight degradation by-products of these β-CMs. However the limitation of this research was inadvertency of screening of all samples components [19]. Although, not all the researches were considered to do a detailed analyzes for all components [20].

Conclusion

In this paper was analyzed the techniques that was used for the determination of hazardous components in dairy products. During the research there was analyzed a large amount of information, research papers, statistics for the last 10 years from the international scientific portals such as Science Direct, Web of Science and other sources. More than 40 researches were considered; as a result all of the research papers were oriented on the determination of mycotoxins, amino acids, fatty acids, preservatives, colorants, hormones in the contamination of dairy products. Determination of these components in milk by chromatographic methods is a very terrible issue to ensure consumers ‘safety and to avoid, even removal company productions from the market of milk. Dairy products are highly complex compound that chromatography methods allow identifying the components even in very small concentrations that is why this method is acceptable for analysis of hazardous components in dairy products. For the sample preparation were considered Solid Phase extraction and Liquid-Liquid extraction were should be taken into account pH of the solution, in most researches it was equal to 4, and complete absorption of the main components so that they do not interfere with further analysis. Accordingly considered chromatographic methods almost 80 percent of analyzes were organized by gas chromatography and high performance of liquid chromatography methods, using available and cognitive mobile phase as ACN, in some cases it was dilution with another acids. In comparison with other methods for determination of hazardous components in dairy products, the most selective method was High Performance of Liquid Chromatography with high separation efficiency, having a good possibility to determine the composition of milk samples deeply. For the future time is required to provide the analyzes of dairy products due to this methods.

References

1. Visioli F., Strata A. (2014) Milk, Dairy products, and their functional effects on humans: A Narra-

tive Review of Recent Evidence. Advances in nutrition, vol. 5, pp. 131-143.

2. Mansson H.L. (2001) Nutritional Value and Technological suitability of milk from various animal species used for dairy production. Comprehensive reviews in food science and food safety, vol. 10, pp. 291-302

3. Nadeem R., Ki-Hyun K. (2018) Quantification techniques for important environmental contaminants in milk and dairy products. Trends in Analytical Chemistry, vol. 98, pp. 79-94.

4. Gurban A., Epure P., Oancea F., Doni M. (2017) Achievements and prospects in electrochemical-based biosensing platforms for aflatoxin M1 Detection in Milk and Dairy Products. Food Chemistry, vol. 46, p. 2951.

5. Fischer W.J., Schilter B., Tritscher R., Stadler H. (2011) Contamination Resulting From Farm and Dairy Practices. Encyclopedia of Dairy Sciences, pp. 887-897.

6. Kulbayeva A., Sheikin D. (2016) Food Industry of the Republic of Kazakhstan. Rating Agency of the RFCA, vol. 12, p. 4.

7. Fashi A., Yaftian M., Zamani A. (2015) Determination of melamine in dairy products using electromembrane–LPME followed by HPLC. Food Chemistry, vol. 188, pp. 92-98.

8. Smirnov Y.N. (2012) Determination of Melamine in dairy products. Epac-Service.

9. Tutelyan V.A., Eller K.I. (2008) Determination of melamine in milk and milk products. Russian Academy of Medical Sciences, No. 4.1.2420-08.

10. Gao P., Li J., Li Z., Hao J., Zan L. (2016) Establishment and application of milk fingerprint by gel filtration chromatography. Journal of dairy science, vol. 99, pp. 9493-9501

11. Tian H., Wang J., Zhang Y., Li S., Jiang J. (2016) Quantitative multiresidue analysis of antibiotics in milk and milk powder by ultra-performance liquid chromatography coupled to tandem quadrupole mass spectrometry. Journal of chromatography B, vol. 1033, pp. 172-179.

12. Slimani K., Féret A., Pirotais Y. (2017) Liquid chromatography-tandem mass spectrometry multiresidue method for the analysis of quaternary ammonium compounds in cheese and milk products. Journal of chromatography A, vol. 1517, pp. 86-96

13. Moreno-Gonzalez D., Hamed A., Garcia-Campana A., Gamiz-Gracia L. (2017) Evaluation of Hydrophilic Interaction Liquid Chromatography–Tandem Mass Spectrometry and extraction with Molecularly Imprinted Polymers for determination of aminoglycosides in milk and milk-based functional foods. Talanta, vol. 171, pp. 74-80.

14. Tania A.P., Aguiar P., Fernandes Ana I., Pinto F. (2015) Quantification of theophylline or paracetamol in milk matrices by High-Performance Liquid Chromatography. Journal of Pharmaceutical Analysis, vol. 7, pp. 401-405.

15. Lin J., Chen W., Zhu H., Wang C. (2015) Determination of free and total phthalates in commercial whole milk products in different packaging materials by Gas Chromatography-Mass Spectrometry. Journal of Dairy Science, vol. 98, pp. 8278–8284.

16. Wei J. (2014) Analysis of phthalates in milk and milk products by Liquid Chromatography coupled to Quadrupole Orbitrap High-Resolution Mass Spectrometry. Journal of chromatography A, vol. 1362, pp. 110-118.

17. Mondal R., Mary A. (2010) Liquid Chromatography−Tandem Mass Spectrometry (LC−MS/MS) method extension to quantify simultaneously melamine and cyanuric acid in egg powder and soy protein in addition to milk products. Journal of Agricultural and Food Chemistry, vol. 58, pp. 11574-11579.

18. Nguyen D., Busetti F., Johnson S. (2017) Degradation of B-Casomorphins and identification of degradation products during yoghurt processing using Liquid Chromatography coupled with High resolution Mass Spectrometry. Food Research International journal, vol. 106, pp. 98-104.

19. Cemile Y., Gökmen V. (2017) Determination of tryptophan derivatives in kynurenine pathway in fermented foods using Liquid Chromatography Tandem Mass Spectrometry. Food Chemistry, vol. 243, pp. 420-427.

20. Menestrina F. (2016) Chiral analysis of derivatized amino acids from kefir by Gas Chromatography. Microchemical Journal, vol. 128, pp. 267-273.

21. Catrienus D., Badings H. (1990) Determination of free fatty acids in milk and cheese procedures for extraction, clean up, and capillary Gas Chromatographic Analysis. Journal of High Resolution Chromatography, vol. 13, pp. 94-98.

22. Lohninger A., Preis P., Linhart L., Sommoggy S., Landau M., Kaiser E. (1990) Determination of plasma free fatty acids, free cholesterol, cholesteryl esters, and triacylglycerols directly from total Lipid Extract by Capillary Gas Chromatography. Analytical Biochemistry, vol. 186, pp. 243-250.

23. Bashar A., Nebel A., Hanne C., Mortensen G. (2013) Novel method for quantification of individual free fatty acids in milk using an in-solution derivatization approach and Gas Chromatography-

Mass Spectrometry. International Dairy Journal, vol. 32, pp. 199-203.

24. Mannion D., Furey A., Kilcawley K. (2016) Comparison and validation of 2 analytical methods for the determination of free fatty acids in dairy products by Gas Chromatography with Flame Ionization Detection. Journal of Dairy Science, vol. 99, pp. 5047-5063.

25. Milk and milk products. Determination of fatty acid content by gas chromatography method. Russian Research Institute of Dairy Industry of the Russian Academy of Agricultural Sciences, No. 32915-2014, 2016.

26. 26. Shi Y., Zhang C. (2011) Selective determination of trace 17B-Estradiol in dairy and meat samples by Molecularly Imprinted Solid-Phase Extraction and HPLC. Food Chemistry, vol. 126, pp. 1916-1925.

27. Sfakianakis, P., Tzia C. (2016) Flavour profiling by Gas Chromatography–Mass Spectrometry and sensory analysis of yoghurt derived from ultrasonicated and homogenised milk. International Dairy Journal, vol. 75, pp.120-128.

28. Socas-Rodríguez B., Herrera-Herrera A., Hernández-Borges J. (2017) Multiresidue determination of estrogens in different dairy products by Ultra-High-Performance Liquid Chromatography-Triple Quadruple Mass Spectrometry. Journal of Chromatography A, vol. 1496, pp. 58-67.

29. Kocadağlı T., Yılmaz C., Gökmen V. (2014) Determination of melatonin and its isomer in foods by Liquid Chromatography Tandem Mass Spectrometry. Food Chemistry, vol. 153, pp. 151-156.

30. Socas-Rodríguez B., Hernández-Borges J. (2013) Chromatographic analysis of natural and synthetic estrogens in milk and dairy products. Trends In Analytical Chemistry, vol. 44, pp. 58-77.

31. Jia W., Yun L., Xiaogang C. (2014) Multimycotoxin analysis in dairy products by Liquid Chromatography coupled to Quadrupole Orbitrap Mass Spectrometry. Journal of Chromatography A, vol. 1345, pp. 107-114.

32. Martins M., Marina H. (2004) Aflatoxin M1 in yoghurts in Portugal. International journal of food microbiology, vol. 91, pp. 315-317.

33. Xiupin W., Li P. (2015) Rapid screening of mycotoxins in liquid milk and milk powder by Automated Size-Exclusion SPE-UPLC–MS/MS and quantification of matrix effects over the whole chromatographic run. Food Chemistry, vol. 173, pp. 897-904.

34. Vergalet S.C., Verardo A.G. (2017) Rapid determination of cholesterol oxidation products in milk powder based products by Reversed Phase SPE and HPLC-APCI-MS/MS. Food Chemistry, vol. 230, pp. 604-610.

35. Lin Q., Zhang J., Pei W. (2015) Determination of phosphatidylserine in milk-based nutritional products using online Derivatization High-Performance Liquid Chromatography. Journal of Chromatography A, vol. 1381, pp. 260-263.

36. Hernandez F., Jitaru P., Cormant F., Guérin T. (2017) Development and application of a method for Cr(III) determination in dairy products by HPLC–ICP-MS. Food Chemistry, vol. 240, pp. 183-188.

37. Sfakianakis P., Tzia C. (2017) Flavour profiling by Gas Chromatography–Mass Spectrometry and sensory analysis of yoghurt derived from ultrasonicated and homogenised milk. International Dairy Journal, vol. 75, pp. 120-128.

38. Waleska A., Bruno P., Ana Paula S. (2015) Simultaneous determination of synthetic colorants in yogurt by HPLC. Food Chemistry, vol. 183, pp. 154-160.

39. Rodríguez-Gómez R., Jiménez-Díaz I., Zafra-Gómez A. (2015) Improved sample treatment for the determination of fructoligosacharides in milk related products by Liquid Chromatography with Electrochemical and Refractive Index Detection. Talanta, vol. 144, pp. 883-889.

40. Milk and milk products. (2003) Determination of preservatives and synthetic colors content by high performance liquid chromatography method. Russian Research Institute of Dairy Industry of the Russian Academy of Agricultural Sciences, No. 31504-2012.

41. Paulo Vieira C., Marion P. C., Silva V. (2017) Development and validation of RP-HPLC-DAD method for biogenic amines determination in probiotic yogurts. Arabian journal of chemistry, pp. 113-128.

42. Marazuela M.D., Bogialli S. (2009) A review of novel strategies of sample preparation for the determination of antibacterial residues in foodstuffs using Liquid Chromatography-Based Analytical Methods. Analytica Chimica Acta, vol. 645, pp. 5-17.

43. Moretti S., Saluti G., Galarini R. (2017) Residue determination in honey, honey analysis. InTech, p. 376.

44. El Hawari K., Mokh S., Doumyati S., Al Iskandarani M. (2016) Development and validation of a multiclass method for the determination of antibiotic residues in honey using Liquid Chromatography-Tandem Mass Spectrometry. Food Additives & Contaminants: Part A, vol. 34, pp. 582-597.

45. Bijttebier S., D'Hondt E., Noten B., Hermans N. (2014) Ultra high performance liquid chromatography versus high performance liquid chromatography: Stationary phase selectivity for generic carotenoid screening. Journal of Chromatography A, vol. 1332, pp. 46–56.

46. Garballo-Rubio, A. (2018) Determination Of Residual Lactose In Lactose-Free Cow Milk By Hydrophilic Interaction Liquid Chromatography (HILIC) Coupled To Tandem Mass Spectrometry. Journal of Food Composition and Analysis, vol. 66, pp. 39-45.

47. Zhang X. Wang C. Yang L (2017). Determination of eight quinolones in milk using immunoaffinity microextraction in a packed syringe and liquid chromatography with fluorescence detection. Journal of Chromatography B, vol. 1084, pp. 68-74

48. Freitas Rezende F., Souza Santos Cheibub A. (2017) Determination of formaldehyde in bovine milk using a high sensitivity HPLC-UV method. Microchemical Journal, vol. 134, pp. 383-389

49. Faraji M. Adeli M. (2017) Sensitive determination of melamine in milk and powdered infant formula samples by high-performance liquid chromatography using dabsyl chloride derivatization followed by dispersive liquid–liquid microextraction. Food Chemistry, vol. 221, pp. 139-146

50. Lourdes MendesFinete V. DuartePereira Netto A. (2015) Validation of a method of high performance liquid chromatography with fluorescence detection for melamine determination in UHT whole bovine milk. Food Control, vol. 51, pp. 402-407

51. Yao K. Zhang W. Yang L. Gong J. (2015) Determination of 11 quinolones in bovine milk using immunoaffinity stir bar sorptive microextraction and liquid chromatography with fluorescence detection. Journal of Chromatography B, vol. 1033, pp. 67-73

52. Targa Martins M., Barreto F., Barcellos Hoff F. (2016) Multiclass and multi-residue determination of antibiotics in bovine milk by liquid chromatography–tandem mass spectrometry: Combining efficiency of milk control and simplicity of routine analysis. International Dairy Journal, vol. 49, pp. 44-51

53. Dan T. Wang R. Zhang L. (2017) Characterization of volatile compounds in fermented milk using solid-phase microextraction methods coupled with gas chromatography-mass spectrometry. Journal of Dairy Science, vol. 100, pp. 2488-2500

54. Aguinaga N., Campillo N., Viñas P. (2007) Determination of 16 polycyclic aromatic hydrocarbons in milk and related products using solid-phase microextraction coupled to gas chromatography–mass spectrometry. Analytica Chimica Acta, vol. 596, pp. 285-290

55. Negreira N., .Rodríguez I. (2010) Solid-phase microextraction followed by gas chromatography–mass spectrometry for the determination of ink photo-initiators in packed milk. Talanta, vol. 82, pp. 296-303

56. Gómez-Cortés P., Rodríguez-Pino V., Juárez M. (2017) Optimization of milk odd and branched-chain fatty acids analysis by gas chromatography using an extremely polar stationary phase. Food Chemistry, vol. 231, pp. 11-18

57. Arroyoa D., Ortiz C., Luis A. (2011) Optimization of the derivatization reaction and the solid-phase microextraction conditions using a D-optimal design and three-way calibration in the determination of non-steroidal anti-inflammatory drugs in bovine milk by gas chromatography–mass spectrometry. Journal of Chromatography A, vol. 1218, pp. 4487–4497

58. Lin J., Chen W., Zhu H. (2015) Determination of free and total phthalates in commercial whole milk products in different packaging materials by gas chromatography-mass spectrometry. American Dairy Science Association, vol. 98, pp. 1-7

59. Campillo N., Penalver P., Hernández-Córdoba M. (2010) Determination of dimethylselenide and dimethyldiselenide in milk and milk by-products by solid-phase microextraction and gas chromatography with atomic emission detection. Talanta, vol. 80, pp. 1856–1861

60. Hossain S, Islam S., Bhadra S. (2016) Investigation of Formaldehyde Content in Dairy Products Available in Bangladesh by a Validated High Performance Liquid Chromatographic Method. Bangladesh Journals Online, vol. 15, pp. 188-199

61. Wang Y., Li X., Zhang Z. (2016) Simultaneous determination of nitroimidazoles, benzimidazoles, and chloramphenicol components in bovine milk by ultra-high performance liquid chromatography–tandem mass spectrometry. Food Chemistry, vol. 192, pp. 280-287

IRSTI 31.25.15

A.K. Nurlybekova, Yang Ye, J. Jenis

Shanghai Institute of Materia Medica, Chinese Academy of Science, Shanghai, China,
*e-mail: janarjenis@mail.ru

Investigation of liposoluble constituents from the root of *Ligularia narynensis*

Abstract. In this work, chemical constituents of the liposoluble portion from the root part of medicinal plant *Ligularia narynensis* have been determined for the first time. The constituents extracted from the root part of *L. narynensis* by chloroform were analyzed by GC-MS method. Total fifty nine compounds were separated and their relative contents were determined by area normalization in which the major constituents were n-Hexadecanoic acid (13.44%), 9,12-Octadecadienoic acid (Z,Z)- (11.79%), (3aR,4aS,5R,9aS)-5,8-Dimethyl-3-methylene-3a,4,4a,5,6,7,9,9a-octahydroazuleno[6,5-b]furan-2(3H)-one (6.90%), Octadecanoic acid (6.17%), .gamma.-Sitosterol (5.50%), 2(1H)Naphthalenone, 3,5,6,7,8,8a-hexahydro-4,8a-dimethyl-6-(1-methylethenyl)- (4.05%), respectively.

Key words: *Ligularia narynensis*, chloroform extract, liposoluble constituents, GC–MS.

Introduction

Ligularia is the genus of perennial herbs of the family Compositae, containing about 180 Eurasian species, 17 species growing in mountains of Kazakhstan [1]. Some species in this genus have been used for a long time as folk remedies for their antibiotic, antiphlogistic, and antitumor activities [2-5]. More than 27 *Ligularia* species have been used as traditional Kazakh and Chinese medicinal herbs for the treatment of fever, pain, inflammation, and intoxication, and to invigorate blood circulation [6-9]. Previous studies confirmed the presence of sesquiterpenes, triterpenes, sinapyl alcohol derivatives, lignans, alkaloids, and steroids in *Ligularia* [10]. Eremophilane sesquiterpenes are considered as the major secondary metabolites and taxonomic markers of *Ligularia* genus. More than 500 eremophilane sesquiterpenes have been reported from this genus [11; 12]. Additionally, oplopane sesquiterpenes have been reported from *L. narynensis* [13].

We have previously reported the chemical investigation results on total bioactive components from root part of *L. narynensis* such as organic acids (0.64 %), flavonoids (0.52 %), moisture content (5.14 %), total ash (13.24 %), and extractives content (27.7 %). Together with eleven macro-micro elements from the ash of plant (main contents: K (2214.13 μg/mL), Ca (391.31 μg/ml), and Fe (311.73 μg/mL) were determined by using method of multi-element atomic emission spectral analysis. And same time, twenty amino and eight fatty acids were analyzed from this plant. The results showed that major contents of amino acids were glutamate (2452 mg/100g), aspartate (1238 mg/100g) and alanine (748 mg/100g), as well as in fatty acids were oleic (33.5 %) and linoleic (41.2 %) acids, respectively [14].

In our continuously study of the plant, fifty nine liposoluble constituents in chloroform extract from medicinal plant, *L. narynensis* have been identified by GC-MS methods which grown in Almaty region of Kazakhstan for the first time.

Materials and methods

Plant material. The root part of plant *L. narynensis* was collected in September 2017 from Butakovskoe gorge of the Zailiysky Alatau Mountains of Almaty region and identified by Dr. Alibek Ydyrys. Specimens (1217-БН-17) were deposited in the Herbarium of Laboratory Plant Biomorphology, Faculty of Biology and Biotechnology, Al-Farabi Kazakh National University, Almaty, Kazakhstan. The air dried roots of *L. narynensis* were cut into small pieces and stored at room temperature.

Extraction and isolation. The air-dried roots of *L. narynensis* (100 g) were pulverised and extracted with 70% ethyl alcohol (1:1) three times (seven days each time) at room temperature. After evaporation of the solvent under reduced pressure, the residues were

 Printed in Kazakhstan

mixed and suspended in water and then successively partitioned with hexane, chloroform, EtOAc, and n-BuOH to afford the corresponding extracts. The obtained chloroform extract (173 mg) was analyzed by GC-MS method.

Experimental part. To determine the liposoluble constituents' composition was made erenow of the raw material used GC/MS device. The root part of *L. narynensis* were analyzed by Electron Impact Ionization (EI) method on Agilent 7890A-5975C GC-MS (Gas Chromatograph coupled to Mass Spectrometer) fused silica capillary column (30m x 0.25mm; 0.25 µm film thickness), coated with HP-5MS were utilized. The carrier gas was helium (99.999 %). The column temperature was programmed from 50°C (held for 10 min), with 10°C/min rate program to increase temperature to 300^{0}C.

The latter temperature maintained for 40 min (Acquisition parameters full scan; scan range 30-1000 amu). The injector temperature was 310°C. Injection: with a 1 µl. Detector ion source (EI-70eV). Samples were injected by splitting with the split ratio 5:1.

Identification of the compounds: Identification of compounds was done by comparing the NIST and Wiley library data of the peaks and mass spectra of the peaks with those reported in literature. Percentage composition was computed from GC peak areas on HP-5MS column without applying correction factors.

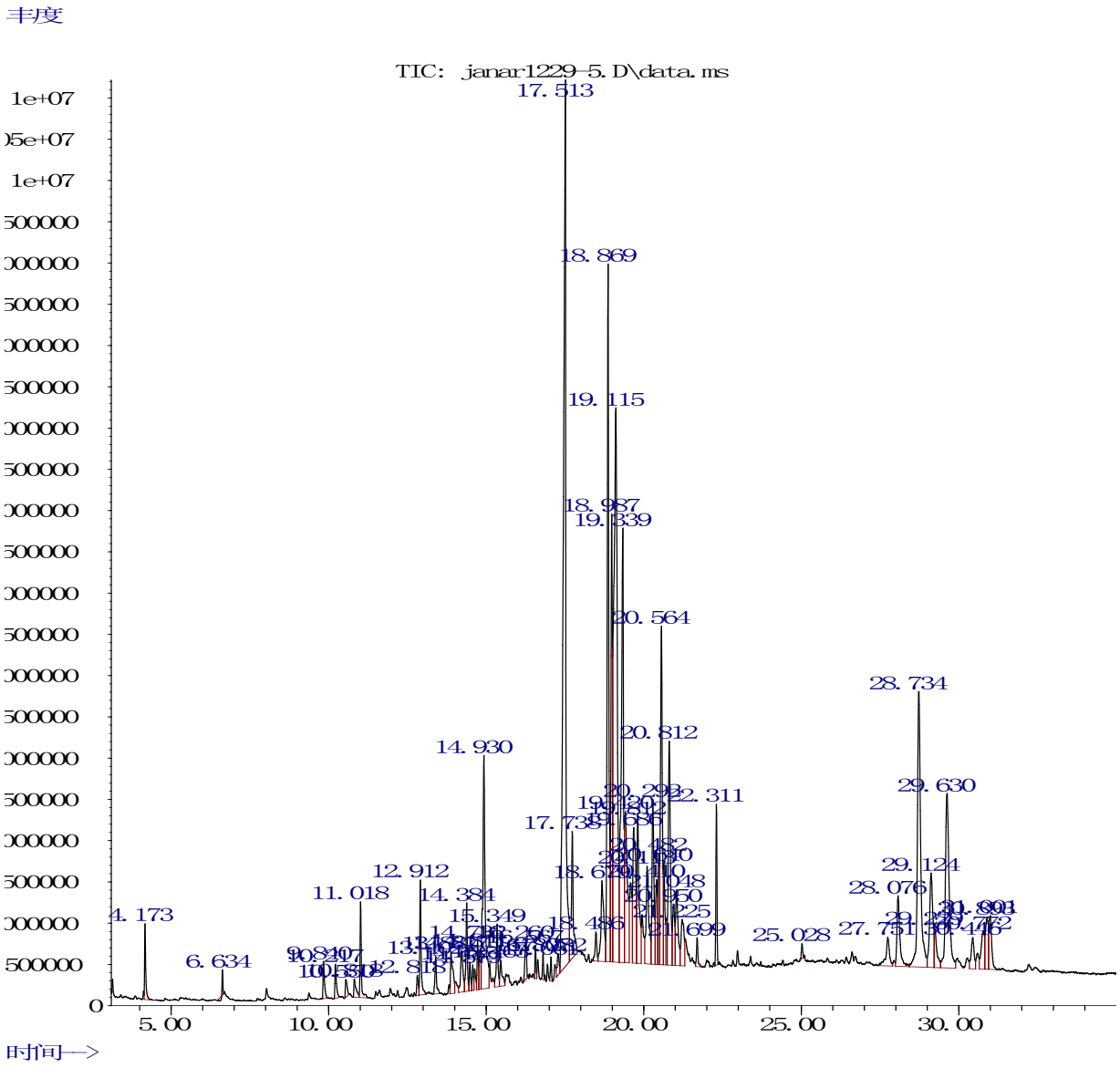

Figure 1 – Total ionization chromatogram of chloroform extract from the root part of *L. narynensis*

Results and discussion

The liposoluble constituents extracted from the root part of *L. narynensis* by chloroform were analyzed by GC-MS method. The yield from whole herbs of *L. narynensis* was found to be 0.173%. Total fifty-nine compounds were separated and their relative contents were determined by area normalization in which the major constituents were n-Hexadecanoic acid (13.44 %), 9,12-Octadecadienoic acid (Z,Z)- (11.79 %), (3aR,4aS,5R,9aS)-5,8-Dimethyl-3-methylene-3a,4,4a,5,6,7,9,9a-octahydroazuleno[6,5-b]furan-2(3H)-one (6.90 %), Octadecanoic acid (6.17 %), .gamma.-Sitosterol (5.50 %), 2(1H)Naphthalenone, 3,5,6,7,8,8a-hexahydro-4,8a-dimethyl-6-(1-methylethenyl)- (4.05 %), 3,6,6-Trimethylundecane-2,5,10-trione (3.94 %), Achillicin (3.86 %), 3-Pyrazolidinone, 1-phenyl- (3.44 %), 2-Pentadecen-4-yne, (Z)- (2.93 %), Linoelaidic acid (2.70 %), Alloaromadendrene (2.34 %), 1-Oxaspiro[2.5]octane, 5,5-dimethyl-4-(3-methyl-1,3-butadienyl)- (1.99 %). GC-MS chromatogram of the liposoluble constituents from root part of *L. narynensis* was presented in Figure 1. Table 1 report the composition of the liposoluble constituents of *L. narynensis*.

According to the report the n-Hexadecanoic acid (13.44 %) might function as an anti-inflammatory agent [15]. Furthermore, this acid has an inhibitory activity. These findings further confirm the medicinal value of plant and its anticancer cytotoxic potential [16; 17]. And second major liposoluble constituent 9,12-Octadecadienoic acid (Z,Z)- (11.79 %) have been reported to have antimicrobial activity [18]. (3aR,4aS,5R,9aS)-5,8-Dimethyl-3-methylene-3a,4,4a,5,6,7,9,9a-octahydroazuleno[6,5-b]furan-2(3H)-one (6.90 %) also called as columellarin has a termiticidal activity [19].

Table 1 – The liposoluble constituents from the root part of *L. narynensis*

Peak No.	Constituents	t_R (min)	Molecular Formula	Structure	MW	Content (%)
1	t-$C_4H_9CH_2C(O)OCH_2CH_3$	4.17	$C_8H_{16}O_2$	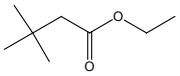	144	0.54
2	Ethane, hexachloro-	6.63	C_2Cl_6	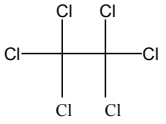	234	0.09
3	2-Methoxy-4-vinylphenol	9.84	$C_9H_{10}O_2$	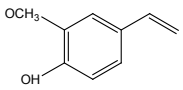	150	0.34
4	Phenol, 2,6-dimethoxy-	10.22	$C_8H_{10}O_3$	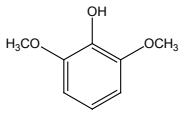	154	0.32
5	Phenol, 4-(ethoxymethyl)-	10.55	$C_9H_{12}O_2$	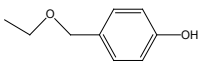	152	0.19
6	Vanillin	10.82	$C_8H_8O_3$	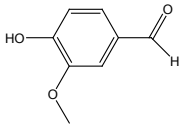	152	0.24
7	Diphenyl ether	11.02	$C_{12}H_{10}O$	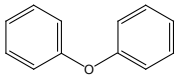	170	0.74

Continuation of table 1

Peak No.	Constituents	t_R (min)	Molecular Formula	Structure	MW	Content (%)
8	2H-1-Benzopyran-2-one, 8-hydroxy-	12.81	$C_9H_6O_3$	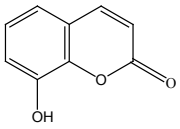	162	0.18
9	2,3,5,6-Tetrafluoroanisole	12.91	$C_7H_4F_4O$	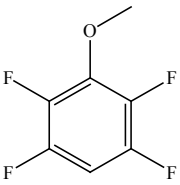	180	0.95
10	(1,4-Dimethylpent-2-enyl)benzene	13.40	$C_{13}H_{18}$	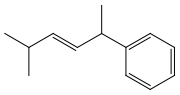	174	0.36
11	Benzaldehyde, 4-hydroxy-3,5-dimethoxy-	13.89	$C_9H_{10}O_4$	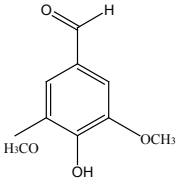	182	0.60
12	7-Oxabicyclo[4.1.0]heptan-3-ol, 6-(3-hydroxy-1-butenyl)-1,5,5-trimethyl-	14.22	$C_{13}H_{22}O_3$	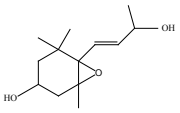	226	0.62
13	(4R,4aR)-4,4a-Dimethyl-6-(prop-1-en-2-yl)-1,2,3,4,4a,7-hexahydronaphthalene	14.38	$C_{15}H_{22}$	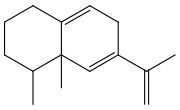	202	0.78
14	(E)-2,6-Dimethoxy-4-(prop-1-en-1-yl) phenol	14.49	$C_{11}H_{14}O_3$	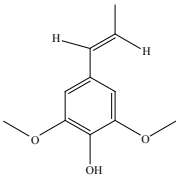	194	0.24
15	.beta.-Vatirenene	14.59	$C_{15}H_{22}$	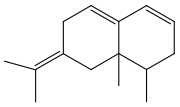	202	0.19
16	Ethanone, 1-(4-hydroxy-3,5-dimethoxyphenyl)-	14.74	$C_{10}H_{12}O_4$	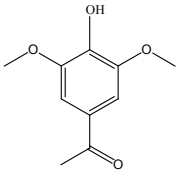	196	0.36
17	Coniferyl aldehyde	14.81	$C_{10}H_{10}O_3$	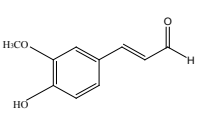	178	0.42

Continuation of table 1

Peak No.	Constituents	t_R (min)	Molecular Formula	Structure	MW	Content (%)
18	3-Pyrazolidinone, 1-phenyl-	14.93	$C_9H_{10}N_2O$	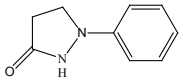	162	3.44
19	2-Cyclohexen-1-one, 4-hydroxy-3,5,5-trimethyl-4-(3-oxo-1-butenyl)-	15.35	$C_{13}H_{18}O_3$	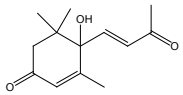	222	0.62
20	(S,E)-4-Hydroxy-3,5,5-trimethyl-4-(3-oxobut-1-en-1-yl)cyclohex-2-enone	15.47	$C_{13}H_{18}O_3$	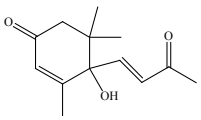	222	0.35
21	Benzene, 1,4-diethyl-2-methyl-	16.26	$C_{11}H_{16}$	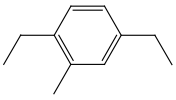	148	0.41
22	2H-Benz[e]inden-3-ol, 3,3a,4,5-tetrahydro-3a-methyl-, (3S-cis)-	16.57	$C_{14}H_{16}O$	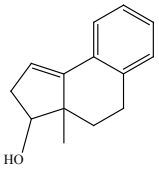	200	0.21
23	Isopulegol	16.81	$C_{10}H_{18}O$	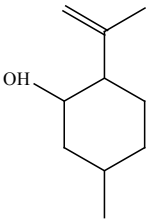	154	0.17
24	Hexadecanoic acid, methyl ester	17.06	$C_{17}H_{34}O_2$	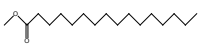	270	0.16
25	trans-Sinapaldehyde	17.28	$C_{11}H_{12}O_4$	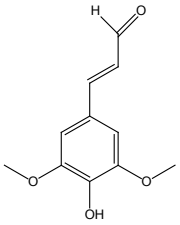	208	0.26
26	n-Hexadecanoic acid	17.52	$C_{16}H_{32}O_2$	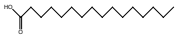	256	13.44
27	Hexadecanoic acid, ethyl ester	17.74	$C_{18}H_{36}O_2$	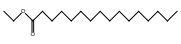	284	1.68
28	1H-Indene, 2-butyl-5-hexyloctahydro-	18.48	$C_{19}H_{36}$	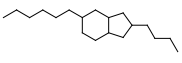	264	0.30
29	Pallensin	18.68	$C_{15}H_{20}O_4$	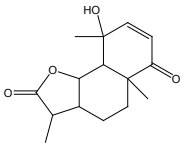	264	1.43

Continuation of table 1

Peak No.	Constituents	t_R (min)	Molecular Formula	Structure	MW	Content (%)
30	(3aR,4aS,5R,9aS)-5,8-Dimethyl-3-methylene-3a,4,4a,5,6,7,9,9a-octahydroazuleno[6,5-b]furan-2(3H)-one	18.87	$C_{15}H_{20}O_2$	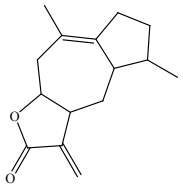	250	6.90
31	Achillicin	18.99	$C_{17}H_{22}O_5$	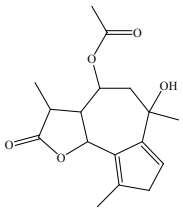	246	3.86
32	9,12-Octadecadienoic acid (Z,Z)-	19.12	$C_{18}H_{32}O_2$	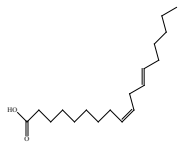	280	11.79
33	Octadecanoic acid	19.34	$C_{18}H_{36}O_2$	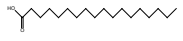	284	6.17
34	Linoelaidic acid	19.42	$C_{18}H_{32}O_2$		280	2.70
35	Alloaromadendrene	19.68	$C_{15}H_{24}$	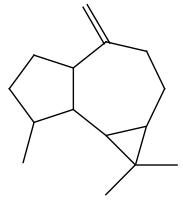	204	2.34
36	1H-Indene-1,3(2H)-dione, 2-(2-methylbutylidene)-	19.81	$C_{14}H_{14}O_2$	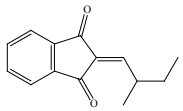	214	1.98
37	Benzo[f]quinoline, 2-methyl-	20.11	$C_{14}H_{11}N$	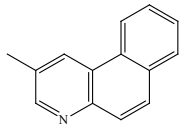	193	1.64
38	1-Oxaspiro[2.5]octane, 5,5-dimethyl-4-(3-methyl-1,3-butadienyl)-	20.30	$C_{14}H_{22}O$	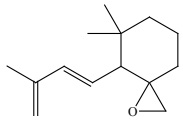	206	1.99
39	Longifolenaldehyde	20.41	$C_{15}H_{24}O$	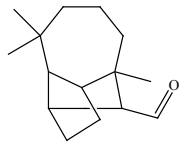	220	0.88
40	11,13-Dimethyl-12-tetradecen-1-ol acetate	20.48	$C_{18}H_{34}O_2$	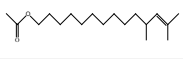	282	0.97

Continuation of table 1

Peak No.	Constituents	t_R (min)	Molecular Formula	Structure	MW	Content (%)
41	3,6,6-Trimethylundecane-2,5,10-trione	20.56	$C_{14}H_{24}O_3$	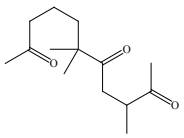	240	3.94
42	(-)-Isolongifolol, methyl ether	20.64	$C_{16}H_{28}O$	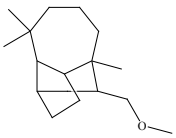	236	0.96
43	2-Pentadecen-4-yne, (Z)-	20.81	$C_{15}H_{26}$	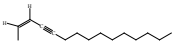	206	2.93
44	Cedrol	20.95	$C_{15}H_{26}O$	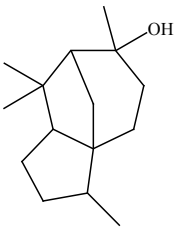	222	0.79
45	2-Heptyne, 7-bromo-	21.05	$C_7H_{11}Br$	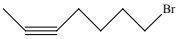	174	1.15
46	2(1H)-Naphthalenone, octahydro-4a-methyl-7-(1-methylethyl)-, (4a.alpha.,7.beta.,8a.beta.)-	21.23	$C_{14}H_{24}O$	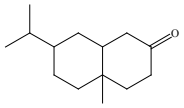	208	0.85
47	1,4-Dioxaspiro[4.5]decan-8-one, 7-(hydroxymethyl)-	21.70	$C_9H_{14}O_4$	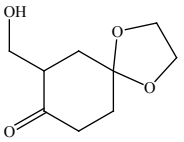	186	0.26
48	Bis(2-ethylhexyl) phthalate	22.31	$C_{24}H_{38}O_4$	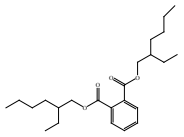	390	1.05
49	Pyridine-3-carboxamide, oxime, N-(2-trifluoromethylphenyl)-	25.03	$C_{13}H_{10}F_3N_3O$	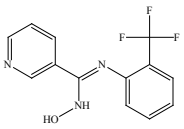	281	0.11
50	Campesterol	27.75	$C_{28}H_{48}O$	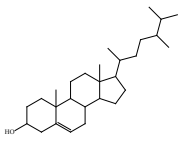	400	0.61
51	Stigmasterol	28.08	$C_{29}H_{48}O$	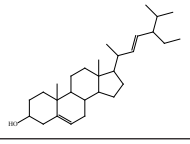	412	1.26

Continuation of table 1

Peak No.	Constituents	t_R (min)	Molecular Formula	Structure	MW	Content (%)
52	.gamma.-Sitosterol	28.73	$C_{29}H_{50}O$	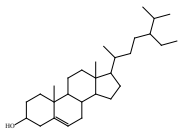	414	5.50
53	.beta.-Amyrin	29.12	$C_{30}H_{50}O$	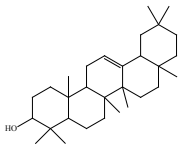	426	1.86
54	.alpha.-Amyrin	29.23	$C_{30}H_{50}O$	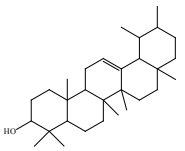	426	0.66
55	2(1H)Naphthalenone, 3,5,6,7,8,8a-hexahydro-4,8a-dimethyl-6-(1-methylethenyl)-	29.64	$C_{15}H_{22}O$	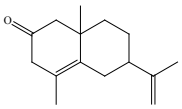	426	4.05
56	.beta.-Amyrone	30.44	$C_{30}H_{48}O$	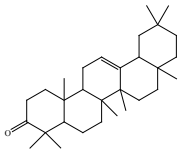	424	0.55
57	Lupeol	30.77	$C_{30}H_{50}O$	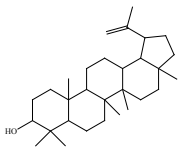	426	0.76
58	Taraxasterol	30.89	$C_{30}H_{50}O$	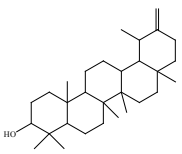	426	0.87
59	Urs-12-en-3-ol, acetate, (3.beta.)-	30.99	$C_{32}H_{52}O_2$	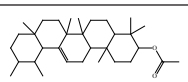	468	0.95

Conclusion

In summary, the investigation of the liposoluble constituents from roots of *L. narynensis* of Kazakhstan have been made for the first time. As the results of this study fifty nine liposoluble compounds were quantified from medicinal plant in which the major constituents were n-Hexadecanoic acid (13.44%), 9,12-Octadecadienoic acid (Z,Z)- (11.79%), (3aR,4aS,5R,9aS)-5,8-Dimethyl-3-methylene-3a,4,4a,5,6,7,9,9a-octahydroazuleno[6,5-b]furan-2(3H)-one (6.90%), Octadecanoic acid (6.17%), .gamma.-Sitosterol (5.50%), 2(1H)Naphthalenone, 3,5,6,7,8,8a-hexahydro-4,8a-dimethyl-6-(1-methylethenyl)- (4.05%), respectively. Presence of these bioactive constituents, may indicate that the plant extract has anti-inflammatory, antimicrobial and anticancer activities. From the results we can estimate that *L. narynensis* extracts poetically useful in medicine. Further and comprehensive investigation is scheduled to be implemented in the next research stage.

Acknowledgement

The work was supported by grants from Ministry of Education and Science of Kazakhstan (0118PK00458).

References

1. Baitenov M.S. (2001) Flora of Kazakhstan. Gylym, Kazakhstan, pp. 206-207.

2. Xue G., Chang-Jun L., Wei-Dong X., Tong S., Zhong-Jian J. (2006) New Oplopane-Type Sesquiterpenes from Ligularia narynensis. Helvetica Chimica Acta., vol. 89., pp. 1387-1394.

3. Wang Q., Chen T.H., Bastow K.F., Morris-Natschke S.L., Lee K.H., Chen D.F. (2013) Songaricalarins A-E, cytotoxic oplopane sesquiterpenes from Ligulaira songarica. J Nat Prod., vol. 76, pp. 305–310.

4. Saito Y., Taniguchi M., Komiyama T., Ohsaki A., Okamoto Y., Gong X., Kuroda C., Tori M. (2013) Four new compounds from Ligularia virgaurea: isolation of eremophilane and noreremophilane sesquiterpenoids and the absolute configuration of 2α-hydroxyeremophil-11-en-9-one by CD spectrum and DFT calculation. Tetrahedron, vol. 69, pp. 8505–8510.

5. Wu Y.X., Chen Y.J., Liu C.M., Gao K. (2012) Four new sesquiterpenoids from Ligularia cymbulifera. J Asian Nat Prod Res., vol. 14, pp. 1130–1136.

6. Xu X., Konirhan B., Zakaria B., Jin X.G., Yili A., Jenis J. (2009) The Kazakh Herbal Medicine. Ethnic publishing house, Beijing, book 1, p.39.

7. Wang R. (2012) The Kazakh Herbal Medicine. Xinjiang Science and Technology press, Urumqi, book 3, p.58.

8. Xue G., Zhong J. J. (2008) A new 8-O-40-type neolignan from Ligularia narynensis. Chinese Chemical Letters, vol. 19, p. 71–72.

9. Chen L.S. (1987) Chin. Tradit. Herb. Drugs, vol. 18, p. 1431.

10. Yang J.L., Wang R., Shi Y.P. (2011) Nat. Prod. Bioprospect., pp. 1-24.

11. Yan-Ming W., Jian-Qiang Zh., Jun-Li Y., Yan-Duo T., Li-Juan M., Yan-Ping Sh. (2017) Chemical constituents from Ligularia purdomii (Turrill) Chittenden. Biochemical Systematics and Ecology, vol. 72, p. 11.

12. Wu L., Liao Z.X., Liu C., Jia H.Y., Sun J.Y. (2016) Chem. Biodivers., vol. 13, pp. 645-671.

13. Gao X., Xie W.D., Jia Z.J. 2008 () Four new terpenoids from the roots of Ligularia narynensis. Journal of Asian Natural Products Research, vol. 10, pp. 185-192.

14. Nurlybekova A.K., Yang Ye, Dyusebaeva M.A., Abilov Zh. A., Jenis J. (2018) Investigation of chemical constituents of Ligularia narynensis. News of NAS RK, vol. 4, p. 10.

15. Vasudevan A., Kalarickal V.D., Pradeep K.M., Ponnuraj K., Chittalakkottu S. Madathilkovilakathu H. (2012) Anti-Inflammatory Property of n-Hexadecanoic Acid: Structural Evidence and Kinetic Assessment. Chem Biol Drug Des., vol. 80, pp. 434–439.

16. Harada, H., Yamashita U., Kurihara H., Fukushi F., Kawabata J., Kamei Y. (2002) Antitumor activity of palmitic acid found as a selective cytotoxic substance in a marine red alga. Anticancer Res., vol. 22, pp. 2587-2590.

17. Lokesh R., Kannabiran K. (2017) Cytotoxic Potential of N-hexadecanoic Acid Extracted from Kigelia pinnata Leaves. Asian Journal of Cell Biology., vol. 12, pp. 20-27.

18. Rahman M.M., Ahmad S.H., Mohamed M.T.M., Ab Rahman M.Z. (2014) Antimicrobial Compounds from Leaf Extracts of Jatropha curcas, Psidium guajava, and Andrographis paniculata. Scientific World Journal, p. 8.

19. Yasutaka W., Tohru M., Tsuyoshi Y. (2005) Investigating Antitermitic Compounds from Australian White Cypress Heartwood (Callitris glaucophylla Thompson et Johnson) Against Coptotermes formosanus Shiraki. Journal of Essential Oil Research, vol. 17, pp. 346-350.

IRSTI 31.21.29

[1*]G. Tuleushov, [2]Martin Attfield

[1]Eurasian National University, Astana, Kazakhstan
[2]School of Chemistry, The University of Manchester, Manchester, United Kingdom
[*]e-mail: tuleushov_g@akb.nis.edu.kz

Synthesis of metal organic framework materials by performing linker exchanges using solvothermal procedure

Abstract. Metal organic frameworks are crystalline nanoporous material constructed from metal ions and bridging organic linkers. These materials are currently receiving considerable research interest due to their adsorption properties and high surface area, which could be used for gas storage and separation. The research involves two main procedures: 1) synthesis of ZIF-76 with LTA framework and performing linker insertion using SALE technique.
Key words: metal organic frameworks, zeolite-imidazolate frameworks, N,N-diethylformamide, N,N-dimethylacetamide.

Introduction

Metal organic frameworks (MOF) are hybrid porous solids which are derived from inorganic (metal nodes) and organic units (organic linkers) in order to build up one, two and three-dimensional frameworks (Figure 1). Metal and organic components are bonded covalently and feature highly ordered crystalline structures [1].

In the last 20 years, metal-organic frameworks (MOFs) have gained considerable attention from researchers because of their potential useful applications such as carbon dioxide capture, storage of hydrogen fuels, gas separation and catalysis [2]. Moreover, MOFs are gaining importance in thin–film devices, membranes and biomedical imaging [3]. Each year, thousands of metal-organic compounds are prepared and studied by chemists [1]. The scope of this studies ranges from topological analysis to molecular synthesis, from optical and absorptive properties to ferroelectric properties and from applications in biomedicine to gas storage [1]. Porosity and large surface area are the main valuable features of metal-organic frameworks (MOFs). Larger storage spaces can be synthesised with longer organic linkers; however, within the MOFs these can form interpenetrating structures. To avoid such structures, MOF needs to be synthesized with a topology which inhibits interpenetration. The synthesis of metal organic frameworks can be carried out at a low temperature. The solvothermal method is utilised above 100^0C. For many syntheses, water and organic solvents, such as pyridine and alcohols can be used. The main parameters of MOF synthesis are temperature, pH and concentration [1].

Solvent-Assisted Linker Exchange of MOF

The synthesis of MOFs from *de novo* suffers from several vagaries such as low solubility, undesirable topologies and loss of sensitivity [4]. However, a recently discovered synthetic method called Solvent-Assisted Linker Exchange (SALE) circumvents the these problems. SALE is based on a heterogeneous reaction, where parent MOF crystals react with a concentrated solution of linkers. SALE circumvents the problem related with linker solubility ensuring the efficient use of precious linkers and leads to the production of the desired MOF material. The heterogeneous reaction pathway enables alteration of MOF crystals by using multitopic linkers. In addition, SALE solves problems associated with catenation and produces MOFs with longer, mixed linkers.

Zeolite A zeolitic-imidazolate frameworks – ZIF-76

The Zeolitic Imidazolate Frameworks (ZIFs) are the most important subfamily of MOFs due to their large use in water softening, selective separation of nitrogen and oxygen gas mixtures and petroleum cracking [5]. ZIFs are composed from bivalent metal cations, such as Co (II), Cu (II), and imidazolate ligands. The main difference of ZIFs from zeolites is their pore size, which tends to be larger than their inorganic analogs [6].

 Printed in Kazakhstan

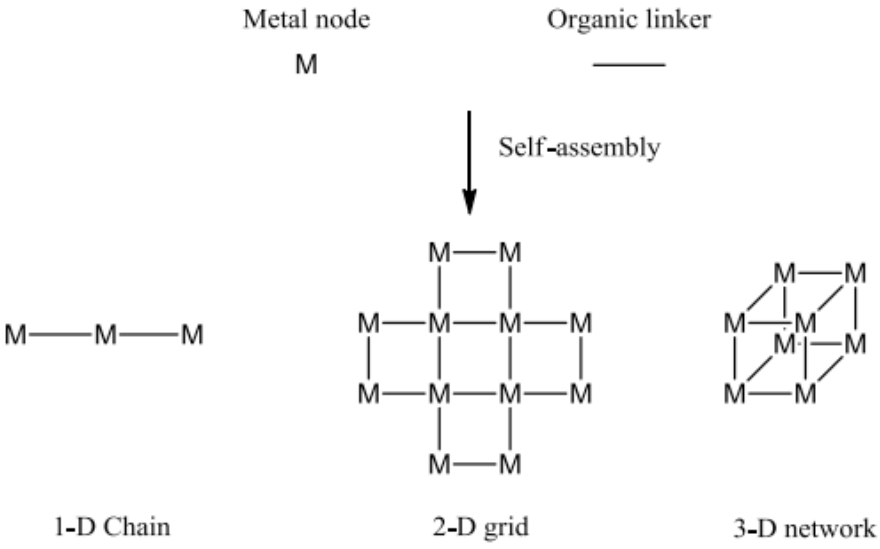

Figure 1 – Different classes of MOF structure[1]

Among the most studied LTA-type ZIFs is $[Zn(Im)_{1.5}(5\text{-}ClbIm)_{0.5}]$ (ZIF-76, Im – Imidazolate, ClbIm – 5-chlorobenzimidazolate) [7]. In ZIF-76, each organic linker connects to two Zn^{2+} centres forming a cubic crystal with a three-dimensional porous framework. Their crystalline properties, such as large pore volume and good stability make them of particular interest for gas adsorption. However, synthesis of ZIF-76 requires an expensive organic linker, 5-chlorobenzimidazolate. To circumvent the problem and retain the LTA framework topology of ZIF, it is important to use relatively inexpensive, structurally related organic linkers such as benzimidazole (bIm). The research is concentrated on synthesising a new LTA-topology $[Zn(Im)_{2-x}(bIm)_x]$ by applying the SALE technique.

Materials and methods

Synthesis

Preparation of ZIF-76 by solvothermal synthesis

The synthesis of ZIF-76 was performed by method described by Yaghi's group. $8.66x10^{-4}$ mol of 5-chlorobenzimidazole (5-ClbIm) and $17.25x10^{-4}$ mol of imidazole (Im) were mixed together in 5 ml of diethylformamide (DEF) and 5 ml of dimethylformamide (DMF). $8.59x10^{-4}$ mol zinc nitrate hexahydrate $Zn(NO_3)_2 \cdot 6H_2O$ were added to this solution. Following the $Zn(NO_3)_2 \cdot 6H_2O$ $12.96x10^{-4}$ mol of NaOH were added in addition. The synthesis was carried out in 20 ml glass vials, which were heated in an oven at 90 ºC for five days. The solid products separated from solution via vacuum suction and washed with DMF. After separation solid product was immersed in methanol for three days refreshing the methanol every day. Finally, ZIF-76 materials were dried at 50 ºC for an hour.

Solvent-assisted linker exchange (SALE) procedure

The ZIF-76 prepared by solvothermal syntheses were used as a starting material for solvent-assisted linker exchange operation. ZIF-76 (55.15 mg, 0.22 mmol) and bIm (100 mg, 1.47 mmol) were placed to 20 ml glass vials and dissolved in 10 ml of DMF. In other case the mixture of ZIF-76 and bIm were dissolved in 10 ml of 1-proponol and DMA and placed in a Teflon-lined autoclave. The mixtures in DMF, 1-propanol and DMA were heated in an oven at 100ºC for 5 days [8].

Characterization Techniques

The characterization of all the samples was carried out using powder X-ray diffraction (PXRD), elemental analysis, scanning electron microscopy and EDS.

Results and discussion

PXRD pattern of parent and daughter ZIF-76 material

The crystallinity and phase purity of synthesized ZIF-76 was confirmed by PXRD as shown in figure 2 and structure is found to be related to the LTA topology

After the SALE reaction reached completion, the integrity of the parent LTA framework in the new

ZIF-76 was confirmed by PXRD analysis as shown in figure 2. All the products of SALE experiment were phase pure and retained the ZIF-76 PXRD pattern, but with lower intensities and sharpness as the diffraction peak. The work carried out by P. Lu et al. showed that keeping the ZIF-76 in different solvents at 100 ºC does not decompose the structure of the sample but declines the crystalinity [9]. In addition, decrease of intensities and crystallinity could be an indication of possible linker exchange. Obviously the decrease of intensity after linker exchange can be seen at 2θ position between 5.57º and 20º as seen in figure 2.

The PXRD pattern exhibits shifting of peaks to higher angle in all exchanged ZIFs compared to parent material (approximately 0.152º) as shown in figure 2. Shifts could be indication of a reduction in the unit cell parameter compared to starting ZIF-76 material and possible linker exchange. Moreover, systematic shift of peaks at 2θ can be caused by zero or sample displacement error.

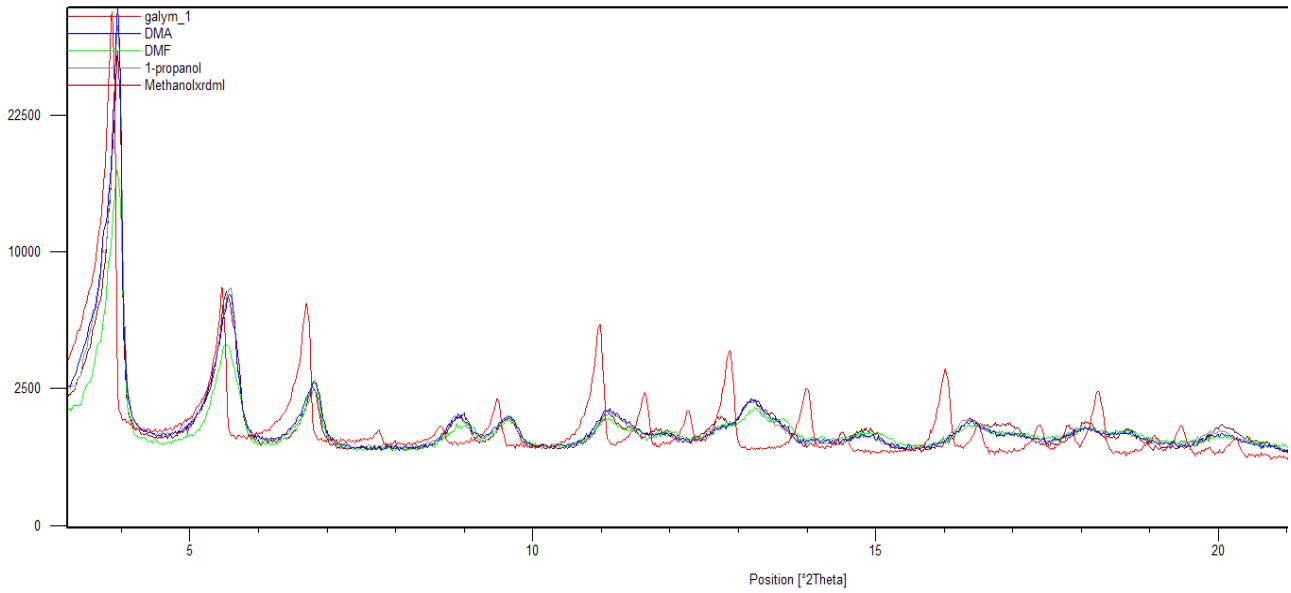

Figure 2 – Comparison of PXRD pattern of parent and exchanged ZIF material

Scanning electron analysis of parent and daughter ZIF-76 material

The size of crystals and morphology of synthesized ZIF-76 material were investigated by Scanning Electron Microscopy. The pure ZIF-76 showed good crystallinity. From the figure 3 it can be seen that ZIF-76 have a cuboctahedron morphology with two destinct facets {100} and {111}. From the SEM it can be observed that {100} face shows square shape while {111} face exhibits triangle shape as expected for cubic symmetry.

The SEM images of all ZIF-76 materials were showed decrease in crystal shape after SALE procedure. The SEM images show that degree of crystal shape from high to low is the ZIFs in methanol, 1-propanol, DMF, DMA . In addition the SEM images of ZIF-76 in methanol and 1-propanol still demonstrates cuboctahedron morphology with two destinct {100} and {111} facets indicating that crystal morphology has been retained.

Elemental analysis and Energy Dispersive Spectroscopy of parent and daughter ZIF-76

To show the evidence of linker exchange elemental analysis (pure ZIF-76, 1-propanol) and EDS (pure ZIF-76, in DMA, DMF, 1-propanol, methanol) were carried out. The main characteristic data of successful of SALE procedure was 0% percentage of chlorine in the product. The pure ZIF-76 contains 5-ClbIm linker. However, the exchange of 5-ClbIm to bIm decreases the percentage of chlorine or in perfect case no chlorine molecules should be detected in composition. Exchanged 5-ClbIm linkers are fully dissolved in solution and removed by vacuum sanction. From the figure 4 it can be seen that intensity of chlorine rapidly decreased indicating exchange of 5-ClbIm to bIm.

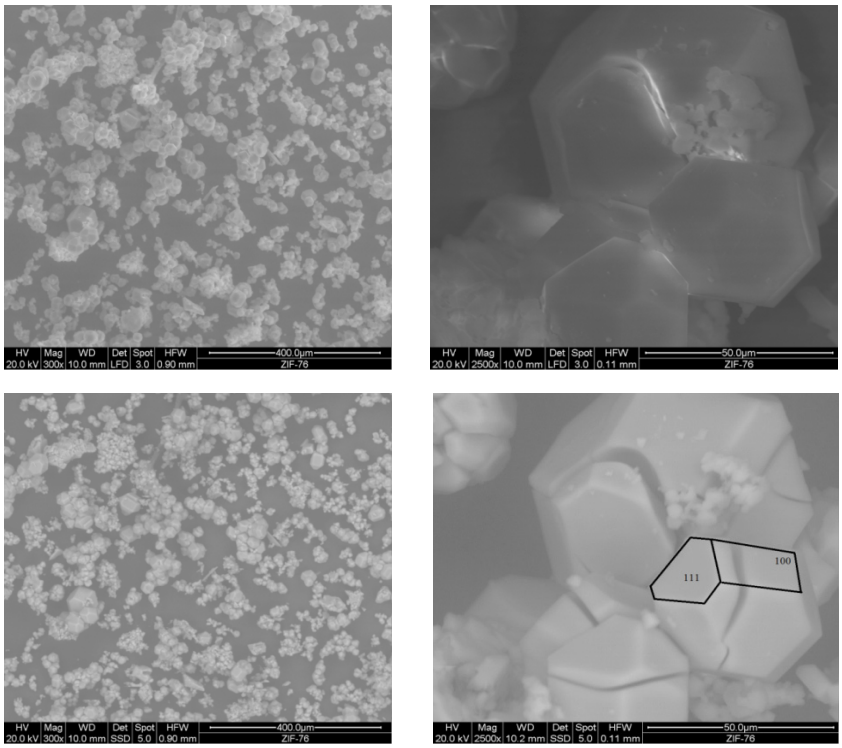

Figure 3 – Scanning electron microscopy images
of secondary and backscattered pure ZIF-76 crystals

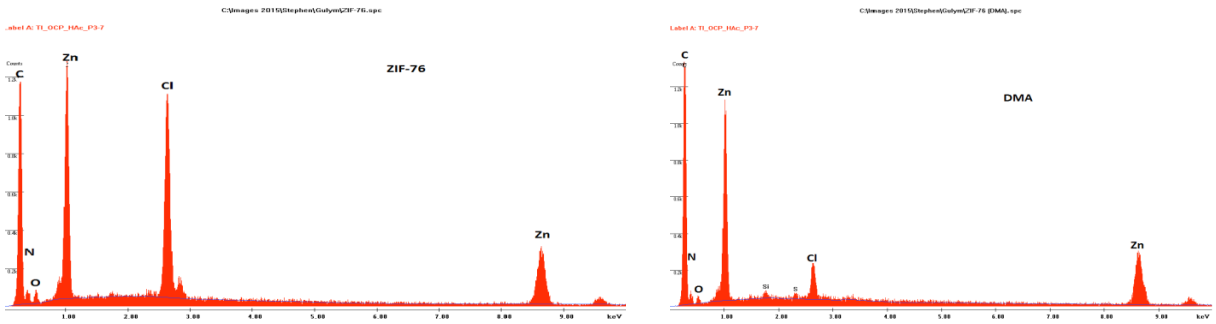

Figure 4 – EDX plot of starting ZIF-76 and after SALE in DMA

Table 1 – The percentage of elements present in ZIF-76 and after the SALE procedure (elemental analysis)

Found	C	H	N	Cl	Zn:Cl ratio
Calculated percentage of elements present from the ZIF-76	42.29	2.48	19.72	23.03	1.85:1
ICP: Reactant ZIF-76	42.28	2.95	20.26	8.86	2.89:1
EDS: Reactant ZIF-76	60.34		6.67	8.50	2.7:1
EDS: Sample 1. DMA	62.80		6.59	1.97	13.5:1
EDS: Sample 2. DMF	68.81		4.29	1.77	12.6:1
EDS: Sample 3. 1-propanol	69.52		5.33	2.59	7.8:1
ICP: Sample 3. 1-propanol	51.75	2.51	18.77	3.31	7.5:1
EDS: Sample 4. Methanol	70.06		4.95	2.80	7.1:1

The elemental analysis of all the samples is given in table 1. The elemental analysis of ZIF-76 after exchange of 5-ClbIm to bIm in propanol gave atomic ratio of Zn to Cl of 7.5:1, which is consistent with EDS (7.8:1). From the EDS it is easy to conclude that the conversion of linker exchange from high to low is DMA, DMF, 1-propanol, methanol. Another noteworthy pattern from the SEM, EDS and elemental analysis is that SALE experiment in DMA and DMF shows good linker exchange but with poor crystal shape. In contrast, SALE experiment in methanol and 1-propanol shows poor linker exchange but with good crystal shape. It indicates that SALE reduces the crystallinity and importance of solvent as a reaction medium.

Conclusion

The new version of ZIF-76 with bIm ligand cannot be achived by direct solvothermal synthesis technique. However, a recently discovered technique known as solvent-assisted linker exchange (SALE) can overcome the above mentioned problem. The findings presented in this project show that successful linker exchange can be achieved in the appropriate solvent. All the data from CHN analysis, Cl analysis, SEM, EDS suggest that the most successful linker exchange was achieved in DMA solvent. The percentage of chlorine in parent ZIF-76 was measured to be about 8%. However, this number falls to approximately 2% in DMA indicating that the majority of 5-ClbIm linker is replaced by bIm ligand. The SEM analysis of parent and all daughter ZIF-76 showed that after SALE, the crystal shape declined. SALE in methanol and 1-propanol demonstrated a good crystal shape compared to ZIF-76 in DMF and DMA. All SALE experiments were carried out with the same reaction time, temperature and ratios. The only variable factor was the reaction medium. From these results it is clear that the solvent size and polarity play an important role in succesful linker exchange. It was observed that the less polar the solvent, the higher the linker conversion. In addition, succesful linker exchange is dependent on the linkers pK_a. The pK_a of 5-ClbIm and bIm is approximately the same and they can replace each other. However, the pK_a of imidazole is about 14.5 indicating that the zinc – nitrogen bond is too strong and stable to be converted by weaker ligands. The adsorption analysis of newly synthesised ZIF-76 in DMA showed that the surface area and pore size significantly decreased. The decline in adsorptivity properities of daughter ZIF-76 can be related to the partial loss of crystallinity as was proven by PXRD analysis. Finally, the accurate selection of ligand and solvent system can improve construction of the porous structures, producing bigger pore sizes.

References

1. Furukawa H., Cordova E. K., O'Keefe M., O. M. Yaghi, Science, 2013, 341, 1.
2. L. C. Rowsell and O. M. Yaghi, Microporous Mesoporous Mater., 2004, 73, 3-14.
3. RSC, http://goo.gl/nB5snZ, [accessed 25th February, 2015].
4. O. Karagiaridi, W. Bury, J. E. Mondloch, J. T. Hupp and O. K. Farha, Angew. Chem. Int. Ed, 2014, 53, 4530-4540.
5. Omar M. Yaghi et al., Nature Materials, 2007, 6, 501-506.
6. Omar M. Yaghi et al., PNAS, 2006, 103, 10186-10191.
7. P. Cubillas, M. W. Anderson and M. P. Attfield, Chem. Eur. J., 2013, 19, 8236-8243.
8. Omar M. Yaghi et al., Nature Materials, 2007, 6, 501-506.
9. Ping-Wei Lu, 2014, Synthesis of Zeolite-imidazolate Framework ZIF-76 with LTA framework by new routes, MSc dissertation, The University of Manchester.